

## Metallic Nanoparticles and Carbon-Based Materials for the Fabrication of Electrochemical Biosensors aiming the Mycotoxin Analysis in Food

Alexandre L. B. Baccaro, Poliana Cardoso, Roberta H. Piccoli, Tatiana C. Bufalo, Roberta C. Martins, Thaina M. Vilela, Ana Carolina F. Alves, Laíse N. S. Pereira, Fabiana S. Felix



8<sup>th</sup> BRAZILIAN MEETING ON  
CHEMICAL SPECIATION



Sao Pedro, Sao Paulo, Brazil

November, 9<sup>th</sup> to 14<sup>th</sup>, 2025



## Dear Colleagues and Friends,

We are excited to announce the 8<sup>th</sup> Brazilian Meeting on Chemical Speciation (8<sup>th</sup> EspeQBrasil) and the 17<sup>th</sup> Rio Symposium on Atomic Spectrometry (17<sup>th</sup> RSAS), which will be held jointly at the beautiful Hotel Fazenda Fonte Colina Verde in São Pedro City, São Paulo State, Brazil. This event will bring together researchers, professionals, and experts from diverse fields to share the latest advancements and innovations in chemical speciation and atomic spectrometry.

We are thrilled to provide a platform for fruitful discussions, knowledge exchange, and networking opportunities. During the event days, attendees will have the chance to engage in inspiring sessions, collaborate on new ideas, and explore solutions to some of the most pressing scientific challenges.

We look forward to welcoming you to this exciting event and hope you make the most of this enriching experience!



[Topics of 8<sup>th</sup> EspeQBrasil](#)



[Topics of 17<sup>th</sup> RSAS](#)

REGISTRATION

SUBMISSION

VENUE

CONTACT

# BrJAC

Brazilian Journal of Analytical Chemistry

**VISÃO FOKKA - COMMUNICATION AGENCY**

## Aims & Scope

BrJAC is a double-blind peer-reviewed research journal, dedicated to the diffusion of significant and original knowledge in all branches of Analytical Chemistry and Bioanalytical Chemistry. It is addressed to professionals involved in science, technology, and innovation projects at universities, research centers and in industry. The **BrJAC welcomes** the submission of research papers reporting studies devoted to new and significant analytical methodologies, putting in evidence the scientific novelty, impact of the research, and demonstrated analytical or bioanalytical applicability. BrJAC **strongly discourages** those simple applications of routine analytical methodologies, or the extension of these methods to new sample matrices, unless the proposal contains substantial novelty and unpublished data, clearly demonstrating advantages over existing ones.

BrJAC is a quarterly journal that publishes original, unpublished scientific articles, reviews and technical notes. In addition, it publishes interviews, points of view, letters, sponsor reports, and features related to analytical chemistry.

For complete information on ethics and policies on conflicts of interest, copyright, reproduction of already published material, preprints, use of AI by authors and reviewers and studies involving biological material, in addition to the manuscript submission and peer review system, please visit 'About us' and 'Author Guidelines' at [www.brjac.com.br](http://www.brjac.com.br).

ISSN 2179-3425 printed

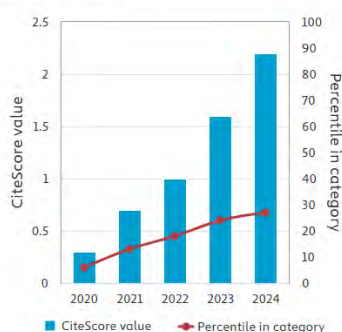
ISSN 2179-3433 electronic

## Indexing Sources

# Scopus

CiteScore<sub>2024</sub> 2.2  
 SJR<sub>2024</sub> 0.207  
 SNIP<sub>2024</sub> 0.305  
 CiteScoreTracker<sub>2025</sub> 1.5  
 Last updated on 5 Sept., 2025  
[Access source details](#)

CiteScore trend



IF<sub>2024</sub> 1.1  
 JCI<sub>2024</sub> 0.19



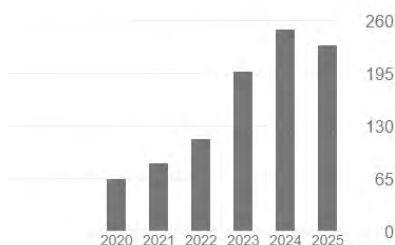
BrJAC is in the Qualis B3 stratum  
 according to preliminary list  
 published on 29 December, 2022

# Google

scholar

Cited by

	All	Since 2020
Citations	1098	947
h-index	15	15
i10-index	29	24



Last updated on 8 September, 2025

## Manager Editor

Silvana Odete Pisani, PhD

## Publisher

Lilian Freitas  
 MTB: 0076693/ SP  
[lilian.freitas@visaofokka.com.br](mailto:lilian.freitas@visaofokka.com.br)

## Advertisement

Luciene Campos  
[luciene.campos@visaofokka.com.br](mailto:luciene.campos@visaofokka.com.br)

**Art Director:** Adriana Garcia

**WebMaster:** Daniel Letieri



BrJAC is associated to the  
 Brazilian Association of Scientific Editors



BrJAC is published quarterly by:  
**Visão Fokka Communication Agency**  
 Av. Washington Luiz, 4300 - Bloco G - 43  
 13042-105 – Campinas, SP, Brazil  
[contato@visaofokka.com.br](mailto:contato@visaofokka.com.br)  
[www.visaofokka.com.br](http://www.visaofokka.com.br)



## **EDITORIAL BOARD**

### **Editor-in-Chief**

**Marco Aurélio Zezzi Arruda**

*Full Professor / Institute of Chemistry, University of Campinas, Campinas, SP, BR*

### **Editor for Reviews**

**Érico Marlon de Moraes Flores**

*Full Professor / Dept. of Chemistry, Federal University of Santa Maria, Santa Maria, RS, BR*

### **Associate Editors**

**Elcio Cruz de Oliveira**

*Technical Consultant / Technol. Mngmt. at Petrobras Transporte S.A. and Aggregate Professor at the Post-graduate Program in Metrology, Pontifical Catholic University, Rio de Janeiro, RJ, BR*

**Elias Ayres Guidetti Zagatto**

*Full Professor / Center of Nuclear Energy in Agriculture, University of São Paulo, Piracicaba, SP, BR*

**Jez Willian Batista Braga**

*Associate Professor / Institute of Chemistry, University of Brasília, DF, BR*

**Leandro Wang Hantao**

*Professor / Institute of Chemistry, University of Campinas, Campinas, SP, BR*

**Mauro Bertotti**

*Full Professor / Institute of Chemistry, University of São Paulo, São Paulo, SP, BR*

**Pedro Vitoriano Oliveira**

*Full Professor / Institute of Chemistry, University of São Paulo, São Paulo, SP, BR*

**Victor Gábor Mihucz**

*Associate Professor / Faculty of Science, Eötvös Loránd University, Budapest, Hungary*

## **EDITORIAL ADVISORY BOARD**

**Auro Atsushi Tanaka**

*Full Professor / Dept. of Chemistry, Federal University of Maranhão, São Luís, MA, BR*

**Carlos Roberto dos Santos**

*Manager of the Decentralized Laboratories Department at CETESB, São Paulo, SP, BR*

**Christopher M. A. Brett**

*Full Professor / Dept. of Chemistry, University of Coimbra, PT*

**Eduardo Costa de Figueiredo**

*Associate Professor / Faculty of Pharmaceutical Sciences, Federal University of Alfenas, MG, BR*

## **EDITORIAL ADVISORY BOARD (Continuation)**

**Fabio Augusto**

*Full Professor / Institute of Chemistry, University of Campinas, Campinas, SP, BR*

**George L. Donati**

*Associate Research Professor / Department of Chemistry, Wake Forest University, Winston-Salem, NC, USA*

**Gisele Simone Lopes**

*Full Professor / Analytical Chemistry and Physical Chemistry Department, Federal University of Ceara, Fortaleza, CE, Brazil*

**Janusz Pawliszyn**

*Full Professor / Department of Chemistry, University of Waterloo, Ontario, CA*

**Joaquim de Araújo Nóbrega**

*Full Professor / Dept. of Chemistry, Federal University of São Carlos, São Carlos, SP, BR*

**Márcia Andreia Mesquita Silva da Veiga**

*Associate Professor / Dept. of Chemistry, Faculty of Philosophy, Sciences and Letters of Ribeirão Preto, University of São Paulo, SP, BR*

**Márcia Foster Mesko**

*Full Professor / Federal University of Pelotas, Pelotas, RS, BR*

**Márcio das Virgens Rebouças**

*Global Process Technology / Specialty Chemicals Manager, Braskem S.A., Campinas, SP, BR*

**Marco Tadeu Grassi**

*Associate Professor / Dept. of Chemistry, Federal University of Paraná, Curitiba, PR, BR*

**Mariela Pistón**

*Full Professor / Faculty of Chemistry, Universidad de la República, Montevideo, UY*

**Pablo Roberto Richter Duk**

*Full Professor / University of Chile, Santiago, CL*

**Ricardo Erthal Santelli**

*Full Professor / Analytical Chemistry, Federal University of Rio de Janeiro, RJ, BR*

**Rodolfo Wuilloud**

*Associated Professor / Facultad de Ciencias Exactas y Naturales, Universidad Nacional de Cuyo, AR*

**Wendell Karlos Tomazelli Coltro**

*Associate Professor / Institute of Chemistry, Federal University of Goiás, Goiânia, GO, BR*

## CONTENTS

<b>Editorial</b> .....	1-2
<i>Leandro Wang Hantao</i>	
<b>Interview</b>	
Professor Jörg Feldmann kindly granted an interview to BrJAC .....	3-6
<i>Jörg Feldmann</i>	
<b>Point of View</b>	
Analytical Chemistry at a Crossroads: Integrity, Reproducibility, and Societal Impact .....	7-9
<i>Emanuel Carrilho</i>	
<b>Letter</b>	
Elemental determination in Fuels and Biofuels: The Challenges and Opportunities for Analytical Chemistry .....	10-13
<i>Paola de Azevedo Mello</i>	
<b>Review</b>	
Metallic Nanoparticles and Carbon-Based Materials for the Fabrication of Electrochemical Biosensors aiming the Mycotoxin Analysis in Food.....	14-66
<i>Alexandre Luiz Bonizio Baccaro, Poliana Cardoso, Roberta Hilsdorf Piccoli, Tatiana Cardoso e Bufalo, Roberta Castro Martins, Thaina M. Vilela, Ana Carolina de Faria Alves, Laíse Nayra dos Santos Pereira, Fabiana S. Felix</i>	
<b>Articles</b>	
Development and Validation of a Stability-Indicating High-Performance Liquid Chromatography with Diode-Array Detection Method for Oclacitinib Using Analytical Quality by Design Approach .....	67-89
<i>Dalton de Assis de Souza, Danilo Raul Ossufo Momade, Allan Michael Junkert, Alexandre de Fátima Cobre, Dile Pontarolo Stremel, Raul Edison Luna Lazo, Luana Mota Ferreira, Roberto Pontarolo</i>	
Geochemical Hydrocarbon Markers in River Sediments from a Densely Populated Area of Curitiba, Brazil .....	90-116
<i>Lucélia Taverna, Fabricio Augusto Hansel, Cesar Alexandro da Silva, Vânia Ribeiro Ferreira, Emerson Luís Yoshio Hara, Rafael Garrett Dolatto, Marco Tadeu Grassi</i>	
Vortex-Assisted Liquid-Liquid Microextraction Based on Hydrophobic Deep Eutectic Solvent for Nickel Determination in Water Samples by Smartphone Digital Image Colorimetry .....	117-131
<i>Airton Vicente Pereira, Orlando Fatibello-Filho, Geovanna Morgado da Penha, Emily Amábilé Tavares</i>	
Development of a Flow-Batch Analyzer for the On-Site Automated Determination of Residual Chlorine in Drinking Water.....	132-143
<i>Guillermo Roth, Justina Medina, Moisés Knochen</i>	
<b>Technical Note</b>	
Sample Preparation Methods Focusing on Soy Biotechnological Samples: Towards Greener Application .....	144-151
<i>João G. Veneziani Kamezawa, Lilian Seiko Kato, Elisânia Kelly Barbosa Fonseca, Marco Aurélio Zezzi Arruda</i>	

## **CONTENTS (Continuation)**

### **Feature**

48 <sup>th</sup> RASBQ 2025: Brazilian Chemistry's Stage for Innovation and Collaboration .....	152-156
---	---------

### **Sponsor Reports**

Impurity Analysis of Gabapentin by HPLC-UV-CAD.....	157-162
---	---------

*Ruben Pawellek, Adrian Leistner, Ulrike Holzgrabe – Thermo Scientific*

A Streamlined Laboratory Workflow for the Analysis of Common Contaminants according to the U.S. EPA 8270E and 8081B Methods using GC-MS/MS .....	163-177
--	---------

*Sarah Crumlett, Mark Belmont, Terry Jeffers, Adam Ladak, Giulia Riccardino, and Daniel Kutscher*

*Thermo Scientific*

New Performance for High Volume Agriculture Laboratories .....	178-184
--	---------

*Milestone*

### **Sponsor Releases**

TSQ Altis Plus Triple Quadrupole Mass Spectrometer.....	185
---	-----

*Thermo Scientific*

Thermo Scientific TSQ 9610 Triple Quadrupole GC-MS/MS System .....	187
--	-----

*Thermo Scientific*

ETHOS UP High Performance Microwave Digestion System .....	189
--	-----

*Milestone*

### **Releases**

Pittcon Conference & Expo .....	191
---------------------------------	-----

SelectScience® Pioneers online Communication and Promotes Scientific Success .....	193
--	-----

CHROMacademy is the Leading Provider of eLearning for Analytical Science .....	195
--	-----

<b>Notices of Books</b> .....	197
-------------------------------	-----



<b>Periodicals &amp; Websites</b> .....	198
---	-----


<b>Events</b> .....	199
---------------------	-----

<b>Author Guidelines</b> .....	200
--------------------------------	-----



## EDITORIAL

Leandro Wang Hantao  

Professor at the Dept. of Analytical Chemistry, Institute of Chemistry, University of Campinas   
Campinas, SP, Brazil

It is with great pleasure that we present Issue 49 of the *Brazilian Journal of Analytical Chemistry* (BrJAC), featuring a diverse collection of contributions for our scientific community.

This issue opens with an insightful interview with Prof. Jörg Feldmann (University of Graz, Austria), in which he reflects on his career and shares valuable perspectives on the evolving role of Analytical Chemistry. We also highlight a thought-provoking point-of-view article by Prof. Emanuel Carrilho, titled "Analytical Chemistry at a Crossroads: Integrity, Reproducibility, and Societal Impact". This timely discussion encourages us to rethink how our field addresses the challenges of scientific rigor and societal relevance. Additionally, Prof. Paola de Azevedo Mello contributes a letter that enriches this vibrant dialogue about the difficulties in elemental determination in fuels and biofuels.

The research articles in this issue illustrate both the breadth and depth of contemporary analytical science. A review article explores the use of metallic nanoparticles and carbon-based materials in the fabrication of electrochemical biosensors, with a focus on mycotoxin analysis in food—highlighting the importance of advanced materials in addressing food safety challenges.


Several original contributions further demonstrate the innovative spirit of our community:

- The development and validation of a stability-indicating HPLC-DAD method for oclacitinib, applying the principles of Analytical Quality by Design (AQbD).
- A chemical investigation of hydrocarbon markers in river sediments from a densely populated area of Curitiba, Brazil, with implications for environmental monitoring.
- The proposal of a vortex-assisted liquid-liquid microextraction technique using hydrophobic deep eutectic solvents, combined with smartphone-based digital image colorimetry for nickel determination in water samples.
- The development of a flow-batch analyzer designed for on-site automated determination of residual chlorine in drinking water, emphasizing practical solutions for public health.
- Completing the issue, a Technical Note discussing sample preparation methods for soy biotechnological samples, pointing toward greener analytical approaches and sustainable practices in food and agricultural sciences.

Taken together, these contributions highlight the dynamism of Analytical Chemistry in addressing fundamental questions, technological challenges, and pressing societal needs. We are confident that the works presented in this issue will inspire reflection, innovation, and collaboration among researchers and practitioners alike.

We wish you an excellent reading experience.



**Leandro Wang Hantao** is currently Associate Professor at the Institute of Chemistry at UNICAMP, Campinas, SP, Brazil. He is a member of the São Paulo State Academy of Sciences (ACIESP) and a full member of the Brazilian Chemical Society (SBQ). His research group specialises in analytical chemistry. Among the current lines of research, the following stand out: (i) sample preparation for the analysis of organic compounds, (ii) chromatographic techniques, (iii) mass spectrometry, and (iv) data processing. His research group is highly active in the fields of food analysis, forensic chemistry, metabolomics, and petrochemistry. [CV](#) 

## INTERVIEW



### Professor Jörg Feldmann kindly granted an interview to BrJAC

Professor Jörg Feldmann was educated in Germany. After 25 years in Canada and Scotland working on the development of novel elemental speciation methods for unraveling biological and environmental pathways of trace elements, he moved to Austria. At the University of Graz, he became Head of the Analytical Chemistry Department and was recently appointed Head of the Institute of Chemistry. Currently, he is focusing mainly on the development of new platforms for fluorine and per- and polyfluoroalkyl substance (PFAS) analysis and is additionally investigating arsenic and mercury transformations and bioaccumulation pathways in the marine environment and in rice cultivation. Professor Feldmann has published more than 350 papers (h-index of 76), given over 180 invited lectures, and educated more than 50 PhD students.

He has also received many awards, including the 2015 European Plasma Spectrochemistry Award, the 2016 RSC Interdisciplinary Award and Medal, the 2020 Award for Industrial Engagement, and the 2023 Award for Excellence in Teaching, and was elected a Fellow of the Royal Society of Edinburgh in 2018.

**BrJAC:** What was your childhood like?

**Prof. Feldmann:** I grew up in a working-class environment in Germany and left school at 15 when I embarked on an apprenticeship in the chemical industry. I hated my job and I realized that I needed to get my life and a job in my own hands. I went back to school to get my qualifications to go to university and study chemistry.

**BrJAC:** What early influences encouraged you to study chemistry? Did you have any influencers, such as a teacher?

**Prof. Feldmann:** In my early years I did chemical experiments at home and in the garden. I carried out explosions and was fascinated about the science of this. In school I had to give a full lesson to the class, since I was always annoying the teacher. "Stop talking or I'll do choke chemistry (that meant no experiments), and if you know it better, you do the next lesson," she said, and I accepted it. I hated school but I loved chemistry and wanted to see the world.

**BrJAC:** What was the beginning of your career in chemistry like?

**Prof. Feldmann:** I realized that I was interested in environmental chemistry, which was not taught in Germany at the time, but I studied geology on the side and I did my Master project in geochemistry in South Africa, already doing some elemental speciation in gold solubilities under hypothetical Precambrian atmospheres. This is all I wanted: chemistry of the environment and in a faraway country with a different culture. But I did not continue with a PhD, although most people did this back in Germany. I decided to work for a city

council as environmental officer to assess contaminated land in the city. But my work was shallow and I could not travel the world. Then I got a phone call from Alfred Hirner, who had founded a new institute of environmental analytical chemistry at the University of Essen, and he had heard that I was a chemist and interested in environmental and analytical chemistry. He offered me a PhD position (and a part-time lecturer position). I developed the first coupling of gas chromatography to ICP-MS in 1991 to analyze volatile metal species in landfill gas and I loved it. When on the matrix printer the numbers were coming out, we knew that we had discovered something novel—this was exiting.

**BrJAC:** What has changed in your profile, ambitions, and performance since the time you started your career?

**Prof. Feldmann:** When I was about to finish my PhD, I did not want to stay in Germany, otherwise I had no plans. But I realized that with a PhD the world opens up, and I applied to the Alexander von Humboldt Foundation, who send out the best-qualified PhD to the world in order to return to Germany. I received a scholarship and went to Bill Cullen at the University of British Columbia in Vancouver, Canada. I worked there on hot springs and volcanic exhalations, trying to develop new skills such as microbiology and working in a hot lab with radioactive material. Even at that point I had no idea what I wanted to do later in life. I never planned anything but I was determined not to go back with my new family to Germany and I decided to go to Aberdeen in Scotland. I loved Scotland when I visited this wonderful country for one month, climbing the hills on the west coast, during my undergraduate years in Germany. At the same time, I had the opportunity to go to large, successful groups in elemental speciation (to Alfredo Sanz-Medel in Spain or Olivier Donard in France), but I wanted to build up my own lab from scratch and that is what I did. I was lucky—I specialized in elemental speciation and that was hip at the time, so I received a lot of funding and attracted great people to work with me as PhDs and postdocs.

**BrJAC:** Could you comment briefly on the recent evolution of analytical chemistry, bearing in mind your contributions?

*... if you come with interesting questions like “why do sheep not die when they eat more than 13 g of arsenic per year?” or “why are whale strandings increasing?” people will flock to you.*

**Prof. Feldmann:** When I started with elemental analysis, I moved from AAS to ICP-MS very quickly. Plasma spectrochemistry was always at the heart of my research in speciation analysis. I always wanted to explain environmental and biological processes in which metals and metalloids were centerpieces, but I found out that the right tools and methods were not available to characterize these processes. Hence, my team needed to develop first of all new analytical methods and then they could apply those to answer environmental or biological scientific questions. This has always been my focus and still is. We

were the first to do elemental mapping in soft tissues using laser ablation ICP-MS and coupled HPLC simultaneously to electrospray mass spectrometry and elemental mass spectrometry (ICP-MS) to identify and quantify novel elemental species such as arsenolipids and mercury phytochelatins. But using only one type of analytical technique is not enough in most cases, and we should use the entire toolbox of analytical chemistry to analyze environmental samples. Hence, synchrotron techniques such as XANES/EXAFS or Raman and electrochemical methods are often needed. Thus, I tried to team up with the best in the world for those techniques and this has been very successful. But the most important collaborations have been with life scientists (soil scientists, geneticists, marine biologists, archaeologists, geologists, epidemiologists, etc.) in working on grand environmental questions. Without these collaborations I would not have been able to answer any of those interesting questions or prove or disprove sometimes outrageous hypotheses. I guess if you work in analytical science, you have to do a good job, and if you come with interesting questions like “why do sheep not die when they eat more than 13 g of arsenic per year?” or “why are whale strandings increasing?” people will flock to you.

**BrJAC:** What are your lines of research? You have published many scientific papers—would you highlight any?

**Prof. Feldmann:** Most of my research has focused on arsenic from biovolatilization, to arsenic metabolism in sheep and humans, to arsenic in rice. The latter gave me the most satisfaction. Then our work in Aberdeen together with Andy Meharg was instrumental in setting guideline values for a maximum legal limit of inorganic arsenic in rice worldwide, and in particular in the EU.

Then, of course, there is the mercury work I did together with Eva Krupp on mercury in plants and in whales in forming mercury nanoparticles, and recently in the decommissioning of offshore oil and gas.

**BrJAC:** What is your opinion about the current progress of chemistry research in Word? What are the recent advances and challenges in scientific research?

**Prof. Feldmann:** Our latest endeavor is fluorine speciation with an emphasis on using mass balance approaches in PFAS analysis. I realized 15 years ago that the approach we use in elemental speciation would be very beneficial for PFAS analysis, since we have more than 12,000 different PFAS and only up to 50 are routinely measured with target analysis using LC-MS/MS. Using elemental analysis like atomic spectrometry (AAS and ICP-MS) can help with monitoring the PFAS. But we are only at the beginning right now. I would compare the current situation with arsenic speciation in the 1990s. So, the challenges are to get a sensitive and robust fluorine detector like we have for metals and metalloids, which can be coupled to chromatography, flow field fractionation for particulates, or to laser ablation for fluorine mapping, and to do reliable total fluorine analysis at the ultra-trace level. If you have any ideas, please contact me.

**BrJAC:** For you, what have been the most important recent achievements in analytical chemistry research? What are the landmarks? What has changed in this scenario with the COVID-19 pandemic?

*"I think classical environmental analytical chemistry has to move to automation, i.e., not only for measurements but for sample preparation and for data analysis. AI-guided approaches for data analysis are becoming more and more important since we often get gigabyte data and use only a fraction in nontargeted analysis."*

**Prof. Feldmann:** I think classical environmental analytical chemistry has to move to automation, i.e., not only for measurements but for sample preparation and for data analysis. Here, fully automated systems are needed that have been developed in proteomics and other disciplines. AI-guided approaches for data analysis are becoming more and more important since we often get gigabyte data and use only a fraction in nontargeted analysis. We neglect most of our data. What COVID-19 has shown us is that we cannot stop developing sophisticated analytical methods for well-funded labs, but we need to simplify the methods so that our methodologies can

be used in less developed economies. We developed, for example, a field-deployable method for inorganic arsenic in rice where an untrained rice farmer can do the analysis and get an answer in one hour as to whether his or her rice can be exported to countries with legal maximum limits for this carcinogenic compound. Recently we even replaced nitric acid with Coca-Cola in the extraction step to make it applicable in rural countries—so, a traffic light system like we have had with the COVID-19 quick tests; that is where we have a social impact and this fits well to the SDGs (Sustainable Development Goals).

**BrJAC:** There are, in Brazil and across the world, several conferences on chemistry. To you, how important are these meetings to the chemistry scientific community?

**Prof. Feldmann:** We have experienced extraordinary times of lockdowns and no in-person conferences. This has resulted in a communication breakdown between scientists, despite the fact that we have all had the technology to listen to lectures all around the world without traveling. The most important parts of those conferences are the breaks and evenings. This is the time science comes alive and new ideas for new projects are born. This is not happening if you sit alone in front of a computer. Hence, scientists in Brazil



keep going and organizing conferences and workshops at which, in a relaxed atmosphere, networking opportunities are generated. I am thankful for those conferences in Brazil.

**BrJAC:** What is the importance of awards for the development of science and new technologies?

**Prof. Feldmann:** Awards are a great tool for all ages but mostly for young researchers. These awards are an acknowledgment of all the hard work from a research community. This helps young researchers especially who are still on the brink of getting a permanent position to get a job or to secure funding to develop new technologies.

**BrJAC:** What advice would you give to a young scientist who wants to pursue a career in chemistry?

**Prof. Feldmann:** As I mentioned before, I did not have a career plan myself, and I hated school and university at first, but my eyes were always open for opportunities. You can have a career in chemistry in industry or in government organizations. You do not have to decide early on what you want to do, there will always be time to change. You will find out during your Master or PhD if academia or industry or working for legislators is for you. All have their pros and cons. If you like training people and you are thrilled by developing new ideas without borders, then academia is the place for you. But you need to be prepared to work some extra hours (unpaid but maybe rewarded with prizes). If you want to earn money and have a brilliant idea, go down the entrepreneur route, but here you need to hunt more for funding than in academia, but it can be rewarding. A nine to five job, if something like that exists, is best found in a large chemical or pharmaceutical company. But you do not have to decide during your Master or PhD and you may get opportunities during this time. Go to conferences and meetings; these are the places where opportunities are.


**BrJAC:** For what would you like to be remembered?

**Prof. Feldmann:** No idea. I am not retired yet and I have still some exciting projects ahead of me. No idea if they work but this is research. If this fails, remember me as a crazy Germanic Scottish guy who likes to come to South America and likes to work with those wonderful Brazilians on interesting projects in environmental chemistry.

## POINT OF VIEW

# Analytical Chemistry at a Crossroads: Integrity, Reproducibility, and Societal Impact

Emanuel Carrilho  

Grupo de Bioanalítica, Microfabricação e Separações, Instituto de Química de São Carlos, Universidade de São Paulo  Av. Trabalhador São-carlense, 400, 13566-590 São Carlos, SP, Brazil

Over four decades at the University of São Paulo (three as professor), I have witnessed the transformation of analytical and bioanalytical chemistry from a discipline often seen as “supportive” to one that is at the center stage of some of the most critical scientific and technological advances of our time. From the development of DNA sequencing technologies in Boston during my doctoral studies<sup>1</sup> to my sabbatical years at Harvard working on microfluidic paper-based devices,<sup>2</sup> I have seen how analytical chemistry has evolved, contributing to our understanding of life, environment, health, and how it can serve society. Today, analytical chemistry faces significant opportunities and tough challenges. On one hand, our methods enable precision diagnostics, environmental monitoring, and quality control for industries in our modern society. On the other hand, we confront a crisis of reproducibility that erodes the public trust in science and widens persistent gaps in connecting academic excellence with societal benefit.

Analytical chemistry has long been the “invisible science” that guarantees reliability. As I argued previously,<sup>3</sup> it is time we innovate from the bottom up. The COVID-19 pandemic reminded us that diagnostics are not ancillary, but central to public health. Brazil responded with creativity, producing molecular tests and even initiating vaccine development. Yet, our dependency on imported reagents and instrumentation exposed the fragility of our system. This paradox — intellectual strength but industrial weakness — must be addressed at the governmental level if we are to transform knowledge into impact.

The societal impact of analytical chemistry goes beyond health crises. It is central in fields such as food safety, drug development, forensic science, and climate monitoring. Our discipline ensures that decisions are based on solid data, but the credibility of science rests not only on data but also on integrity. For students and colleagues alike, I often stress that analytical chemistry is about more than numbers — it is about truth. Selective reporting, inadequate validation, and neglect of uncertainty undermine not only the quality of science but also the faith in it.

As researchers and educators, we carry the responsibility of transmitting ethical practices to the younger generations. This involves rigor in data handling, transparency in reporting, and humility in acknowledging limitations. Journals, funding agencies, and universities must reinforce ethics and responsible research, but ultimately it is at the laboratory bench where integrity is practiced daily. Unfortunately, we have seen an unprecedented number of paper retractions from journals, and not only from the predatory publishers.<sup>4</sup>

The issue of reproducibility has emerged as a defining challenge for modern science.<sup>5</sup> A recent study we conducted confirmed that analytical chemistry is not immune to this crisis. We found that method validation and measurement uncertainty are frequently misapplied, leading to results that cannot be reproduced with confidence. In nearly one-third of the papers analyzed, uncertainties exceeded 100% at the lowest concentration levels, resulting in questionable conclusions.<sup>6</sup>

These findings are not isolated, and concerns have been raised across disciplines regarding insufficient statistical training, inadequate replication, and a lack of data transparency. In chemistry, these deficiencies are particularly concerning because our results often serve as the basis for regulatory approval, industrial processes, and clinical decisions. The path forward requires collective efforts. First, we must integrate chemical metrology, method validation, and quality assurance into curricula from undergraduate levels to graduate school. Second, journals should enforce clearer standards for reporting validation and uncertainty, let alone the use of artificial intelligence. Third, open science practices — including data sharing — must become the norm rather than the exception.

Reversing the reproducibility crisis and reinforcing research integrity requires cultural change and education. We must teach future chemists not only how to generate data but also how to ensure that those data can withstand scrutiny and serve society. After all, what good is an analytical breakthrough if it cannot be trusted, reproduced, or applied to real-world challenges?

Analytical and bioanalytical chemistry stand at a crossroads. We have never been more central to the scientific enterprise, but we must also face the truths revealed by the reproducibility crisis. By embracing integrity, rigor, and innovation, we can restore confidence in our results and amplify our impact on society. More than that, we should be able to bring to the spotlight the reasons for unethical behavior in producing data, writing papers, and pushing the productivity numbers (and the toll it takes on the mental health of young researchers). As a professor who has trained generations of chemists at USP, I remain convinced that the way to move forward relies on education, transparency, and the pursuit of truth. Only then will our discipline live up to its promise — to provide the reliable answers upon which science, technology, and society rely.



## REFERENCES

- (1) Carrilho, E.; Ruiz-Martinez, M. C.; Berka, J.; Smirnov, I.; Goetzinger, W.; Miller, A. W.; Brady, D.; Karger, B. L. Rapid DNA Sequencing of More Than 1000 Bases per Run by Capillary Electrophoresis Using Replaceable Linear Polyacrylamide Solutions. *Anal. Chem.* **1996**, 68, 19, 3305–3313. <https://doi.org/10.1021/ac960411r>
- (2) Carrilho, E.; Martinez, A. W.; Whitesides, G. M. Understanding wax printing: a simple micropatterning process for paper-based microfluidics. *Anal. Chem.* **2009**, 81(16), 7091-7095. <https://doi.org/10.1021/ac901071p>
- (3) Carrilho, E. Analytical and Bioanalytical Chemistry – It is time we innovate. *Braz. J. Anal. Chem.* **2022**, 9 (35), 5–6. <http://dx.doi.org/10.30744/brjac.2179-3425.point-of-view.ecarrilho.N35>
- (4) The Retraction Watch Database by Crossref. <https://retractiondatabase.org/RetractionSearch.aspx?>
- (5) Baker, M. 1500 scientists lift the lid on reproducibility. *Nature* **2016**, 533, 452–454. <https://doi.org/10.1038/533452a>
- (6) Ferreira, B. D.; Olivares, I. R. B.; Carrilho, E.; Paccos, V. H. P. Is everything wrong in analytical chemistry? A study on reproducibility. *Accred. Qual. Assur.* **2025**, 30, 361–366. <https://doi.org/10.1007/s00769-025-01649-7>

**Disclosure:** To be truthful to the point of view, I declare that artificial intelligence was used to edit, improve, and proofread the text.



**Emanuel Carrilho**, FRSC, is a Full Professor at the University of São Paulo (USP) with a Master's degree in Analytical Chemistry from USP (1990) with focus in instrumentation for supercritical fluid chromatography, and a Ph.D. from Northeastern University, Boston, USA (1997) in bioanalytical chemistry, helping in the development of DNA sequencing technologies that led to the sequencing of the Human Genome Project. Later, (2007-2009) he spent a sabbatical leave at Harvard University in the Whitesides Group, working on the emergence of microfluidic paper-based analytical devices ( $\mu$ PAD) and wax-printing. The Carrilho group, or BioMicS – Bioanalytical, Microfabrication, and Separations Group, develops new bioanalytical methods and instrumentation covering the broad aspects of genomics, proteomics,

and metabolomics for human health, applied cell and microbiology in microfluidic platforms like organs-on-a-chip, searching for biomarkers for cancer, rare, and neglected diseases. Dr. Carrilho has supervised over 60 graduate students and a dozen of post-docs, has published about 200 papers with 9,000 citations, and an h index of 41.  

## LETTER

# Elemental Determination in Fuels and Biofuels: The Challenges and Opportunities for Analytical Chemistry

Paola de Azevedo Mello  

Departamento de Química, Universidade Federal de Santa Maria , 97105-900, Santa Maria, RS, Brazil

While the fossil fuel industry continues to face upheavals, with discoveries of new fields, the global demand for energy and fuels drives research into alternative and renewable energies, such as biomass. This trend has been reinforced by recognizing the negative impacts of burning fossil fuels and using fossils as raw materials for industry to supply everyday demands.

In this scenario, analytical methods that are already established in laboratories worldwide must be updated to align with the trends and advances, providing new methods for the unique demands of this instigating sector, which has peculiar compositions and a broad scope of analytes. Heavy and light crude oil, coal, gas, different biomass types and their derived products are challenging samples that require experience and rigorous protocols for chemical characterization.

In terms of composition, petroleum from different reservoirs presents variations in chemical composition, both in their major hydrocarbons and in the types of elements present.<sup>1</sup> In contrast, biomass encompasses a diverse range, including lignocellulosic raw materials, waste, garbage, and agro-industrial residues, among others. This results in a diversity of compositions that significantly differ from hydrocarbon mixtures typical of fossil raw materials.<sup>2</sup>

Figure 1 summarizes the key aspects relevant to each context. When it comes to elemental composition, it is worth mentioning that the elements that most deserve attention in fossil raw materials and their fractions/products due to their presence and inherent impacts, in addition to sulfur (and nitrogen), are nickel and vanadium, alkaline and alkaline earth elements in petroleum and arsenic, cadmium, lead and mercury (in coal and natural gas).<sup>3</sup> In biomass raw materials and in the products and fractions derived from their conversion, the primary elements of interest are typically sodium, potassium, calcium, magnesium, aluminum, iron, copper, phosphorus, sulfur and chlorine.<sup>4</sup>



**Figure 1.** The key aspects of fossil fuels and biofuels covering the raw materials, main products and composition and target elements.



A literature search covering the last 50 years indicates that some studies focused on elemental determination in fossil fuels began to be published at the beginning of the selected period (Figure 2). Conversely, it was only at the end of the last century that researchers began to focus on biofuels. More recently, there has been an increase in publications addressing both fossil and renewable fuels.

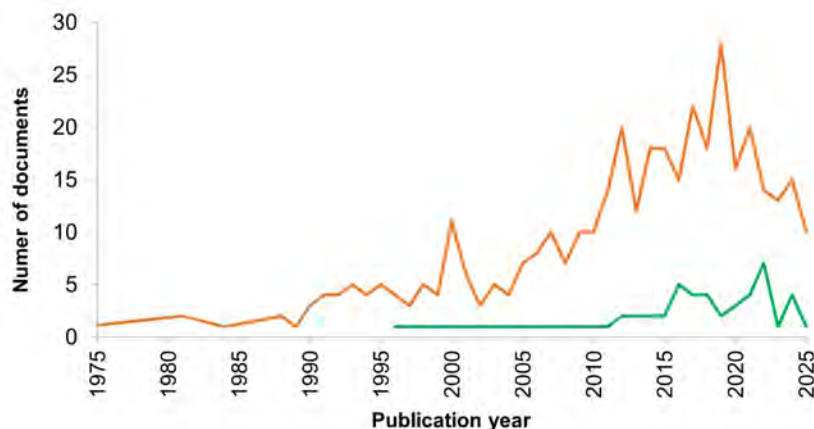


**Figure 2.** Number of articles published in the last decades on the topic of crude oil (orange line) or biofuels and biomass (green line) and elemental (or metal) determination. Data were obtained from Web of Science, on August 2025 (filter for document types - article or review article).

Although the industry requires methods for elemental determination, with official protocols for each type of raw material or product, the accuracy of these methods for various materials must be critically evaluated, especially due to the diversity of the matrices. Hence, while laboratories are relatively well equipped with methods to attend the requirements of petroleum industry, which has a relatively large number of standards from different entities, such as the American Society for Testing and Materials, the Institute of Petroleum, the Brazilian National Agency for Petroleum, Natural Gas and Biofuels), methods for biomass and biofuels remain relatively scarce. This scarcity is justified by technical limitations, and the recent and less widespread use of these materials, thereby justifying the smaller range of possibilities in terms of official standards. Nevertheless, the growing interest in alternatives to fossil fuels, in a way, justifies the scientific community's engagement to ensure accuracy, precision, and adequate detection and quantification limits, which is in line with the current trends in analytical chemistry and green/white chemistry.<sup>1,5</sup>

Despite the advances in instrumentation enabling powerful detection capabilities through techniques, such as atomic absorption, mass spectrometry or optical emission spectrometry, analyzing samples with variable compositions remains a challenge.<sup>1,6-9</sup> Some elements are relatively less impaired by interferences, particularly those that are not difficult to ionize in inductively coupled plasmas or microwave-induced plasmas. However, the limitations related to determining non-metals (due to the low emission wavelengths) and the low mass-to-charge ratio for mass spectrometry (e.g. Cl, Br, S, and P) hinder method development, especially at low concentrations. In this context, methods for non-metals, particularly the halogens and for the speciation analysis, seem to be the main bottlenecks, regardless of the sample type within this context.<sup>10-12</sup>

Equipment continues to be improved to expand applications, although for samples with oil-based compositions or solids, one remaining limitation is related to the introduction systems that work well with aqueous solutions. Some examples of successful applications are documented, although they often encounter interferences and difficulties with calibration. Moreover, direct analysis is also possible, with techniques such as X-ray fluorescence spectrometry, but limitations in the supply chain of calibration standards and matrices is not capable of covering all the range of composition. Thus, matrix-interferences continue to restrict the scope of matrices and analytes that can be measured accurately.

Sample preparation that converts samples to aqueous solutions is a common strategy that facilitates conventional calibration and fast analysis with conventional nebulization systems. Nevertheless, decomposing organic-based matrices can be a problem even with powerful systems allowing high pressure and temperature, namely high-performance microwave-assisted systems.<sup>13</sup> Primary challenges to circumvent include gas samples and samples from non-conventional crude oil reservoirs, in addition to the samples composed of mixtures of fossil fuels and biomass-derived fractions.

Hence, considering the task of determining the elemental composition of fossil fuels and biofuels (and general biomass-derived fractions), the application of classical and conventional methods, especially in the context of the petroleum industry, is by itself a critical aspect. These methods often involve the use of protocols based on high amounts of solvents that take hours to develop, compared to the current precepts in the development of analytical methods, despite ensuring ease of execution and assuring accuracy and reproducibility. This represents a target for analytical chemistry, which is centered on developing alternatives that address these problems. In addition, developing systematic evaluations, adjusting conditions for various types of matrices and elements, and achieving the necessary quantification limits are other points of attention. Lastly, in addition to the inherent limitations of the chosen or available method or technique, overcoming the lack of certified reference materials is another obstacle to overcome. Despite this, research in this area has continued to garner increasing attention from researchers and economic and global efforts.


## REFERENCES

- (1) Shishkova, I.; Stratiev, D.; Kolev, I. V.; Nenov, S.; Nedanovski, D.; Atanassov, K.; Ivanov, V.; Ribagin, S. Challenges in petroleum characterization - a review. *Energies (Basel)* **2022**, *15* (20), 7765. <https://doi.org/10.3390/en15207765>
- (2) Wang, Z.; Burra, K. G.; Lei, T.; Gupta, A. K. Co-pyrolysis of waste plastic and solid biomass for synergistic production of biofuels and chemicals-a review. *Prog. Energy Combust. Sci.* **2021**, *84*, 100899. <https://doi.org/10.1016/j.pecs.2020.100899>
- (3) Shi, Q.; Wu, J. Review on sulfur compounds in petroleum and its products: state-of-the-art and perspectives. *Energy & Fuels* **2021**, *35* (18), 14445–14461. <https://doi.org/10.1021/acs.energyfuels.1c02229>
- (4) Vassilev, S. V.; Vassileva, C. G.; Song, Y.-C.; Li, W.-Y.; Feng, J. Ash contents and ash-forming elements of biomass and their significance for solid biofuel combustion. *Fuel* **2017**, *208*, 377–409. <https://doi.org/10.1016/j.fuel.2017.07.036>
- (5) Cai, J.; He, Y.; Yu, X.; Banks, S. W.; Yang, Y.; Zhang, X.; Yu, Y.; Liu, R.; Bridgwater, A. V. Review of physicochemical properties and analytical characterization of lignocellulosic biomass. *Renewable Sustainable Energy Rev.* **2017**, *76*, 309–322. <https://doi.org/10.1016/j.rser.2017.03.072>
- (6) Thomaidis, N. S. Simultaneous or sequential multi-element graphite furnace atomic absorption spectrometry techniques: advances within the last 20 years. *At. Spectrosc.* **2021**, *42* (6). <https://doi.org/10.46770/AS.2021.707>
- (7) Sánchez, R.; Sánchez, C.; Lienemann, C.-P.; Todolí, J.-L. Metal and Metalloid Determination in biodiesel and bioethanol. *J. Anal. At. Spectrom.* **2015**, *30* (1), 64–101. <https://doi.org/10.1039/C4JA00202D>
- (8) Gab-Allah, M. A.; Goda, Emad. S.; Shehata, A. B.; Gamal, H. Critical review on the analytical methods for the determination of sulfur and trace elements in crude oil. *Crit. Rev. Anal. Chem.* **2020**, *50* (2), 161–178. <https://doi.org/10.1080/10408347.2019.1599278>
- (9) Sánchez, R.; Todolí, J. L.; Lienemann, C.-P.; Mermet, J.-M. Determination of trace elements in petroleum products by inductively coupled plasma techniques: a critical review. *Spectrochim. Acta, Part B* **2013**, *88*, 104–126. <https://doi.org/10.1016/j.sab.2013.06.005>
- (10) Caumette, G.; Lienemann, C.-P.; Merdrignac, I.; Bouyssiére, B.; Lobinski, R. Element speciation analysis of petroleum and related materials. *J. Anal. At. Spectrom.* **2009**, *24* (3), 263. <https://doi.org/10.1039/b817888g>

- (11) Mello, P. A.; Pereira, J. S. F.; Mesko, M. F.; Barin, J. S.; Flores, E. M. M. Sample preparation methods for subsequent determination of metals and non-metals in crude oil- a review. *Anal. Chim. Acta.* **2012**, 746, 15–36. <https://doi.org/10.1016/j.aca.2012.08.009>
- (12) Holkem, A. P.; Voss, M.; Schlesner, S. K.; Helfer, G. A.; Costa, A. B.; Barin, J. S.; Müller, E. I.; Mello, P. A. A green and high throughput method for salt determination in crude oil using digital image-based colorimetry in a portable device. *Fuel* **2021**, 289, 119941. <https://doi.org/10.1016/j.fuel.2020.119941>
- (13) Druzian, G. T.; Nascimento, M. S.; Picoloto, R. S.; Mesko, M. F.; Flores, E. M. M.; Mello, P. A. Ultra-trace Hg determination in crude oils by CV-ICP-MS: overcoming the limitations of sample preparation to determine sub-ppb levels. *J. Anal. At. Spectrom.* **2022**, 37 (9), 1799–1805. <https://doi.org/10.1039/D2JA00169A>





**Paola de Azevedo Mello** has bachelor's in industrial chemistry (2004), a Master's degree in Analytical Chemistry in 2007 and a PhD in Chemistry in 2011. She is currently an Associate Professor at the Federal University of Santa Maria (UFSM) in Brazil. She has two maternity leaves (2018 and 2021).

Paola de A. Mello has experience in analytical chemistry, focusing on atomic spectrometry (AAS, ICP OES and ICP-MS), development of sample preparation methods, and speciation analysis using LC and GC-coupled techniques. She has supervised three PhD students, ten Master's students and fifty undergraduate students. She has published over 120 peer-reviewed international papers and reviews. She has been a member of the Chemistry Committee of the Rio Grande do Sul State Foundation for Research (FAPERGS) since 2017, and has been Director of the Analytical Chemistry Division of the Brazilian Chemical Society (SBQ) since 2024. She was awarded in 2020 with the Brazilian Women in Chemistry and Related Sciences Award by C&EN and CAS (ACS) and received the PhosAgro/UNESCO/IUPAC Grant in Green Chemistry, in 2024. 

REVIEW

# Metallic Nanoparticles and Carbon-Based Materials for the Fabrication of Electrochemical Biosensors aiming the Mycotoxin Analysis in Food

Alexandre Luiz Bonizio Baccaro<sup>1</sup> , Poliana Cardoso<sup>2</sup> , Roberta Hilsdorf Piccoli<sup>2</sup> ,  
Tatiana Cardoso e Bufalo<sup>3</sup> , Roberta Castro Martins<sup>4</sup> , Thaina M. Vilela<sup>1</sup> , Ana Carolina  
de Faria Alves<sup>1</sup> , Laíse Nayra dos Santos Pereira<sup>5</sup> , Fabiana S. Felix<sup>1\*</sup>  

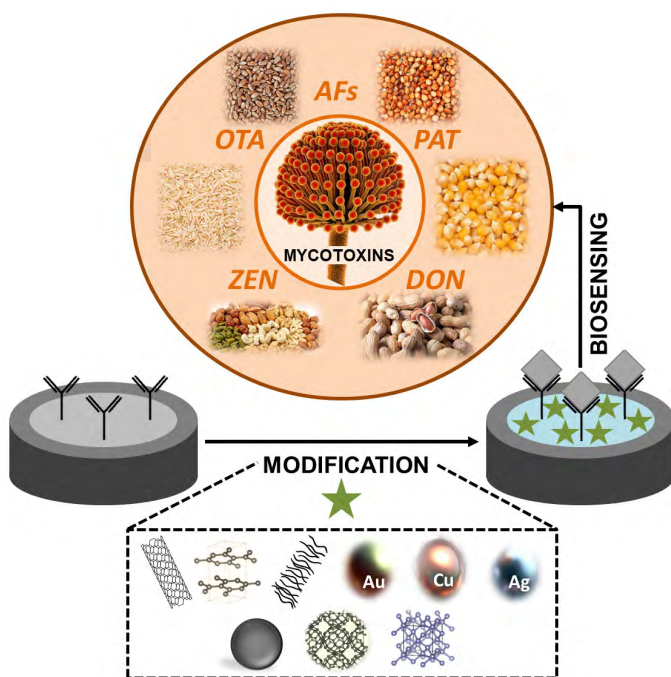
<sup>1</sup>Departamento de Química/ICN, Universidade Federal de Lavras  Trevo Rotatório Professor Edmir Sá Santos, s/n, CP. 3037, 37.203-202, Lavras, MG, Brazil

<sup>2</sup>Departamento de Ciências dos Alimentos, Escola de Ciências Agrárias, Universidade Federal de Lavras, CP. 3037, 37200-900, Lavras, MG, Brazil

<sup>3</sup>Departamento de Física/ICN, Universidade Federal de Lavras, CP. 3037, 37200-900, Lavras, MG, Brazil

<sup>4</sup>Departamento de Ciências Florestais/ESAL, Universidade Federal de Lavras, CP. 3037, 37.203-202, Lavras, MG, Brazil

<sup>5</sup>Instituto Federal de Educação, Ciência e Tecnologia do Maranhão  Campus Zé Doca. Rua da Tecnologia, 215, 65365-000, Zé Doca, MA, Brazil



Mycotoxins are low molecular-weight compounds produced by fungi genera as secondary metabolites during pre- and post-harvest storage of crops and foodstuff. Many reports show highly concerning issues ascribed to their carcinogenic, genotoxic, immunosuppressive, and teratogenic properties. Biosensors are compact analytical devices incorporating a biological or biologically-derived recognition element that might be either integrated within or intimately associated with a physicochemical transducer. The most applied bioreceptors are the enzymes (biosensors), DNA and RNA nucleic acids (genosensors), antibodies (immunosensors), aptamers (aptasensors) or living cells (microbial biosensors). The integration of nanotechnology to the biosensors field brought sensitivity and versatility for bioassays, since nanomaterials might play the role as new signal markers, surface substrates for functionalization and fixation of biomolecules, and generation source

**Cite:** Baccaro, A. L. B.; Cardoso, P.; Piccoli, R. H.; Bufalo, T. C.; Martins, R. C.; Vilela, T. M.; Alves, A. C. F.; Pereira, L. N. S.; Felix, F. S. Metallic Nanoparticles and Carbon-Based Materials for the Fabrication of Electrochemical Biosensors aiming the Mycotoxin Analysis in Food. *Braz. J. Anal. Chem.* 2025, 12 (49), pp 14-66. <http://dx.doi.org/10.30744/brjac.2179-3425.RV-189-2024>

Submitted December 20, 2024; Resubmitted April 26, 2025; Accepted June 7, 2025; Available online July 4, 2025.



of analytical signals. For electrochemical biosensors, nanostructures can enhance the sensitivity of electrochemical techniques by filling the gap between the converter and the biorecognition element. Metal nanoparticles are used to improve the analytical sensitivity by refining the electrical connectivity of the interface, increasing both the chemical accessibility of analytes and the sensing surface with higher amounts of bioaffinity recognition sites. Gold nanoparticles are among the most used nanostructures due to their unique electrocatalytic activity and conductivity. In turn, carbon-based nanomaterials are very appealing considering their large specific surface area and high electron transfer rates. Carbon nanotubes (CNTs) and graphene oxide materials are the most employed carbon-based materials. There is no doubt that the whole bioassay has become more versatile, robust, and dynamic with the introduction of the nanoscience, consolidating in an emerging field with current intense research. Hence, this work reviews some selected applications of electrochemical metallic and carbon-based nanobiosensors for the determination of mycotoxins in food, revisiting important fundamentals of the electrochemical bioassay.

**Keywords:** mycotoxins contamination, foodstuff analysis, immunosensors, aptasensors, genosensors, electrochemistry

## INTRODUCTION

The class of the mycotoxins is a group of low molecular-weight compounds produced by filamentous fungi in food. They are secreted as secondary metabolites of several fungi species, like *Aspergillus*, *Fusarium*, *Penicillium*, and *Alternaria*, during pre- and post-harvest of crops and foodstuff storage. Among commonly studied mycotoxins are the aflatoxins (AF), ochratoxins (OTA), and patulin (PAT).<sup>1</sup> Aflatoxins are the most investigated group, including the aflatoxins B1, B2, G1 and G2, produced by *Aspergillus flavus*. They have drawn a lot of attention due to their high cytotoxicity and carcinogenicity.<sup>2</sup> *Aspergillus* and *Penicillium* genus produce the ochratoxins mycotoxins, which include ochratoxin A ascribed to toxic pathologies on the human renal system. *Penicillium* strains can additionally produce some tremorgenic mycotoxins. Other mycotoxins include the trichothecene group generated by the *Fusarium* genus, which can cause oral lesions such as dermatitis, irritation, and bleeding.<sup>3</sup> That is why mycotoxins are contaminants that need to be continuously monitored in critical stages of the food chain to preserve the quality of human life. That includes inspections of raw materials, food supply and processing, final products, and also the storage.<sup>4</sup> Considering the mycotoxins maximum levels allowed in cereals and related cereal products by e.g. the European Commission Regulation (1881/2006), there is a substantial challenge for detecting such low concentrations at ppb magnitude order in complex food products. For total aflatoxin (TAF) the maximum concentration allowed is 4 ng/g, while for deoxynivalenol (DON) is from 200 to 500 ng/g, for zearalenone (ZEN) is from 20 to 50 ng/g and, for ochratoxin A (OTA) is 0.5 ng/g. Still, the identification of emerging mycotoxins and their synergistic effects<sup>5</sup> usually requires the use of multi-target procedures, demanding advanced instrumental methods such as the liquid chromatography-electrospray ionization-tandem mass spectrometry (LC-ESI/MS) with long sample processing times, and high instrument costs that impair the screening of a large number of samples.<sup>6</sup>

Many benchtop analytical methods are available to accurately and sensitively detect mycotoxins in foods: thin-layer chromatography,<sup>7</sup> capillary electrophoresis,<sup>8</sup> liquid chromatography coupled with mass spectrometry,<sup>9</sup> and Raman spectroscopy<sup>10</sup> are some examples. However, analytical chemistry is quickly evolving in the last decades, making field measurements feasible (at least for screening analysis) that accelerate the decision-making for the agriculture niche.<sup>11,12</sup> A fast overview of the situation regarding the eventual mycotoxins contamination can not only help in terms of the producers awareness, but with the number of samples to be collected, processed, prepared, and analyzed, saving time and money.<sup>13</sup> This reality can still be highly improved by the full substitution of the lab-bench techniques by *in situ* specific techniques with improved accuracy, precision, and sensitivity. That is the main reason why mycotoxin immunoassay development has approached and nearly surpassed chromatographic methods.<sup>6</sup> Hundreds of immunoassay methods have been developed addressing the fast mycotoxins detection using ELISA, flow



injection immunoassay (FIIA), chemiluminescence (CL) immunoassay, lateral flow immunoassay (LFIA), and flow immunoassay.<sup>6,14–16</sup> Among other immunological methods, ELISA and LFIAS stand out for their simplicity, agility, and long-term stability under different climatic conditions, ascribing them to be suitable for onsite mycotoxin detection.<sup>6</sup>

Another way to perform *in situ* determinations is by the development of miniaturized electrochemical nanoimmunosenors. Immunosensors are a class of highly-specific biosensors that use antibodies as recognizing bioreceptor agents, which specifically interact with the analyte, forming surface immunocomplexes.<sup>17</sup> Among the immunological bioreceptors, aptamers are attracting much attention recently due to their low cost, reasonable stability, and good applicability in wide ranges of pH and temperatures, with the so-called label-free detection.<sup>18</sup> The signal is triggered by the analyte bonding that changes the aptamer conformation or hybridization.<sup>19</sup> Many transducing mechanisms are possible with special regard to electrochemical methods that are considerably simple and sensitive enough for most of the studied applications.<sup>20,21</sup> Meanwhile, the nanotechnology serves several purposes once applied to electrochemical immunosensors.

Nanomaterials are materials with at least one of their dimensions in the range between 1 and 100 nm or are composed of them as the basic unity in a three-dimensional space.<sup>22</sup> Considering their reduced nanosizes, they show large surface area to volume ratios with many special physical and chemical properties when compared to bulk materials, as their catalytic effect due to their higher ratios of reactive surface sites,<sup>23,24</sup> and the quantum effect<sup>25</sup> for very small sizes. By applying different strategies of synthesis as the ball milling, sputtering, electron beam evaporation, laser ablation, and electrospraying (top-down physical processes);<sup>26,27</sup> or the sol-gel synthesis, hydrothermal synthesis, co-precipitation method, microemulsion technique, and chemical vapor deposition (bottom up chemical processes),<sup>27,28</sup> different nanostructures can be obtained as metallic nanoparticles (MNP), nanotubes (NTs), nanowires (NW), nanorods (NR), carbon allotropes, quantum dots (QD), or even their mixing in nanostructured composites. Their composition comprises many materials, including metals, metal oxides, dendrimers, mesoporous silica, micelle, liposome, magnetic materials, polymers, and carbon-based materials<sup>29–31</sup> (Figure 1).

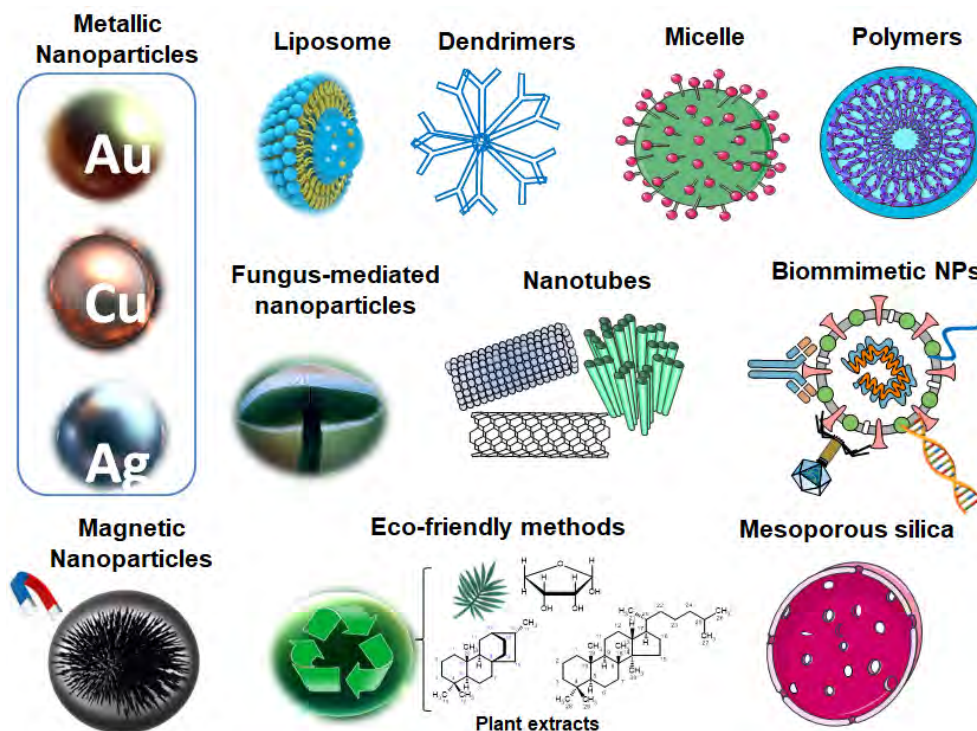


Figure 1. Different nanostructured materials.

Nowadays, the research on nanomaterials field is growing fast as well as its applications in physics, chemistry, materials, biology, and medicine. Additionally, many nanomaterials hold promise to improve the processes of food storage, quality monitoring, food processing, food packaging, and food safety detection and control, consolidating one of the most appealing tools to revolutionize the food production chain.<sup>32</sup> And it is not different for the science of biosensors. Nanomaterials can play different roles: starting from the replacement of traditional markers and signal amplifiers,<sup>4,33</sup> passing through surface functionalization<sup>34</sup> and fixation<sup>35</sup> with biomolecules, until the generation of fluorescence analytical signals.<sup>6</sup> They confer sensitivity and versatility to the analytical methodologies and, regarding specifically to the electrochemical biosensors, nanostructures are used to fill the gap between the converter and the bioreceptor, greatly enhancing the yet high sensitivity of electrochemical techniques.<sup>36</sup> Currently, the modification of electrode surface to access the contamination of mycotoxins in food has applied<sup>37</sup> carbon-based nanomaterials, metal or metal oxide nanoparticles, quantum dots, metal-organic frameworks (MOFs), and covalent organic frameworks (COFs).

Carbon-based nanomaterials are interesting materials considering their large specific surface area and high performance at the electron transfer step.<sup>38</sup> Among them, the carbon nanotubes (CNTs) are the most employed carbon-based nanomaterial used for electrochemical detection. CNTs are classified in two groups according to the number of layers of graphene sheets: the single-walled CNTs (SWCNTs) and multi-walled CNTs (MWCNTs). For instance, Yang *et al.*<sup>39</sup> developed a SWCNTs/chitosan-functionalized glass carbon electrode (GCE) immunosensor for the highly sensitive detection of Fumonsin B1 (FB1) in corn. Liu *et al.*<sup>40</sup> applied the MWCNTs to develop a nanobody-based voltammetric immunosensor with horseradish peroxidase concatemer-modified hybridization chain reaction (HRP-HCR) for the detection of aflatoxin B1 (AFB1). Tungsten disulfide (WS<sub>2</sub>) and gold nanoparticles (AuNPs) were used to enhance the surface area by the formation of a hierarchical nanocomposite, still improving the material conductivity and the loading capacity of the recognition molecules. Graphene Oxide (GO) is a 2D nanosheet of carbon monolayer with stratified structure and more appealing physical properties than the CNT with, *e.g.*, larger surface area, higher thermal and electrical conductivities. Considering these advantages, GO-based electrochemical sensors have gained great attention of researches.

For instance, Bulbul *et al.*<sup>41</sup> developed a GO-based screen printed carbon electrode (SPCE) to assemble an electrochemical aptasensor for the detection of Ochratoxin A (OTA) with the synergistic contribution of GO and the nanoceria. The GO layer accomplished the role of immobilizing the aptamer and increasing the electron transfer rate, enhancing the sensitivity of the analytical methodology. Li *et al.*<sup>42</sup> created a programmable ratiometric electrochemical aptasensor for the detection of aflatoxin B1 (AFB1) in peanut by using a thionine-functionalized reduced GO (THI-rGO) deposited on a glassy carbon electrode (GCE). Positive charges of THI promoted the dispersibility and prevented the aggregation of the reduced form of graphene (r-GO). AuNPs were electrostatically adsorbed on the THI-rGO surface as the conjugated sites for the s-DNA and the ferrocene-labeled aptamer (fc-apt, signal probe) were fixed to the electrode by the base pairing with the s-DNA. The presence of AFB1 in the sample led to the formation of the Fc-apt-AFB1 complex, which stripped the probe from the electrode, fading the current intensity of Fc and increasing the current intensity of THI. Finally, some alternatives to the bottom-up synthesis approach have been recently created and, an example of them is the self-assembly chemical vapor deposition, which allowed the development of microporous 3D graphene.<sup>37</sup> Ong *et al.*<sup>43</sup> prepared 3D-graphene nickel to assemble an electrochemical aptasensor for the selective biosensing of deoxinivalenol (DON). The nanoflorets on the surface of 3D graphene nickel increased the material surface area for the bonding of biomolecules, besides the enhancement of charge transfer properties, consolidating an effective alternative for the DON detection in food and feed samples.

Metals nanoarchitectures have been applied to electrochemical biosensors to improve the analytical sensitivity of methodologies by refining the electrical connectivity of the interface, increasing the chemical accessibility of analytes and the sensing surface by improving the amount of anchored bioaffinity recognition sites.<sup>37</sup> Gold nanostructures as, *e.g.*, spheres, rods, wires, urchins, stars, and cages have been abundantly applied due to their unique electrocatalytic activities and conductivities, providing anchoring sites for thiolate

recognition molecules or redox species through direct bonds with sulfur (S) or nitrogen (N) groups. As a good example, Wu *et al.*<sup>44</sup> developed an electrochemical aptasensor for the detection of AFB1 by the direct deposition of gold nanoparticles (AuNPs) onto a bare glassy carbon electrode (GCE). The role of these AuNPs was to improve the interface electron transfer capacity, allowing the consolidated aptasensor to effectively measure the content of AFB1 in real samples of peanut oil with interesting recovery ratio between 94.5 and 106.7%. One should bear in mind that these gold nanoparticles show physical characteristics of solid spheres, allowing only the outer sphere area to be covered with the anchoring sites of biorecognition elements. Therefore, new nanoarchitectures had to be designed to increase the overall electroactive surface. For instance, the use of porous gold nanocages (AuNCs) with inner and outer walls can improve the effective area for the aptamer immobilization on a screen-printed carbon electrode (SPCE), as reported by An *et al.*<sup>45</sup> As a result, a highly sensitive aptasensor was obtained for AFB1 sensing in a so-called label-free method. By exposing the sensing interface to the AFB1 it was possible to initiate the formation of the aptamer/AFB1 complex, increasing the interfacial electron transfer resistance on the SPCE and leading to a methodology with a very low limit of detection (LOD) of 0.03 pg mL<sup>-1</sup>.

Electrochemical immunosensors, as all kinds of currently existing immunosensors, can be divided in two main classes: the labelled and label-free types.<sup>46</sup> For the labelled type (Figure 2a), a molecular component as an enzyme is anchored to either the biorecognition element (antibody) or the target molecule (antigen), acting as an electroactive probe that generates and/or amplifies the signal associated with the formation of the immunocomplex, allowing the target detection. The label-free electrochemical immunosensor (Figure 2b) enable the direct detection of the target analyte without labels or redox reporters, which is a tendency in the immunoassay field. These methodologies use e.g. the formation of the antibody-antigen (Ab-Ag) immunocomplexes to produce the detectable electrical signal. One of them is immobilized on the electrode surface to establish the sensing interface. Then, the target analyte binds to form the Ab-Ag complex, changing the interface electrical properties, which include variations in the surface area, electron transfer, and even diffusivity. These events are detectable and allow quantifications to be accomplished by electrochemical techniques such as amperometry, voltammetry, or electrochemical impedance spectroscopy (EIS).<sup>47</sup>

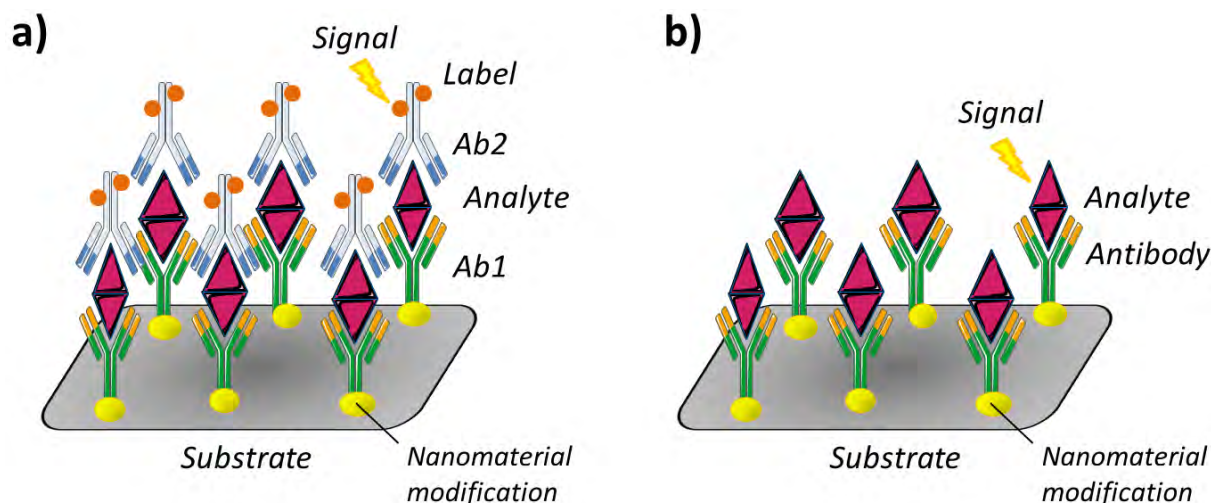


**Figure 2.** Schematics of: a) a labeled-type immunosensor with the capture antibody (Ab1) and the detection antibody (Ab2); b) a label-free immunosensor with analyte direct detection.

The direct label-free detection shows as its main advantages the elimination of labelling or conjugation steps, simplifying the procedures, reducing the duration and complexity of assays, and minimizing the risks of contamination and interference from the labelling reagents.<sup>48</sup> However, challenges on the label-free immunosensors include the lower sensitivity once compared to labelled assays due to the absence of the



signal amplification step that is typical of labelled reporter molecules,<sup>49</sup> and the potential to eventually allow non-specific binding,<sup>50</sup> since label-free methodologies rely a lot on the surface properties of the transducer and the immobilized biorecognition elements. Layer-by-layer electrochemical characterization is recently advancing as a tool for the development of label-free immunosensors,<sup>51</sup> providing important insights into the relations of structure and functionality of the electrochemical components of the immunosensor, and driving the design of immunological chains. The use of electrochemical complementary techniques as cyclic voltammetry (CV), electrochemical impedance spectroscopy (EIS), and chronoamperometry allow the real-time systematic monitoring of the properties of each deposited layer, enabling the optimization. Precise control of assembling steps is accessed, optimizing the concentration, incubation time and pH of bioreceptors, blocking agents, and the formation of the Ab-Ag complex. Nice reviews discussing such subjects of label-free electrochemical immunosensors can be found elsewhere.<sup>46,52-54</sup>

This comprehensive review aims to didactically explain the advances of metallic nanoparticles (MNPs) and carbon-based materials to assemble both sensitive and highly specific biosensors for the detection and quantification of mycotoxins that affect crops and the foodstuff production chain. After briefly contextualizing the problem of the mycotoxins in food, the fundamentals of biosensors are presented by introducing the different bioreceptors used as the specific recognition biomolecules, the conventional transducers used for biosensing, and the electrochemical transducers. Finally, distinctive selected applications from the last decades of metallic nanoparticles and carbon-based immunosensors for the mycotoxin detection are discussed, pointing out challenges, opportunities, and perspectives for future research.

## THE RISK OF MYCOTOXINS IN FOOD

Mycotoxins represent a category of food contaminant whose presence in edible material is considered unacceptable. It is defined as the fungal secondary metabolites produced by filamentous fungi, meaning the diverse group of microorganisms with a single unit structure of slender filaments, providing morphological complexity and capacity to secrete large amounts of different enzymes.<sup>55,56</sup> Secondary metabolites (also known as natural products) are chemical compounds playing fungal interactions with other organisms or plants, while primary metabolites comprise essential compounds for fungi growth that cannot be obtained from the medium. Accordingly, secondary metabolites are the result of a truncated process of polymerization of the primary metabolites by an enzymatic cocktail that vastly alters their bioactivities.<sup>57,58</sup> Concerning the food safety, although the Fungi kingdom encompasses a variety of organisms from unicellular yeasts, multicellular molds, until the macroscopic mushrooms, solely mycotoxins are significant inasmuch as yeasts and molds may cause food spoilage without safety implications. It is worth highlighting that the toxins produced by mushrooms or even those affecting only plants or lower animals (insects) are not included in the definition of mycotoxin.<sup>30</sup> Furthermore, the toxic response of animals and humans to the ingestion of mycotoxins can happen at different stages of the agrifood chain – before and after the harvest, during the processing or storage.<sup>59-61</sup>

Mycotoxins are thermally stable under conventional food-processing temperatures (80 – 121 °C), displaying high bioaccumulation ability and carrying-over into animal fluids, organs, and tissues even in very low concentrations.<sup>62,63</sup> Typical environmental agents as humidity, temperature, insect damage, and weather status are suitable scenarios for the growth of mycotoxin-producing fungi in agricultural products. Meanwhile, the occurrence of mycotoxin in food and beverages is caused by direct contamination of plant materials, animal tissues, milk, and eggs after the intake of contaminated feed.<sup>64-66</sup> Mycotoxins represent a very diverse group differing from each other structurally, which results in different toxic levels: over 500 different mycotoxins have been recognized and, indeed, one fungal species may produce more than one type of mycotoxin, and several fungal species may simultaneously grow in food and feed products. Favorably, there are around 20 mycotoxins found in food and feed produced by *Fusarium*, *Penicillium*, *Claviceps*, *Alternaria* and *Aspergillus* that can impact the human and animal health.<sup>67</sup> *Fusarium* (Figure 3) produces the specific mycotoxins Deoxynivalenol, Nivalenol, Zearalenone, and Fumonisin, while *Alternaria* synthesizes Alternariol, *Penicillium* the Ochratoxin and Patulin, and *Aspergillus* the Aflatoxins and Ochratoxin.<sup>68</sup> Furthermore, plant

metabolism has the potential to engender toxic byproducts from mycotoxins, which is an emerging concept called “hidden mycotoxins”.<sup>69</sup> A compilation of the most prominent mycotoxigenic fungi in the food industry can be found in Table I.

**Table I.** Important mycotoxins related to agriculture, economics, public health and their effects on humans

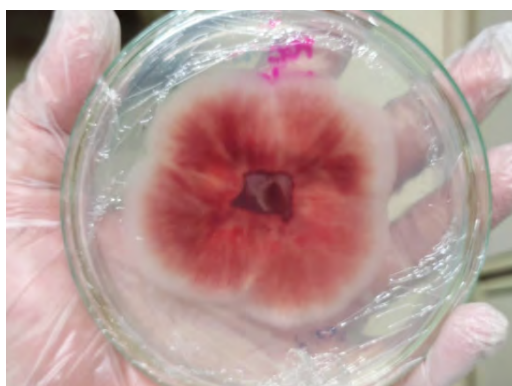
Mycotoxin	Types of mycotoxins	Main Production Fungi	Food Source	Human Risks	Authors
Aflatoxins (AFs)	AFB <sub>1</sub> , AFB <sub>2</sub> , AFG <sub>1</sub> , AFG <sub>2</sub> , AFM <sub>1</sub> , AFM <sub>2</sub>	<i>Aspergillus</i> spp., <i>A. flavus</i> , <i>A. parasiticus</i> , <i>A. niger</i> , <i>A. nomius</i> , <i>A. tubingensis</i> , <i>Fusarium</i> spp., <i>Mucor</i> spp.	Grains (maize and rice), peanuts, seeds, spices, dried fruits; animal products (milk and meat)	Carcinogenic, genotoxic, liver damage, hepatocellular carcinoma	56, 70–75
Ochratoxin A (OTA)	--	<i>Fusarium</i> spp., <i>Aspergillus</i> spp., <i>A. carbonarius</i> , <i>A. ochraceus</i> , <i>Penicillium</i> spp., <i>P. nordicum</i> , <i>P. verrucosum</i>	Cereals, particularly maize, wheat, oat, barley, coffee, grapes, raisins, red wines, meat (pork and poultry), milk, infant formula and infant cereals	Carcinogenic, genotoxicity, cytotoxicity, mutagenic, teratogenic, hepatotoxic, immunosuppressive	76–79
Fumonisin (FUM)	FA <sub>1</sub> , FA <sub>2</sub> , FA <sub>3</sub> , PHFA <sub>3a</sub> , PHFA <sub>3b</sub> , HFA <sub>3</sub> , FAK <sub>1</sub> , FBK <sub>1</sub> , FB <sub>1</sub> , Iso-FB <sub>1</sub> , PHFB <sub>1a</sub> , PHFB <sub>1b</sub> , HFB <sub>1</sub> , FB <sub>2</sub> , FB <sub>3</sub> , FB <sub>4</sub> , FB <sub>5</sub> , FC <sub>1</sub> , N-acetyl- FC <sub>1</sub> , Iso-FC <sub>1</sub> , N-acetyl- iso-FC <sub>1</sub> , OH-FC <sub>1</sub> , N-acetyl OH-FC <sub>1</sub> , FC <sub>3</sub> , FC <sub>4</sub> , FP <sub>1</sub> , FP <sub>2</sub> , FP <sub>3</sub>	<i>Fusarium</i> spp., <i>F. sacchari</i> , <i>F. proliferatum</i> , <i>F. verticillioides</i>	Maize and maize products, coffee, banana	Carcinogenic, esophageal cancer, neural tube defect disease, cells apoptosis, neurotoxicity, immunotoxicity, reproductive toxicity, tissue and organ toxicity	80–84
Zearalenone (ZEA)	--	<i>Fusarium</i> spp., <i>F. graminearum</i> , <i>F. culmorum</i> , <i>F. cerealis</i> , <i>F. equiseti</i> , <i>F. crookwellense</i> , <i>F. semitectum</i>	Maize, sorghum, wheat, rice, barley, nuts, soybeans, sesame	Hepatotoxic, immunotoxic, carcinogenic, nephrotoxic effects, severe reproductive and sexual dysfunctions	75, 78

(continues on next page)



**Table I.** Important mycotoxins related to agriculture, economics, public health and their effects on humans (continuation)

Mycotoxin	Types of mycotoxins	Main Production Fungi	Food Source	Human Risks	Authors
Patulin (PAT)	--	<i>Fusarium</i> spp., <i>F. sacchari</i> , <i>F. proliferatum</i> , <i>Penicillium</i> spp., <i>P. expansum</i>	Fruits and processed products	Cytotoxicity, genotoxicity	76, 85–87
Deoxynivalenol (DON)	--	<i>Fusarium</i> spp., <i>F. andiyazi</i> , <i>F. fujikuroi</i> , <i>F. temperatum</i> , <i>F. subglutinans</i>	Cereal crops, maize, oat	Nausea, vomiting, diarrhea	75,88
Citrinin (CIT)	--	<i>Penicillium</i> spp., <i>P. citrinum</i> , <i>P. verrucosum</i> , <i>P. expansum</i> , <i>Aspergillus</i> spp., <i>A. carneus</i> , <i>A. niveus</i> , <i>A. terreus</i> , <i>Monascus</i> spp., <i>M. ruber</i>	Cereal and fruits, grains, spices and condiments, citrus fruits, herbs, processed fruit juices, beers	Carcinogenicity, nephrotoxic, genotoxic	86, 87, 89, 90
Alternaria (AT)	AOH, AME, ALT, ATX-I, ATX-II, ATXII, TeA	<i>Alternaria</i> spp., <i>A. alternata</i>	Cereal crops, vegetables, citrus fruits	Genotoxic, mutagenicity	87, 91
Trichothecenes (TH)	--	<i>Fusarium</i> spp., <i>F. langsethiae</i> , <i>F. sporotrichioides</i>	Cereal crops, oat	Problems in the hematologic and immune systems	92, 93

**Figure 3.** Reddish pigment bikaverin produced by mycotoxigenic fungi *Fusarium oxysporum*.

Under favorable conditions as elevated temperatures, torrential rain, high moisture, and poor hygienic practices, field and storage fungi<sup>94</sup> can be produced. The agriculture products, food, and other commodities might be contaminated in the field or during any step of the harvest, handling, transportation, or storage. Therefore, mycotoxin contamination poses a worldwide threat to the international trade, social development, and the human health itself. Plant-derived foods as vegetables, cereals, and fruits are liable to the growth of

mycotoxin-production fungi due to their nutritional components that are essential for these microorganisms.<sup>95–97</sup> As an example of the aforementioned posed risk, Azaiez *et al.*<sup>98</sup> reported that 160 samples from a total of 228 fruits purchased from the Tunisia and Spain markets were contaminated with mycotoxins, with incidence ratios of 83% for red dates, 80% for raisings, 64% for figs, 59% for apricots, and 26% for plums. And still of these, 51% of the samples were contaminated with more than one mycotoxin at the same time, achieving until six types for the same product.

Furthermore, Kosicki *et al.*<sup>99</sup> analyzed the content of deoxynivalenol (DON), nivalenol, T-2 and HT-2 toxins, zearalenone (ZEN), fumonisins (FMs), ochratoxin A (OTA), and aflatoxins (AFs) in 143 maize silage samples, 295 maize samples, 480 complete feed samples, and 466 small grain cereal samples. DON and ZEN showed the highest incidence ratios of 89% and 92% in corn, 86% and 88% in corn silage, and 97% and 98% in small grains samples. Their contents exceed the EU recommendation in 24 samples. Regarding to the completed feed samples, more than 90% of them were contaminated with ZEN, HT-2 and T-2 toxins. In other study,<sup>100</sup> 17 *Alternaria* free and modified mycotoxins were investigated in 56 tomato sauce, 39 sunflower seed oil, and 100 wheat flour samples. The most frequently-found mycotoxins were: alternariol monomethyl ether (AME: 1.2–6.6 ng g<sup>-1</sup>), alternariol (AOH: 0.5–1.3 ng g<sup>-1</sup>), tentoxin (66–161 ng g<sup>-1</sup>), and tenuazonic acid (0.1–0.5 ng g<sup>-1</sup>).

Concerning the mycotoxins in animal-origin foodstuff<sup>101</sup> as flesh, dairy products, milk and milk products, poultry, and eggs, the occurrence is also increasing due to the improper storage and the limited ability of animals to degrade mycotoxins after consuming feed and other contaminated food, which usually takes from 10 to 19 days to be completely eliminated from their organism.<sup>102</sup> Thus, the intake of animal tissues with mycotoxin residues for a long period exposes the consumer to potential chronic poisoning. Zadravec *et al.*<sup>103</sup> studied the incidence of mycotoxins in Croatian products of traditional dry-cured meat, finding out that the OTA contamination up to 6.86 mg kg<sup>-1</sup> was more frequently than the AFB1 up to 1.92 mg kg<sup>-1</sup>, achieving 14% against 8% of samples, respectively. Xu *et al.*<sup>104</sup> quantified the content of mycotoxins, pesticides, and veterinary drugs in eggs using a QuEChERS and magnetic multi-walled carbon nanotubes-based UPLC-MS/MS method. They found the incidence over 23% of the samples with three kinds of analytes. Aflatoxin B1 (AFB1) was detected in more than 10 egg samples with high contents of 83.1, 83.6, 142.0, and 144.9 mg kg<sup>-1</sup> in 4 samples. In another work,<sup>105</sup> residual amounts up to 0.039 mg kg<sup>-1</sup> of aflatoxin M1 (AFM1) were found in milk and skimmed milk samples. Finally, Cao *et al.*<sup>106</sup> analyzed multiple mycotoxins in human blood, urine, and edible animal tissues (as liver and muscle) from swine and chickens. They found out that 5 samples were contaminated with AFB1, and one swine liver sample was simultaneously contaminated with AFM1, AFB1, and AFB2. These findings by themselves indicate the serious danger of the humans' exposure to mycotoxins by the ingestion of animal-based foods.

Traditional oriental medicines are another class of products vulnerable to fungal contamination and consequent residues of aflatoxins (AFs), ochratoxins (OTs), zearalenone (ZEN), and fumonisins (FMs) mycotoxins.<sup>107–111</sup> Root herbs,<sup>112</sup> ginseng,<sup>112,113</sup> red yeast rice,<sup>114</sup> *Radix Paeoniae Alba*,<sup>115</sup> and edible medicinal foods as lotus seed, ginger, malt, and yam, show rich nutrient contents that provide ideal substrates for the growth and reproduction of various fungi from the planting to the storage processes, exhibiting increased chances of mycotoxin contamination which reduce the product quality and efficacy. For instance, lotus seed is frequently used as an edible medicinal food in pharmacy compounding and is even highly ingested in the table diet, showing high market value. But with the high rate of mycotoxin pollution, its ingestion is becoming a threat to human health.<sup>111</sup> For example, 30% of batches of lotus seed samples purchased from the China market showed AFB1, FB2, T-2, and ZEN contamination and, as a worse scenario, some samples were contaminated with more than 3 mycotoxins simultaneously.<sup>116</sup> Wei *et al.*<sup>109</sup> revealed a very concerning conjuncture too: one or more mycotoxins were detected in 26 commercially available lotus seed samples, with AFB1, AFB2, OTA, and CIT as the predominant toxins.

Chinese yam and malt are other kinds of food or traditional oriental medicine susceptible to mycotoxins contamination. An investigation<sup>117</sup> of 27 batches of yam, yam powder, and related products collected from several markets and pharmacies showed that one normal sample and four mold samples were contaminated

with different mycotoxins, achieving AFB1 concentrations that exceeded the maximum residue level in 2 mold samples. Bolechova *et al.*<sup>118</sup> analyzed 52 batches of barley and malt samples collected from the Czech Republic, and they found out that all of them were contaminated with one mycotoxin at least. Finally, Xiao *et al.*<sup>119</sup> reported that 2 out of 16 malt samples obtained were contaminated with OTA. Other edible and medicinal foods exposed to the mycotoxin contamination are the Hibiscus sabdariffa,<sup>108</sup> Areca catechu<sup>120</sup> and locusts.<sup>121</sup> It is important to mention that some mycotoxins as the aflatoxins (AFs) can transfer from the raw types of *Hordei Fructus Germinatus*, *Lilii Bulbus*, *Bombyx Batryticatus*, and *Nelumbinis Semen* to their decoctions,<sup>122</sup> posing serious risk over the customers that ingest the decoctions prepared from these edible medicinal foods contaminated with AFs. So, one should be aware of the heavy exposition to mycotoxins from the consumption of traditional oriental medicines, generally considered as “more natural” or even “healthier” by the consumers.

Lastly, even infants and young children might be exposed to mycotoxins contamination, especially those who consume domestic and industrially processed complementary foods. Ojuri *et al.*<sup>123</sup> studied the exposure of children to AFs at Nigeria and concluded that those under 12 months of age were less exposed than kids from 12 to 24 months. Furthermore, about 69% and 75% of infants and young children which consumed household grains and “Tom Bran” (a cereal-legume weaning food) were co-exposed to mycotoxins with commensurate risks and, 47% of them were co-exposed to until four types of mycotoxins: aflatoxins (AFs), citrinin (CIT), fumonisins (FMs), and ochratoxins (OTA).

Considering the above, it is predictable the urgency to develop quick and sensitive analytical methodologies for the simultaneous high-throughput detection and quantification of multiple mycotoxins in food, agricultural products, and pharmaceuticals to guarantee the quality and safety of such products. Several immunosensors have been reported exploiting the broad application in mycotoxin determinations, since worldwide scenario with global warming and climate changes seems to harden the food safety control regarding to mycotoxin contamination, mainly, due to the acclimatization of mycotoxigenic fungi to the new environmental conditions, potentially becoming even more aggressive pathogens.<sup>124,125</sup>

## TYPES OF BIOSENSORS AND THEIR BIORECEPTORS

According to the gold book of the International Union of Pure and Applied Chemistry (IUPAC)<sup>126</sup> and its recommendations in the glossary for chemists of terms used in biotechnology<sup>127</sup> from 1992, a biosensor is “a device that uses specific biochemical reactions mediated by isolated enzymes, immunosystems, tissues, organelles or whole cells to detect chemical compounds usually by electrical, thermal or optical signals.”. According to more recent IUPAC<sup>128</sup> recommendations from 1999, a biosensor is an independently integrated receptor transducer device that is capable of providing selective quantitative or semiquantitative analytical information using a biological recognition element. Considering that two-to-three decades have passed since these IUPAC definitions, the concept of biosensor have expanded and some new alternative approaches have been proposed, incorporating novel sensing principles and different recognition elements, such as e.g. the aptamers,<sup>129</sup> and the molecularly imprinted polymers.<sup>130</sup> Therefore, ultimately, a “biosensor” is short for “biological sensor” and is defined as a compact analytical device incorporating a biological or biologically-derived sensing element that might be either integrated within or intimately associated with a physicochemical transducer.<sup>131</sup>

There are two fundamental operating principles of a biosensor: the “biological recognition” and the “real sensing”. So, generally, biosensors can be divided in three basic components connected in series: (i) a biological recognition system, usually called “bioreceptor”; (ii) a transducer and; (iii) the microelectronics. The basic functioning principle of a biosensor is to detect the molecular recognition step and to convert it into another type of signal using a transducer. The recognition system provides a degree of selectivity to the sensor for the target analyte, meanwhile the interaction between the analyte with the bioreceptor should produce a measurable response effect on the transducer, transforming the biological information into a measurable electrical or optical signal.<sup>131</sup> Its purpose is to provide fast, real-time, accurate, precise, and reliable information about the target analyte. Ideally (but rarely fully achieved), it should be a device

capable of responding continuously, reversibly, and shall barely perturb the sample, finding applications in several fields like medicine, agriculture, and food safety.<sup>132</sup>

As stated, biosensors<sup>133,134</sup> show a biological component that act as the real sensor, and the electronic component to detect and transmit the generated signal. So, the biological material is immobilized in direct contact with the transducer. The analyte shall interact with this biological material to form a bounded analyte that is responsible for the electronic response that is measured. In some cases, the analyte is converted into a product that might be associated with the release of heat, gases, electrons or hydrogen ions. The role of the transducer is to transform the product-linked changes into electrical signal, which can be amplified and measured. This relations lead to some proper classification of biosensors as: an affinity sensor (binding of analyte and the recognition bioelement), a metabolic sensor (analyte leads to chemical changes used to the analytical measurements), and a catalytic sensor (biological element combines with the analyte forming an auxiliary substrate).<sup>135</sup> Further biosensor classifications are regarded to the type of bioreceptor and transducer used. Figure 4 shows examples of typical bioreceptors currently used for the assembling of biosensors.

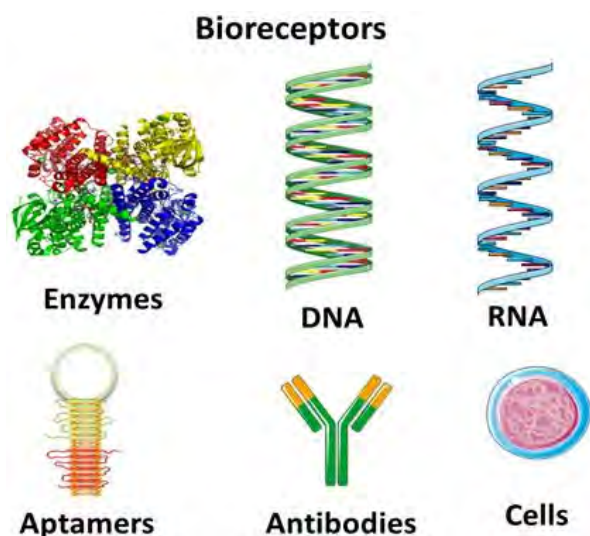


**Figure 4.** Bioreceptors currently used for the assembling of biosensors.

As above mentioned, bioreceptors<sup>136</sup> are the recognition key elements that confer some specificity to the bioelectronic device, featuring as a significant distinguishing characteristic of a biosensor. In terms of constitution, a bioreceptor is a molecular species that uses a biochemical mechanism for recognition, being responsible for the binding of the analyte on the surface of the sensor for the measurement. The types of molecular recognition can be classified as static or dynamic molecular recognitions.<sup>137</sup> The static molecular recognition is usually compared in analogy to a “lock and key” mechanism with a 1:1 complexation between a host molecule and a guest molecule to form the host-guest complex. To achieve advanced status of recognition by the static model, the recognition sites should be highly specific for the guest molecules. In the dynamic molecular recognition, there are two guests and two binding sites and the binding of the first guest to the first site affects the association constant of the second guest with the second binding site, consolidating an allosteric control system. For positive allosteric systems, the binding of the first guest increases the association constant of the second guest, while for the negative allosteric system, the binding of the first guest decreases the association constant of the second guest. Dynamic molecular recognition is particularly important since it provides a clear mechanism to regulate the binding in complex biological systems, and is currently being studied for applications in high functional chemical sensors using bioreceptors and further



molecular devices. Regarding to the classification of bioreceptors, they can be generally subdivided in five major categories: enzyme, antibody/antigen, nucleic acid/DNA, cellular structure/cell, and biomimetic. The sampling component contains a so-called biosensitive layer, comprising bioreceptors or is even made by the covalent attaching of bioreceptors to the transducer. The most common bioreceptors used in the literature are the enzymes and antibodies.<sup>131</sup>

Enzymes are commonly used as bioreceptors<sup>138,139</sup> due to their specific binding capabilities and catalytic activity, coining the term “biosensor” for such sensors. When the detection in a biosensor is amplified by a catalytic reaction, the recognition is classified as a biocatalytic mechanism.<sup>140</sup> Despite of a small group of catalytic ribonucleic acids, all the enzymes are proteins (Figure 4) and some of them even do not require further chemical groups than their own amino acid residues to exert their catalytic activity. Some others require a cofactor as Fe(II), Mn(II) or Zn(II) inorganic ions or even more complex organic or organometallic coenzymes. The catalytic activity of enzymes leads to high sensitivities and lower limits of detection (LODs) than reference binding techniques, depending only on the integrity of their native protein conformation.<sup>131</sup> When enzymes are denatured or dissociated into their subunits, their catalytic activity is inhibited. So, enzyme-coupled receptors<sup>141</sup> can be used to modify the recognition mechanism by the modulation of the enzyme activity by the binding of a ligand, enhancing the enzymatic activity by an enzyme cascade with complex reactions. Enzymes are usually the primary choice for biosensors by most authors since they are natural proteins with high specificity to the substrate, which is catalytically converted into a product, *i.e.*, without the enzyme consumption during the reaction. Their mechanism of operation might involve (*i*) the conversion of the analyte into a detectable product, (*ii*) the detection of an analyte that acts as an enzyme inhibitor or activator, or even (*iii*) the monitoring of the enzyme properties upon interaction with the analyte.<sup>131</sup>

Antibodies<sup>142</sup> can be used as bioreceptors to detect specific antigens, consolidating the so-called immunosensors. Immunoassay embraces the most specific analytical methodologies with extremely low LODs and is applicable to a wide range of analytes, especially for the identification and quantification of proteins.<sup>131</sup> The term immunoassay is used for tests based on immunoreactions, while the term “immunosensor” is specifically applied to describe the whole instrument as short of “immunoreactions-based biosensors”. Antibodies are heavy plasma proteins with about 150 kDa. Also called glycoproteins, they show two heavy chains and two light chains forming the traditional Y shape (Figure 4). They are produced by animals as an immunological response to antigens foreign agents. The antibody binds the antigen with high affinity, allowing analytical methods to detect the target analyte even in the presence of interfering substances of the sample matrix. There are two types of antibodies applied in immunosensors: the polyclonal, highly sensitive but less specific due to the possibility of recognition of different epitopes (antigen binding sites) on their target antigen and; the monoclonal that are produced from one type of immune cells and are bounded to the same epitope of their specific antigen without cross-reactions, making their immunoassays highly specific.<sup>143</sup> Monoclonal antibodies are excellent to be used as the primary antibody in immunoassays or for the detection of specific antigens in the presence of interfering molecules, being considerably less susceptible to background staining than polyclonal antibodies.<sup>131</sup>

The hybridization of DNA or RNA (Figure 4) can be used as another biorecognition mechanism with highly specific affinity from the binding reaction between two single-stranded DNA (ssDNA) chains to form a double-stranded DNA (dsDNA), the so-called nucleic acids-based biosensors.<sup>144,145</sup> DNA biosensors or genosensors<sup>146</sup> detect the individual nucleotides that comprise the specific DNA genome molecule with rapid and non-destructive sequencing of DNA molecules. The biological recognition agent is the ssDNA with specific oligonucleotides that is commonly called the DNA probe and is combined with a transducer. Among the different types of genosensors figures the optical, the piezoelectric, and the electrochemical, the last one with great advantages of simplicity, rapidness, low cost, high sensitivity, and prone to the development of inexpensive portable devices.<sup>131</sup> Electrochemical genosensors usually monitors the sequence-specific hybridization events measuring the oxidation signal of DNA electroactive nucleotide bases, detecting the DNA electroactive indicators forming complexes with DNA nitrogenous bases or enzyme-labeling oligonucleotides. The electrochemical impedance spectroscopy (EIS) is a very important electrochemical technique for the



study of DNA hybridization, being an effective method for probing interfacial properties as the capacitance or the electron-transfer resistance of DNA-modified electrodes, sparing the use of oligonucleotide labeling for the DNA detection.<sup>147–149</sup>

A typical genosensor configuration uses the ssDNA probe sequence immobilized within the biosensor recognition layer, place where base-pairing interactions recruit the target DNA to the surface.<sup>131</sup> The repetitive and uniform structure of DNA makes a well-defined assembly on the recognition surface, where the critical dynamics of target capture happens to generate the recognition signal. So, it is crucial for the device performance to immobilize the nucleic acid probe sequences in a predictable manner while keeping their inherent affinity for the target DNA. The recognition event depends mainly on the method used for the signal transduction. In the electrochemical DNA biosensor,<sup>150,151</sup> the three main events of detection mechanism are (i) the formation of the DNA recognition layer, (ii) the actual hybridization event, and (iii) the conversion of the hybridization event into an electrical signal, which happens basically by label-free or labeled immunoassays. For the label-free detection,<sup>152</sup> the decrease or increase of the oxidation or reduction peak current of electroactive DNA bases (e.g. guanine or adenine) is directly monitored. This detection pathway relies on the intrinsic DNA signal with guanine and adenine being the most electroactive bases of DNA due to their easy adsorption and oxidation on carbon-based electrodes. The electrochemical signal from free adenine and guanine usually decreases with their binding with thymine and cytosine after hybridization. In the labeled detection,<sup>153</sup> the alteration of the oxidation or reduction peak current is monitored for the electrochemical label that selectively binds with the dsDNA/SSDNA. There are two types of label-based electrochemical detection of DNA hybridization: the intercalative redox active probe, which basically the hybrid modified electrode is immersed in a solution with the redox-active molecule and the DNA binding molecule and; the redox-active probe, which is constituted of a capture probe, the target, and a signaling probe. The signaling probe is tagged with e.g. ferrocene, enzyme or metal nanoparticle and serves to label the target upon hybridization. The flow of electrons to the electrode only happens when the target is present and the specific hybridization of both signaling and capture probes is achieved.<sup>131</sup> This principle has been used in a DNA chip technology<sup>154</sup> called *eSensor™* developed by the Motorola Life Science Inc.

Aptamers<sup>156</sup> can be used as the recognition element in the so-called aptasensors.<sup>157,158</sup> Aptamers are single-stranded RNA or DNA molecules that bind to their target molecules (usually proteins) with high affinity and specificity (Figure 4). They are more stable and adapted to the real sample conditions, rivaling the antibodies in an interesting number of applications. Aptamers are very small in size (from 30 to 100 nucleotides) once compared to other biorecognition molecules as antibodies or enzymes. This characteristic allows an efficient immobilization process with high aptamers density and easier production, miniaturization, integration, and biosensor automation than with antibodies. After the selection, aptamers can be synthesized with high purity and reproducibility.<sup>131</sup> They are classified as DNA, RNA, or peptide aptamers. DNA aptamers<sup>159</sup> are chemically stable and allow the reusability of biosensors,<sup>160</sup> while the RNA aptamers<sup>161</sup> are susceptible to degradation by endogenous ribonucleases found in cell lysates and serum, being able to be used for only single-shot measurements in biological matrices.<sup>162</sup> Furthermore, DNA and RNA can be chemically modified to undergo analyte-dependent conformational changes. Possible aptamers detection modes include the label-free methods as e.g. the surface plasmon resonance (SPR) and the quartz crystal microbalance (QCM), and labeled methods as the electrochemical, fluorescence, chemiluminescence, and field effect transistor ones.<sup>131</sup> Aptamers are typically isolated from combinatorial libraries by an *in vitro* process of evolution called systematic evolution of ligands by exponential enrichment, or simply SELEX. SELEX process<sup>163,164</sup> is used for the election of aptamers with high specificity in binding and function due to their nucleotide sequence and shape. SELEX stages involve: (i) the library generation containing 1 x 10<sup>9</sup> single-stranded oligonucleotides with random sequence region flanked by the binding site; (ii) the binding and separation by the incubation of the library with the immobilized target molecule, the consequent filtering of unbound nucleic acids from the solution, and the elution of the bound nucleic acids from the target and; (iii) the amplification, which the bound nucleic acids are copied using the polymerase chain reaction (PCR) to create a new library and, this new library will be further used in a new round of SELEX to optimize the

quality of aptamers, proceeding until the identification of the highest binding species through competitive binding methodologies.<sup>165</sup>

Aptasensors can be classified according to the transduction mechanism. Electrochemical aptasensors<sup>166</sup> use an electrode surface as a platform to immobilize the sensing aptamer and the analyte-binding event is monitored based on current (or potential) variations using the faradaic impedance spectroscopy (FIS), differential pulse voltammetry, alternating current voltammetry, square-wave voltammetry, potentiometry, or amperometry.<sup>166</sup> The receptor-target interaction can lead to an increase or decrease of the detector response, consolidating a positive or a negative readout signal, respectively. Optical aptasensors<sup>167,168</sup> use label-based aptamers with fluorophores, luminophores, enzymes or nanoparticles, or label-free detection systems as the surface plasmon resonance (SPR). Considering the possible analytical formats, fluorescence and colorimetry are the most relevant techniques, while the SPR rely on changes generated in the optical parameters of the layer closest to the sensitive surface.<sup>169</sup> Finally, mass sensitive aptasensors are devices that measure any property that scales proportionally with the mass associated with the sensitive surface that is assembled with capture probes. They are considered label-free bioassays using SPR, QCM or surface acoustic wave for analytical measurements.<sup>157</sup>

Microbial biosensors<sup>170,171</sup> are analytical devices that immobilize living microorganisms (Figure 4) onto a transducer for the detection of target analytes. Bacteria and fungi are usually used to detect specific molecules or simply to sense the overall state of the surrounding environment. Analytical response comes from the specific interaction between enzymes or proteins (the “real” bioreceptors) contained in the immobilized living cells, avoiding the expensive and time-consuming process of purification.<sup>172</sup> The microorganisms of microbial biosensors can be integrated to several transducers as amperometric, potentiometric, calorimetric, conductometric, luminometric, and fluorimetric ones. The measurement principle is based on the metabolism of the microorganism that is usually accompanied by the oxygen or carbon dioxide consumption.<sup>173</sup> The integration of the microorganism to the transducer is pivotal to achieve a reliable and reusable microbial biosensor. During its functioning, the analyte enters the cell and is converted using the intracellular enzymes, consuming cosubstrates and generating products that can be readily detected using e.g. electrochemical sensors. The monitoring of dissolved oxygen concentrations, medium ionic composition, and other parameters in the layer of immobilized cells can be used as metabolic indicators of the cell state, and act as the background for the electrochemical determination of the biologically electroactive compounds of interest.<sup>131</sup>

## CONVENTIONAL TRANSDUCERS FOR BIOSENSORS

The transducer is the component of the biosensor with the noble role of converting the biorecognition event into a detectable analytical signal, which can be of electrochemical (potentiometry, conductometry, impedimetry, amperometry or voltammetry), optical (colorimetric, fluorescence, luminescence, interferometry), calorimetric (thermistor), mass change (piezoelectric or acoustic wave) or magnetic nature.<sup>131</sup>

Optical biosensors<sup>174,175</sup> are powerful analysis tools that induce a change in the phase, amplitude, polarization or frequency of an input light in response to the physical or chemical change produced by the biorecognition process. As the main advantages are the specificity, remote sensing, isolation from electromagnetic interferences, quick processing, real-time measurements, multiple channels and multi parameters detection, compact design, minimally invasive for *in vivo* measurements, possibility of choice of optical components for biocompatibility, and the detailed information obtained from the analytes. The instrumentation components are the light source, the optical transmission medium (as fibers and waveguides), the immobilized biological recognition elements, and the optical detection system. Optical biosensors can be generally classified on diverse parameters with two possible detection protocols: the fluorescence-based detection and the label-free detection.<sup>131</sup>

In the fluorescence-based detection,<sup>176,177</sup> either the target molecules or the biorecognition molecules are labeled with fluorescence tags as dyes, and the intensity of fluorescence indicates both the presence of the target molecules and the strength of interaction between the target and the biorecognition molecules. For instance, nucleic acids or antibodies can be used to tag with a fluorochrome and convert the hybridization

interaction between two complementary DNA strands into an optical signal.<sup>178</sup> Label-free modes use non-labelled target molecules that are detected in their natural form without molecular modifications, which is a more rare option considering that most of the biological-sensing elements and target analytes do not possess intrinsic spectral properties. Whole cells can be used in fluorescent biosensors too by immobilizing them on the surface of a bioactive sensor layer that is usually placed in front of the tip of an optical fiber bundle to generate the fluorescent signal. Optical fibers are required to direct the excitation radiation on the fluorescent bioelement and convey the fluorescence radiation up to the fluorimeter. Optical translucent supports are important to improve the simplicity and reliability of fluorescent-based biosensors, enabling the fluorescent detection emitted by algal cells.<sup>131</sup>

A common fluorescence protocol used for the biosensing is the sandwich-type assay,<sup>179,180</sup> which the analyte is selectively bound to a surface by a targeting molecule (as antibodies) that are covalently immobilized on the surface of a well or other cell. The analyte molecule is labelled with a fluorescent tag and its surface concentration may be measured by highly sensitive fluorescence spectroscopy. Several green fluorescent proteins have been extensively used for the assembling of fluorescent protein-based biosensors, or simply FP-based biosensors.<sup>181</sup> In such biosensors, the sensing element consists of one or more polypeptide chains that act as the molecular recognition element by suffering conformational changes upon the binding with the analyte that changes the fluorescence pattern. FP-based biosensors can be further classified into three types of assay considering their structure: the Förster or fluorescent resonance energy transfer (FRET)-based biosensors,<sup>182</sup> the bimolecular fluorescence complementation (BiFC)-based biosensors and, the single FP-based biosensors.<sup>131</sup>

FRET<sup>183</sup> is the phenomenon of nonradiative energy transfer between an excited blue-shifted fluorescent chromophore (the donor, in a higher energy state) and a chromophore with a red-shifted absorption spectrum (the acceptor) through a dipole-dipole coupling. More importantly, the efficiency of the energy transfer is determined by the distance and orientation between the donor and the acceptor proteins, and the recording of fluorescence emission spectrum can be used to determine the proximity of the two chromophores. In the FRET-based biosensors,<sup>182</sup> two fluorescent proteins are genetically linked either to each end of a polypeptide chain (the molecular recognition element: MRE) or two separate polypeptides, MRE and the analyte protein. Upon interaction with the analyte, conformation of the protein changes and so the distance between the two chromophores, changing the fluorescence intensities of both donor and acceptor that is measured by the FRET efficiency. Increased FRET efficiency indicates that the two FPs are aligned together, while the decreased FRET efficiency indicates that both are separated. These FRET-based biosensors are widely applied to detect a range of molecular events as protein binding interactions, protein conformational changes, enzyme activities, and the concentration of biomolecules. The (BiFC)-based biosensors<sup>184</sup> are used to visualize the protein-protein interaction in live cells. Here, the FP and MRE are splitted up and the MRE is linked to one portion and the analyte protein is linked to the other portion. When both proteins interact, the two fragments are fused together, refolding properly into the 3D-structure that produces a typical fluorescence signal. In the FP-based biosensors, the MRE can be either exogenous or endogenous and the analyte binding to the MRE causes conformational changes of the fluorescent protein and, consequently, alters its fluorescent properties.<sup>131</sup> Fluorescence is an extremely sensitive technique with LODs down to a single-molecule detection,<sup>185</sup> besides the fact that it is relatively easy and cheap to perform and allows quantitative and kinetic measurements of molecular interactions. On the other hand, major drawbacks reside in the additional complexity of time-resolved instrumentation in time, frequency domains or in both, and is not suitable for the real-time monitoring.

The optical label-free protocols<sup>186</sup> for biosensing usually use the surface plasmon resonance (SPR)<sup>187</sup> to observe the binding interactions between an injected analyte and an immobilized biomolecule in real time. For the conventional SPR measurements, a thin metallic film is coated on one side of a prism to separate the sensing medium from the optical disperser element. The SPR effect is sensitive to the binding of the analyte due to the mass increase that causes a proportional increase in the interface refractive index, which is experimentally observed by the shift in the resonance angle. SPR biosensors use the surface plasmon

electromagnetic waves to detect the changes from the target analyte interaction with the biorecognition element on the sensor. Therefore, when a target analyte interacts with the immobilized biomolecule on the sensor surface, it produces changes in the refractive index and these changes produces a variation in the propagation constant of the surface plasmon wave, and so this variation is measured to produce the analytical reading. A spectrometer is usually used to measure the absorption spectrum of the sample in real-time monitoring without radioactivity and fluorescence. Several biorecognition elements have been incorporated with SPR biosensors such as proteins, antibodies-antigens, nucleic acids, and enzymes.<sup>188,189</sup> Advantages of SPR biosensors are the high detection sensitivity, the real-time detection, the anti-interference capability, the absence of samples pretreatment, rapidness, and the high throughput of analysis with less reagents and samples. Biological applications include the measurement of adsorption and desorption kinetics, antigen-antibody binding, and the epitope mapping for the determination of biomolecular structures and interactions of proteins, DNA, and viruses.<sup>131</sup>

Luminescence<sup>190,191</sup> is the emission of light from an electronically excited state returning to the ground state in a compound. Chemiluminescence<sup>192</sup> occurs during the course of some chemical reactions when an electronically-excited state is generated. As the rate of photons production can be monitored, the produced light intensity depends on the rate of the luminescent reaction and is directly proportional to the concentration of the limiting reactant involved. Considering the modern detection instrumentation,<sup>193</sup> the light intensity can be measured at very low levels, allowing the development of sensitive analytical methods with the aid of optical fibers and photomultiplier tubes (PMTs). In the chemiluminescent biosensor,<sup>194,195</sup> the reaction between the analyte and the immobilized biomolecule that has been marked with a chemiluminescence species will generate light as a result of a biochemical reaction. It is an emerging tool for the diagnosis with extremely high sensitivity along with the simple instrumentation of devices, fast dynamic response, and wide calibration range. Chemiluminescent-based transducers have been widely applied for biosensing of nucleic acid hybridization,<sup>196</sup> with LODs as lower as  $10^{-13}$  mol L<sup>-1</sup> magnitude order, and is gradually substituting the fluorescence for the development of biochips and microarrays. Nevertheless, chemiluminescence transduction shows as the main drawbacks the lower accuracy according to the short lifetime, the non-suitability for real-time monitoring, and is still considered an expensive method.<sup>131</sup>

The piezoelectric biosensor<sup>197</sup> is a class of microelectrochemical system based on the changes in the resonance frequency of an oscillating crystal due to the interaction between the bioreceptor and the analyte. The transducer is made of a piezoelectric material as quartz with the surface coated with the biosensing material, which vibrates on a certain frequency that can be modulated by the circumstances in the surrounding environment.<sup>198</sup> Once coated with the biosensing material, the actual frequency depends on the mass of the crystal and the coating. The resonant frequency can be easily measured with accuracy, making it possible to calculate the mass of analyte adsorbed on the crystal surface. Piezoelectric methods are sensitive and can use antibodies, enzymes, and antigens as biological elements to achieve LODs down to the picogram levels. There are two main types of piezoelectric sensors: the bulk acoustic wave piezoelectric sensors (BAW) and the surface acoustic wave piezoelectric sensors (SAW).<sup>131</sup>

As explained, piezoelectric acoustic wave sensors apply an oscillating electric field to create a mechanical wave that propagates through the substrate and is then transformed back into an electric field for the measurement. The bulk wave happens when the wave propagates through the substrate, and devices operate in thickness shear mode resonator (TSM)<sup>199</sup> or the shear-horizontal acoustic plate mode (SH-APM).<sup>200</sup> TSM is commonly widely referred to as the quartz crystal microbalance (QCM), and is considered as the best-known and simplest acoustic wave device.<sup>201</sup> The BAW simplest configuration<sup>202</sup> uses a quartz material sandwiched between two metallic electrodes. The natural oscillating frequency of the material and the coating deposit thickness are used as design parameters to obtain the desired operating frequencies. However, if the wave propagates on the surface of the substrate, it is known as a surface acoustic wave (SAW). SAW sensors<sup>202</sup> are made of a thick plate of a piezoelectric material, that is usually quartz, to sense the so-called Rayleigh waves that propagate along the upper surface of crystals. The most common SAW devices are the SAW sensor<sup>203</sup> and the shear-horizontal surface acoustic wave (SH-SAW) sensor,<sup>204</sup>



also known as the surface transverse wave (STW) sensor. SAW-based sensors are built on single crystal piezoelectric materials and, according to the different cut angles, it can produce largely different results. That is why the design of the sensor needs to be adapted for each application by selecting the appropriate design alternative.<sup>131</sup>

The piezoelectric transducer has been used for the DNA and protein detection with LODs as low as  $1 \text{ ng cm}^{-2}$ .<sup>205</sup> Its applications embrace the diagnostic detection of cholera toxin,<sup>206</sup> hepatitis B,<sup>206</sup> hepatitis C,<sup>207</sup> and foodborne pathogen detection,<sup>208</sup> achieving a LOD of  $8.6 \text{ pg L}^{-1}$  for the DNA of hepatitis B virus, and  $25 \text{ ng mL}^{-1}$  for cholera toxin detection.<sup>206</sup> As its main advantages we can point it out the low production cost, high sensitivity, small size and portability, fast response, robustness, high accuracy, and compatibility with integrated circuit technologies.<sup>131</sup>

Magnetoelastic biosensors<sup>209,210</sup> work similarly to the quartz crystal microbalance (QCM) except for the magnetoelasticity principle instead of piezoelectricity. A magnetoelastic material changes its dimensions once exposed to a magnetic field, so a thin strip of such kind of material forms the resonator with the shape of a tuning fork. When the strip with the coated biomolecules film is exposed to a short magnetic pulse, it starts to oscillate emitting a magnetic field in return. The frequency, amplitude, and damping of this emitted magnetic field supply the information about the sensor status and the coating surrounding it. As an application, magnetoelastic biosensors have been used for the monitoring of blood coagulation.<sup>211</sup> The ribbon magnetoelastic sensor oscillates at a fundamental frequency and shifts it linearly in response to an applied mass load of changing elasticity. The sensor emit the magnetic flux that is detected by a remotely located pickup coil without any physical direct connection. During the blood coagulation, its viscosity changes due to the formation of a soft fibrin clot, shifting the characteristic resonance frequency of the magnetoelastic sensor, and enabling the real-time continuous monitoring of this biological event. The signal output might be monitored as a function of time and distinct blood clotting profiles can be found and compared. Advantages of magnetoelastic biosensor are the wireless detection with antenna-to-sensor range of a few decimeters in air and a few centimeters in liquids, the non-invasive and passive sensor without the need of batteries or other power supply sources, and the low sensor cost since it is made from cheap materials and is well suited for disposable sensors applications.<sup>131</sup>

Field effect transistor-based biosensors (or FET-based biosensors),<sup>212,213</sup> as the name suggests, are based on one of the most commonly used semiconductor devices of electronics. All FETs show three terminals called the source (S), the drain (D), and the gate (G). There is no physical contact between the source and the drain, but it does exist a current path that is called the conduction channel S-D. The gate-to-source voltage ( $V_{gs}$ ) will turn on or off the device considering that FET-type devices can work as switches. The strength of the generated electric field serves as a control mechanism that is associated with the voltage applied to the gate. For a *n*-type FET, the applied gate voltage will cause electrons to pass through the S-D channel. If a positive voltage is applied to the gate of an *n*-type FET, a channel is created and the charge effect on the conductance across the channel increases accordingly. However, if a negative gate voltage is applied, the *n*-type channel will pinch off. For a *p*-type FET, quite the opposite is observed as the positive (negative) gate voltage will turn off (on) the transistor device. Therefore, a FET uses an electric field to control the conduction channel and its charge-carriers. The flow of charge-carriers between the source and the drain can be tuned by modifying the size and the shape of the conducting channel by the application of an electric field to the gate. In analogy, the FET-based biosensor have been developed to study biomolecular interactions that are the key drivers of biological responses for *in vitro* or *in vivo* systems. FET-type biosensor is one of the most appealing electrical biosensors considering its sensitive measurements, portable instrumentation, easy operation with small sample consumption, low-cost under mass production, and high analytical speed.<sup>131</sup>

The biosensor configuration<sup>212,213</sup> consists of a nanowire channel between the source and the drain terminals. The surface of this nanowire is biofunctionalized so that the biorecognition binding can create an electric field, similar to the electric field control of conventional FETs by the gate. Then, the FET sensor is connected to an electronic circuit so as the specific conductance of the sensor surface can be monitored. The configuration of FET-type biosensors includes all the three usual terminals of FET (gate, source and



drain), with the gate being generally replaced by a biofilm layer material with a receptor enzyme, antibody, DNA or other type of biorecognition molecule. The analyte interaction with this biorecognition molecules in the biomodified gate modulates the channel conductivity, leading to changes in the drain current that brings the desired quantitative analytical information. As an example of application, ion-selective field effect transistors (ISFET)<sup>214</sup> have been applied to selectively measure the ion activity in electrolytes, since they act as conventional ion-selective electrodes with low output impedance. The association of the ISFET with a membrane modified with biorecognition materials (as enzymes or microbes) allows the measurement of organic compounds activity with very high specificity.<sup>215</sup>

Calorimetric biosensors<sup>216</sup> measure the changes in temperature during the reaction between the biorecognition element and the suitable analyte. These changes in the temperature can be correlated to the amount of reactants consumed or the products formed. The heat change is measured by the device using either a thermistor of metal oxides or a thermopile of ceramic semiconductors. The major advantages<sup>131</sup> of thermal detection are the stability, increased sensitivity, and miniaturization possibility. These methodologies are classified as label-free assays and are used for the screening of biomolecules interactions. Calorimetry can rapidly detect e.g. the DNA hybridization, and is currently being used in food industry.<sup>217</sup>

## ELECTROCHEMICAL BIOSENSORS

Electrochemical detection is the main transducing method used in biosensors due to the low cost, ease of use, portability, and simplicity of device construction.<sup>218,219</sup> The electrochemical reaction that is being monitored usually generates a measurable current (amperometry), charge accumulation or potential (potentiometry), or even alters the conductive properties of an electrolyte between two measuring electrodes in a conductivity cell (conductometry).<sup>220</sup> Electrochemical impedance spectroscopy (EIS) is another transducing alternative for biosensors, measuring both resistance and reactance of bioelectrodes.<sup>220</sup> As a surface technique, electrochemical detection offers advantages for the biosensing as the independence from reaction volume, the use of very small sample volumes,<sup>221</sup> and the high sensitivity that allows achieving very low LODs with little or none sample preparation.<sup>222,223</sup> Besides, electrochemical measurements are not affected by sample components as chromophores, fluorophores, and can be accomplished in turbid samples as, e.g., whole blood, without interference from fat globules, red blood cells, hemoglobin, and bilirubin.<sup>224,225</sup>

Voltammetric techniques are characterized by the application of a potential to a working electrode (WE) by an auxiliary electrode (AE) and the measurement of the generated current.<sup>226</sup> The potential applied on the WE is referenced against the reference electrode (RE). The current is a result of the electrolysis observed in the whole electrochemical cell by means of a reduction (cathodic current) or oxidation (anodic current) of the analyte on the surface of the WE. The current is controlled by the kinetics of the electrochemical reaction that might be ruled, e.g., by the mass transport rate of the analyte from the bulk of the solution to the electrode surface, once the system might be considered electrochemically reversible and a high enough potential is applied.<sup>226</sup> The term voltammetry is usually regarded to those techniques which the potential is scanned over a set potential range, forming a peak or plateau as the expected analytical response. Voltammetric methods include the linear sweep voltammetry, cyclic voltammetry, hydrodynamic voltammetry, differential pulse voltammetry, square-wave voltammetry, AC voltammetry, polarography, and stripping voltammetry.<sup>226</sup>

In amperometry the generated current is monitored in function of time while a constant potential is sustained at the WE against the RE.<sup>227</sup> The absence of a scanning potential is what distinguishes the amperometry from the voltammetry. The technique is applied by stepping the potential directly to the desired value and then measuring the consequent current or, in flow injection analysis (FIA), by passing samples across the biased WE. The measured current is usually directly proportional to the concentration of the electroactive species present in the sample. Some authors sustain that amperometric biosensors have additional selectivity since the potential used for the detection is characteristic of the oxidation or reduction of the analyte species.<sup>218</sup> The amperometric detection is usually used with biocatalytic or affinity assays due to its simplicity and low LODs achieved.<sup>228</sup> Advantageously, the fixed potential during the whole experiment allows the stabilization of the background current, decreasing the capacitive component on it. Furthermore, amperometry permits

the use of the hydrodynamic condition that enhances significantly the mass transport of the analyte to the electrode surface<sup>226,229</sup> by the WE rotating or vibrating in relation to the solution,<sup>230,231</sup> or during the flow analysis when the sample solution is pumped and passes over the stationary electrode.<sup>229,232,233</sup>

Electrochemical sensors are part of electrochemical cells that consist of three electrodes: the working electrode (WE) of a chemically stable solid conductive materials as platinum, gold, or carbon materials; the reference electrode (RE), with a stable and known potential usually consisting of silver metal coated with a layer of silver chloride (Ag/AgCl) immersed in a separated compartment with a porous junction containing saturated KCl (3.5 mol L<sup>-1</sup>); and a platinum auxiliary electrode (AE) to apply the potential. This three-electrode system is mainly interesting due to the fact that the potential is applied by the AE instead of the RE, protecting the RE from changing its potential. The two-electrode systems with the WE and the RE are only used if the current-density is low enough ( $< \mu\text{A cm}^{-2}$ ) for the RE to carry the charge without no adverse biasing effect.<sup>227</sup> It is usually preferred for disposable sensors considering that the long-term stability of RE is not necessary, and the project shows lower costs. These three electrodes are easily miniaturized with new dimensions on the order of  $\mu\text{m}$  or smaller,<sup>234-236</sup> exhibiting higher sensitivities<sup>220</sup> and requiring lower sample volumes of  $\mu\text{L}$  or less.<sup>237,238</sup> Also, electrochemical detectors and their controlling instrumentation are easily miniaturized with relatively low cost by micromachining, manufacturing field-portable instruments for biosensing purposes. Considering that working currents are temperature-dependent in voltammetry, the detection cell shall be maintained in a constant temperature for running the calibration with standards and the sample, so as accurate and precise results can be obtained.<sup>239</sup>

Screen-printed (SPEs) minielectrode systems with WE, RE, and AE have become popular in electrochemical biosensors for their low cost, ease fabrication, and fast mass production using thick films technology.<sup>221</sup> SPEs are produced by printing different inks on various types of plastic or ceramic substrates. As an example, polyester screens are generally used for printing with patterns designed by the analyst according to the analytical purpose. The composition of several inks used for printing the electrodes determines the selectivity and the sensitivity required for each analysis.<sup>131</sup> SPE can even be miniaturized for microfluidic systems and portable meters. The typical patterned WE is made of conductive carbon ink with rough surface and uncertain surface area.<sup>240</sup> As an application example, disposable SPEs have been widely used in biosensors to measure the blood glucose content.<sup>241</sup>

Interdigitated array (IDA) electrodes are good amperometric transducers for biosensors. They are made of two pairs of WEs made of parallel strips of metal fingers that are interdigitated and separated by an insulating material.<sup>242,243</sup> One electrode array is used as the anode and the other as the cathode. The main advantage of IDA is the redox cycling of the electroactive product or mediator, which happens once different potentials are applied to the pair of electrodes, causing the oxidation-reduction cycling for reversible electrochemical reactions. Lower LODs are achieved due to the multiple contribution of each redox active species to the measured current,<sup>242,243</sup> improving consistently the signal-to-noise ratio. The signal enhancement increases as the spacing and width of the metal fingers decrease altogether with the diffusion distances for the redox species. Typical IDA signal enhancements are about 3 to 10 times and can achieve 1000 times depending on the cell dimensions.<sup>243</sup> In terms of applications, IDA has been consistently used as detector in electrochemical immunoassay.<sup>244</sup>

Handling small volumes of liquids with high precision is one of the challenges in the development of the next generation of electrochemical biosensors. Devices are becoming smaller and more sophisticated, so the difficulty in handling the analytical reagents for the electrodes production is increasing. Liquid-handling biosensor devices allow the detection of biomolecular interactions in a liquid. The use of labels is spared and the methods are performed with high-throughput. Some interesting advances in transducers designs make possible the production of one million measurements points on a 1 cm<sup>2</sup> chip. This kind of approach still suffers from a poor incorporation of the biological reagent onto the surface of such arrays. Ink-jet techniques are suitable for depositing droplets of less than 1 nL in volume with very high speeds and still poor droplet resolution. Other liquid-handling techniques include the syringe-type processes as the "Cravo deposition", usually involving "touching off" a droplet onto a surface. Another method picks up reagents on

a “pin” with a concave head and deposits it onto the surface of the device, a technique adapted from certain pharmaceutical applications. Additional developments on the fabrication techniques of electrochemical biosensors involve lithography and photolithography processes.<sup>131</sup>

Conductometry detection monitors changes in the electrical conductivity of the sample solution or a medium, as their composition changes during the course of a chemical reaction. Conductometric biosensors often use enzymes as the biorecognition element as their conversion products with electric charge increase the medium conductivity. Such systems have been applied for the detection mode in biosensors of environmental and clinical analysis. For instance, a tyrosinase biosensor was developed to measure ppb amounts of diuron and atrazine pollutants.<sup>245</sup> They also have been applied for the detection of foodborne pathogens as enterohemorrhagic *Escherichia coli* O157:H7 and *Salmonella* spp. using a low volume immunosensor with a sandwich-type immunoassay.<sup>246</sup> Drug detection of methamphetamine in human urine is another subject that has been accomplished using a conductometric biosensor.<sup>247</sup>

Potentiometric sensors are based on the measurement of the potential of electrochemical cells while draining negligible current. Conventional examples include the glass pH electrode and ion-selective electrodes for K(I), Ca(II), Na(I), and Cl(I). An electrochemical cell with two electrodes is used to measure the potential across a membrane that selectively reacts with the charged ions of interest. Potentiometric biosensors can be produced by coating electrodes with a biological element as an enzyme to catalyze the formation of the ion that is specifically detected by the electrode. As an application example, a penicillin sensor has been developed by coating a pH electrode with penicillinase that catalyzes a reaction of penicillin that also generates protons (H<sup>+</sup>).<sup>248</sup> As the electrode senses the pH reduction on its surface, an indirect correlation with the penicillin content might be drawn.

Electrochemical impedance spectroscopy (EIS) is a technique that measures the resistive and capacitive properties of a material using small amplitude sinusoidal AC excitation signals, typically between 2 and 10 mV,<sup>227,249</sup> and over a wide range of frequencies to obtain spectra. Both in-phase and out-of-phase current responses are determined to access the resistive and capacitive components of the impedance, usually using fitting models of analogic circuits. The electron-transfer resistance is accessed at high frequencies while mass transfer rate at low frequencies. Regarding to biosensing, impedimetric detectors were used for affinity biosensors at first,<sup>241</sup> being used for the monitoring of the Ab-Ag complex binding on the electrode surface. Small changes in the impedance are proportional to the concentration of the measured species, as the antigen (Ag). During next stages of development, the surface of the WE could be modified with a highly specific biological recognition element and, during the detection step, a known tension signal was applied to this electrode and the resulting current was measured. The electron transfer resistance at the electrode/solution interface changes slightly by the binding of the analyte, allowing the recording of positive or negative signal readouts.

As shown at Figure 5, the formation of antibody-antigen conjugated layers might provide a label-free immunoassay, which the formation of a blocking layer (Ab-Ag) gradually suppresses current amperometric signals using a redox probe. By EIS, the increase on the charge-transfer resistance can be observed for such immunological system, allowing the characterization of the bioelectrode surface in addition to evaluating the kinetics of Ab-Ag binding.<sup>250</sup>

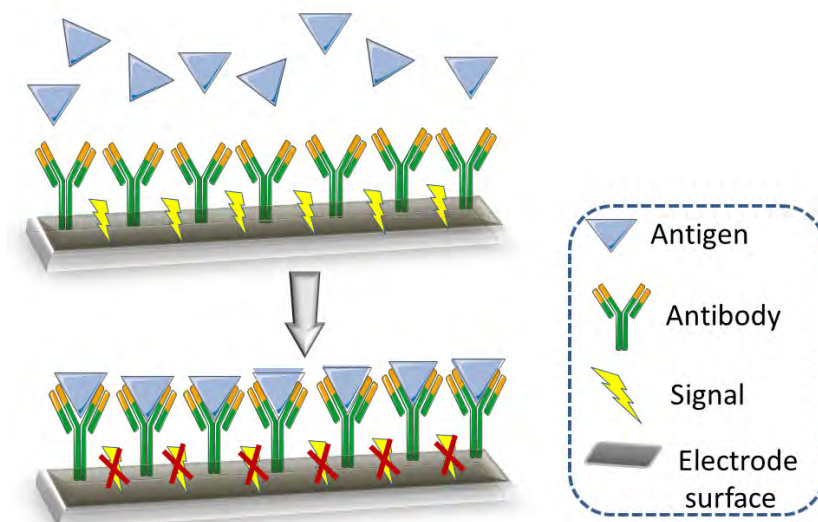


**Figure 5.** Formation of the blocking layer by the Antibody-Antigen complex in a hypothetical non-labeled assay with redox probe.

The direct monitoring of the formation of Ab-Ag conjugated layers provides a label-free detection mode with many advantages as higher signal-to-noise ratios, easy detection, lower costs of assay, faster experiments, and shorter detector response times. Nevertheless, the surface regeneration after the first measurement of an impedimetric biosensor is typically time-consuming, and measurements are not enough reproducible, which constitutes one of the biggest limitations of immunosensors involving the Ab-Ag complexes with high affinity constants. Sometimes, own regeneration conditions can be aggressive enough to damage and release the immunoreagent that is bounded to the bioelectrode.<sup>241</sup>

Now, once compared to the EIS, amperometric detection shows some drawbacks as the necessity of an easy accessibility of the participating species of the biologically-mediated redox reaction to the analyte solution and to the electrode surface. Still, redox mediators have been used to help overcome this accessibility and proximity limitations, but it causes the detection to be limited by the mass transfer rate of the mediator itself. Furthermore, additional redox active species of the sample matrix (e.g. urate and ascorbate) can contribute indistinctly to the amperometric signal depending on the detection potential of choice. Impedimetric immunosensors monitoring the Ab-Ag complex can bypass all these aforementioned limitations, since they are insensitive to most possible matrix disturbances once the impedimetric detection have been carefully designed to minimize nonspecific binding of the analyte.<sup>251</sup> Nanomaterials as gold nanoparticles and carbon nanotubes are very beneficial to chemical impedance sensors due to the increased electrode surface area, improved electrical conductivity of the sensing interface, higher chemical accessibility of the analyte, and some possible electrocatalytic effects.<sup>249</sup>

Miniaturization is a trend in the analytical chemistry and in order to design and fabricate small electrochemical biosensors, bioelectrodes need to be greatly reduced in size. Manufacturing capabilities of depositing microelectrodes on surfaces are growing and microelectrodes can easily be assembled on microfluidic chips using the vapor deposition technologies.<sup>221</sup> Microelectrodes are defined as electrodes with a diameter in the micrometer scale and can be made as disks or cylinders of carbon fibers or metal microwires.<sup>234,235</sup> Their applications include the measure of electroactive species in small critical places as inside mammalian brains<sup>234</sup> and live biological cells.<sup>252</sup> This is possible considering that electrochemical reactions occur on the electrode surface instead of the bulk solution, and very small sensing microelectrodes can be easily inserted in very small drops or spaces without disturbance or damage. For instance, carbon fiber microelectrodes have been used to detect 190 zmol of catecholamine released from a single stimulated rat nerve cell to monitor this species in cultures of adrenal cells.<sup>253</sup> The release of serotonin from neuronal vesicles have been monitored achieving 4.8 zmol LOD,<sup>254</sup> and a detector in microvolume electrochemical immunoassay



have been developed, both using carbon fiber microelectrodes too.<sup>238</sup> The measured currents are usually in the nA to pA magnitude order, so as the method can be classified as nondestructive,<sup>234</sup> besides the fact that the signal amplification is almost mandatory.<sup>221</sup>

Despite of the continuous development of several types of transducers for biosensors, the electrochemical type is very interesting for portable point-of-care devices since they are small, simple, easy to use, cost-effective, and disposable for most of the cases. Electrochemical sensors are the smallest among all types of sensors (including the optical and piezoelectric sensors), providing the bioassays with the great advantage of portability that allowed the miniaturization of instruments to small pocket-size devices that are applicable even for the consumer home use. Furthermore, the sensitivity and response of the electrochemical sensors are considerably higher than most of optical or piezoelectric sensors. That is why there is an immense motivation in the literature to explore the field of electrochemical biosensors, especially for the detection and quantification of analytes with very low concentrations in sample matrices with challenging interferences, such as those found for mycotoxins in food.

## METALLIC NANOPARTICLES BIOSENSORS FOR MYCOTOXINS DETECTION

Metal-based nanoparticles (MNPs) are commonly applied for electrochemical sensing due to the enhancement of both sensitivity and selectivity of proposed methodologies. Gold, platinum, palladium, silver, copper and cobalt are some examples of pure metals used in nanoparticulate form for the assembling of sensors.<sup>255</sup> Besides, MNPs show interesting biocompatibility and good conductivity. They might act as immobilizing platforms,<sup>256</sup> electron transfer enhancers,<sup>257</sup> catalysts of chemiluminescent reactions,<sup>258</sup> amplifiers of mass<sup>259</sup> and refractive index.<sup>260</sup> They can even work as electron conductors transporting the charge to the receiving transducer.<sup>257</sup> Furthermore, MNPs can directly act as suitable mediators for modified electrodes due to their high electrical conductivity without great cost increase on the sensing project. That is true since there is a considerable cost difference between noble metal macroelectrodes and synthesized NPs. In general, their synthesis is accomplished by the reduction of the precursor metal salt in the presence of capping agents such as phosphines, thiols, polymers, and amines.<sup>261–263</sup>

An example of a nanobiosensor assembling with MNPs involves: (i) the deposition of a mediator on the substrate electrode to catalyze the biochemical redox reaction; (ii) the immobilization of MNPs on the mediator-modified electrode to work as the immobilizing platform and; (iii) the immobilization of the biomolecule recognition agent. The detection mechanism indicates that the analyte is converted to the specific product, which involves an oxidation or reduction reaction. The biomolecule changes its form to the reduced or oxidized form, while the mediator regenerates it to the original active species. Finally, the analytical signal is generated by the donation (acceptance) of electrons by the underlying substrate electrode to (from) the mediator.<sup>264</sup>

Among the aflatoxin, AFB1 might be considered as one of the most hazardous due to its toxic, carcinogenic, mutagenic, and genotoxic character.<sup>265</sup> It is found in contaminated and moldy crops and beverages. Many electrochemical biosensors have been developed for AFB1 detection.<sup>266–269</sup> Most of them are cheap and easy to operate, despite of their lack of sensitivity in comparison to the maximum permissible limits of AFB1 established by rulers worldwide. For US and China, the tolerable limit for foodstuff is 20 ng/g, while for Korea and Japan is 10 ppb. For rice in the EU, the tolerable limit is 5 ng/g.<sup>270</sup>

Zhang *et al.*<sup>271</sup> developed an electrochemical immunosensor for the detection of AFB1 using Pd–Au nanoparticles supported on functionalized PDDA–MWCNT nanocomposites (CNTs / PDDA / Pd–Au immunosensor). The PDDA (positively-charged polyelectrolyte) was used to avoid the aggregation of MWCNTs, facilitating their dispersion in aqueous medium and allowing the formation of homogenous films on the electrode. PDDA still enriched the surface of CNTs with positive charges that promoted the adsorption of the negatively-charged Pd–AuNPs. These MNPs were used as the supporting substrate for the antibody immobilization. The analytical performance of CNTs/PDDA/Pd–Au immunosensor was studied using the differential pulse voltammetry under optimal conditions found. A satisfactory linear relation with AFB1 concentration in the range between 0.05 and 25 ng/mL was obtained with a LOD of 0.03 ng/mL. Comparing



with other reported AFB1 biosensors, the linear range showed 4 orders of magnitude in concentration that is higher than the one found for CNT-ionic liquid,<sup>266</sup> Silica gel-ionic liquid,<sup>272</sup> Prussian blue,<sup>273</sup> and AFB1-BSA<sup>274</sup> biosensors; it is comparable to the one of chitosan/Au nanoparticles,<sup>269</sup> and barely worse than the one for the Polypyrrole/pyrrolepropylic acid.<sup>275</sup> It showed one of the best LOD values, only worse than the Silica gel-ionic liquid.<sup>267</sup> The analysis of real samples showed recovery tests in the range between 98.2% (50 µg/kg) and 103.2% (100 µg/kg) for samples of non-contaminated spiked rice with simple sample treatments. Ultimately, the CNTs/PDDA/Pd-Au immunosensor showed interesting low LOD with satisfactory reproducibility, selectivity, and storage stability. The strategy is still valid for the immobilization of other antigens using their corresponding antibodies for the quantification of other toxins.

Wang *et al.*<sup>35</sup> proposed the use of metal ions as signal tags for the design and fabrication of sensitive immunosensors. Signal tags are used for the amplification of the transduction signal to improve the methodologies sensitivity. The most common tags are the enzymes, dyes, and quantum dots. Metal ions are compelling tags since they are cheap, readily available, and can be sensitively detected using stripping analysis voltammetry. Most difficulties of using metals as tags reside in the fact that it is hard to establish a direct contact of targets and the metal ions information. Therefore, the authors addressed this challenge by replacing Ca(II) ions by Cu(II) in the hydroxyapatite composition to consolidate an ion-exchange approach, forming the Cu-apatite. AuNPs were used to modify the screen-printed carbon electrode (SPCE) and complete the competitive-type immunosensor, where Cu(II) ions were released from apatite through acidolysis and its concentration was determined by stripping voltammetry, successfully establishing correlation with the analyte quantities. A satisfactory linear relation was observed between the peak current and the logarithm of AFB1 concentration in the range of 1 pg/mL to 100 ng/mL with LOD of 0.2 pg/mL. Comparing to other immunoassays of the until-date literature,<sup>270,273,276–283</sup> the Cu(II)-tag immunosensor showed superior performance with detection range meeting the limits for the AFB1 in human foodstuff in the European Union (2 ng/mL), and in the United States (20 ng/mL). Milk and peanut butter were used as real samples spiked with 1 ng/mL and 20 ng/mL of AFB1 for recovery tests, respectively. Recoveries in the range of 95.5-110% and 90-102% were observed, with small issues concerning the accuracy and the matrix effect. Nevertheless, the prototype concept has been proved, reducing the production cost of the immunosensor and making possible the use of leaked metal ions as signal tags.

Bhardwaj *et al.*<sup>284</sup> fabricated an electrochemical label-free immunosensor via antigen-antibody interactions using chemically prepared graphene quantum dots modified with gold nanoparticles (GQDs-AuNPs) that were deposited on hydrolyzed ITO by electrophoretic deposition (EPD). AFB1 antibodies were immobilized by cross-coupling chemistry using N-ethylN-(3-dimethylamino propyl) carbodiimide (EDC) and N-Hydroxy succinimide (NHS). GQDs were preferred over conventional graphene nanosheets due to the limited number of edge planes and the zero graphene band-gap, which improves the surface reactivity, dispersibility, biocompatibility, and the ratio of edge-to-basal planes that favors the bio-nano conjugation<sup>285</sup>. That remarkably increases the rate of heterogeneous charge-transfer, improving the immunosensor sensitivity and stability. AuNPs were combined with GQDs for the immunosensor assembling due to its high electrical conductivity and catalytic properties,<sup>286</sup> offering a multifold signal enhancement that provides precision, accuracy, and sensitivity for the involved methodologies. The electrochemical response of the BSA/anti-AFB1/GQD-AuNPs/ITO immunosensor was evaluated by cyclic voltammetry in the presence of ferricyanide/ferrocyanide redox probe, showing an anodic peak signal that is directly proportional to the AFB1 concentration until 1.0 ng/mL. The signal positive readout has been explained by the formation of an electro-transfer layer by the Ag-Ab immunocomplex, some possible changes in the conformational structure, and improvements of the conductive pathway between the redox couples and the transducer. Sensitivity and LOD were of 382 µA/ng mL<sup>-1</sup> cm<sup>-2</sup> and 0.008 ng/mL, respectively. Results were compared to other until-date published immunosensors, and GQDs-AuNPs/ITO showed comparable LOD results to PEDOT/AuNPs/ITO<sup>287</sup> and SWCNTs/Chitosan,<sup>288</sup> while much better value than PTH/Au/GCE,<sup>289</sup> CNTs/c PDDA/Pd-Au,<sup>271</sup> CS-AuNPs/gold microelectrode,<sup>290</sup> and rGO/ITO.<sup>291</sup> Non-contaminated maize with several spiked concentrations of AFB1 was used as real sample, achieving linear range between 0.1 ng/mL–2.5 ng/mL and LOD of 0.11 ng/mL, demonstrating the

applicability of BSA/anti-AFB1/GQD-AuNPs/ITO to the real analysis of AFB1 in maize even in concentrations under the maximum tolerance level of EU regulations.

Table II summarizes the electrochemical biosensors discussed according to the type of biomaterial, the target mycotoxin, the type of sample, LOD, and linear range of response.

**Table II.** Information of electrochemical biosensors discussed, including the type of material, the target mycotoxin, the type of sample, the limit of detection (LOD), and the linear range

Electrochemical biosensors	Mycotoxin / sample	LOD	Linear Range	Refs.
SPCE/Au NPs	AFB1/ corn	0.2 pg mL <sup>-1</sup>	0.001 - 100 ng mL <sup>-1</sup>	35
GCE/AuNPs	AFB1/ olive oil	0.05 ng mL <sup>-1</sup>	0.1 - 10 ng mL <sup>-1</sup>	266
Graphene/Polymer/AuNPs	AFB1/ rice	3.3 pg mL <sup>-1</sup>	0.01 - 10 ng mL <sup>-1</sup>	268
Au/nanomagnetic material	AFB1/ rice	0.01 ng mL <sup>-1</sup>	0.03 - 10 ng mL <sup>-1</sup>	269
GCE/Pd-Au/PDDA (MWCNTs)	AFB1/ corn	0.05 ng mL <sup>-1</sup>	0.1 - 10 ng mL <sup>-1</sup>	271
GCE/cysteine/MAB	AFB1/ rice	0.1 ng mL <sup>-1</sup>	0.1 - 10 ng mL <sup>-1</sup>	274
CGE/Pd-Au/ MWCNTs	AFB1/ corn	0.05 ng mL <sup>-1</sup>	0.1 - 10 ng mL <sup>-1</sup>	271
QCM electrode/AuNP	AFB1/ rice	0.05 ng mL <sup>-1</sup>	0.05 - 10 ng mL <sup>-1</sup>	276
Au electrode	AFB1/ peanut	0.05 ng mL <sup>-1</sup>	0.05 - 10 ng mL <sup>-1</sup>	281
ITO electrode	AFB1/ maize	0.1 ng mL <sup>-1</sup>	0.1 - 3.0 ng mL <sup>-1</sup>	284
GCE/ Au-Ag/graphene/GQD	AFB1/ aqueous solutions	0.05 ng mL <sup>-1</sup>	0.05 - 10 ng mL <sup>-1</sup>	286
GCE/ZnS QDs	SEB/ aqueous solutions	0.1 ng mL <sup>-1</sup>	0.1 - 10 ng mL <sup>-1</sup>	287
GCE/ SWCNTs	AFB1/ corn	0.02 ng mL <sup>-1</sup>	0.05 - 10 ng mL <sup>-1</sup>	288
GCE/PTH/AuNPs	AFB1 /food sample	0.07 ng mL <sup>-1</sup>	0.6 - 2.4 ng mL <sup>-1</sup>	289
SPCE/MWCNTs	AFB1/ wheat	0.05 ng mL <sup>-1</sup>	0.1 - 10 ng mL <sup>-1</sup>	290
AuNPs/MWCNTs/CS	AFB1/ wheat	0.002 ng mL <sup>-1</sup>	0.001 - 100 ng mL <sup>-1</sup>	292
Au/Bi2S3/ERGO/CF	AFB1/ cornflour	8 pg mL <sup>-1</sup>	10 pg - 20 ng mL <sup>-1</sup>	293
AuNPs/Zn/Ni-ZIF-8-800@ graphene	AFB1/ peanut oil	0.18 ng mL <sup>-1</sup>	0.18 - 100 ng mL <sup>-1</sup>	294
Au electrode	OTA/ coffee	0.15 ng mL <sup>-1</sup>	0.5 - 100 ng mL <sup>-1</sup>	295
CF/PdNPs	OTA/ coffee	0,096 ng mL <sup>-1</sup>	0.5 - 20 ng mL <sup>-1</sup>	296
Au/SPGE/CMD	AFB1/pistachio	1 ng mL <sup>-1</sup>	0.5 - 1 ng mL <sup>-1</sup>	297

## CARBON-BASED ELECTROCHEMICAL BIOSENSORS FOR MYCOTOXINS DETECTION

Carbon chains might organize themselves in several forms to assemble different structures, resulting in diverse materials as graphene, diamond, graphite, carbon nanotubes, fullerenes, carbon fibers, and carbon black (Figure 6).<sup>298</sup> These materials can display different properties despite their same chemical composition depending on their electronic structure. They are classified according to their geometric structure: particles admit the shape of tubes, horns, spheres or ellipsoids. Tube-shaped or corner-shaped particles are called carbon nanotubes (CNTs) or carbon nanorods (CNHs), respectively. 0D nanodiamonds, 1D nanotubes,

and 2D graphene nano-sheets can act as nanocomposites<sup>299</sup> (Figure 6). Advances in carbon nanomaterial synthesis have resulted in sensing systems that show improved analytical performance, providing new detection routes.<sup>298</sup>

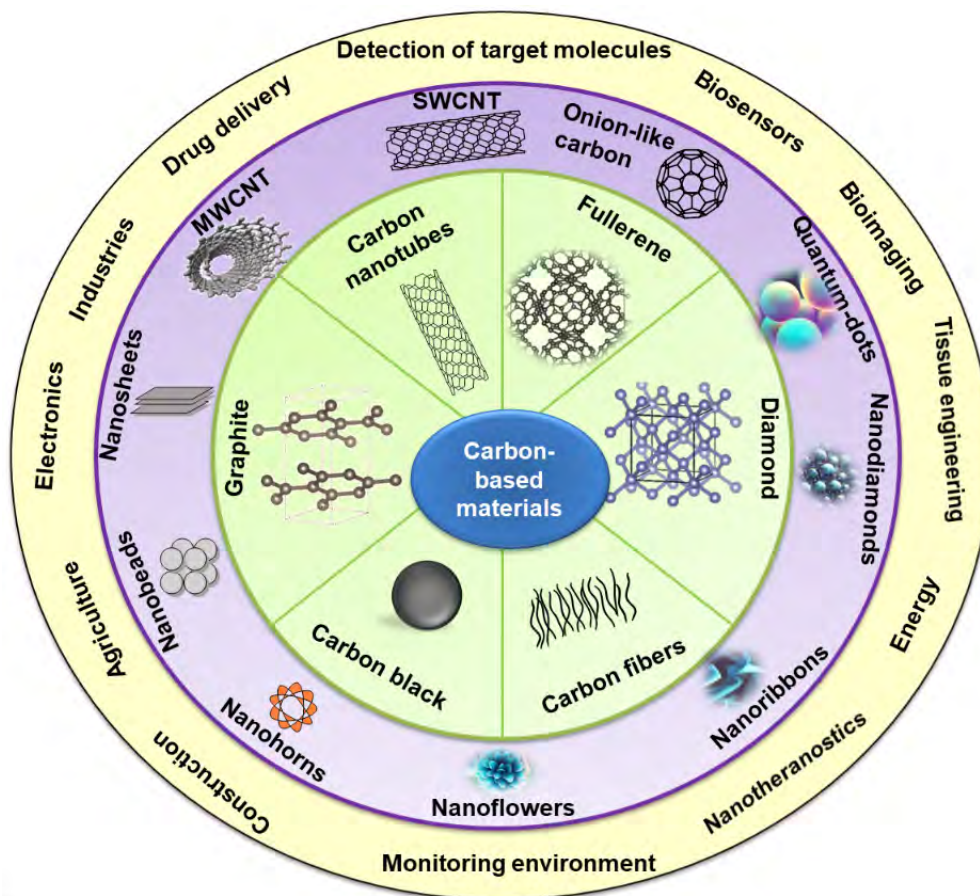


**Figure 6.** Carbon-based materials and their applications.

Furthermore, carbon-based sensors have demonstrated biocompatibility, good sensitivity, selectivity, and low LODs for a wide range of molecules. Due to their unique characteristics, carbon nanomaterials are among the most investigated materials.<sup>298</sup> They show high specific surface areas, high electrical conductivity, and flexibility that ascribe them to a wide range of applications including electronics, construction, agriculture, energy, nanotheranostics, and the detection of toxins in foodstuff.<sup>300–303</sup> Herein, we will focus our discussion on the two main carbon-based materials used for mycotoxin nanobiosensing: graphene-type and carbon nanotubes materials, although some important applications can be found elsewhere for carbon nanofibers,<sup>304</sup> nanodiamonds,<sup>305</sup> fullerene,<sup>306</sup> and Carbon-Black.<sup>307</sup>

Honeycomb two-dimensional graphene gained considerable attention since its discovery in 2004.<sup>308</sup> Curiously, graphene shows very alike physical and chemical intrinsic properties than graphite as the high surface area and the numerous surface active sites. The difference comes from the higher electron transfer kinetics of such active sites, and the increased thermal conductivity, mechanical flexibility, and biocompatibility<sup>309</sup> that make graphene very compelling for the application in electrochemical sensing platforms. There are many reported methods for the graphene preparation,<sup>309,310–316</sup> but the most scalable, cost-effective, and productive is the graphite exfoliation on graphene-type materials as graphite oxides (GO).<sup>317</sup> GO is obtained as a highly oxidized form of graphene that is produced by its surface reaction with strong oxidizing agents, resulting in a material with excellent surface functionality and amphiphilicity.<sup>318</sup> The Hummer's method

(Figure 7) is frequently used to synthesize the graphene oxide and includes the oxidation of graphite by potassium permanganate and sulfuric acid,<sup>319</sup> followed by the sonication to generate the graphite functionalized salts, the GO precursor. This material should be reduced to form the reduced-graphene oxide (rGO) analogue with interesting properties for desirable electrochemical applications. Many reduction pathways can be followed as the thermal annealing or the chemical reduction with hydrazine or sodium borohydride.<sup>320</sup>

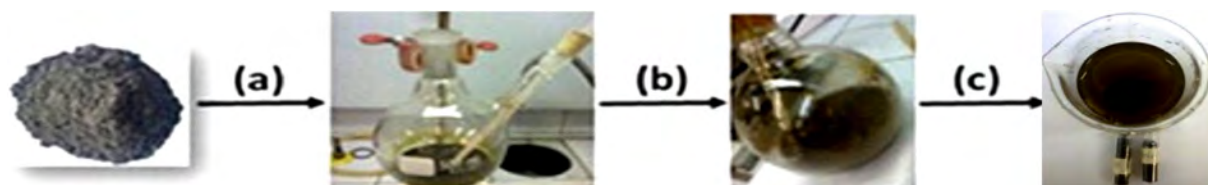


**Figure 7.** Schematic representation of graphite oxidation to obtain GO using Hummer's method: system containing graphite powder, sodium nitrate, sulfuric acid, and potassium permanganate (a), addition of hydrogen peroxide and deionized water (b), and resulting material after centrifugation and drying (c).

In general, pristine graphene is considered chemically inert and interacts with other molecules by weak physical adsorption, being necessary the introduction of surface defects or functional groups to improve its reactivity by the adjustment of surface and electronic properties. Surface functionalization can turn pristine graphene or GO into chemically sensitive and dispersible materials, making them suitable for sensing applications. Covalent functionalization is one of the most common surface modification methods for graphene. The structural change may take place both on the basal surface and at the margins/corners. Graphene can be covalently functionalized through reactions with its unsaturated bonds so as amino, hydroxyl, sulfonate, or alkyl groups are introduced through covalent bonding.<sup>321,322</sup> These groups can also act as anchoring sites to embed proteins, amino acids, and polymers.<sup>322,323</sup> The covalent carbon-carbon bonding involving the basal plane of carbon atoms offers key advantages such as the greater stability of the hybrid material, the controllability over the functionalization degree, and the reproducibility. As a disadvantage, although covalent strategies can effectively install functionalities, they unavoidably cause a loss of the free  $\pi$ -electron charge-carriers.<sup>320</sup> The non-covalent functionalization basically requires the adsorption of appropriate atoms on the graphene surface, which does not influence the material conductivity.<sup>324</sup> The polymer wrapping, the adsorption of surfactants or small aromatic molecules and their interactions with porphyrins or biomolecules as DNA are all examples of non-covalent functionalization.<sup>298</sup> This method allows the reversible functionalization while preserving the original structure of graphene. However, physical adsorption is nonspecific and there is little control over the degree of functionalization, being less stable, reproducible, and susceptible to environmental conditions during applications.<sup>325</sup>

Carbon nanotubes (CNTs) are cylindrical structures made of carbon atoms arranged in a hexagonal lattice. CNTs can be divided into two types: single-walled carbon nanotubes (SWCNTs) and multi-walled carbon nanotubes (MWCNTs).<sup>326-328</sup> SWCNTs consist of a single graphene sheet rolled into a seamless cylinder with diameters on the nanometer size, ranging from 0.4 to 3 nm.<sup>329</sup> MWCNTs consist of multiple concentric layers of graphene sheets with larger outer diameter compared to SWCNTs, typically ranging from 2 to 100 nm.<sup>330</sup> The presence of multiple layers contributes to the MWCNTs enhanced mechanical performance compared to SWCNTs, still exhibiting higher thermal conductivity and efficient heat transfer along graphene layers. CNTs exhibit remarkable electrical, mechanical, and chemical properties<sup>327,331</sup> and their good charge-transfer characteristic is appealing for their application in the assembling of electrochemical biosensors and sensing platforms. Common methods of CNT synthesis include electric arc discharge,<sup>327</sup> chemical vapor deposition (CVD),<sup>331</sup> laser ablation,<sup>329</sup> chemical vapor infiltration (CVI),<sup>332</sup> and template-assisted synthesis.<sup>333</sup> Considering the differences between the synthesis methodologies, materials should be purified prior to the chromatographic separation.<sup>334,335</sup> CNTs purification consists on the dissolution of contaminating catalysts and fullerenes by-products, and the removal of the remaining graphite large particles and further



aggregates by simple filtration. The main strategies are the acid treatment,<sup>336</sup> ultrasonication,<sup>337</sup> filtration (or chromatographic method),<sup>335</sup> thermal or oxidative treatment,<sup>338</sup> and density gradient ultracentrifugation (DGU).<sup>339</sup>

Although CNTs exhibit remarkable physical and chemical properties, their low dispersibility in aqueous and organic solvents has hindered their early application.<sup>340</sup> To circumvent this hindrance the functionalization has been used to modify CNTs surface, attaching functional groups or molecules to increase their ease of dispersion, manipulation, and processability. Main functionalization strategies are based on substitution reactions, such as the replacement of carbon atoms in the tube wall by boron or nitrogen. The choice of functionalization method depends on the desired properties, stability, and intended applications. CNTs are functionalized by irreversibly binding polymers to their walls or at defect points located at edges: the so-called grafts.<sup>340</sup> Functionalization can be achieved through covalent or non-covalent methods (Figure 8) as seen above for graphene. For the electrochemical biosensing applications, the non-covalent biomolecular functionalization<sup>341</sup> is the most relevant strategy, since it allows biomolecules as DNA, proteins, and antibodies to be attached to CNTs as the biorecognition element for specific analyte targeting.

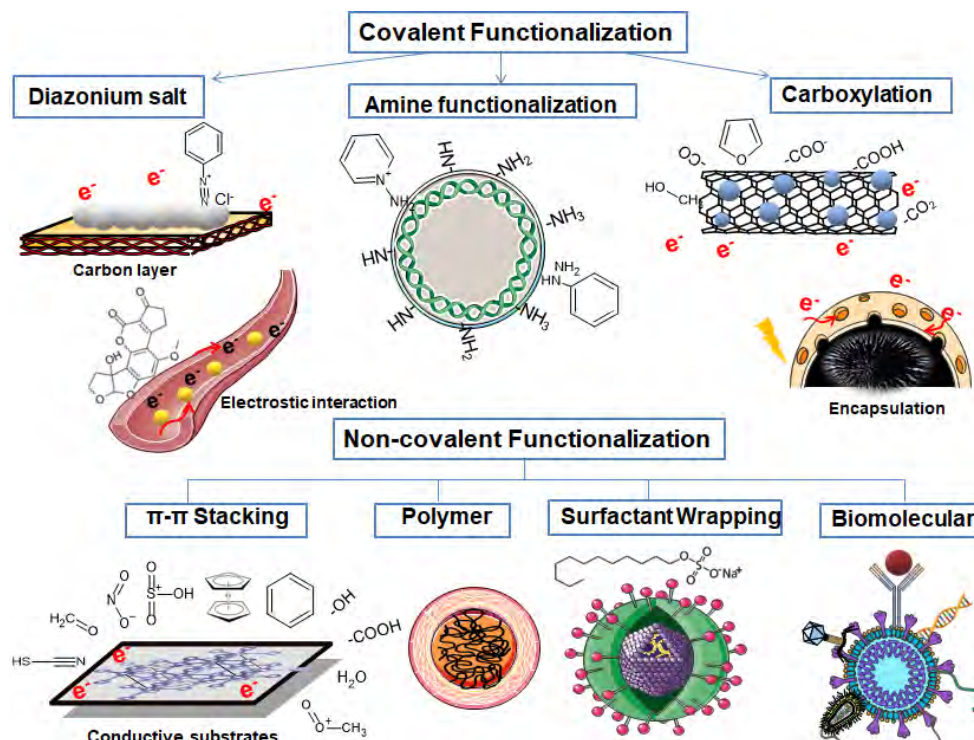


**Figure 8.** Different kinds of functionalization strategies used for carbon nanotubes (CNTs).

Gaozhi Ou *et al.*<sup>304</sup> developed a label-free electrochemical immunosensor for the determination of aflatoxin B1 (AFB1) based on Au nanoparticles decorated with urchin-like  $\text{Bi}_2\text{S}_3$  ( $\text{Au}/\text{Bi}_2\text{S}_3$ ) anchored on electrochemically reduced graphene oxide (ERGO) modified carbon fiber (CNFs) microelectrode ( $\text{Au}/\text{Bi}_2\text{S}_3/\text{ERGO}/\text{CF}$ ). Under the optimum conditions, the label-free electrochemical immunosensor detected AFB1 within the linear range of  $10 \text{ pg mL}^{-1}$  to  $20 \text{ ng mL}^{-1}$  with a LOD of  $8 \text{ pg mL}^{-1}$  and sensitivity of  $0.48 \text{ } \mu\text{A}/\text{ng mL}^{-1}$ . The immunosensor was applied to detect AFB1 in corn flour samples, offering excellent reliability and accuracy compared with typical detection methods. Glassy carbon electrode modified with nickel/nickel hydroxide NPs-decorated reduced graphene oxide ( $\text{Ni}/\text{Ni}(\text{OH})_2\text{-rGO}$ ) was used for non-enzymatic detection of xanthomegnin.<sup>342</sup>  $\text{Ni}/\text{Ni}(\text{OH})_2\text{-rGO}$  composites were synthesized through a simple microwave-assisted technique with a less harmful reducing agent. The sensor exhibited a limit of detection



of  $0.12 \mu\text{mol L}^{-1}$ . The selectivity, stability, and analytical recovery proved the potential use of the sensor for the detection of xanthomegnin in real samples.

Molecularly imprinted electrochemical sensors were exploited to detect zearalenone (ZEA) by the synergistic effect of reduced graphene nanoribbons (rGNRs) and gold nanoparticles (AuNPs).<sup>343</sup> The oxidized GNRs were firstly produced by an improved Hummers' oxidation method, and then reduced and modified with AuNPs onto a glassy carbon electrode by electrodeposition. It was found that the constructed sensor showed a wide linear range of  $1\text{--}500 \text{ ng mL}^{-1}$  for ZEA, with a LOD as low as  $0.34 \text{ ng mL}^{-1}$ . Singh *et al.*<sup>344</sup> prepared composite c-MWCNTs/ITO electrodes by one-step electrophoretic deposition of c-MWCNTs on ITO glass. BSA/anti-AFB1/MWCNTs/ITO immune electrode was prepared by covalently coupling aflatoxin monoclonal antibodies. The results showed that the method had high sensitivity in the linear range of  $0.25\text{--}1.375 \text{ ng mL}^{-1}$  and LOD of  $0.08 \text{ ng/mL}$ .

Wang *et al.*<sup>345</sup> developed a molecularly imprinted electrochemical method using a stepwise approach for the detection of AFB1 in gutter oil. Au/Pt bimetallic nanoparticles were electrodeposited on glassy carbon electrode modified with MWCNTs. The performance of the imprinted sensor showed a linear range of  $1.0 \times 10^{-10}$  to  $1.0 \times 10^{-5} \text{ mol L}^{-1}$  with a LOD of  $0.03 \text{ nmol L}^{-1}$ . Zhang *et al.*<sup>346</sup> developed an electrochemical immunosensor for detection of aflatoxin B1 in agricultural products by modifying multi-walled carbon nanotubes (MWCNTs) with ferrocene (FC) fixed on the surface of a screen-printed carbon electrode (SPCE) via MWCNTs and chitosan (CS). The increase in the specific surface area of SPCE modified by Fc/MWCNT/CS facilitated the binding of AFB1-Bovine serum albumin, while the excellent electrical conductivity of Fc/MWCNT/CS promoted a good electron transfer rate. These advantages not only amplified the immunosensor signal, but also improved the immunosensor sensitivity and stability.

Solis *et al.*<sup>347</sup> developed an electrochemical microfluidic immunosensor for T-2 quantification in wheat germ samples. The detection was carried out using a competitive immunoassay method with monoclonal anti-T-2 antibodies that were immobilized on poly(methyl methacrylate) (PMMA) in a central channel. A platinum wire modified with reduced graphene oxide (rGO)-nanoporous gold (NPG) was used as the working electrode and positioned at the end of this channel. The detection mechanism comprised the T-2 competition with T-2-horseradish peroxidase (HRP) for the specific recognizing sites of immobilized anti-T-2 monoclonal antibodies, so as HRP in the presence of hydrogen peroxide catalyzes de oxidation of 4-tert-butylcatechol (4-TBC) which reduction was monitored at the nanostructured electrode at  $-0.15 \text{ V}$  (vs. Ag/AgCl). According to authors, the new microfluidic assay contributed to the *in situ* analysis of mycotoxins in agricultural samples, making it faster and even more secure.

Jubeen *et al.*<sup>348</sup> prepared an overview of the scenario of recent studies using electrochemical sensors and biosensors for mycotoxin detection for food safety. Authors provide a critical inspiration for future applications of electrochemical analysis and point-of-care testing for mycotoxins, pointing out the electrochemical sensors as a viable method for addressing specificity and sensitivity in detection, considering their ease of use, sensitivity, low cost, and miniaturization capability. Many graphene-based devices are herein discussed as well. Kalambate *et al.*<sup>349</sup> reported a review which outlines a variety of electrochemical sensing platforms. Authors claim that the electrochemical sensing platforms emerged as feasible devices to address specificity and sensitivity issues, even privileging the effectiveness, efficiency, and user-friendly nature. The review offers valuable perspectives on the existing challenges, discussing great advancements using graphene-based nanocomposites. Jiang *et al.*<sup>350</sup> reviewed the significant work on electrochemical sensors for mycotoxins detection in food samples aiming the mechanisms and portable use for the toxin detection, including carbon nanostructured materials. They summarized recent advances providing a new perspective on future trends of portability.

Yang *et al.*<sup>351</sup> developed a immunosensor for the mycotoxin FB1 detection in food, based on chitosan functionalized nitrogen-doped graphene and polyaniline (N-G@PANI@CS) with electrodeposited gold nanoparticles (AuNPs) on its surface. The immunosensor showed a broad linear range of  $0.50 \text{ ng mL}^{-1}$  to  $800.00 \text{ ng mL}^{-1}$  and LOD of  $0.07 \text{ ng mL}^{-1}$ . Authors discuss that their study provides a novel, reliable, and convenient mean to detect FB1 in contaminated food. Deng *et al.*<sup>352</sup> reported a study with an ultrasensitive

Nafion-immobilized functionalized multiwalled carbon nanotube (MWCNT)-based electrochemical (EC) immunosensor for the trace detection of AFB1. Nafion is herein used to stabilize the MWCNTs suspension to provide uniform distribution of the material all over the surface of gold electrodes. MWCNTs were used as signal amplifiers with large surface area, several active sites for anti-AFB1 monoclonal antibodies (mAbs) coupling, and high conductivity to improve the charge-transport. The immunosensor selectivity was herein tested in the presence of three other types of mycotoxins, while the methodology accuracy was studied by measuring the AFB1 concentrations in fortified malt, lotus seed, and hirudo samples, achieving 92.08 to 104.62% of recovery.

Zhang *et al.*<sup>353</sup> reported a chitosan–graphene nanosheets (CS-GNs) electrochemical immunosensor. The CS-GN nanocomposite was used as a modifier layer to increase the specific surface area and biocompatibility of the immunosensor, enhancing the electron-transfer rate and the efficiency of the antibody immobilization. Results showed good correlation between the current transients and the AFB1 immunoreaction with interesting specificity and stability. Linear range was from 0.05 to 25 ng/mL with LOD of 0.021 ng/mL and recovery rates ranging from 97.3% to 101.4% in real corn samples. Authors claim that their methodology show promising performance, indicating a remarkable prospect for the mycotoxins detection in grains.

Carbon-based materials such as graphene and CNTs highlighted here have gained significant attention in the development of biosensors due to their exceptional electrical, mechanical, and chemical properties. All applications of carbon-based immunosensors discussed in this review are summarized in Table III.

**Table III.** Main carbon-based immunosensors discussed, including the material, the target mycotoxin, the type of sample, limit of detecton (LOD), and linear range

Nanoimmunosensor	Mycotoxin / sample	LOD	Linear Range	Refs.
Au/Bi <sub>2</sub> S <sub>3</sub> /ERGO/CF	AFB1 / cornflour	8 pg mL <sup>-1</sup>	10 pg mL <sup>-1</sup> – 20 ng mL <sup>-1</sup>	304
AuNP-rGNR	ZEA / –	0.34 ng mL <sup>-1</sup>	1 – 500 ng mL <sup>-1</sup>	343
c-MWCNTs/ITO	AFB1 / –	0.08 ng mL <sup>-1</sup>	0.25 – 1.375 ng mL <sup>-1</sup>	344
(POPD)-grafted Au/Pt MWCNT	AFB1 / hogwash oil	0.03 nmol L <sup>-1</sup>	10 <sup>-10</sup> – 10 <sup>-5</sup> mol L <sup>-1</sup>	345
Fc/MWNT/CS SPCE	AFB1 / agricultural products	0.159 pg mL <sup>-1</sup>	10 <sup>-3</sup> – 2 10 <sup>-4</sup> ng mL <sup>-1</sup>	346
PMMA rGO-NPG T-2 HRP	T-2 / wheat germ	0.10 µg kg <sup>-1</sup>	0.0 – 1000 µg kg <sup>-1</sup>	347
AuNPs/N-G@PANI@CS	FB1 / –	0.07 ng mL <sup>-1</sup>	0.50 – 800.00 ng mL <sup>-1</sup>	351
Nafion–MWCNT	AFB <sub>1</sub> / fortified malt, lotus seed, and hirudo	0.021 ng mL <sup>-1</sup>	0.05 – 100 ng mL <sup>-1</sup>	352
CS-GNs	AFB1 / corn	0.021 ng mL <sup>-1</sup>	0.05 – 25 ng mL <sup>-1</sup>	353

## CHALLENGES AND FUTURE RESEARCH DIRECTIONS

Despite of significant advancements in the development of electrochemical nanoimmunosensors for mycotoxin detection in food, several challenges remain that must be addressed to fully achieve their potential in commercial applications and real-world use. These challenges span issues related to sensor sensitivity, selectivity, matrix effects, and practical deployment in diverse food matrices. Addressing these challenges will require multidisciplinary approaches, collaboration, and continued innovation.

**Matrix Effects and Sample Preparation:** one of the most pressing challenges in the detection of mycotoxins in food using electrochemical sensors is the interference from complex sample matrices. Sometimes, the detection of mycotoxins based on a single analytical signal has proven to be false negative or false positive due to matrix effects.<sup>354</sup> Agricultural products and foodstuffs often contain various components as proteins,

lipids, sugars that can affect the accuracy and reproducibility of sensor measurements. The presence of these matrix components can lead to signal interference, reducing the effectiveness of electrochemical sensors. While ultrafiltration techniques and fouling-resistant coatings have been explored as solutions, these methods often require further refinement to ensure their practical feasibility. Future research should focus on developing robust sample preparation protocols that effectively mitigate matrix effects while maintaining the integrity and sensitivity of the sensors. An example is the use of multimodal biosensors<sup>355</sup> that can generate different analytical signals resulting in linearity increase and accuracy.

**Improving Sensitivity, Selectivity, and Reproducibility:** although electrochemical nanobiosensors offer enhanced sensitivity and selectivity compared to traditional methods, further optimization is needed. The current generation of sensors often faces limitations in detecting mycotoxins at low concentrations, particularly when multiple toxins are present in a sample.<sup>356</sup> Enhancing the sensitivity and selectivity of these sensors will require advances in nanomaterial design, sensor surface functionalization, and the development of more efficient biorecognition elements. Furthermore, reproducibility remains a key challenge, especially when sensors are exposed to variable environmental conditions. Future research should focus on improving the consistency and reliability of electrochemical nanobiosensors to ensure their suitability for commercial applications.<sup>357,358</sup>

**Labeled vs. Label-Free Sensors:** a significant challenge resides in the choice between labeled and label-free bioassay protocols. While labeled biosensors often provide higher sensitivities, they require additional steps for label conjugation and detection, potentially complicating the sensing process. Label-free biosensors, on the other hand, offer advantages in terms of simplicity and cost, but they may struggle to match the sensitivity of labeled systems. Future research could explore hybrid approaches that combine the benefits of both labeled and label-free technologies, improving the overall performance and versatility of electrochemical nanobiosensors.<sup>46</sup>

**Integration with Portable and Wearable Devices:** one of the most promising aspects of electrochemical nanobiosensors is their potential integration with portable and wearable devices for real-time mycotoxin monitoring.<sup>350</sup> The growing demand for point-of-care testing<sup>358</sup> and continuous monitoring of food safety in various settings as agricultural fields and food processing plants has led to increasing interest in wearable electrochemical biosensors.<sup>359</sup> However, the development of flexible, durable, and user-friendly sensors that can operate in real-world conditions remains a significant challenge. Research into the integration of electrochemical sensors with flexible substrates,<sup>360</sup> microfluidics,<sup>361</sup> and wireless communication systems is essential to overcome these hurdles. Wearable devices that can offer real-time and continuous monitoring of mycotoxins would provide a valuable tool for food safety professionals and consumers.<sup>359</sup>

**Multiplexed Detection for Simultaneous Monitoring:** another critical challenge in mycotoxin analysis is the need for simultaneous detection of multiple mycotoxins in a single sample.<sup>356</sup> Many electrochemical nanoimmunosensors have been designed for the detection of a single target, and the ability to perform multiplexed detection remains limited. Developing sensors capable of simultaneously detecting a wide range of mycotoxins in complex food matrices will be a significant breakthrough.<sup>362</sup> Advances in microfluidics,<sup>361</sup> sensor arrays,<sup>363</sup> and signal processing algorithms<sup>364</sup> could enable the development of these multiplexed systems, expanding the applications of electrochemical sensors in food safety monitoring.

**Commercialization and Regulatory Approvals:** finally, one of the biggest challenges for the widespread adoption of electrochemical nanobiosensors is the commercialization process, including obtaining regulatory approvals. For these sensors to be accepted by regulatory bodies, they must meet stringent requirements for accuracy, reliability, and reproducibility. Additionally, manufacturers must address issues related to production scalability, cost-efficiency, and users training. Ongoing collaboration between researchers, industry

stakeholders, and regulatory agencies will be crucial to ensure that electrochemical nanobiosensors can be effectively deployed in the real world.

## CONCLUSIONS AND PERSPECTIVE

Herein we have revised the types and mechanisms of biosensors based on the biorecognition elements (enzymes, antibodies, cells, aptamers, and nucleic acids), the transducers (electrochemical, optical, piezoelectric, magnetoelastic, FET, calorimetric, and acoustic), and the applied metallic and carbon-based (graphene and CNTs) nanomaterials. The application of such nanomaterials in biosensors led the field to a rapid growth in the recent decade due to the employment of new biorecognition elements and transducers, progress in miniaturization, design and manufacture of nanostructured devices at micro-level, besides the new techniques of nanomaterials synthesis, bringing together life and physical scientists with engineers and further technology professionals. The sensing technology in general has become more versatile, robust, and dynamic with the introduction of the nanoscience, improving significantly the transduction mechanisms with greater sensitivity, quicker detection, shorter response time, and better reproducibility by the application of different nanomaterials, each one with its own characteristics within biosensors. Electrochemical biosensors are not different from that: they have much to gain in terms of sensitivity by coupling with nanomaterial science.

Besides the clear advantages of using nanostructured materials in biosensors applications, some major drawbacks unfortunately still hinder the evolution of applications for the next level. Examples of some important issues are the insufficient investigation on the sustainability of nanostructures in sensor applications and in the fabrication of such nanostructures, and the few studies about nanomaterials toxicity that may change according to their physical properties. These limitations certainly should be better investigated and addressed during the expansion of new nanostructured materials for their use in biosensors. Still, most biosensor devices for biomedical applications require large sample volumes for detection, otherwise leading to some false-positive or false-negative results. Electrochemical nanobiosensors devices can help that since they require very low sample volumes with fast, versatile, and reliable results using simple instrumentation that even favors the point-of-care testing approach with portable devices.<sup>133</sup>

With that said, it is important to remind that very few biosensors have attained the commercial success at global level, besides the electrochemical glucose sensors and lateral flow pregnancy tests. Production costs of the nanostructure-based biosensors should be better revised and optimized so as affordable device costs altogether with rapid and reliable results in a user-friendly interface can lead to commercial success. For instance, nanomaterials should be incorporated in tiny “lab-on-a-biochip” devices integrating the sample handling and the multiplexed analysis. Also, electrochemical biosensors still should improve in terms of the simultaneous quantification of multiple biomarkers. New prototypes should embrace the artificial intelligence with nanotechnology for designs and fabrication. Therefore, more research should be done in this regard to turn the ongoing biosensor academic research into commercially viable prototypes by industries in the near future.<sup>133</sup>

Regarding to the deleterious effects of fungi and their mycotoxins, a number of detrimental health effects in humans have been reported. As the mycotoxins are secondary metabolites of fungal pathogens, they represent a diverse range of chemical structures. Most researches have focused on major incidence toxins as aflatoxins, fumonisins, trichothecenes, zearalenone, ochratoxin A, and patulin. Some mycotoxin groups even contain structurally related analogs. Afterwards, a suitable combination of biorecognition element, bio-fabrication, and compatible transducers will be the solution for the successful development of efficient and robust mycotoxin biosensors. Many up-to-date developed biosensors can detect profusely only a few or particular mycotoxins, while the future trend is most certainly the development of the multiplexed biosensing-based detection. Upcoming methods for biosensor developments seem to integrate multiple detection technologies with application of genetically engineered microbes. Evaluation of biological contaminants related to emerging diseases to avoid chronic illness with high mortality is one feasible possibility of future direction of toxins investigations.<sup>365</sup>



In recent years, the mycotoxin biosensors development emerged as a field of intense research due to their capacity of specifically detecting such toxic molecules in very low concentrations even in complex sample matrices. The combination of nanomaterials with biomolecules to fabricate single molecule multifunctional nanocomposites, nanoelectrodes, and nanofilms seem to be a trend to be explored. However, the single-molecule biosensors with high throughput assay shall be also focused on. Metabolite biosensors with multiple targets, mechanisms of action, and applications in metabolic engineering are an upcoming subject of research too. Ultimately, considering the further advance of nanomaterials science, the imminent research theme in biosensors is expected to be mostly focused on the transducer technology, the sample matrix treatment, and the development of new biorecognition sensing elements.<sup>365</sup>

### Conflicts of interest

The authors declare no conflicts of any possible nature.

### Acknowledgements

The authors are grateful to FAPEMIG [BPD-01048-22 - Finance code 001], CAPES [Finance code 001], and EMBRAPA-CAFÉ [Notice 20/2018 and code 145].

### REFERENCES

- (1) Anfossi, L.; Giovannoli, C.; Baggiani, C. Mycotoxin Detection. *Curr. Opin. Biotechnol.* **2016**, *37*, 120–126. <https://doi.org/10.1016/j.copbio.2015.11.005>
- (2) Evtugyn, G.; Hianik, T. Electrochemical Immuno- and Aptasensors for Mycotoxin Determination. *Chemosensors* **2019**, *7* (1), 10. <https://doi.org/10.3390/chemosensors7010010>
- (3) Pohanka, M.; Jun, D.; Kuca, K. Mycotoxin Assays Using Biosensor Technology: A Review. *Drug Chem. Toxicol.* **2007**, *30* (3), 253–261. <https://doi.org/10.1080/01480540701375232>
- (4) Tothill, I. Biosensors and Nanomaterials and their Application for Mycotoxin Determination. *World Mycotoxin J.* **2011**, *4* (4), 361–374.
- (5) Freire, L.; Sant'Ana, A. S. Modified Mycotoxins: An Updated Review on Their Formation, Detection, Occurrence, and Toxic Effects. *Food Chem. Toxicol.* **2018**, *111*, 189–205. <https://doi.org/10.1016/j.fct.2017.11.021>
- (6) Zhou, S.; Xu, L.; Kuang, H.; Xiao, J.; Xu, C. Immunoassays for Rapid Mycotoxin Detection: State of the Art. *Analyst* **2020**, *145* (22), 7088–7102. <https://doi.org/10.1039/D0AN01408G>
- (7) Matysik, G.; Giry, H. Gradient Thin-Layer Chromatography and Densitometry Determination of Alternaria Mycotoxins. *Chromatographia* **1996**, *42* (9–10), 555–558. <https://doi.org/10.1007/BF02290291>
- (8) Kecskeméti, Á.; Nagy, C.; Biró, P.; Szabó, Z.; Pócsi, I.; Bartók, T.; Gáspár, A. Analysis of Fumonisin Mycotoxins with Capillary Electrophoresis – Mass Spectrometry. *Food Addit. Contam., Part A* **2020**, *37* (9), 1553–1563. <https://doi.org/10.1080/19440049.2020.1778797>
- (9) Pallarés, N.; Sebastià, A.; Martínez-Lucas, V.; González-Angulo, M.; Barba, F. J.; Berrada, H.; Ferrer, E. High Pressure Processing Impact on Alternariol and Aflatoxins of Grape Juice and Fruit Juice-Milk Based Beverages. *Molecules* **2021**, *26* (12), 3769. <https://doi.org/10.3390/molecules26123769>
- (10) Chen, R.; Li, S.; Sun, Y.; Huo, B.; Xia, Y.; Qin, Y.; Li, S.; Shi, B.; He, D.; Liang, J.; Gao, Z. Surface-Enhanced Raman Spectroscopy Aptasensor for Simultaneous Determination of Ochratoxin A and Zearalenone Using Au@Ag Core-Shell Nanoparticles and Gold Nanorods. *Microchim. Acta* **2021**, *188* (8), 281. <https://doi.org/10.1007/s00604-021-04919-6>
- (11) Ghaani, M.; Azimzadeh, M.; Büyüktaş, D.; Carullo, D.; Farris, S. Electrochemical Sensors in the Food Sector: A Review. *J. Agric. and Food Chem.* **2024**, *72* (44), 24170. <https://doi.org/10.1021/acs.jafc.4c09423>
- (12) Das, J.; Mishra, H. N. Recent advances in sensors for detecting food pathogens, contaminants, and toxins: A review. *Eur. Food Res. Technol.* **2022**, *248* (4), 1125. <https://doi.org/10.1007/s00217-021-03951-3>

- (13) Focker, M.; Van der Fels-Klerx, H. J. Economics applied to food safety. *Curr. Opin. Food Sci.* **2020**, *36*, 18. <https://doi.org/10.1016/j.cofs.2020.10.018>
- (14) Singh, J.; Mehta, A. Rapid and Sensitive Detection of Mycotoxins by Advanced and Emerging Analytical Methods: A Review. *Food Sci. Nutr.: Curr. Issues Answers* **2020**, *8* (5), 2183–2204. <https://doi.org/10.1002/fsn3.1474>
- (15) Matabaro, E.; Ishimwe, N.; Uwimbabazi, E.; Lee, B. H. Current Immunoassay Methods for the Rapid Detection of Aflatoxin in Milk and Dairy Products. *Comp. Rev. Food Sci. Food Safe* **2017**, *16* (5), 808–820. <https://doi.org/10.1111/1541-4337.12287>
- (16) Sarter, S.; Zakhia, N. Chemiluminescent and Bioluminescent Assays as Innovative Prospects for Mycotoxin Determination in Food and Feed. *Luminescence* **2004**, *19* (6), 345–351. <https://doi.org/10.1002/bio.791>
- (17) Bahadır, E. B.; Sezgintürk, M. K. A Review on Impedimetric Biosensors. *Artif. Cells, Nanomed., Biotechnol.* **2016**, *44* (1), 248–262. <https://doi.org/10.3109/21691401.2014.942456>
- (18) Xu, G.; Huo, D.; Hou, J.; Zhang, C.; Zhao, Y.; Hou, C.; Bao, J.; Yao, X.; Yang, M. An Electrochemical Aptasensor of Malathion Based on Ferrocene/DNA-Hybridized MOF, DNA Coupling-Gold Nanoparticles and Competitive DNA Strand Reaction. *Microchem. J.* **2021**, *162*, 105829. <https://doi.org/10.1016/j.microc.2020.105829>
- (19) Irfan Azizan, M. A.; Taufik, S.; Norizan, M. N.; Abdul Rashid, J. I. A Review on Surface Modification in the Development of Electrochemical Biosensor for Malathion. *Biosens. Bioelectron.:X* **2023**, *13*, 100291. <https://doi.org/10.1016/j.biosx.2022.100291>
- (20) Heydari-Bafrooei, E.; Ensafi, A. A. Nanomaterials-Based Biosensing Strategies for Biomarkers Diagnosis, a Review. *Biosens. Bioelectron.:X* **2023**, *13*, 100245. <https://doi.org/10.1016/j.biosx.2022.100245>
- (21) Khan, A.; Haque, M. N.; Kabiraz, D. C.; Yeasin, A.; Rashid, H. A.; Sarker, A. C.; Hossain, G. A Review on Advanced Nanocomposites Materials Based Smart Textile Biosensor for Healthcare Monitoring from Human Sweat. *Sens. Actuators, A* **2023**, *350*, 114093. <https://doi.org/10.1016/j.sna.2022.114093>
- (22) Cai, X.; Xie, Z.; Li, D.; Kassymova, M.; Zang, S.-Q.; Jiang, H.-L. Nano-sized metal-organic frameworks: Synthesis and applications. *Coord. Chem. Rev.* **2020**, *417*, 213366. <https://doi.org/10.1016/j.ccr.2020.213366>
- (23) Rosado, T. F.; Costa, I. P.; Nadier, J.; De Avillez, R. R.; Xing, Y.; Solórzano, G.; Silva, A. C. A.; Dourado, A. H. B.; Dos Santos, C. C.; Faria, V. W.; Fraga, M. A.; Júnior, J.; Tanaka, A. A.; Garcia, M. A. S.; Da Silva, A. G. M. Beyond Surface: Correlating Cul /Cull and O-Vacancy Surface Sites in CuxO Nanocubes with Their Activities as Noble Metal-Free Anodes for Fuel Cells. *Surf. Interfaces* **2023**, *40*, 102889. <https://doi.org/10.1016/j.surf.2023.102889>
- (24) Fiorio, J. L.; Gothe, M. L.; Kohlrausch, E. C.; Zardo, M. L.; Tanaka, A. A.; De Lima, R. B.; Da Silva, A. G. M.; Garcia, M. A. S.; Vidinha, P.; Machado, G. Nanoengineering of Catalysts for Enhanced Hydrogen Production. *Hydrogen* **2022**, *3* (2), 218–254. <https://doi.org/10.3390/hydrogen3020014>
- (25) Volokitin, Y.; Sinzig, J.; de Jongh, L. J.; Schmid, G.; Vargaftik, M. N.; Moiseev, I. I. Quantum-size effects in the thermodynamic properties of metallic nanoparticles. *Nature* **1996**, *384* (6610), 621–623. <https://doi.org/10.1038/384621a0>
- (26) Chen, F.; Yan, T.; Bashir, S.; Jingbo Louise Liu. *Synthesis of Nanomaterials Using Top-down Methods*. Elsevier eBooks, 2022, pp 37–60. <https://doi.org/10.1016/b978-0-323-99877-2.00007-2>
- (27) Abid, N.; Khan, A. M.; Shujait, S.; Chaudhary, K.; Ikram, M.; Imran, M.; Haider, J.; Khan, M.; Khan, Q.; Maqbool, M. Synthesis of nanomaterials using various top-down and bottom-up approaches, influencing factors, advantages, and disadvantages: A review. *Adv. Colloid Interface Sci.* **2022**, *300*, 102597. <https://doi.org/10.1016/j.cis.2021.102597>
- (28) Lin, H. K.; Yan, T.-H.; Bashir, S.; Jingbo Louise Liu. *Synthesis of Nanomaterials Using Bottom-up Methods*. Elsevier eBooks, 2022, pp 61–110. <https://doi.org/10.1016/b978-0-323-99877-2.00003-5>

- (29) Ren, R.; Lim, C.; Li, S.; Wang, Y.; Song, J.; Lin, T.-W.; Muir, B. W.; Hsu, H.-Y.; Shen, H.-H. Recent Advances in the Development of Lipid-, Metal-, Carbon-, and Polymer-Based Nanomaterials for Antibacterial Applications. *Nanomaterials* **2022**, 12 (21), 3855. <https://doi.org/10.3390/nano12213855>
- (30) Bissessur, R. *Nanomaterials Applications*. Elsevier eBooks, 2020, pp 435–453. <https://doi.org/10.1016/b978-0-12-816806-6.00018-2>
- (31) Afolabi, O. A.; Pandurangan, M. T.; Kanny, K. *Types of Biobased Nanomaterials*. In: Ahmed, S. (Eds.). *Biobased Nanomaterials*. Springer, 2023, pp 17-43. [https://doi.org/10.1007/978-981-97-0542-9\\_2](https://doi.org/10.1007/978-981-97-0542-9_2)
- (32) Thiruvengadam, M.; Rajakumar, G.; Chung, I.-M. Nanotechnology: Current Uses and Future Applications in the Food Industry. *3 Biotech.* **2018**, 8 (1), 74. <https://doi.org/10.1007/s13205-018-1104-7>
- (33) Campanile, R.; Scardapane, E.; Forente, A.; Granata, C.; Germano, R.; Di Girolamo, R.; Minopoli, A.; Velotta, R.; Della Ventura, B.; Iannotti, V. Core-Shell Magnetic Nanoparticles for Highly Sensitive Magnetoelastic Immunosensor. *Nanomaterials* **2020**, 10 (8), 1526. <https://doi.org/10.3390/nano10081526>
- (34) Chen, H.; Li, Y.; Song, Y.; Liu, F.; Deng, D.; Zhu, X.; He, H.; Yan, X.; Luo, L. A Sandwich-Type Electrochemical Immunosensor Based on Spherical Nucleic Acids-Templated Ag Nanoclusters for Ultrasensitive Detection of Tumor Biomarker. *Biosens. Bioelectron.* **2023**, 223, 115029. <https://doi.org/10.1016/j.bios.2022.115029>
- (35) Wang, H.; Zhang, Y.; Chu, Y.; Ma, H.; Li, Y.; Wu, D.; Du, B.; Wei, Q. Disposable Competitive-Type Immunoassay for Determination of Aflatoxin B1 via Detection of Copper Ions Released from Cu-Apatite. *Talanta* **2016**, 147, 556–560. <https://doi.org/10.1016/j.talanta.2015.10.040>
- (36) Huang, X.; Zhu, Y.; Kianfar, E. Nano Biosensors: Properties, Applications and Electrochemical Techniques. *J. Mater. Res. Technol.* **2021**, 12, 1649–1672. <https://doi.org/10.1016/j.jmrt.2021.03.048>
- (37) Lin, X.; Yu, W.; Tong, X.; Li, C.; Duan, N.; Wang, Z.; Wu, S. Application of Nanomaterials for Coping with Mycotoxin Contamination in Food Safety: From Detection to Control. *Crit. Rev. Anal. Chem.* **2022**, 54 (2), 355–388. <https://doi.org/10.1080/10408347.2022.2076063>
- (38) Xie, F.; Yang, M.; Jiang, M.; Huang, X.-J.; Liu, W.-Q.; Xie, P.-H. Carbon-Based Nanomaterials – a Promising Electrochemical Sensor toward Persistent Toxic Substance. *TrAC, Trends Anal. Chem.* **2019**, 119, 115624. <https://doi.org/10.1016/j.trac.2019.115624>
- (39) Yang, X.; Zhou, X.; Zhang, X.; Qing, Y.; Luo, M.; Liu, X.; Li, C.; Li, Y.; Xia, H.; Qiu, J. A Highly Sensitive Electrochemical Immunosensor for Fumonisin B1 Detection in Corn Using Single-Walled Carbon Nanotubes/Chitosan. *Electroanalysis* **2015**, 27 (11), 2679–2687. <https://doi.org/10.1002/elan.201500169>
- (40) Liu, X.; Wen, Y.; Wang, W.; Zhao, Z.; Han, Y.; Tang, K.; Wang, D. Nanobody-Based Electrochemical Competitive Immunosensor for the Detection of AFB1 through AFB1-HCR as Signal Amplifier. *Microchim. Acta* **2020**, 187 (6). <https://doi.org/10.1007/s00604-020-04343-2>
- (41) Bulbul, G.; Hayat, A.; Andreescu, S. A. Generic Amplification Strategy for Electrochemical Aptasensors Using a Non-Enzymatic Nanoceria Tag. *Nanoscale* **2015**, 7 (31), 13230–13238. <https://doi.org/10.1039/c5nr02628h>
- (42) Li, Y.; Liu, D.; Zhu, C.; Shen, X.; Liu, Y.; You, T. Sensitivity Programmable Ratiometric Electrochemical Aptasensor Based on Signal Engineering for the Detection of Aflatoxin B1 in Peanut. *J. Hazard. Mater.* **2020**, 387, 122001. <https://doi.org/10.1016/j.jhazmat.2019.122001>
- (43) Ong, C. C.; Siva Sangu, S.; Illias, N. M.; Chandra Bose Gopinath, S.; Saheed, M. S. M. Iron Nanoflorets on 3D-Graphene-Nickel: A “Dandelion” Nanostructure for Selective Deoxynivalenol Detection. *Biosens. Bioelectron.* **2020**, 154, 112088. <https://doi.org/10.1016/j.bios.2020.112088>
- (44) Wu, S. S.; Wei, M.; Wei, W.; Liu, Y.; Liu, S. Electrochemical Aptasensor for Aflatoxin B1 Based on Smart Host-Guest Recognition of  $\beta$ -Cyclodextrin Polymer. *Biosens. Bioelectron.* **2019**, 129, 58–63. <https://doi.org/10.1016/j.bios.2019.01.022>

- (45) An, K.; Lu, X.; Wang, C.; Qian, J.; Chen, Q.; Hao, N.; Wang, K. Porous Gold Nanocages: High Atom Utilization for Thiolated Aptamer Immobilization to Well Balance the Simplicity, Sensitivity, and Cost of Disposable Aptasensors. *Anal. Chem.* **2019**, *91* (13), 8660–8666. <https://doi.org/10.1021/acs.analchem.9b02145>
- (46) Cancelliere, R.; E. Paialunga; A. Grattagliano; Micheli, L. Label-Free Electrochemical Immunosensors: A Practical Guide. *TrAC, Trends Anal. Chem.* **2024**, *180*, 117949–117949. <https://doi.org/10.1016/j.trac.2024.117949>
- (47) Ricci, F.; Adornetto, G.; Palleschi, G. A Review of Experimental Aspects of Electrochemical Immunosensors. *Electrochim. Acta* **2012**, *84*, 74–83. <https://doi.org/10.1016/j.electacta.2012.06.033>
- (48) Zhang, P.; Wang, R. Label-Free Biosensor. *Biosensors* **2023**, *13* (5), 556. <https://doi.org/10.3390/bios13050556>
- (49) Holmes, C.; Tabrizian, M. *Surface Functionalization of Biomaterials*. In: Vishwakarma, A.; Sharpe, P.; Shi, S., Ramalingam, M. (Eds.). *Stem Cell Biology and Tissue Engineering in Dental Sciences*. Academic Press, 2015. Chapter 14, pp 187–206. <https://doi.org/10.1016/B978-0-12-397157-9.00016-3>
- (50) Shanbhag, M. M.; Manasa, G.; Mascarenhas, R. J.; Mondal, K.; Shetti, N. P. Fundamentals of Bio-Electrochemical Sensing. *Chem. Eng. J. Adv.* **2023**, *16*, 100516. <https://doi.org/10.1016/j.cej.2023.100516>
- (51) Cancelliere, R.; Albano, D.; Brugnoli, B.; Buonasera, K.; Leo, G.; Margonelli, A.; Rea, G. Electrochemical and Morphological Layer-By-Layer Characterization of Electrode Interfaces during a Label-Free Impedimetric Immunosensor Build-Up: The Case of Ochratoxin A. *Appl. Surf. Sci.* **2021**, *567*, 150791. <https://doi.org/10.1016/j.apsusc.2021.150791>
- (52) Vestergaard, M.; Kerman, K.; Tamiya, E. An Overview of Label-Free Electrochemical Protein Sensors. *Sensors* **2007**, *7* (12), 3442–3458. <https://doi.org/10.3390/s7123442>
- (53) Rahn, K. L.; Peramune, U.; Zhang, T.; Anand, R. K. Label-Free Electrochemical Methods for Disease Detection. *Annu. Rev. Anal. Chem.* **2023**, *16* (1), 49–69. <https://doi.org/10.1146/annurev-anchem-091622-085754>
- (54) Sang, S.; Wang, Y.; Feng, Q.; Wei, Y.; Ji, J.; Zhang, W. Progress of New Label-Free Techniques for Biosensors: A Review. *Crit. Rev. Biotechnol.* **2015**, *36* (3), 1–17. <https://doi.org/10.3109/07388551.2014.991270>
- (55) Wikandari, R.; Hasniah, N.; Taherzadeh, M. J. The role of filamentous fungi in advancing the development of a sustainable circular bioeconomy. *Bioresour. Technol.* **2022**, *345*, 126531. <https://doi.org/10.1016/j.biortech.2021.126531>
- (56) Rietjens, I. M. C. M.; Pascale, M.; Pellegrino, G.; Ribera, D.; Venâncio, A.; Wang, D.; Korzeniowski, K. The definition of chemical contaminants in food: ambiguity and consequences. *Regul. Toxicol. Pharmacol.* **2024**, *155*, 105739. <https://doi.org/10.1016/j.yrtph.2024.105739>
- (57) Keller, N. P. Fungal secondary metabolism: regulation, function and drug discovery. *Nat. Rev. Microbiol.* **2019**, *17* (3), 167–180. <https://doi.org/10.1038/s41579-018-0121-1>
- (58) Keller, N. P.; Turner, G.; Bennett, J. W. Fungal secondary metabolism—from biochemistry to genomics. *Nat. Rev. Microbiol.* **2005**, *3* (12), 937–947. <https://doi.org/10.1038/nrmicro1286>
- (59) Dijksterhuis, J. Fungal spores: Highly variable and stress-resistant vehicles for distribution and spoilage. *Food Microbiol.* **2019**, *81*, 2–11. <https://doi.org/10.1016/j.fm.2018.11.006>
- (60) Nguyen, T. B. H.; Foulong-Oriol, M.; Jany, J. L.; le Floch, G.; Picot, A. New insights into mycotoxin risk management through fungal population genetics and genomics. *Crit. Rev. Microbiol.* **2024**, *26*, 1–22. <https://doi.org/10.1080/1040841x.2024.2392179>
- (61) Garcia, D.; Ramos A. J.; Sanchis, V.; Marín S. Predicting mycotoxins in foods: a review. *Food Microbiol.*, **2009**, *26* (8), 757–769. <https://doi.org/10.1016/j.fm.2009.05.014>
- (62) Mousavi Khaneghah, A.; Fakhri, Y.; Gahruie, H. H.; Niakousari, M.; Sant’Ana, A. S. Mycotoxins in Cereal-Based Products during 24 Years (1983–2017): A Global Systematic Review. *Trends Food Sci. Technol.* **2019**, *91*, 95–105. <https://doi.org/10.1016/j.tifs.2019.06.007>



- (63) Escrivá, L.; Font, G.; Manyes, L.; Berrada, H. Studies on the presence of mycotoxins in biological samples: An overview. *Toxins* **2017**, 9 (8), 251. <https://doi.org/10.3390/toxins9080251>
- (64) Dey, D. K.; Kang, J.I.; Bajpai, V.K.; Kim, K.; Lee, H.; Sonwal, S.; Simal-Gandara, J.; Xiao, J.; Ali, S.; Huh, Y.S.; Han, Y.K.; Shukla, S. Mycotoxins in food and feed: Toxicity, preventive challenges, and advanced detection techniques for associated diseases. *Crit. Rev. Food Sci. Nutr.* **2023**, 63 (27), 8489-8510. <https://doi.org/10.1080/10408398.2022.2059650>
- (65) Magnoli, A. P.; Poloni, V. L.; Cavaglieri, L. Impact of mycotoxin contamination in the animal feed industry. *Curr. Opin. Food Sci.* **2019**, 29, 99-108. <https://doi.org/10.1016/j.cofs.2019.08.009>
- (66) Gonçalves, R. A.; Schatzmayr, D.; Albalat, A.; Mackenzie, S. Mycotoxins in aquaculture: Feed and food. *Rev. Aquac.* **2020**, 12 (1), 145-175. <https://doi.org/10.1111/raq.12310>
- (67) Köpke, U.; Thiel, B.; Elmholt, S. *Strategies to reduce mycotoxin and fungal alkaloid contamination in organic and conventional cereal production systems*. In: Cooper, J.; Niggli, U.; Leifert, C. (Eds.). *Handbook of organic food safety and quality*. Woodhead Publishing, 2007. Chapter 17, pp 353-391. <https://doi.org/10.1533/9781845693411.3.353>
- (68) Bennett, J. W.; Klich, M. Mycotoxins, *Clin. Microbiol. Rev.* **2003**, 16 (3), 497-516. <https://doi.org/10.1128/cmr.16.3.497-516.2003>
- (69) Veprikova, Z.; Zachariasova, M.; Dzuman, Z.; Zachariasova, A.; Fenclova, M.; Slavikova, P.; Vaclavikova, M.; Mastovska, K.; Hengst, D.; Hajslova, J. Mycotoxins in plant-based dietary supplements: hidden health risk for consumers. *J. Agric. Food Chem.* **2015**, 63 (29), 6633-6643. <https://doi.org/10.1021/acs.jafc.5b02105>
- (70) Orlov, A. V.; Zolotova, M. O.; Novichikhin, D. O.; Belyakov, N. A.; Protasova, S. G.; Nikitin, P. I.; Sinolits, A. V. Stannous Chloride-Modified Glass Substrates for Biomolecule Immobilization: Development of Label-Free Interferometric Sensor Chips for Highly Sensitive Detection of Aflatoxin B1 in Corn. *Biosensors* **2024**, 14, 531. <https://doi.org/10.3390/bios14110531>
- (71) Yadav, N.; Yadav, S.S.; Chhillar, A.K.; Rana, J.S. An Overview of Nanomaterial Based Biosensors for Detection of Aflatoxin B1 Toxicity in Foods. *Food Chem. Toxicol.* **2021**, 152, 112201. <https://doi.org/10.1016/j.fct.2021.112201>
- (72) Ayofemi Olalekan Adeyeye, S. Aflatoxigenic fungi and mycotoxins in food: a review. *Crit. Rev. Food Sci. Nutr.* **2019**, 60, 709–721. <https://doi.org/10.1080/10408398.2018.1548429>
- (73) Akullo, J. O.; Amayo, R.; Okello, D. K.; Mohammed, A.; Muyinda, R.; Magumba, D.; Mweetwa, A. M. Aflatoxin contamination in groundnut and maize food products in Eastern and Northern Uganda. *Cogent Food Agric.* **2023**, 9 (1). <https://doi.org/10.1080/23311932.2023.2221015>
- (74) Sujayasree, O. J.; Chaitanya, A. K.; Bhoite, R.; Pandiselvam, R.; Kothakota, A.; Gavahian, M.; Mousavi Khaneghah, A. Ozone: An advanced oxidation technology to enhance sustainable food consumption through myco-toxin degradation. *Ozone:Sci. Eng.* **2022**, 44(1), 17–37. <https://doi.org/10.1080/01919512.2021.1948388>
- (75) Adácsi, C.; Kovács, S.; Pócsi, I.; Pusztahelyi, T. Elimination of Deoxynivalenol, Aflatoxin B1, and Zearalenone by Gram-Positive Microbes (Firmicutes). *Toxins* **2022**, 14, 591–591. <https://doi.org/10.3390/toxins14090591>
- (76) Assunção, R.; Pinhão, M.; Loureiro, S.; Alvito, P.; Silva, M. J. A multi-endpoint approach to the combined toxic effects of patulin and ochratoxin a in human intestinal cells. *Toxicol. Lett.* **2019**, 313, 120–129. <https://doi.org/10.1016/j.toxlet.2019.06.002>
- (77) Nikolchina, I.; Rodrigues, P. A. preliminary study on mycobiota and ochratoxin a contamination in commercial palm dates (*Phoenix dactylifera*). *Mycotoxin Res.* **2021**, 37, 215–220. <https://doi.org/10.1007/s12550-021-00432-0>
- (78) El-Sayed, R. A.; Jebur, A. B.; Kang, W.; El-Demerdash, F. M. An overview on the major mycotoxins in food products: characteristics, toxicity, and analysis. *J. Future Foods* **2022**, 2, 91–102. <https://doi.org/10.1016/j.jfutfo.2022.03.002>
- (79) Lee, H. J.; Kim, H. D.; Ryu, D. Practical Strategies to Reduce Ochratoxin A in Foods. *Toxins* **2024**, 16, 58. <https://doi.org/10.3390/toxins16010058>

- (80) Taguali, S. C.; Riolo, M.; Dopazo, V.; Meca, G.; Cacciola, S. O. Characterization of mycotoxins produced by two *Fusarium* species responsible for postharvest rot of banana fruit. *J. Plant Pathol.* **2024**, *106*, 1785–1800. <https://doi.org/10.1007/s42161-024-01751-8>
- (81) Stoev, S. D. Balkan Endemic Nephropathy – Still continuing enigma, risk assessment and underestimated hazard of joint mycotoxin exposure of animals or humans. *Chem.-Biol. Interact.* **2017**, *261*, 63–79. <https://doi.org/10.1016/j.cbi.2016.11.018>
- (82) Silva Júnior, S.; Isabel, M.; Machado, D. C.; Medeiros, P. L.; Rodrigues, C. G. Alphatoxin Nanopore Detection of Aflatoxin, Ochratoxin and Fumonisin in Aqueous Solution. *Toxins* **2023**, *15* (3), 183–183. <https://doi.org/10.3390/toxins15030183>
- (83) Qu, L.; Wang, L.; Ji, H.; Fang, Y.; Lei, P.; Zhang, X.; Jin, L.; Sun, D.; Dong, H. Toxic Mechanism and Biological Detoxification of Fumonisin. *Toxins* **2022**, *14*, 182–182. <https://doi.org/10.3390/toxins14030182>
- (84) Di Paola, D.; Iaria, C.; Capparucci, F.; Arangia, A.; Crupi, R.; Cuzzocrea, S.; Spanò, N.; Gugliandolo, E.; Peritore, A. F. Impact of Mycotoxin Contamination on Aquatic Organisms: Toxic Effect of Aflatoxin B1 and Fumonisin B1 Mixture. *Toxins* **2022**, *14*, 518. <https://doi.org/10.3390/toxins14080518>
- (85) Sánchez-torres, P. Emerging alternatives to control fungal contamination. *Curr. Opin. Food Sci.* **2025**, *61*, 101255. <https://doi.org/10.1016/j.cofs.2024.101255>
- (86) Pushparaj, K.; Meyyazhagan, A.; Pappuswamy, M.; Khaneghah, A. M.; Liu, W.; Balasubramanian, B. Occurrence, identification, and decontamination of potential mycotoxins in fruits and fruit by-products. *Food Front.* **2023**, *4*, 32–46. <https://doi.org/10.1002/fft2.198>
- (87) Rovetto, E. I.; Luz, C.; Spada, F. L.; Meca, G.; Riolo, M.; Cacciola, S. O. Diversity of Mycotoxins and Other Secondary Metabolites Recovered from Blood Oranges Infected by *Colletotrichum*, *Alternaria*, and *Penicillium* Species. *Toxins* **2023**, *15* (7), 407–407. <https://doi.org/10.3390/toxins15070407>
- (88) Dong, T.; Qiao, S.; Xu, J.; Shi, J.; Qiu, J.; Ma, G. Effect of Abiotic Conditions on Growth, Mycotoxin Production, and Gene Expression by *Fusarium fujikuroi* Species Complex Strains from Maize. *Toxins* **2023**, *15*, 260. <https://doi.org/10.3390/toxins15040260>
- (89) Wang, M.; Jiang, N.; Xian, H.; Wei, D.; Shi, L.; Feng, X. A single-step solid phase extraction for the simultaneous determination of 8 mycotoxins in fruits by ultra-high performance liquid chromatography tandem mass spectrometry. *J. Chromatogr. A* **2016**, *1429*, 22–29. <https://doi.org/10.1016/j.chroma.2015.12.004>
- (90) Kamle, M.; Mahato, D. K.; Gupta, A.; Pandhi, S.; Sharma, N.; Sharma, B.; Mishra, S.; Arora, S.; Selvakumar, R.; Saurabh, V.; Dhakane-Lad, J.; Kumar, M.; Barua, S.; Kumar, A.; Gamlath, S.; Kumar, P. Citrinin Mycotoxin Contamination in Food and Feed: Impact on Agriculture, Human Health, and Detection and Management Strategies. *Toxins* **2022**, *14*, 85. <https://doi.org/10.3390/toxins14020085>
- (91) Gotthardt, M.; Asam, S.; Gunkel, K.; Moghaddam, A. F.; Baumann, E.; Kietz, R.; Rychlik, M. Quantitation of Six *Alternaria* Toxins in Infant Foods Applying Stable Isotope Labeled Standards. *Front. microbiol.* **2019**, *10*, 1–14. <https://doi.org/10.3389/fmicb.2019.00109>
- (92) Gil-Serna, J.; Patiño, B.; Verheecke-Vaessen, C.; Vázquez, C.; Medina, Á. Searching for the *Fusarium* spp. Which Are Responsible for Trichothecene Contamination in Oats. Using Metataxonomy to Compare the Distribution of Toxigenic Species in Fields from Spain and the UK. *Toxins* **2022**, *14*, 592–592. <https://doi.org/10.3390/toxins14090592>
- (93) Polak-Śliwińska, M.; Paszczyk, B. Trichothecenes in Food and Feed, Relevance to Human and Animal Health and Methods of Detection: A Systematic Review. *Molecules* **2021**, *26*, 454–454. <https://doi.org/10.3390/molecules26020454>
- (94) Nleya, N.; Adetunji, M.; Mwanza, M. Current Status of Mycotoxin Contamination of Food Commodities in Zimbabwe. *Toxins* **2018**, *10* (5), 89. <https://doi.org/10.3390/toxins10050089>
- (95) Ayelign, A.; De Saeger, S. Mycotoxins in Ethiopia: Current Status, Implications to Food Safety and Mitigation Strategies. *Food Control* **2020**, *113*, 107163. <https://doi.org/10.1016/j.foodcont.2020.107163>

- (96) Kebede, H.; Liu, X.; Jin, J.; Xing, F. Current Status of Major Mycotoxins Contamination in Food and Feed in Africa. *Food Control* **2020**, *110*, 106975. <https://doi.org/10.1016/j.foodcont.2019.106975>.
- (97) Oliveira, I. S.; da Silva Junior, A. G.; de Andrade, C. A. S.; Oliveira, M. D. L. Biosensors for Early Detection of Fungi Spoilage and Toxigenic and Mycotoxins in Food. *Curr. Opin. Food Sci.* **2019**, *29*, 64–79. <https://doi.org/10.1016/j.cofs.2019.08.004>
- (98) Azaiez, I.; Font, G.; Mañes, J.; Fernández-Franzón, M. Survey of Mycotoxins in Dates and Dried Fruits from Tunisian and Spanish Markets. *Food Control* **2015**, *51*, 340–346. <https://doi.org/10.1016/j.foodcont.2014.11.033>
- (99) Kosicki, R.; Błajet-Kosicka, A.; Grajewski, J.; Twarużek, M. Multiannual Mycotoxin Survey in Feed Materials and Feedingstuffs. *Anim. Feed Sci. Technol.* **2016**, *215*, 165–180. <https://doi.org/10.1016/j.anifeedsci.2016.03.012>
- (100) Puntischer, H.; Cobankovic, I.; Marko, D.; Warth, B. Quantitation of Free and Modified Alternaria Mycotoxins in European Food Products by LC-MS/MS. *Food Control* **2019**, *102*, 157–165. <https://doi.org/10.1016/j.foodcont.2019.03.019>
- (101) Adegbeyeye, M. J.; Reddy, P. R. K.; Chilaka, C. A.; Balogun, O. B.; Elghandour, M. M. M. Y.; Rivas-Caceres, R. R.; Salem, A. Z. M. Mycotoxin toxicity and residue in animal products: Prevalence, consumer exposure and reduction strategies – A review. *Toxicon* **2020**, *177*, 96–108. <https://doi.org/10.1016/j.toxicon.2020.01.007>
- (102) Cui, X.; Ishfaq, M.; Li, R.; Jin, H.; Guo, Z.; Yang, Y.; Satha, H.; Li, J.; Cheng, P.; Zhang, X. Development of a UPLC-FLD Method for Detection of Aflatoxin B1 and M1 in Animal Tissue to Study the Effect of Curcumin on Mycotoxin Clearance Rates. *Front. Pharmacol.* **2017**, *8*, 1–10. <https://doi.org/10.3389/fphar.2017.00650>
- (103) Zadavec, M.; Vahčić, N.; Brnić, D.; Markov, K.; Frece, J.; Beck, R.; Lešić, T.; Pleadin, J. A study of surface moulds and mycotoxins in Croatian traditional dry-cured meat products. *Int. J. Food Microbiol.* **2020**, *317*, 108459. <https://doi.org/10.1016/j.ijfoodmicro.2019.108459>
- (104) Xu, X.; Xu, X.; Han, M.; Qiu, S.; Hou, X. Development of a Modified QuEChERS Method Based on Magnetic Multiwalled Carbon Nanotubes for the Simultaneous Determination of Veterinary Drugs, Pesticides and Mycotoxins in Eggs by UPLC-MS/MS. *Food Chem.* **2019**, *276*, 419–426. <https://doi.org/10.1016/j.foodchem.2018.10.051>
- (105) Zhao, Y.; Yuan, Y.; Bai, X.-B.; Liu, Y.-M.; Wu, G.; Fa-Shu, Y.; Liao, X. Multi-Mycotoxins Analysis in Liquid Milk by UHPLC-Q-Exactive HRMS after Magnetic Solid-Phase Extraction Based on PEGylated Multi-Walled Carbon Nanotubes. *Food Chem.* **2020**, *305*, 125429–125429. <https://doi.org/10.1016/j.foodchem.2019.125429>
- (106) Cao, X.; Li, X.; Li, J.; Niu, Y.; Shi, L.; Fang, Z.; Zhang, T.; Ding, H. Quantitative Determination of Carcinogenic Mycotoxins in Human and Animal Biological Matrices and Animal-Derived Foods Using Multi-Mycotoxin and Analyte-Specific High Performance Liquid Chromatography-Tandem Mass Spectrometric Methods. *J. Chromatogr. B* **2018**, *1073*, 191–200. <https://doi.org/10.1016/j.jchromb.2017.10.006>
- (107) Zhang, L.; Zheng, Y.; Fu, R.; Chen, Y.; Liu, X. Contribution of Blocking Positions on the Curing Behaviors, Networks and Thermal Properties of Aromatic Diamine-Based Benzoxazines. *Thermochim. Acta* **2018**, *668*, 65–72. <https://doi.org/10.1016/j.tca.2018.08.012>
- (108) Liu, X.; Ying, G.; Sun, C.; Yang, M.; Zhang, L.; Zhang, S.; Xing, X.; Li, Q.; Kong, W. Development of an Ultrasonication-Assisted Extraction Based HPLC with a Fluorescence Method for Sensitive Determination of Aflatoxins in Highly Acidic Hibiscus Sabdariffa. *Front. Pharmacol.* **2018**, *9*, 1–9. <https://doi.org/10.3389/fphar.2018.00284>
- (109) Wei, F.; Liu, X.; Liao, X.; Shi, L.; Zhang, S.; Lu, J.; Zhou, L.; Kong, W. Simultaneous Determination of 19 Mycotoxins in Lotus Seed Using a Multimycotoxin UFLC-MS/MS Method. *J. Pharm. Pharmacol.* **2019**, *71* (7), 1172–1183. <https://doi.org/10.1111/jphp.13101>



- (110) Liu, X.; Ying, G.; Liao, X.; Sun, C.; Wei, F.; Xing, X.; Shi, L.; Sun, Y.; Kong, W.; Zhou, L. Cytometric Microbead Magnetic Suspension Array for High-Throughput Ultrasensitive Detection of Aflatoxin B1. *Anal. Chem.* **2018**, *91* (1), 1194–1202. <https://doi.org/10.1021/acs.analchem.8b05278>
- (111) Liao, X.; Sun, C.; Wei, F.; Zhou, L.; Kong, W. Exploration of the Safe Water Content and Activity Control Points for Medicinal and Edible Lotus Seeds from Mildew. *AMB Express* **2020**, *10* (1), 89. <https://doi.org/10.1186/s13568-020-01019-1>
- (112) Su, C.; Hu, Y.; Gao, D.; Luo, Y.; Chen, A. J.; Jiao, X.; Gao, W. Occurrence of Toxigenic Fungi and Mycotoxins on Root Herbs from Chinese Markets. *J. Food Prot.* **2018**, *81* (5), 754–761. <https://doi.org/10.4315/0362-028x.jfp-17-405>
- (113) Bi, B.; Bao, J.; Xi, G.; Xu, Y.; Zhang, L. Determination of multiple mycotoxin residues in Panax ginseng using simultaneous UPLC-ESI-MS/MS. *J. Food Saf.* **2018**, *38* (4), e12458. <https://doi.org/10.1111/jfs.12458>
- (114) Jiang, F.; Li, P.; Zong, C.; Yang, H. Surface-Plasmon-Coupled Chemiluminescence Amplification of Silver Nanoparticles Modified Immunosensor for High-Throughput Ultrasensitive Detection of Multiple Mycotoxins. *Anal. Chim. Acta* **2020**, *1114*, 58–65. <https://doi.org/10.1016/j.aca.2020.03.052>
- (115) Yao, X.; Meng, W.; Sun, W.; Li, D.; Yu, Z.; Tong, L. Simultaneous Qualitative and Quantitative Analysis of 21 Mycotoxins in Radix Paeoniae Alba by Ultra-High Performance Liquid Chromatography Quadrupole Linear Ion Trap Mass Spectrometry and QuEChERS for Sample Preparation. *J. Chromatogr. B* **2016**, *1031*, 202–213. <https://doi.org/10.1016/j.jchromb.2016.07.008>
- (116) Huang, P.; Kong, W.; Wang, S.; Wang, R.; Lu, J.; Yang, M. Multiclass Mycotoxins in Lotus Seeds Analysed by an Isotope-Labelled Internal Standard-Based UPLC-MS/MS. *J. Pharm. Pharmacol.* **2018**, *70* (10), 1378–1388. <https://doi.org/10.1111/jphp.12974>
- (117) Li, M.; Kong, W.; Li, Y.; Li, H.; Liu, Q.; Dou, X.; Ouyang, Z.; Yang, M. High-Throughput Determination of Multi-Mycotoxins in Chinese Yam and Related Products by Ultra Fast Liquid Chromatography Coupled with Tandem Mass Spectrometry after One-Step Extraction. *J. Chromatogr. B* **2016**, *1022*, 118–125. <https://doi.org/10.1016/j.jchromb.2016.04.014>
- (118) Bolechová, M.; Benešová, K.; Běláková, S.; Čáslavský, J.; Pospíchalová, M.; Mikulíková, R. Determination of Seventeen Mycotoxins in Barley and Malt in the Czech Republic. *Food Control* **2014**, *47*, 108–113. <https://doi.org/10.1016/j.foodcont.2014.06.045>
- (119) Xiao, K.; Wang, K.; Qin, W.; Hou, Y.; Lu, W.; Xu, H.; Wo, Y.; Cui, D. Use of Quantum Dot Beads-Labeled Monoclonal Antibody to Improve the Sensitivity of a Quantitative and Simultaneous Immunochromatographic Assay for Neuron Specific Enolase and Carcinoembryonic Antigen. *Talanta* **2017**, *164*, 463–469. <https://doi.org/10.1016/j.talanta.2016.12.003>
- (120) Liu, H.; Luo, J.; Kong, W.; Liu, Q.; Hu, Y.; Yang, M. UFLC-ESI-MS/MS Analysis of Multiple Mycotoxins in Medicinal and Edible Areca Catechu. *Chemosphere* **2016**, *150*, 176–183. <https://doi.org/10.1016/j.chemosphere.2016.02.032>
- (121) Kong, D.; Kong, W.; Yang, X.; Yang, M. Contamination Parts and Residue Levels of Multi-Mycotoxins in Medicinal and Edible Locust. *Front. Pharmacol.* **2018**, *9*, 1–9. <https://doi.org/10.3389/fphar.2018.00480>
- (122) Nian, Y.; Wang, H.; Ying, G.; Yang, M.; Wang, Z.; Kong, W.; Yang, S. Transfer Rates of Aflatoxins from Herbal Medicines to Decoctions Determined by an Optimized High-Performance Liquid Chromatography with Fluorescence Detection Method. *J. Pharm. Pharmacol.* **2017**, *70* (2), 278–288. <https://doi.org/10.1111/jphp.12856>
- (123) Ojuri, O. T.; Ezekiel, C. N.; Eskola, M. K.; Šarkanj, B.; Babalola, A. D.; Sulyok, M.; Hajšlová, J.; Elliott, C. T.; Krska, R. Mycotoxin Co-Exposures in Infants and Young Children Consuming Household- and Industrially-Processed Complementary Foods in Nigeria and Risk Management Advice. *Food Control* **2019**, *98*, 312–322. <https://doi.org/10.1016/j.foodcont.2018.11.049>
- (124) Casu, A.; Leggieri, M. C.; Toscano, P.; Battilani, P. Changing climate, shifting mycotoxins: A comprehensive review of climate change impact on mycotoxin contamination. *Compr. Rev. Food Sci. Food Saf.* **2024**, *23* (2), e13323. <https://doi.org/10.1111/1541-4337.13323>



- (125) Chhaya, R. S.; O'Brien, J.; Cummins, E. Feed to fork risk assessment of mycotoxins under climate change influences-recent developments. *Trends Food Sci. Technol.* **2022**, 126, 126-141. <https://doi.org/10.1016/j.tifs.2021.07.040>
- (126) McNaught, A. D.; Wilkinson, A. (Eds.). *The IUPAC Compendium of Chemical Terminology*. Wiley, NY, 2014. <https://doi.org/10.1351/goldbook.b00663>
- (127) Nagel, B.; Dellweg, H.; Gierasch, L. M. Glossary for Chemists of Terms Used in Biotechnology (IUPAC Recommendations 1992). *Pure Appl. Chem.* **1992**, 64 (1), 143–168. <https://doi.org/10.1351/pac199264010143>
- (128) Thévenot, D. R.; Toth, K.; Durst, R. A.; Wilson, G. S. Electrochemical Biosensors: Recommended Definitions and Classification. *Biosens. Bioelectron.* **2001**, 16 (1-2), 121–131. [https://doi.org/10.1016/s0956-5663\(01\)00115-4](https://doi.org/10.1016/s0956-5663(01)00115-4)
- (129) Wang, W.; He, Y.; He, S.; Deng, L.; Wang, H.; Cao, Z.; Feng, Z.; Xiong, B.; Yin, Y. A Brief Review of Aptamer-Based Biosensors in Recent Years. *Biosensors* **2025**, 15 (2), 120. <https://doi.org/10.3390/bios15020120>
- (130) Saylan, Y.; Kılıç, S.; Denizli, A. Biosensing Applications of Molecularly Imprinted-Polymer-Based Nanomaterials. *Processes* **2024**, 12 (1), 177–177. <https://doi.org/10.3390/pr12010177>
- (131) Karunakaran, C.; Rajkumar, R.; Bhargava, K. Introduction to Biosensors. In: Karunakaran, H.; Rajkumar, R.; Bhargava, K. (Eds.). *Biosensors and Bioelectronics*. Elsevier, 2015. Chapter 1, pp 1–68. <https://doi.org/10.1016/b978-0-12-803100-1.00001-3>
- (132) Luong, J. H. T.; Male, K. B.; Glennon, J. D. Biosensor Technology: Technology Push versus Market Pull. *Biotechnol. Adv.* **2008**, 26 (5), 492–500. <https://doi.org/10.1016/j.biotechadv.2008.05.007>
- (133) Varnakavi, N.; Lee, N. A Review on Biosensors and Recent Development of Nanostructured Materials-Enabled Biosensors. *Sensors* **2021**, 21 (4), 1109. <https://doi.org/10.3390/s21041109>
- (134) Chadha, U.; Bhardwaj, P.; Agarwal, R.; Rawat, P.; Agarwal, R.; Gupta, I.; Panjwani, M.; Singh, S.; Ahuja, C.; Selvaraj, S. K.; Banavoth, M.; Sonar, P.; Badoni, B.; Chakravorty, A. Recent Progress and Growth in Biosensors Technology: A Critical Review. *Ind. Eng. Chem.* **2022**, 109, 21–51. <https://doi.org/10.1016/j.jiec.2022.02.010>
- (135) Turner, A. P. F. Biochemistry: Biosensors-Sense and Sensitivity. *Science* **2000**, 290 (5495), 1315–1317. <https://doi.org/10.1126/science.290.5495.1315>
- (136) Kumar, A.; Mahato, K. *Recent Advancements in Bioreceptors and Materials for Biosensors*. Elsevier eBooks, 2024. <https://doi.org/10.1016/b978-0-443-15380-8.00007-2>
- (137) Apetrei, C. (Ed.). *Frontiers in Bioactive Compounds*. Bentham Science Publishers, Sharjah, UAE, 2016. <https://doi.org/10.2174/97816810834141160101>
- (138) Newman, J. D.; Setford, S. J. Enzymatic Biosensors. *Mol. Biotechnol.* **2006**, 32 (3), 249–268. <https://doi.org/10.1385/mb:32:3:249>
- (139) Gupta, U.; Gupta, V.; Arun, R. K.; Chanda, N. Recent Advances in Enzymatic Biosensors for Point-Of-Care Detection of Biomolecules. *Biotechnol. Bioeng.* **2022**, 119 (12), 3393–3407. <https://doi.org/10.1002/bit.28251>
- (140) Shahbaz, A.; Hussain, N.; Azeem Intisar; Bilal, M.; Hafiz. Immobilized Enzymes-Based Biosensing Cues for Strengthening Biocatalysis and Biorecognition. *Catal. Lett.* **2021**, 152 (9), 2637–2649. <https://doi.org/10.1007/s10562-021-03866-4>
- (141) Alberts, B.; Heald, R.; Johnson, A.; Morgan, D., *Molecular Biology of the Cell*. Norton & Company, NY, 2022.
- (142) Prajapati, V.; Shrivastav, P. S. Bioreceptors for Antigen–Antibody Interactions. In: Inamuddin, T. A. (Ed.). *Biosensors Nanotechnology*. Wiley, 2023. Chapter 16, pp 371–394. <https://doi.org/10.1002/9781394167135.ch16>
- (143) Pohanka, M. Monoclonal and Polyclonal Antibodies Production - Preparation of Potent Biorecognition Element. *J. Appl. Biomed.* **2009**, 7 (3), 115–121. <https://doi.org/10.32725/jab.2009.012>

- (144) Drummond, T. G.; Hill, M. G.; Barton, J. K. Electrochemical DNA Sensors. *Nat. Biotechnol.* **2003**, 21 (10), 1192–1199. <https://doi.org/10.1038/nbt873>
- (145) Vitae, J.; Castaneda, G.; Carvajal Barbosa, L.; Cepeda, D.; Felipe, A.; Torres, L.; Mercedes, M.; Cortes, A.; Rivera Monroy, Z.; Torres, A.; Arias Cortes, M.; Castaned, J. Nucleic Acid-Based Biosensors: Analytical Devices for Prevention, Diagnosis and Treatment of Diseases. *Vitae* **2021**, 28, 347259. <https://doi.org/10.17533/udea.vitae.v28n3a347259>
- (146) Yang, M.-S.; McGovern, M. E.; Thompson, M. Genosensor Technology and the Detention of Interfacial Nucleic Acid Chemistry. *Anal. Chim. Acta* **1997**, 346 (3), 259–275. [https://doi.org/10.1016/s0003-2670\(97\)90055-6](https://doi.org/10.1016/s0003-2670(97)90055-6)
- (147) Low, S. S.; Loh, H.-S.; Boey, J. S.; Khiew, P. S.; Chiu, W. S.; Tan, M. T. T. Sensitivity Enhancement of Graphene/Zinc Oxide Nanocomposite-Based Electrochemical Impedance Genosensor for Single Stranded RNA Detection. *Biosens. Bioelectron.* **2017**, 94, 365–373. <https://doi.org/10.1016/j.bios.2017.02.038>
- (148) Mohan, S.; Nigam, P.; Kundu, S.; Prakash, R. A Label-Free Genosensor for BRCA1 Related Sequence Based on Impedance Spectroscopy. *Analyst* **2010**, 135 (11), 2887. <https://doi.org/10.1039/c0an00258e>
- (149) Bonanni, A.; Pividori, M. I.; Valle, M. del. Application of the Avidin–Biotin Interaction to Immobilize DNA in the Development of Electrochemical Impedance Genosensors. *Anal. Bioanal. Chem.* **2007**, 389 (3), 851–861. <https://doi.org/10.1007/s00216-007-1490-x>
- (150) Surucu, O.; Öztürk, E.; Kuralay, F. Nucleic Acid Integrated Technologies for Electrochemical Point-Of-Care Diagnostics: A Comprehensive Review. *Electroanalysis* **2021**, 34 (2), 148–160. <https://doi.org/10.1002/elan.202100309>
- (151) Szymczyk, A.; Ziółkowski, R.; Malinowska, E. Modern Electrochemical Biosensing Based on Nucleic Acids and Carbon Nanomaterials. *Sensors* **2023**, 23 (6), 3230. <https://doi.org/10.3390/s23063230>
- (152) Mir, M.; Katakis, I. Target Label-Free, Reagentless Electrochemical DNA Biosensor Based on Sub-Optimum Displacement. *Talanta* **2008**, 75(2), 432–441. <https://doi.org/10.1016/j.talanta.2007.11.035>
- (153) Kokkinos, C. Electrochemical DNA Biosensors Based on Labeling with Nanoparticles. *Nanomaterials* **2019**, 9 (10), 1361. <https://doi.org/10.3390/nano9101361>
- (154) Lemieux, B.; Aharoni, A.; Schena, M. Overview of DNA Chip Technology. *Mol. Breed.* **1998**, 4 (4), 277–289. <https://doi.org/10.1023/a:1009654300686>
- (155) Motorola Clinical Microsensors, eSensor® 4800 system. Available at: <https://www.life-sciences-usa.com/product/esensor-4800-system-motorola-clinical-microsensors-group-ciphergen-2001-4444.html> (accessed on April 2025).
- (156) Adachi, T.; Nakamura, Y. Aptamers: A Review of Their Chemical Properties and Modifications for Therapeutic Application. *Molecules* **2019**, 24(23), 4229. <https://doi.org/10.3390/molecules24234229>
- (157) Lim, Y. C.; Kouzani, A. Z.; Duan, W. Aptasensors: A Review. *J. Biomed. Nanotechnol.* **2010**, 6 (2), 93–105. <https://doi.org/10.1166/jbn.2010.1103>
- (158) Shkempi, X.; Svobodova, M.; Skouridou, V.; Bashammakh, A. S.; Alyoubi, A. O.; O'Sullivan, C. K. Aptasensors for Mycotoxin Detection: A Review. *Anal. Biochem.* **2021**, 644, 114156. <https://doi.org/10.1016/j.ab.2021.114156>
- (159) Breaker, R. DNA Aptamers and DNA Enzymes. *Curr. Opin. Chem. Biol.* **1997**, 1 (1), 26–31. [https://doi.org/10.1016/s1367-5931\(97\)80105-6](https://doi.org/10.1016/s1367-5931(97)80105-6)
- (160) Hong, K. L.; Sooter, L. J. Single-Stranded DNA Aptamers against Pathogens and Toxins: Identification and Biosensing Applications. *BioMed. Res. Int.* **2015**, 2015, 419318. <https://doi.org/10.1155/2015/419318>
- (161) Kang, K. N.; Lee, Y. S. RNA Aptamers: A Review of Recent Trends and Applications. In: Zhong, J. J. (Ed.). *Future Trends in Biotechnology. Advances in Biochemical Engineering/Biotechnology*. Springer, 2012. pp 153–169. [https://doi.org/10.1007/10\\_2012\\_136](https://doi.org/10.1007/10_2012_136)

- (162) Tombelli, S.; Minunni, M.; Mascini, M. Analytical Applications of Aptamers. *Biosens. Bioelectron.* **2005**, *20* (12), 2424–2434. <https://doi.org/10.1016/j.bios.2004.11.006>
- (163) Zhuo, Z.; Yu, Y.; Wang, M.; Li, J.; Zhang, Z.; Liu, J.; Wu, X.; Lu, A.; Zhang, G.; Zhang, B. Recent Advances in SELEX Technology and Aptamer Applications in Biomedicine. *Int. J. Mol. Sci.* **2017**, *18* (10), 2142. <https://doi.org/10.3390/ijms18102142>
- (164) Lyu, C.; Khan, I. M.; Wang, Z. Capture-SELEX for Aptamer Selection: A Short Review. *Talanta* **2021**, *229*, 122274. <https://doi.org/10.1016/j.talanta.2021.122274>
- (165) Kohlberger, M.; Gadermaier, G. SELEX: Critical Factors and Optimization Strategies for Successful Aptamer Selection. *Biotechnol. Appl. Biochem.* **2021**, *69* (5), 1771–1792. <https://doi.org/10.1002/bab.2244>
- (166) Sassolas, A.; Blum, L. J.; Leca-Bouvier, B. D. Electrochemical Aptasensors. *Electroanalysis* **2009**, *21* (11), 1237–1250. <https://doi.org/10.1002/elan.200804554>
- (167) Feng, C.; Dai, S.; Wang, L. Optical Aptasensors for Quantitative Detection of Small Biomolecules: A Review. *Biosens. Bioelectron.* **2014**, *59*, 64–74. <https://doi.org/10.1016/j.bios.2014.03.014>
- (168) ul ain Zahra, Q.; Khan, Q. A.; Luo, Z. Advances in Optical Aptasensors for Early Detection and Diagnosis of Various Cancer Types. *Front. Oncol.* **2021**, *11*, 1–7. <https://doi.org/10.3389/fonc.2021.632165>
- (169) Song, M.; Khan, I.; Wang, Z. Research Progress of Optical Aptasensors Based on AuNPs in Food Safety. *Food Anal. Methods* **2021**, *14* (10), 2136–2151. <https://doi.org/10.1007/s12161-021-02029-w>
- (170) Lei, Y.; Chen, W.; Mulchandani, A. Microbial Biosensors. *Anal. Chim. Acta* **2006**, *568* (1-2), 200–210. <https://doi.org/10.1016/j.aca.2005.11.065>
- (171) Su, L.; Jia, W.; Hou, C.; Lei, Y. Microbial Biosensors: A Review. *Biosens. Bioelectron.* **2011**, *26* (5), 1788–1799. <https://doi.org/10.1016/j.bios.2010.09.005>
- (172) Dako, E.; Bernier, A.-M.; Dadie, A. T.; Jankowski, C. K. The Problems Associated with Enzyme Purification. In: Ekinici, D. (Ed.). *Chemical Biology*. Intech, 2012. Chapter 2, pp 19–40. <https://doi.org/10.5772/33307>
- (173) Inda, M. E.; Lu, T. K. Microbes as Biosensors. *Annu. Rev. Microbiol.* **2020**, *74* (1), 337–359. <https://doi.org/10.1146/annurev-micro-022620-081059>
- (174) Singh, A. K.; Mittal, S.; Das, M.; Saharia, A.; Tiwari, M. Optical Biosensors: A Decade in Review. *Alexandria Eng. J.* **2023**, *67*, 673–691. <https://doi.org/10.1016/j.aej.2022.12.040>
- (175) Uniyal, A.; Srivastava, G.; Pal, A.; Taya, S. A.; Muduli, A. Recent Advances in Optical Biosensors for Sensing Applications: A Review. *Plasmonics* **2023**, *18* (2), 735–750. <https://doi.org/10.1007/s11468-023-01803-2>
- (176) Strianese, M.; Staiano, M.; Ruggiero, G.; Labella, T.; Pellecchia, C.; D'Auria, S. Fluorescence-Based Biosensors. *Methods Mol. Biol.* **2012**, *875*, 193–216. [https://doi.org/10.1007/978-1-61779-806-1\\_9](https://doi.org/10.1007/978-1-61779-806-1_9)
- (177) Ligler, F.S. Fluorescence-Based Optical Biosensors. In: Pavesi, L.; Fauchet, P. M. (Eds.). *Biophotonics. Biological and Medical Physics, Biomedical Engineering*. Springer, 2008. Chapter 11, pp 199–215. [https://doi.org/10.1007/978-3-540-76782-4\\_11](https://doi.org/10.1007/978-3-540-76782-4_11)
- (178) Kim, H.; Ju, J.; Lee, H. N.; Chun, H.; Seong, J. Genetically Encoded Biosensors Based on Fluorescent Proteins. *Sensors* **2021**, *21* (3), 795. <https://doi.org/10.3390/s21030795>
- (179) Nishi, K.; Isobe, S.-I.; Zhu, Y.; Kiyama, R. Fluorescence-Based Bioassays for the Detection and Evaluation of Food Materials. *Sensors* **2015**, *15* (10), 25831–25867. <https://doi.org/10.3390/s151025831>
- (180) Pei, X.; Zhang, B.; Tang, J.; Liu, B.; Lai, W.; Tang, D. Sandwich-Type Immunosensors and Immunoassays Exploiting Nanostructure Labels: A Review. *Anal. Chim. Acta* **2013**, *758*, 1–18. <https://doi.org/10.1016/j.aca.2012.10.060>

- (181) Ibraheem, A.; Campbell, R. E. Designs and Applications of Fluorescent Protein-Based Biosensors. *Curr. Opin. Chem. Biol.* **2010**, *14* (1), 30–36. <https://doi.org/10.1016/j.cbpa.2009.09.033>
- (182) Verma, A. K.; Noumani, A.; Yadav, A. K.; Solanki, P. R. FRET Based Biosensor: Principle Applications Recent Advances and Challenges. *Diagnostics* **2023**, *13* (8), 1375–1375. <https://doi.org/10.3390/diagnostics13081375>
- (183) Beljonne, D.; Curutchet, C.; Scholes, G. D.; Silbey, R. J. Beyond Förster Resonance Energy Transfer in Biological and Nanoscale Systems. *J. Phys. Chem. B* **2009**, *113* (19), 6583–6599. <https://doi.org/10.1021/jp900708f>
- (184) Shi, Z.; Gao, X.; Zhang, W.; Chen, B.; Wang, M.; Liao, K.; Wang, Z.; Ren, L.; Zhai, Y.; Qiu, Y.; Wang, X.; Lin, Y. Novel Bimolecular Fluorescence Complementation (BiFC) Assay for Visualization of the Protein–Protein Interactions and Cellular Protein Complex Localizations. *Mol. Biotechnol.* **2023**, *66* (9), 2548–2557. <https://doi.org/10.1007/s12033-023-00860-6>
- (185) Haustein, E.; Schwille, P. Single-Molecule Spectroscopic Methods. *Curr. Opin. Struct. Biol.* **2004**, *14* (5), 531–540. <https://doi.org/10.1016/j.sbi.2004.09.004>
- (186) Khansili, N.; Rattu, G.; Krishna, P. M. Label-Free Optical Biosensors for Food and Biological Sensor Applications. *Sens. Actuators, B* **2018**, *265*, 35–49. <https://doi.org/10.1016/j.snb.2018.03.004>
- (187) Singh, P. SPR Biosensors: Historical Perspectives and Current Challenges. *Sens. Actuators, B* **2016**, *229*, 110–130. <https://doi.org/10.1016/j.snb.2016.01.118>
- (188) Chiu, N.-F. The Current Status and Future Promise of SPR Biosensors. *Biosensors* **2022**, *12* (11), 933. <https://doi.org/10.3390/bios12110933>
- (189) Ravindran, N.; Kumar, S.; Yashini, M.; Rajeshwar, S.; Mamathi, C. A.; Thirunavookarasu, N. S.; C K, Sunil, C. K. Recent Advances in Surface Plasmon Resonance (SPR) Biosensors for Food Analysis: A Review. *Crit. Rev. Food Sci. Nutr.* **2021**, 1–23. <https://doi.org/10.1080/10408398.2021.1958745>
- (190) Waychunas, G. A. Luminescence Spectroscopy. *Rev. Mineral. Geochem.* **2014**, *78* (1), 175–217. <https://doi.org/10.2138/rmg.2014.78.5>
- (191) Kulmala, S.; Suomi, J. Current Status of Modern Analytical Luminescence Methods. *Anal. Chim. Acta* **2003**, *500* (1), 21–69. <https://doi.org/10.1016/j.aca.2003.09.004>
- (192) Dodeigne, C. Chemiluminescence as Diagnostic Tool. A Review. *Talanta* **2000**, *51* (3), 415–439. [https://doi.org/10.1016/S0039-9140\(99\)00294-5](https://doi.org/10.1016/S0039-9140(99)00294-5)
- (193) Sheetanshu, G.; Dharendra, K.; Ahmed, A.; Mohamed, A. E. A.; Costanza, F.; Paola, D.; Ali, R. A. M. Modern Optical Sensing Technologies and Their Applications in Agriculture. *Afr. J. Agric. Res.* **2024**, *20* (10), 896–909. <https://doi.org/10.5897/ajar2024.16714>
- (194) Roda, B.; Deo, S. K.; O'Connor, G.; Moraskie, M.; Giordani, S.; Marassi, V.; Roda, A.; Daunert, S. Shining Light on Biosensors: Chemiluminescence and Bioluminescence in Enabling Technologies. *TrAC, Trends Anal. Chem.* **2024**, *180*, 117975. <https://doi.org/10.1016/j.trac.2024.117975>
- (195) Deshpande, K. B.; Lizy Kanungo. Chemiluminescence and Fluorescence Biosensors for Food Application: A Review. *Sens. Actuators Rep.* **2023**, *5*, 100137–100137. <https://doi.org/10.1016/j.snr.2022.100137>
- (196) Herzer, S.; Englert, D. F. Nucleic Acid Hybridization. In: Gerstein, A. S. (Ed.). *Molecular Biology Problem Solver: A Laboratory Guide*. Wiley, 2001. Chapter 14, pp 399–460. <https://doi.org/10.1002/0471223905.ch14>
- (197) Skládal, P. Piezoelectric Biosensors. *TrAC, Trends Anal. Chem.* **2016**, *79*, 127–133. <https://doi.org/10.1016/j.trac.2015.12.009>
- (198) Pohanka, M. The Piezoelectric Biosensors: Principles and Applications, a Review. *Int. J. Electrochem. Sci.* **2017**, *12* (1), 496–506. <https://doi.org/10.20964/2017.01.44>
- (199) Bandey, H. L.; Martin, S. J.; Cernosek, R. W.; Hillman, A. R. Modeling the Responses of Thickness-Shear Mode Resonators under Various Loading Conditions. *Anal. Chem.* **1999**, *71* (11), 2205–2214. <https://doi.org/10.1021/ac981272b>



- (200) Miao, H.; Li, F. Shear Horizontal Wave Transducers for Structural Health Monitoring and Nondestructive Testing: A Review. *Ultrasonics* **2021**, *114*, 106355–106355. <https://doi.org/10.1016/j.ultras.2021.106355>
- (201) Wang, L.; Song, J.; Yu, C. The Utilization and Advancement of Quartz Crystal Microbalance (QCM): A Mini Review. *Microchem. J.* **2024**, *199*, 109967. <https://doi.org/10.1016/j.microc.2024.109967>
- (202) Benes, E.; Groschl, M.; Seifert, F.; Pohl, A. Comparison between BAW and SAW Sensor Principles. *IEEE Trans. Ultrason. Ferroelectr. Freq. Control* **1998**, *45* (5), 1314–1330. <https://doi.org/10.1109/58.726458>
- (203) Priya, R. B.; Venkatesan, T.; Pandiyarajan, G.; Pandya, H. M. A Short Review of SAW Sensors. *J. Environ. Nanotechnol.* **2015**, *4* (4), 15–22. <https://doi.org/10.13074/jent.2015.12.154171>
- (204) Brugger, M. S.; Schnitzler, L. G.; Nieberle, T.; Wixforth, A.; Westerhausen, C. Shear-Horizontal Surface Acoustic Wave Sensor for Non-Invasive Monitoring of Dynamic Cell Spreading and Attachment in Wound Healing Assays. *Biosens. Bioelectron.* **2020**, *173*, 112807–112807. <https://doi.org/10.1016/j.bios.2020.112807>
- (205) Nirschl, M.; Blüher, A.; Erler, C.; Katzschner, B.; Vikholm-Lundin, I.; Auer, S.; Vörös, J.; Pompe, W.; Schreiter, M.; Mertig, M. Film Bulk Acoustic Resonators for DNA and Protein Detection and Investigation of in Vitro Bacterial S-Layer Formation. *Sens. Actuators A: Phys.* **2009**, *156* (1), 180–184. <https://doi.org/10.1016/j.sna.2009.02.021>
- (206) Chen, H.; Hu, Q.-Y.; Yue-Zheng; Jiang, J.-H.; Shen, G.-L.; Yu, R.-Q. Construction of Supported Lipid Membrane Modified Piezoelectric Biosensor for Sensitive Assay of Cholera Toxin Based on Surface-Agglutination of Ganglioside-Bearing Liposomes. *Anal. Chim. Acta* **2009**, *657* (2), 204–209. <https://doi.org/10.1016/j.aca.2009.10.036>
- (207) Skládal, P.; Riccardi, C. dos S.; Yamanaka, H.; da Costa, P. I. Piezoelectric Biosensors for Real-Time Monitoring of Hybridization and Detection of Hepatitis c Virus. *J. Virol. Methods* **2004**, *117* (2), 145–151. <https://doi.org/10.1016/j.jviromet.2004.01.005>
- (208) Serra, B.; Gamella, M.; Reviejo, A. J.; Pingarrón, J. M. Lectin-Modified Piezoelectric Biosensors for Bacteria Recognition and Quantification. *Anal. Bioanal. Chem.* **2008**, *391* (5), 1853–1860. <https://doi.org/10.1007/s00216-008-2141-6>
- (209) Saiz, P. G.; de Luis, R. F.; Lasheras, A.; Arriortua, M. I.; Lopes, A. C. Magnetoelastic Resonance Sensors: Principles, Applications, and Perspectives. *ACS Sens.* **2022**, *7* (5), 1248–1268. <https://doi.org/10.1021/acssensors.2c00032>
- (210) Ren, L.; Yu, K.; Tan, Y. Applications and Advances of Magnetoelastic Sensors in Biomedical Engineering: A Review. *Materials* **2019**, *12* (7), 1135. <https://doi.org/10.3390/ma12071135>
- (211) Chen, X.; Wang, Q.; Deng, J.; Hu, N.; Liao, Y.; Yang, J. An Amplitude Analysis-Based Magnetoelastic Biosensing Method for Quantifying Blood Coagulation. *Biosensors* **2025**, *15* (4), 219. <https://doi.org/10.3390/bios15040219>
- (212) Suryaganesh, M.; Samuel, T. S. A.; Kumar, T. A.; Velammal, M. N. Advanced FET-Based Biosensors—a Detailed Review. *Lect. Notes Netw. Syst.* **2021**, *281*, 273–284. [https://doi.org/10.1007/978-981-16-4244-9\\_22](https://doi.org/10.1007/978-981-16-4244-9_22)
- (213) Park, J.; Nguyen, H. H.; Woubit, A.; Kim, M. Applications of Field-Effect Transistor (FET)-Type Biosensors. *Appl. Sci. Conver. Technol.* **2014**, *23* (2), 61–71. <https://doi.org/10.5757/asct.2014.23.2.61>
- (214) Janata, J. Historical Review. Twenty Years of Ion-Selective Field-Effect Transistors. *Analyst* **1994**, *119* (11), 2275. <https://doi.org/10.1039/an9941902275>
- (215) Ma, X.; Peng, R.; Mao, W.; Lin, Y.; Yu, H. Recent Advances in Ion-Sensitive Field-Effect Transistors for Biosensing Applications. *Electrochem. Sci. Adv.* **2022**, *3* (3), e2100163. <https://doi.org/10.1002/elsa.202100163>
- (216) Abdelhamid, H. N. Calorimetric Biosensors. In: Hasnain, M. S.; Nayak, A. K.; Aminabhavi, T. M (Eds.). *Fundamentals of Biosensors in Healthcare*. Academic Press, 2024. Chapter 15, pp 359–372. <https://doi.org/10.1016/B978-0-443-21658-9.00009-7>

- (217) Kirchner, P.; Oberländer, J.; Friedrich, P.; Berger, J.; Rysstad, G.; Keusgen, M.; Schöning, M. J. Realisation of a Calorimetric Gas Sensor on Polyimide Foil for Applications in Aseptic Food Industry. *Sens. Actuators, B* **2012**, 170, 60–66. <https://doi.org/10.1016/j.snb.2011.01.032>
- (218) Eggins, B. R. *Chemical Sensors and Biosensors*. Wiley, Chichester, 2004.
- (219) Wang, J. *Analytical Electrochemistry*. Wiley, Hoboken, 2006.
- (220) Grieshaber, D.; MacKenzie, R.; Vörös, J.; Reimhult, E. Electrochemical Biosensors - Sensor Principles and Architectures. *Sensors* **2008**, 8 (3), 1400–1458. <https://doi.org/10.3390/s80314000>
- (221) Ronkainen-Matsuno, N. J.; Thomas, J. H.; Brian, H. H.; Heineman, W. R. Electrochemical Immunoassay Moving into the Fast Lane. *TrAC, Trends Anal. Chem.* **2002**, 21 (4), 213–225. [https://doi.org/10.1016/s0165-9936\(02\)00401-6](https://doi.org/10.1016/s0165-9936(02)00401-6)
- (222) Bauer, C.; Eremenko, A. V.; Ehrentreich-Förster, E.; Bier, F. F.; Makower, A.; Halsall, H. B.; Heineman, W. R.; Scheller, F. W. Zeptomole-Detecting Biosensor for Alkaline Phosphatase in an Electrochemical Immunoassay for 2,4-Dichlorophenoxyacetic Acid. *Anal. Chem.* **1996**, 68 (15), 2453–2458. <https://doi.org/10.1021/ac960218x>
- (223) Jenkins, S. H.; Heineman, W. R.; Halsall, H. B. Extending the Detection Limit of Solid-Phase Electrochemical Enzyme Immunoassay to the Attomole Level. *Anal. Biochem.* **1988**, 168 (2), 292–299. [https://doi.org/10.1016/0003-2697\(88\)90321-1](https://doi.org/10.1016/0003-2697(88)90321-1)
- (224) Brajter-Toth, A.; Chambers, J. Q. *Electroanalytical Methods of Biological Materials*. CRC Press, Boca Raton, 2002. <https://doi.org/10.1201/9780203908907>
- (225) Yao, H.; Jenkins, S. H.; Pesce, A. J.; Halsall, H. B.; Heineman, W. R. Electrochemical Homogeneous Enzyme Immunoassay of Theophylline in Hemolyzed, Icteric, and Lipemic Samples. *Clin. Chem.* **1993**, 39 (7), 1432–1434. <https://doi.org/10.1093/clinchem/39.7.1432>
- (226) Heineman, W. R.; Kissinger, P. T. *Laboratory Techniques in Electroanalytical Chemistry*. CRC Press, NY, Basel, 1996.
- (227) Bartlett, P. N. *Bioelectrochemistry*. John Wiley & Sons, NY, 2008.
- (228) Halsall H. B.; Heineman W. R. Electrochemical immunoassay: an ultrasensitive method. *J. Int. Fed. Clin. Chem.* **1990**, 2 (4), 179-87.
- (229) Trojanowicz, M.; Szewczyńska, M.; Wcisło, M. Electroanalytical Flow Measurements-Recent Advances. *Electroanalysis* **2003**, 15 (5-6), 347–365. <https://doi.org/10.1002/elan.200390041>
- (230) Wijayawardhana, C. A.; Purushothama, S.; Cousino, M. A.; Halsall, H. B.; Heineman, W. R. Rotating Disk Electrode Amperometric Detection for a Bead-Based Immunoassay. *J. Electroanal. Chem.* **1999**, 468 (1), 2–8. [https://doi.org/10.1016/s0022-0728\(99\)00115-1](https://doi.org/10.1016/s0022-0728(99)00115-1)
- (231) Wijayawardhana, C. A.; Halsall, H. B.; Heineman, W. R. Micro Volume Rotating Disk Electrode (RDE) Amperometric Detection for a Bead-Based Immunoassay. *Anal. Chim. Acta* **1999**, 399 (1-2), 3–11. [https://doi.org/10.1016/s0003-2670\(99\)00570-x](https://doi.org/10.1016/s0003-2670(99)00570-x)
- (232) Puchades, R.; Maquieira, A. Recent Developments in Flow Injection Immunoanalysis. *Crit. Rev. Anal. Chem.* **1996**, 26 (4), 195–218. <https://doi.org/10.1080/10408349608050574>
- (233) Jiang, T.; Halsall, H. B.; Heineman, W. R.; Giersch, T.; Hock, B. Capillary Enzyme Immunoassay with Electrochemical Detection for the Determination of Atrazine in Water. *J. Agric. Food Chem.* **1995**, 43 (4), 1098–1104. <https://doi.org/10.1021/jf00052a044>
- (234) Bard, A. J.; Zoski, C. G. *Electroanalytical Chemistry*. CRC Press, Boca Raton, 2010.
- (235) Wightman, R. M. Microvoltammetric Electrodes. *Anal. Chem.* **1981**, 53 (9), 1125A–1134A. <https://doi.org/10.1021/ac00232a004>
- (236) Heinze, J. Ultramicroelectrodes in Electrochemistry. *Angew. Chem. Int. Ed.* **1993**, 32 (9), 1268–1288. <https://doi.org/10.1002/anie.199312681>
- (237) Thomas, J. H.; Ronkainen-Matsuno, N. J.; Farrell, S.; Halsall, H. B.; Heineman, W. R. Microdrop Analysis of a Bead-Based Immunoassay. *Microchem. J.* **2003**, 74 (3), 267–276. [https://doi.org/10.1016/s0026-265x\(03\)00036-5](https://doi.org/10.1016/s0026-265x(03)00036-5)

- (238) Halsall, H. B.; Heineman, W. R.; Farrell, S.; Ronkainen-Matsuno, N. J. Bead-Based Immunoassays with Microelectrode Detection. *Anal. Bioanal. Chem.* **2004**, 379(3), 358–367. <https://doi.org/10.1007/s00216-004-2632-z>
- (239) Kissinger, P. T.; Heineman, W. R. Cyclic Voltammetry. *J. Chem. Educ.* **1983**, 60 (9), 702. <https://doi.org/10.1021/ed060p702>
- (240) Hart, J. P.; Crew, A.; Crouch, E.; Honeychurch, K. C.; Pemberton, R. M. Some Recent Designs and Developments of Screen-Printed Carbon Electrochemical Sensors/Biosensors for Biomedical, Environmental, and Industrial Analyses. *Anal. Lett.* **2004**, 37 (5), 789–830. <https://doi.org/10.1081/al-120030682>
- (241) van Emon, J. M. *Immunoassay and Other Bioanalytical Techniques*. CRC Press, Boca Raton, 2016.
- (242) Ronkainen-Matsuno, N. J.; Thomas, J. H.; Halsall, H. B.; Heineman, W. R. Electrochemical Immunoassay Moving into the Fast Lane. *TrAC, Trends Anal. Chem.* **2002**, 21 (4), 213–225. [https://doi.org/10.1016/s0165-9936\(02\)00401-6](https://doi.org/10.1016/s0165-9936(02)00401-6)
- (243) Niwa, O.; Morita, M.; Tabei, H. Electrochemical Behavior of Reversible Redox Species at Interdigitated Array Electrodes with Different Geometries: Consideration of Redox Cycling and Collection Efficiency. *Anal. Chem.* **1990**, 62 (5), 447–452. <https://doi.org/10.1021/ac00204a006>
- (244) Thomas, J. H.; Sang, K. K.; Hesketh, P. J.; Halsall, H. B.; Heineman, W. R. Bead-Based Electrochemical Immunoassay for Bacteriophage MS2. *Anal. Chem.* **2004**, 76 (10), 2700–2707. <https://doi.org/10.1021/ac035503c>
- (245) Anh, T. M.; Dzyadevych, S. V.; Van, M. C.; Renault, N. J.; Duc, C. N.; Chovelon, J.-M. Conductometric Tyrosinase Biosensor for the Detection of Diuron, Atrazine and Its Main Metabolites. *Talanta* **2004**, 63 (2), 365–370. <https://doi.org/10.1016/j.talanta.2003.11.008>
- (246) Muhammad-Tahir, Z.; Alocilja, E. C. A. Conductometric Biosensor for Biosecurity. *Biosens. Bioelectron.* **2003**, 18 (5-6), 813–819. [https://doi.org/10.1016/s0956-5663\(03\)00020-4](https://doi.org/10.1016/s0956-5663(03)00020-4)
- (247) Yagiuda, K.; Hemmi, A.; Ito, S.; Asano, Y.; Fushinuki, Y.; Chen, C.-Y.; Karube, I. Development of a Conductivity-Based Immunosensor for Sensitive Detection of Methamphetamine (Stimulant Drug) in Human Urine. *Biosens. Bioelectron.* **1996**, 11 (8), 703–707. [https://doi.org/10.1016/0956-5663\(96\)85920-3](https://doi.org/10.1016/0956-5663(96)85920-3)
- (248) Papariello, G. J.; Mukherji, A. K.; Shearer, C. M. Penicillin Selective Enzyme Electrode. *Anal. Chem.* **1973**, 45 (4), 790–792. <https://doi.org/10.1021/ac60326a032>
- (249) Suni, I. I. Impedance Methods for Electrochemical Sensors Using Nanomaterials. *TrAC, Trends Anal. Chem.* **2008**, 27 (7), 604–611. <https://doi.org/10.1016/j.trac.2008.03.012>
- (250) Lakhera, P.; Chaudhary, V.; Jha, A.; Singh, R.; Kush, P.; Kumar, P. Recent Developments and Fabrication of the Different Electrochemical Biosensors Based on Modified Screen Printed and Glassy Carbon Electrodes for the Early Diagnosis of Diverse Breast Cancer Biomarkers. *Mater. Today Chem.* **2022**, 26, 101129. <https://doi.org/10.1016/j.mtchem.2022.101129>
- (251) Ronkainen, N. J.; Halsall, H. B.; Heineman, W. R. Electrochemical Biosensors. *Chem. Soc. Rev.* **2010**, 39 (5), 1747–1763. <https://doi.org/10.1039/b714449k>
- (252) Chien, J. B.; Wallingford, R. A.; Ewing, A. G. Estimation of Free Dopamine in the Cytoplasm of the Giant Dopamine Cell of Planorbis Corneus by Voltammetry and Capillary Electrophoresis. *J. Neurochem.* **1990**, 54 (2), 633–638. <https://doi.org/10.1111/j.1471-4159.1990.tb01918.x>
- (253) Jankowski, J. A.; Schroeder, T. J.; Holz, R. W.; Wightman, R. M. Quantal Secretion of Catecholamines Measured from Individual Bovine Adrenal Medullary Cells Permeabilized with Digitonin. *J. Biol. Chem.* **1992**, 267 (26), 18329–18335. [https://doi.org/10.1016/s0021-9258\(19\)36964-9](https://doi.org/10.1016/s0021-9258(19)36964-9)
- (254) Bruns, D.; Jahn, R. Real-Time Measurement of Transmitter Release from Single Synaptic Vesicles. *Nature* **1995**, 377 (6544), 62–65. <https://doi.org/10.1038/377062a0>
- (255) Malathi, S.; Pakrudheen, I.; Kalkura, S. N.; Webster, T. J.; Balasubramanian, S. Disposable Biosensors Based on Metal Nanoparticles. *Sensors* **2022**, 3, 100169. <https://doi.org/10.1016/j.sintl.2022.100169>



- (256) Turkmen, E.; Bas, S. Z.; Gulce, H.; Yildiz, S. Glucose Biosensor Based on Immobilization of Glucose Oxidase in Electropolymerized Poly(o-Phenylenediamine) Film on Platinum Nanoparticles-Polyvinylferrocenium Modified Electrode. *Electrochim. Acta* **2014**, *123*, 93–102. <https://doi.org/10.1016/j.electacta.2013.12.189>
- (257) Li, Y.; Schluesener, H. J.; Xu, S. Gold Nanoparticle-Based Biosensors. *Gold Bull.* **2010**, *43* (1), 29–41. <https://doi.org/10.1007/BF03214964>
- (258) Tian, D.; Duan, C.; Wang, W.; Li, N.; Zhang, H.; Cui, H.; Lu, Y. Sandwich-Type Electrochemiluminescence Immunosensor Based on N-(Aminobutyl)-N-Ethylisoluminol Labeling and Gold Nanoparticle Amplification. *Talanta* **2009**, *78* (2), 399–404. <https://doi.org/10.1016/j.talanta.2008.11.037>
- (259) Yan, Z.; Yang, M.; Wang, Z.; Zhang, F.; Xia, J.; Shi, G.; Xia, L.; Li, Y.; Xia, Y.; Xia, L. A Label-Free Immunosensor for Detecting Common Acute Lymphoblastic Leukemia Antigen (CD10) Based on Gold Nanoparticles by Quartz Crystal Microbalance. *Sens. Actuators, B* **2015**, *210*, 248–253. <https://doi.org/10.1016/j.snb.2014.12.104>
- (260) Sugawa, K.; Tahara, H.; Yamashita, A.; Otsuki, J.; Sagara, T.; Harumoto, T.; Yanagida, S. Refractive Index Susceptibility of the Plasmonic Palladium Nanoparticle: Potential as the Third Plasmonic Sensing Material. *ACS Nano* **2015**, *9* (2), 1895–1904. <https://doi.org/10.1021/nn506800a>
- (261) Alizadeh, M.; Zarei, M.; Ebratkhan, M.; Amjadi, M. Synthesis of Different Morphologies of Metal and Metal Oxide Nanoparticles and Investigation of Their Catalytic Properties by Optical Methods. *J. Mol. Struct.* **2021**, *1244*, 130943. <https://doi.org/10.1016/j.molstruc.2021.130943>
- (262) Ribeiro, C. A. S.; Albuquerque, L. J. C.; De Castro, C. E.; Pereira, R. M.; Albuquerque, B. L.; Pavlova, E.; Schlüter, L. G.; Batista, B. L.; Bellettini, I. C.; Giacomelli, F. C. Ready-to-Use Room Temperature One-Pot Synthesis of Surface-Decorated Gold Nanoparticles with Targeting Attributes. *J. Colloid Interface Sci.* **2022**, *614*, 489–501. <https://doi.org/10.1016/j.jcis.2022.01.145>
- (263) Kumar, S.; Bukkitgar, S. D.; Singh, S.; Pratibha; Singh, V.; Reddy, K. R.; Shetti, N. P.; Venkata Reddy, Ch.; Sadhu, V.; Naveen, S. Electrochemical Sensors and Biosensors Based on Graphene Functionalized with Metal Oxide Nanostructures for Healthcare Applications. *Chem. Select* **2019**, *4* (18), 5322–5337. <https://doi.org/10.1002/slct.201803871>
- (264) Lawrence, N. S.; Liang, H. Metal Nanoparticles: Applications in Electroanalysis. In Nanostructured Materials in Electrochemistry. In Eftekhari, A. (Ed.). *Nanostructured Materials in Electrochemistry*. Wiley, 2008. Chapter 12, pp 435–457. <https://doi.org/10.1002/9783527621507.ch12>
- (265) Rushing, B. R.; Selim, M. I. Aflatoxin B1: A Review on Metabolism, Toxicity, Occurrence in Food, Occupational Exposure, and Detoxification Methods. *Food Chem. Toxicol.* **2019**, *124*, 81–100. <https://doi.org/10.1016/j.fct.2018.11.047>
- (266) Yu, L.; Zhang, Y.; Hu, C.; Wu, H.; Yang, Y.; Huang, C.; Jia, N. Highly Sensitive Electrochemical Impedance Spectroscopy Immunosensor for the Detection of AFB1 in Olive Oil. *Food Chem.* **2015**, *176*, 22–26. <https://doi.org/10.1016/j.foodchem.2014.12.030>
- (267) Zaijun, L.; Zhongyun, W.; Xiulan, S.; Yinjun, F.; Peipei, C. A Sensitive and Highly Stable Electrochemical Impedance Immunosensor Based on the Formation of Silica Gel-Ionic Liquid Biocompatible Film on the Glassy Carbon Electrode for the Determination of Aflatoxin B1 in Bee Pollen. *Talanta* **2010**, *80* (5), 1632–1637. <https://doi.org/10.1016/j.talanta.2009.09.058>
- (268) Linting, Z.; Ruiyi, L.; Zaijun, L.; Qianfang, X.; Yinjun, F.; Junkang, L. An Immunosensor for Ultrasensitive Detection of Aflatoxin B1 with an Enhanced Electrochemical Performance Based on Graphene/Conducting Polymer/Gold Nanoparticles/the Ionic Liquid Composite Film on Modified Gold Electrode with Electrodeposition. *Sens. Actuators, B* **2012**, *174*, 359–365. <https://doi.org/10.1016/j.snb.2012.06.051>
- (269) Masoomi, L.; Sadeghi, O.; Banitaba, M. H.; Shahrjerdi, A.; Davarani, S. S. H. A Non-Enzymatic Nanomagnetic Electro-Immunosensor for Determination of Aflatoxin B1 as a Model Antigen. *Sens. Actuators, B* **2013**, *177*, 1122–1127. <https://doi.org/10.1016/j.snb.2012.11.067>



- (270) Xu, W.; Xiong, Y.; Lai, W.; Xu, Y.; Li, C.; Xie, M. A Homogeneous Immunosensor for AFB1 Detection Based on FRET between Different-Sized Quantum Dots. *Biosens. Bioelectron.* **2014**, *56*, 144–150. <https://doi.org/10.1016/j.bios.2014.01.007>
- (271) Zhang, S.; Shen, Y.; Shen, G.; Wang, S.; Shen, G.; Yu, R. Electrochemical Immunosensor Based on Pd–Au Nanoparticles Supported on Functionalized PDDA-MWCNT Nanocomposites for Aflatoxin B1 Detection. *Anal. Biochem.* **2016**, *494*, 10–15. <https://doi.org/10.1016/j.ab.2015.10.008>
- (272) Jiang, Y.; Peng, Z.; Zhang, S.; Li, F.; Liu, Z.; Zhang, J.; Liu, Y.; Wang, K. Facile In-Situ Solvothermal Method to Synthesize Double Shell ZnIn2S4 Nanosheets/TiO2 Hollow Nanosphere with Enhanced Photocatalytic Activities. *Ceram. Int.* **2018**, *44* (6), 6115–6126. <https://doi.org/10.1016/j.ceramint.2017.12.244>
- (273) Rejeb, I. B.; Arduini, F.; Arvinte, A.; Amine, A.; Gargouri, M.; Micheli, L.; Bala, C.; Moscone, D.; Palleschi, G. Development of a Bio-Electrochemical Assay for AFB1 Detection in Olive Oil. *Biosens. Bioelectron.* **2009**, *24* (7), 1962–1968. <https://doi.org/10.1016/j.bios.2008.10.002>
- (274) Tan, Y.; Chu, X.; Shen, G.-L.; Yu, R.-Q. A Signal-Amplified Electrochemical Immunosensor for Aflatoxin B1 Determination in Rice. *Anal. Biochem.* **2009**, *387* (1), 82–86. <https://doi.org/10.1016/j.ab.2008.12.030>
- (275) Wang, D.; Hu, W.; Xiong, Y.; Xu, Y.; Ming Li, C. Multifunctionalized Reduced Graphene Oxide-Doped Polypyrrole/Pyrrolepropylic Acid Nanocomposite Impedimetric Immunosensor to Ultra-Sensitively Detect Small Molecular Aflatoxin B1. *Biosens. Bioelectron.* **2015**, *63*, 185–189. <https://doi.org/10.1016/j.bios.2014.06.070>
- (276) Jin, X.; Chen, L.; Jiang, J.; Shen, G.; Yu, R. Piezoelectric Immunosensor with Gold Nanoparticles Enhanced Competitive Immunoreaction Technique for Quantification of Aflatoxin B1. *Biosens. Bioelectron.* **2009**, *24* (8), 2580–2585. <https://doi.org/10.1016/j.bios.2009.01.014>
- (277) Zhang, D.; Li, P.; Zhang, Q.; Zhang, W. Ultrasensitive Nanogold Probe-Based Immunochromatographic Assay for Simultaneous Detection of Total Aflatoxins in Peanuts. *Biosens. Bioelectron.* **2011**, *26* (6), 2877–2882. <https://doi.org/10.1016/j.bios.2010.11.031>
- (278) Shim, W.-B.; Kim, M. J.; Mun, H.; Kim, M.-G. An Aptamer-Based Dipstick Assay for the Rapid and Simple Detection of Aflatoxin B1. *Biosens. Bioelectron.* **2014**, *62*, 288–294. <https://doi.org/10.1016/j.bios.2014.06.059>
- (279) Beizaei, A.; O' Kane, S. L.; Kamkar, A.; Misaghi, A.; Henahan, G.; Cahill, D. J. Highly Sensitive Toxin Microarray Assay for Aflatoxin B1 Detection in Cereals. *Food Control* **2015**, *57*, 210–215. <https://doi.org/10.1016/j.foodcont.2015.03.039>
- (280) Ko, J.; Lee, C.; Choo, J. Highly Sensitive SERS-Based Immunoassay of Aflatoxin B1 Using Silica-Encapsulated Hollow Gold Nanoparticles. *J. Hazard. Mater.* **2015**, *285*, 11–17. <https://doi.org/10.1016/j.jhazmat.2014.11.018>
- (281) Chen, L.; Jiang, J.; Shen, G.; Yu, R. A Label-Free Electrochemical Impedance Immunosensor for the Sensitive Detection of Aflatoxin B1. *Anal. Methods* **2015**, *7* (6), 2354–2359. <https://doi.org/10.1039/C4AY01981D>
- (282) Hu, J.; Ni, P.; Dai, H.; Sun, Y.; Wang, Y.; Jiang, S.; Li, Z. A Facile Label-Free Colorimetric Aptasensor for Ricin Based on the Peroxidase-like Activity of Gold Nanoparticles. *RSC Adv.* **2015**, *5* (21), 16036–16041. <https://doi.org/10.1039/C4RA17327A>
- (283) Wei, S.; Liu, Y.; Yan, Z.; Liu, L. Molecularly Imprinted Solid Phase Extraction Coupled to High Performance Liquid Chromatography for Determination of Aflatoxin M1 and B1 in Foods and Feeds. *RSC Adv.* **2015**, *5* (27), 20951–20960. <https://doi.org/10.1039/C4RA16784H>
- (284) Bhardwaj, H.; Pandey, M. K.; Rajesh; Sumana, G. Electrochemical Aflatoxin B1 Immunosensor Based on the Use of Graphene Quantum Dots and Gold Nanoparticles. *Microchim. Acta* **2019**, *186* (8), article number 592. <https://doi.org/10.1007/s00604-019-3701-5>
- (285) Szabó, T.; Berkesi, O.; Forgó, P.; Josepovits, K.; Sanakis, Y.; Petridis, D.; Dékány, I. Evolution of Surface Functional Groups in a Series of Progressively Oxidized Graphite Oxides. *Chem. Mater.* **2006**, *18* (11), 2740–2749. <https://doi.org/10.1021/cm060258+>

- (286) Yang, H.; Liu, W.; Ma, C.; Zhang, Y.; Wang, X.; Yu, J.; Song, X. Gold–Silver Nanocomposite-Functionalized Graphene Based Electrochemiluminescence Immunosensor Using Graphene Quantum Dots Coated Porous PtPd Nanochains as Labels. *Electrochim. Acta* **2014**, *123*, 470–476. <https://doi.org/10.1016/j.electacta.2014.01.014>
- (287) Sharma, A.; Kumar, A.; Khan, R. Electrochemical Immunosensor Based on Poly (3,4-Ethylenedioxythiophene) Modified with Gold Nanoparticle to Detect Aflatoxin B1. *Mater. Sci. Eng. C* **2017**, *76*, 802–809. <https://doi.org/10.1016/j.msec.2017.03.146>
- (288) Zhang, X.; Li, C.-R.; Wang, W.-C.; Xue, J.; Huang, Y.-L.; Yang, X.-X.; Tan, B.; Zhou, X.-P.; Shao, C.; Ding, S.-J.; Qiu, J.-F. A Novel Electrochemical Immunosensor for Highly Sensitive Detection of Aflatoxin B1 in Corn Using Single-Walled Carbon Nanotubes/Chitosan. *Food Chem.* **2016**, *192*, 197–202. <https://doi.org/10.1016/j.foodchem.2015.06.044>
- (289) Owino, J. H. O.; Arotiba, O. A.; Hendricks, N.; Songa, E. A.; Jahed, N.; Waryo, T. T.; Ngece, R. F.; Baker, P. G. L.; Iwuoha, E. I. Electrochemical Immunosensor Based on Polythionine/Gold Nanoparticles for the Determination of Aflatoxin B1. *Sensors* **2008**, *8* (12), 8262–8274. <https://doi.org/10.3390/s8128262>
- (290) Ma, H.; Sun, J.; Zhang, Y.; Xia, S. Disposable Amperometric Immunosensor for Simple and Sensitive Determination of Aflatoxin B1 in Wheat. *Biochem. Eng. J.* **2016**, *115*, 38–46. <https://doi.org/10.1016/j.bej.2016.08.003>
- (291) Srivastava, S.; Kumar, V.; Ali, M. A.; Solanki, P. R.; Srivastava, A.; Sumana, G.; Saxena, P. S.; Joshi, A. G.; Malhotra, B. D. Electrophoretically Deposited Reduced Graphene Oxide Platform for Food Toxin Detection. *Nanoscale* **2013**, *5* (7), 3043–3051. <https://doi.org/10.1039/c3nr32242d>
- (292) Zhang, L.; Li, Y.; Liu, Y.; Li, H.; Wang, X.; Li, J.; Li, Y. A Novel Electrochemical Aflatoxin B1 Immunosensor Based on Gold Nanoparticle-Modified Multi-Walled Carbon Nanotubes and Chitosan. *New J. Chem.* **2021**, *45*, 15694–15701. <https://doi.org/10.1039/D1NJ02293H>
- (293) Ou, G.; Zhao, A.; Liao, H.; Zhang, Z.; Xiao, F. Au nanoparticles decorated urchin-like Bi<sub>2</sub>S<sub>3</sub> on graphene wrapped carbon fiber microelectrode: Towards electrochemical immunosensor for sensitive determination of aflatoxin B1. *J. Electroanal. Chem.* **2022**, *929*, 117124. <https://doi.org/10.1016/j.jelechem.2022.117124>
- (294) Wang, N.; Liu, Q.; Hu, X.; Wang, F.; Hu, M.; Yu, Q.; Zhang, G. Electrochemical immunosensor based on AuNPs/Zn/Ni-ZIF-8-800@graphene for rapid detection of aflatoxin B1 in peanut oil. *Anal. Biochem.* **2022**, *650*, 114710. <https://doi.org/10.1016/j.ab.2022.114710>
- (295) Oliveira, J. P. de; Burgos-Flórez, F.; Nascimento, I. S. do; Villalba, P. J.; Zucolotto, V. Label-free electrochemical immunosensor for Ochratoxin A detection in coffee. *Food Chem.* **2023**, *372*, 130123. <https://doi.org/10.1016/j.foodchem.2022.130123>
- (296) Kunene, K.; Weber, M.; Sabela, M.; Voiry, D.; Kanchi, S.; Bisetty, K.; Bechelany, M. Highly-efficient electrochemical label-free immunosensor for the detection of ochratoxin A in coffee samples. *Sens. Actuators, B* **2021**, *305*, 127438. <https://doi.org/10.1016/j.snb.2019.127438>
- (297) Kaminiaris, M. D.; Mavrikou, S.; Georgiadou, M.; Paivana, G.; Tsitsigiannis, D. I.; Kintzios, S. An Impedance Based Electrochemical Immunosensor for Aflatoxin B1 Monitoring in Pistachio Matrices. *Chemosensors* **2020**, *8*, 121. <https://doi.org/10.3390/chemosensors8040121>
- (298) Speranza, G. Carbon Nanomaterials: Synthesis, Functionalization and Sensing Applications. *Nanomaterials* **2021**, *11* (4), 967. <https://doi.org/10.3390/nano11040967>
- (299) Kour, R.; Arya, S.; Young, S.-J.; Gupta, V.; Bandhoria, P.; Khosla, A. Review—Recent Advances in Carbon Nanomaterials as Electrochemical Biosensors. *J. Electrochem. Soc.* **2020**, *167* (3), 037555. <https://doi.org/10.1149/1945-7111/ab6bc4>
- (300) Pandey, A.; Guyot-Sionnest, P. Intraband Spectroscopy and Band Offsets of Colloidal II–VI Core/Shell Structures. *J. Chem. Phys.* **2007**, *127* (10), 104710. <https://doi.org/10.1063/1.2766957>
- (301) Luo, L.; Liu, X.; Ma, S.; Li, L.; You, T. Quantification of Zearalenone in Mildewing Cereal Crops Using an Innovative Photoelectrochemical Aptamer Sensing Strategy Based on ZnO-NGQDs Composites. *Food Chem.* **2020**, *322*, 126778. <https://doi.org/10.1016/j.foodchem.2020.126778>

- (302) Isakovski, M. K.; Beljin, J.; Tričković, J.; Rončević, S.; Maletić, S. Current State and Future Perspectives of Carbon-Based Materials in the Environment: Fate and Application. *Recent Pat. Nanotechnol.* **2021**, 15 (3), 183–196. <https://doi.org/10.2174/1872210514666201217150323>
- (303) Pandey, S.; Karakoti, M.; Bhardwaj, D.; Tatrari, G.; Sharma, R.; Pandey, L.; Lee, M.-J.; Sahoo, N. G. Recent Advances in Carbon-Based Materials for High-Performance Perovskite Solar Cells: Gaps, Challenges and Fulfillment. *Nanoscale Adv.* **2023**, 5 (6), 1492–1526. <https://doi.org/10.1039/D3NA00005B>
- (304) Ou, G.; Zhao, A.; Liao, H.; Zhang, Z.; Xiao, F. Au Nanoparticles Decorated Urchin-like Bi<sub>2</sub>S<sub>3</sub> on Graphene Wrapped Carbon Fiber Microelectrode: Towards Electrochemical Immunosensor for Sensitive Determination of Aflatoxin B<sub>1</sub>. *J. Electroanal. Chem.* **2023**, 929, 117124. <https://doi.org/10.1016/j.jelechem.2022.117124>
- (305) Puzyr', A. P.; Purtov, K. V.; Shenderova, O. A.; Luo, M.; Brenner, D. W.; Bondar, V. S. The Adsorption of Aflatoxin B<sub>1</sub> by Detonation-Synthesis Nanodiamonds. *Dokl. Biochem. Biophys.* **2007**, 417 (1), 299–301. <https://doi.org/10.1134/S1607672907060026>
- (306) Kovač, T.; Šarkanj, B.; Klapac, T.; Borišev, I.; Kovač, M.; Nevistić, A.; Strelec, I. Antiaflatoxicogenic Effect of Fullerene C<sub>60</sub> Nanoparticles at Environmentally Plausible Concentrations. *AMB Expr.* **2018**, 8 (1), 14. <https://doi.org/10.1186/s13568-018-0544-0>
- (307) Jafari, S.; Burr, L.; Migliorelli, D.; Galve, R.; Marco, M.-P.; Campbell, K.; Elliott, C.; Suman, M.; Sturla, S. J.; Generelli, S. Smartphone-Based Magneto-Immunosensor on Carbon Black Modified Screen-Printed Electrodes for Point-of-Need Detection of Aflatoxin B<sub>1</sub> in Cereals. *Anal. Chim. Acta* **2022**, 1221, 340118. <https://doi.org/10.1016/j.aca.2022.340118>
- (308) Fang, T.-H.; Wang, T. H.; Yang, J.-C.; Hsiao, Y.-J. Mechanical Characterization of Nanoindented Graphene via Molecular Dynamics Simulations. *Nanoscale Res. Lett.* **2011**, 6 (1), 481. <https://doi.org/10.1186/1556-276X-6-481>
- (309) Wang, Y.; Li, Z.; Wang, J.; Li, J.; Lin, Y. Graphene and Graphene Oxide: Biofunctionalization and Applications in Biotechnology. *Trends Biotechnol.* **2011**, 29 (5), 205–212. <https://doi.org/10.1016/j.tibtech.2011.01.008>
- (310) Sutter, P. W.; Flege, J.-I.; Sutter, E. A. Epitaxial Graphene on Ruthenium. *Nature Mater.* **2008**, 7 (5), 406–411. <https://doi.org/10.1038/nmat2166>
- (311) Kim, K. S.; Zhao, Y.; Jang, H.; Lee, S. Y.; Kim, J. M.; Kim, K. S.; Ahn, J.-H.; Kim, P.; Choi, J.-Y.; Hong, B. H. Large-Scale Pattern Growth of Graphene Films for Stretchable Transparent Electrodes. *Nature* **2009**, 457 (7230), 706–710. <https://doi.org/10.1038/nature07719>
- (312) Dedkov, Y. S.; Fonin, M.; Rüdiger, U.; Laubschat, C. R. Effect in the Graphene/Ni(111) System. *Phys. Rev. Lett.* **2008**, 100 (10), 107602. <https://doi.org/10.1103/PhysRevLett.100.107602>
- (313) Reina, A.; Jia, X.; Ho, J.; Nezich, D.; Son, H.; Bulovic, V.; Dresselhaus, M. S.; Kong, J. Large Area, Few-Layer Graphene Films on Arbitrary Substrates by Chemical Vapor Deposition. *Nano Lett.* **2009**, 9 (1), 30–35. <https://doi.org/10.1021/nl801827v>
- (314) Coraux, J.; N'Diaye, A. T.; Busse, C.; Michely, T. Structural Coherency of Graphene on Ir(111). *Nano Lett.* **2008**, 8 (2), 565–570. <https://doi.org/10.1021/nl0728874>
- (315) Eda, G.; Fanchini, G.; Chhowalla, M. Large-Area Ultrathin Films of Reduced Graphene Oxide as a Transparent and Flexible Electronic Material. *Nature Nanotech* **2008**, 3 (5), 270–274. <https://doi.org/10.1038/nnano.2008.83>
- (316) Huang, L.; Wu, B.; Chen, J.; Xue, Y.; Geng, D.; Guo, Y.; Yu, G.; Liu, Y. Gram-Scale Synthesis of Graphene Sheets by a Catalytic Arc-Discharge Method. *Small* **2013**, 9 (8), 1330–1335. <https://doi.org/10.1002/smll.201202802>
- (317) Park, S.; Ruoff, R. S. Chemical Methods for the Production of Graphenes. *Nature Nanotech* **2009**, 4 (4), 217–224. <https://doi.org/10.1038/nnano.2009.58>
- (318) Chung, C.; Kim, Y.-K.; Shin, D.; Ryoo, S.-R.; Hong, B. H.; Min, D.-H. Biomedical Applications of Graphene and Graphene Oxide. *Acc. Chem. Res.* **2013**, 46 (10), 2211–2224. <https://doi.org/10.1021/ar300159f>



- (319) Ponnammam, D.; Guo, Q.; Krupa, I.; Al-Maadeed, M. A. S. A.; Varughese, K. T.; Thomas, S.; Sadasivuni, K. K. Graphene and Graphitic Derivative Filled Polymer Composites as Potential Sensors. *Phys. Chem. Chem. Phys.* **2015**, *17* (6), 3954–3981. <https://doi.org/10.1039/C4CP04418E>
- (320) Allen, M. J.; Tung, V. C.; Kaner, R. B. Honeycomb Carbon: A Review of Graphene. *Chem. Rev.* **2010**, *110* (1), 132–145. <https://doi.org/10.1021/cr900070d>
- (321) Basta, L.; Moscardini, A.; Fabbri, F.; Bellucci, L.; Tozzini, V.; Rubini, S.; Griesi, A.; Gemmi, M.; Heun, S.; Veronesi, S. Correction: Covalent Organic Functionalization of Graphene Nanosheets and Reduced Graphene Oxide via 1,3-Dipolar Cycloaddition of Azomethine Ylide. *Nanoscale Adv.* **2021**, *3* (21), 6242–6242. <https://doi.org/10.1039/D1NA90092G>
- (322) Ramanathan, T.; Abdala, A. A.; Stankovich, S.; Dikin, D. A.; Herrera-Alonso, M.; Piner, R. D.; Adamson, D. H.; Schniepp, H. C.; Chen, X.; Ruoff, R. S.; Nguyen, S. T.; Aksay, I. A.; Prud'Homme, R. K.; Brinson, L. C. Functionalized Graphene Sheets for Polymer Nanocomposites. *Nature Nanotech* **2008**, *3* (6), 327–331. <https://doi.org/10.1038/nnano.2008.96>
- (323) Farouq, R. Functionalized Graphene/Polystyrene Composite, Green Synthesis and Characterization. *Sci. Rep.* **2022**, *12* (1), 21757. <https://doi.org/10.1038/s41598-022-26270-3>
- (324) Yang, W.; Akhtar, S.; Leifer, K.; Grennberg, H. Noncovalent Functionalization of Graphene in Suspension. *ISRN Org. Chem.* **2013**, *2013*, 1–7. <https://doi.org/10.1155/2013/656185>
- (325) Xiao, Y.; Pang, Y. X.; Yan, Y.; Qian, P.; Zhao, H.; Manickam, S.; Wu, T.; Pang, C. H. Synthesis and Functionalization of Graphene Materials for Biomedical Applications: Recent Advances, Challenges, and Perspectives. *Adv. Sci.* **2023**, *10* (9), 2205292. <https://doi.org/10.1002/adv.202205292>
- (326) Dai, S.; Wu, S.; Duan, N.; Wang, Z. A Near-Infrared Magnetic Aptasensor for Ochratoxin a Based on near-Infrared Upconversion Nanoparticles and Magnetic Nanoparticles. *Talanta* **2016**, *158*, 246–253. <https://doi.org/10.1016/j.talanta.2016.05.063>
- (327) Dai, H. Carbon Nanotubes: Synthesis, Integration, and Properties. *Acc. Chem. Res.* **2002**, *35* (12), 1035–1044. <https://doi.org/10.1021/ar0101640>
- (328) Zamolo, V. A.; Vazquez, E.; Prato, M. Carbon Nanotubes: Synthesis, Structure, Functionalization, and Characterization. In Siegel, J. S., Wu, Y.-T. (Eds.). *Polyarenes II. Topics in Current Chemistry*. Springer, 2013, pp 65–109. [https://doi.org/10.1007/128\\_2012\\_403](https://doi.org/10.1007/128_2012_403)
- (329) Bystrzejewski, M.; Rummeli, M. H.; Lange, H.; Huczko, A.; Baranowski, P.; Gemming, T.; Pichler, T. Single-Walled Carbon Nanotubes Synthesis: A Direct Comparison of Laser Ablation and Carbon Arc Routes. *J. Nanosci. Nanotechnol.* **2008**, *8* (11), 6178–6186. <https://doi.org/10.1166/jnn.2008.SW05>
- (330) Andrews, R.; Jacques, D.; Qian, D.; Rantell, T. Multiwall Carbon Nanotubes: Synthesis and Application. *Acc. Chem. Res.* **2002**, *35* (12), 1008–1017. <https://doi.org/10.1021/ar010151m>
- (331) Yang, G.; Cheng, F.; Zuo, S.; Zhang, J.; Xu, Y.; Hu, Y.; Hu, X. Growing Carbon Nanotubes In Situ Surrounding Carbon Fiber Surface via Chemical Vapor Deposition to Reinforce Flexural Strength of Carbon Fiber Composites. *Polymers* **2023**, *15* (10), 2309. <https://doi.org/10.3390/polym15102309>
- (332) Manocha, L. M.; Patel, H.; Manocha, S.; Roy, A.; Singh, J. P. Development of Carbon/Carbon Composites with Carbon Nanotubes as Reinforcement and Chemical Vapor Infiltration Carbon as Matrix. *J. Nanosci. Nanotechnol.* **2009**, *9* (5), 3119–3124. <https://doi.org/10.1166/jnn.2009.034>
- (333) Zuo, H.; Duan, J.; Lyu, B.; Lyu, W.; Li, Y.; Mei, X.; Liao, Y. Carbon Nanotube Template-Assisted Synthesis of Conjugated Microporous Polytriphenylamine with High Porosity for Efficient Supercapacitive Energy Storage. *Macromol. Rapid Commun.* **2024**, *45* (1), 2300238. <https://doi.org/10.1002/marc.202300238>
- (334) Rajavel, K.; Minitha, C. R.; Ranjith, K. S.; Kumar, R. T. R. Recent Progress on the Synthesis and Applications of Carbon Based Nanostructures. *Recent Pat. Nanotechnol.* **2012**, *6* (2), 99–104. <https://doi.org/10.2174/187221012800270199>
- (335) Eatemadi, A.; Daraee, H.; Karimkhanloo, H.; Kouhi, M.; Zarghami, N.; Akbarzadeh, A.; Abasi, M.; Hanifehpour, Y.; Joo, S. W. Carbon Nanotubes: Properties, Synthesis, Purification, and Medical Applications. *Nanoscale Res. Lett.* **2014**, *9* (1), 393. <https://doi.org/10.1186/1556-276X-9-393>



- (336) Yun, Y.; Shanov, V.; Tu, Y.; Subramaniam, S.; Schulz, M. J. Growth Mechanism of Long Aligned Multiwall Carbon Nanotube Arrays by Water-Assisted Chemical Vapor Deposition. *J. Phys. Chem. B* **2006**, 110 (47), 23920–23925. <https://doi.org/10.1021/jp057171g>
- (337) Li, C.; Yang, Z.; Zhang, X.; Ru, Y.; Gao, D.; Wu, D.; Sun, J. Ultrasonic-Assisted Method for the Preparation of Carbon Nanotube-Graphene/Polydimethylsiloxane Composites with Integrated Thermal Conductivity, Electromagnetic Interference Shielding, and Mechanical Performances. *IJMS* **2022**, 23 (23), 15007. <https://doi.org/10.3390/ijms232315007>
- (338) Guo, J.; Jiang, H.; Teng, Y.; Xiong, Y.; Chen, Z.; You, L.; Xiao, D. Recent Advances in Magnetic Carbon Nanotubes: Synthesis, Challenges and Highlighted Applications. *J. Mater. Chem. B* **2021**, 9 (44), 9076–9099. <https://doi.org/10.1039/D1TB01242H>
- (339) Jang, M.; Kim, S.; Jeong, H.; Ju, S.-Y. Affinity-Mediated Sorting Order Reversal of Single-Walled Carbon Nanotubes in Density Gradient Ultracentrifugation. *Nanotechnology* **2016**, 27 (41), 41LT01. <https://doi.org/10.1088/0957-4484/27/41/41LT01>
- (340) Dubey, R.; Dutta, D.; Sarkar, A.; Chattopadhyay, P. Functionalized Carbon Nanotubes: Synthesis, Properties and Applications in Water Purification, Drug Delivery, and Material and Biomedical Sciences. *Nanoscale Adv.* **2021**, 3 (20), 5722–5744. <https://doi.org/10.1039/D1NA00293G>
- (341) Zhou, Y.; Fang, Y.; Ramasamy, R. Non-Covalent Functionalization of Carbon Nanotubes for Electrochemical Biosensor Development. *Sensors* **2019**, 19 (2), 392. <https://doi.org/10.3390/s19020392>
- (342) Swetha, P. D. P.; Nikitha, A.; Shenoy, M. M.; Shim, Y.-B.; Prasad, K. S. Ni/Ni(OH)<sub>2</sub>-rGO Nanocomposites Sensor for the Detection of Long Forgotten Mycotoxin, Xanthomegnin. *Talanta* **2023**, 253, 123953. <https://doi.org/10.1016/j.talanta.2022.123953>
- (343) Zhou, B.; Xie, H.; Zhou, S.; Sheng, X.; Chen, L.; Zhong, M. Construction of AuNPs/Reduced Graphene Nanoribbons Co-Modified Molecularly Imprinted Electrochemical Sensor for the Detection of Zearalenone. *Food Chem.* **2023**, 423, 136294. <https://doi.org/10.1016/j.foodchem.2023.136294>
- (344) Singh, C.; Srivastava, S.; Ali, Md. A.; Gupta, T. K.; Sumana, G.; Srivastava, A.; Mathur, R. B.; Malhotra, B. D. Carboxylated Multiwalled Carbon Nanotubes Based Biosensor for Aflatoxin Detection. *Sens. Actuators, B* **2013**, 185, 258–264. <https://doi.org/10.1016/j.snb.2013.04.040>
- (345) Wang, Z.; Li, J.; Xu, L.; Feng, Y.; Lu, X. Electrochemical Sensor for Determination of Aflatoxin B1 Based on Multiwalled Carbon Nanotubes-Supported Au/Pt Bimetallic Nanoparticles. *J. Solid State Electrochem.* **2014**, 18 (9), 2487–2496. <https://doi.org/10.1007/s10008-014-2506-z>
- (346) Zhang, H.; Shi, Z.; Cheng, S.; Yang, Q.; Sun, X.; Guo, Y. Ultrasensitive Immunosensor for Aflatoxin B1 Detection Based on Screen-Printed Carbon Electrode Modified by Ferrocene @ Multi-Walled Carbon Nanotubes. *Int. J. Electrochem. Sci.* **2019**, 14 (9), 9170–9180. <https://doi.org/10.20964/2019.09.61>
- (347) Solis, L. N. F.; Silva Junior, G. J.; Bertotti, M.; Angnes, L.; Pereira, S.V.; Fernández-Baldo, M. A.; Regiart, M. Electrochemical microfluidic immunosensor with graphene-decorated gold nanoporous for T-2 mycotoxin detection, *Talanta* **2024**, 273, 125971. <https://doi.org/10.1016/j.talanta.2024.125971>
- (348) Jubeen, F.; Batool, A.; Naz, I.; Sehar, S.; Sadia, H.; Hayat, A.; Kazi, M. Mycotoxins detection in food using advanced, sensitive and robust electrochemical platform of sensors: A review. *Sens. Actuators, A* **2024**, 367, 115045. <https://doi.org/10.1016/j.sna.2024.115045>
- (349) Kalambate, R. P.; Kalambate, P. K.; Khosropour, H.; Thummarati, P.; Chiabchalard, A.; Boonlue, W.; Laiwattanapaisa, W. Exploring advanced functional nanomaterial-based electrochemical sensors for the detection of mycotoxins in food matrices: A comprehensive review. *Chem. Inorg. Mater.* **2024**, 3, 100044. <https://doi.org/10.1016/j.cinorg.2024.100044>
- (350) Jiang, Y.; Sima, Y.; Liu, L.; Zhou, C.; Shi, S.; Wan, K.; Chen, A.; Tang, N.; He, Q.; Liu, J. Research progress on portable electrochemical sensors for detection of mycotoxins in food and environmental samples. *Chem. Eng. J.* **2024**, 485, 149860. <https://doi.org/10.1016/j.cej.2024.149860>

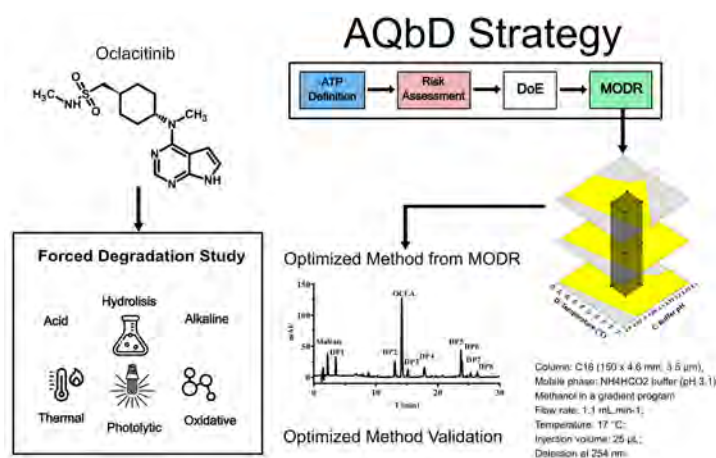
- (351) Yang, Y.; Sun, B.; Ma, Q.; Shi, H.; Dang, Q.; Liu, Y.; Yu, S.; Bao, L.; Yang, L.; Shi, X. A novel electrochemical immunosensor based on AuNPs/N-G@PANI@CS was constructed for the highly sensitive and selective detection of mycotoxin FB1 in food. *J. Food Compos. Anal.* **2025**, *139*, 107083. <https://doi.org/10.1016/j.jfca.2024.107083>
- (352) Deng, K.; Zhang, Y.; Xiao, H.; Hou, Y.; Xu, Q.; Li, Y.; Kong, W.; Ma, L. Nafion-Immobilized Functionalized MWCNT-based Electrochemical Immunosensor for Aflatoxin B1 Detection. *ACS Omega* **2024**, *9* (8), 8754–8762. <https://doi.org/10.1021/acsomega.3c04619>
- (353) Zhang, S.; Wu, C.; Zhao, Z.; Xu, K. An Electrochemical Immunosensor Based on Chitosan–Graphene Nanosheets for Aflatoxin B1 Detection in Corn. *Molecules* **2024**, *29*, 1461. <https://doi.org/10.3390/molecules29071461>
- (354) Pisoschi, A. M.; Iordache, F.; Stanca, L.; Mitranescu, E.; Stoica, L. B.; Geicu, O. I.; Bileanu, L.; Serban, A. I. Biosensors for Food Mycotoxin Determination: A Comparative and Critical Review. *Chemosensors* **2024**, *12* (6), 92–92. <https://doi.org/10.3390/chemosensors12060092>
- (355) Han, Q.; Wang, H.; Wang, J. Multi-Mode/Signal Biosensors: Electrochemical Integrated Sensing Techniques. *Adv. Funct. Mater.* **2024**, *34*, 2403122. <https://doi.org/10.1002/adfm.202403122>
- (356) Stroka, J.; Maragos, C. M. Challenges in the Analysis of Multiple Mycotoxins. *World Mycotoxin J.* **2016**, *9* (5), 847–861. <https://doi.org/10.3920/wmj2016.2038>
- (357) Sadeghi, M.; Sadeghi, S.; Naghib, S. M.; Garshasbi, H. R. A Comprehensive Review on Electrochemical Nano Biosensors for Precise Detection of Blood-Based Oncomarkers in Breast Cancer. *Biosensors* **2023**, *13* (4), 481. <https://doi.org/10.3390/bios13040481>
- (358) Pena-Zacarias, J.; Zahid, M. I.; Nurunnabi, M. Electrochemical Nanosensor-Based Emerging Point-Of-Care Tools: Progress and Prospects. *Wiley Interdiscip. Rev. Nanomed. Nanobiotechnol.* **2024**, *16* (6), e2002. <https://doi.org/10.1002/wnan.2002>
- (359) Wang, M.; Yang, Y.; Min, J.; Song, Y.; Tu, J.; Mukasa, D.; Ye, C.; Xu, C.; Heflin, N.; McCune, J. S.; Hsiai, T. K.; Li, Z.; Gao, W. A Wearable Electrochemical Biosensor for the Monitoring of Metabolites and Nutrients. *Nat. Biomed. Eng.* **2022**, *6*, 1225–1235. <https://doi.org/10.1038/s41551-022-00916-z>
- (360) Jeerapan, I.; Poorahong, S. Review—Flexible and Stretchable Electrochemical Sensing Systems: Materials, Energy Sources, and Integrations. *J. Electrochem. Soc.* **2020**, *167* (3), 037573. <https://doi.org/10.1149/1945-7111/ab7117>
- (361) Guo, L.; Feng, J.; Fang, Z.; Xu, J.; Lu, X. Application of Microfluidic “Lab-On-a-Chip” for the Detection of Mycotoxins in Foods. *Trends Food Sci. Technol.* **2015**, *46* (2), 252–263. <https://doi.org/10.1016/j.tifs.2015.09.005>
- (362) Adunphatcharaphon, S.; Elliott, C. T.; Sooksimuang, T.; Charlermroj, R.; Petchkongkaew, A.; Karoonuthaisiri, N. The Evolution of Multiplex Detection of Mycotoxins Using Immunoassay Platform Technologies. *J. Hazard. Mater.* **2022**, *432*, 128706–128706. <https://doi.org/10.1016/j.jhazmat.2022.128706>
- (363) Zhu, J.; Xu, W.; Yang, Y.; Kong, R.; Wang, J. SsDNA-C3N4 Conjugates-Based Nanozyme Sensor Array for Discriminating Mycotoxins. *Microchim. Acta* **2022**, *190* (1), 6. <https://doi.org/10.1007/s00604-022-05593-y>
- (364) Fu, J.; Yue, X.; Zhang, Q.; Li, P. Early Warning Technologies for Mycotoxins in Grains and Oilseeds: A Review. *Trends Food Sci. Technol.* **2024**, *148*, 104479–104479. <https://doi.org/10.1016/j.tifs.2024.104479>
- (365) Shrivastava, A.; Sharma, R. K. Biosensors for the Detection of Mycotoxins. *Toxin Rev.* **2021**, *41* (2), 618–638. <https://doi.org/10.1080/15569543.2021.1894175>

ARTICLE

# Development and Validation of a Stability-Indicating High-Performance Liquid Chromatography with Diode-Array Detection Method for Oclacitinib Using Analytical Quality by Design Approach

Dalton de Assis de Souza<sup>ID</sup>, Danilo Raul Ossufo Momade<sup>ID</sup>, Allan Michael Junkert<sup>ID</sup>, Alexandre de Fátima Cobre<sup>ID</sup>, Dile Pontarolo Stremel<sup>ID</sup>, Raul Edison Luna Lazo<sup>ID</sup>, Luana Mota Ferreira<sup>ID</sup>, Roberto Pontarolo\*<sup>ID</sup>✉

Programa de Pós-Graduação em Ciências Farmacêuticas, Universidade Federal do Paraná <sup>ROR</sup>. Av. Lothário Meissner, 632, 80210-170, Curitiba, PR, Brazil



This study aimed to develop and validate a stability-indicating method by high performance liquid chromatography to quantify the Oclacitinib (OCLA), on the presence of its degradation products (DPs), by applying Analytical Quality by Design (AQbD) strategy. OCLA was subjected to acidic, alkaline, neutral, photolytic, oxidative, and thermal stress conditions, with degradation products observed under acidic and photolytic conditions. After defining the Analytical Target Profile, the tailing factor, peak purity, and last peak retention time were established as Critical Quality Attributes. The risk assessment led to the designation of the mobile and stationary

phases, the oven temperature, the injection volume and the flow rate as Critical Method Parameters. A screening step was then performed to select categorical variables, and the significant factors were subsequently incorporated into the Box-Behnken Design for method optimization. The optimized method was achieved using Zorbax XBD C18 column (150 x 4.6 mm, 3.5  $\mu$ m), oven temperature 17  $^{\circ}$ C, and injection volume 25  $\mu$ L. The mobile phase consisted of ammonium formate buffer 100 mM, pH 3.1 and methanol, and a flow rate of 1.1 mL min<sup>-1</sup>, eluted by a stepwise gradient. Furthermore, the method demonstrated excellent selectivity and linearity ( $R > 0.999$ ). The theoretical limit of detection was determined to be 5.52  $\mu$ g mL<sup>-1</sup>, while the theoretical limit of quantification was found to be 16.74  $\mu$ g mL<sup>-1</sup>. Furthermore, precision and accuracy were demonstrated with a relative standard deviation below 2.0% and accuracy ranging from 99.87% to 101.38%. Hence, the method was successfully developed, optimized, and validated by applying AQbD approach, becoming a useful methodology for routine quality control of OCLA and its degradation products.

**Cite:** de Souza, D. A.; Momade, D. R. O.; Junkert, A. M.; Cobre, A. F.; Stremel, D. P.; Lazo, R. E. L.; Ferreira, L. M.; Pontarolo, R. Development and Validation of a Stability-Indicating High-Performance Liquid Chromatography with Diode-Array Detection Method for Oclacitinib Using Analytical Quality by Design Approach. *Braz. J. Anal. Chem.* 2025, 12 (49), pp 67-89. <http://dx.doi.org/10.30744/brjac.2179-3425.AR-6-2024>

Submitted January 13, 2024; Resubmitted March 26, 2025; Accepted April 11, 2025; Available online May 21, 2025.

**Keywords:** Forced degradation, liquid chromatography, AQbD, Box-Behnken Design, Janus kinase inhibitor

## INTRODUCTION

Oclacitinib (OCLA), chemically known as N-methyl-1-[4-[methyl(7H-pyrrole[2,3-d]pyrimidine-4-yl)amino]cyclohexyl]methanesulfonamide (Figure 1), is a cyclohexylamine pyrrole derived from pyrimidine.<sup>1</sup> The OCLA functions by inhibiting the activity of Janus kinases 1 and 2 enzymes, which play a role in the signaling pathway involved in inflammatory and immune responses.<sup>2,3</sup> It was approved by the FDA in 2013 to prevent and treat pruritus related to allergic and atopic canine dermatitis.<sup>4,5</sup> Despite its significance, research on analytical methods to determine OCLA in active pharmaceutical ingredient (API) and different formulations is still scarce.

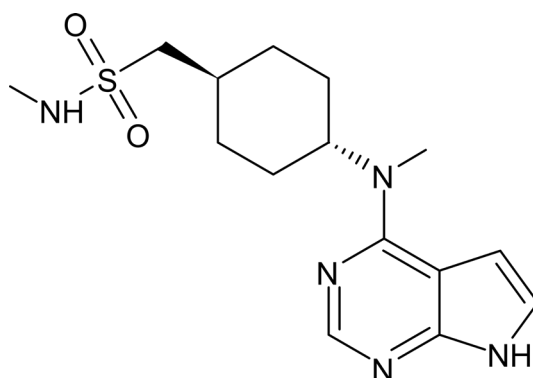


**Figure 1.** The chemical structure of Oclacitinib.

Stability studies aim to provide evidence on drug quality, assessing whether there is variation in the API content or changes in medication characteristics resulting from environmental factors including temperature, humidity, and storage conditions. These modifications are crucial as they directly impact both the drug's efficacy and safety. The presence of DPs may lead to sub-therapeutic doses and/or occurrence of adverse events.<sup>6</sup> Conducting stress tests on the drug compound aids in identifying potential DPs, thereby establishing decomposition pathways and inherent stability of the molecule. Furthermore, it validates the stability-indicating analytical method, ensuring the accurate quantification of the API amidst its degradation products and excipients without interference.<sup>7,8</sup>

A trial-based approach, also known as one-factor-at-a-time (OFaT), is still widely used to develop analytical methods by liquid chromatography. This approach involves altering a chromatographic parameter in each experiment until the desired outcome is achieved. However, it may increase the number of experiments required, as the process relies on the analyst's expertise to rationalize these adjustments. Alternatively, Analytical Quality by Design (AQbD) represents a systematic strategy for developing and validating analytical methods. This approach ensures quality, robustness, and efficiency through the application of risk assessment and multivariate analysis through the design of experiments (DOE).<sup>9-12</sup> Regulatory agencies have recognized the value of AQbD and supported its adoption. The United States Pharmacopeia (USP) is a modern directive that reflects the principles of AQbD, such as USP <1220> "The Analytical Procedure Lifecycle," which describes a sophisticated approach to analytical method development based on sound scientific procedures and quality risk management. Similarly, the International Council for Harmonization (ICH) has developed guidelines such as ICH Q14 and Q2(R2) that align with the AQbD framework, further emphasizing the industry's shift toward a more scientific and risk-based quality assurance model. In this context, the Analytical AQbD approach is directly compatible with ICH Q14 and USP GC <1220>, which advocate a lifecycle management framework for analytical procedures. This framework encompasses Procedure Design, Performance Qualification and Continuous Monitoring, ensuring method robustness and flexibility within predefined Method Operational Design Regions (MODRs).<sup>13,14</sup>



For instance, OCLA has been quantified in the plasma of dogs, cats, and horses through a pharmacokinetic study using liquid chromatography coupled to mass spectroscopy (LC-MS) technique.<sup>15–17</sup> Additionally, our group previously developed a spectrophotometric method for determining OCLA in capsule formulations.<sup>18</sup> To our knowledge, a stability-indicating method utilizing an AQbD approach for OCLA in API to monitor its stability has not been reported. This study aimed to develop a robust stability-indicating HPLC-DAD method based on AQbD for the quantification of OCLA in the presence of its degradation products. Following the establishment of Analytical Target Profiles (ATPs) and Critical Method Attributes (CMAs), a comprehensive risk assessment was conducted to identify and classify Critical Method Parameters (CMPs) as categorical or numerical variables. A screening study was performed to select categorical CMPs, including the type of buffer, organic solvent, and stationary phase, while a preliminary study established fundamental HPLC conditions, such as the initial organic phase ratio, initial organic phase hold time, detection wavelength, and injection volume. These studies also defined the experimental range for further modeling. The method optimization phase employed a Box–Behnken design, a response surface methodology, to evaluate the influence of CMPs on CMAs and establish a robust analytical region, with the optimized parameters positioned at its center. The final method was validated in accordance with ICH and ANVISA guidelines, ensuring its reliability and applicability for laboratory routine.

## **MATERIALS AND METHODS**

### ***Standard and reagents***

Oclacitinib standard was purchased (Nanjing Kaimubo, China, Batch No. 2023031601) with 99.06% purity. The ammonium acetate, HPLC grade acetonitrile (ACN), methanol (MeOH) and tetrahydrofuran (THF) were obtained from J.T.Baker® (New Jersey, USA), formic acid and ammonium formate were from Aldrich (Missouri, USA). Acetic acid and hydrogen peroxide (H<sub>2</sub>O<sub>2</sub>, 30%) was acquired from Labsynth (São Paulo, Brazil). Sodium hydroxide (NaOH) was acquired from ACS Científica (São Paulo, Brazil), and hydrochloric acid (HCl) was acquired from Neon Comercial (São Paulo, Brazil). Ultrapure water was obtained through the Milli-Q® Gradient A10-Millipore purification system (Milford, USA).

### ***Analytical instrumentation***

The analyses were conducted using an Agilent 1100 series HPLC system (Agilent Technologies, California, USA) coupled to a diode-array detector (DAD). The chromatograms were recorded and analyzed through an Agilent ChemStation® version B.04.03[16]. The method development process involved evaluating different combinations of stationary phase, mobile phase, organic modifier and mobile phase pH. The chromatographic columns tested included Agilent Zorbax Eclipse XDB C18 (4.6 mm × 150 mm, 3.5 µm), Waters XBridge BEH C8 (4.6 mm × 150 mm, 5 µm) and Waters Spherisorb® ODS2 (4.6 mm × 150 mm, 5 µm). The mobile phase was composed of 100 mM ammonium acetate buffer (pH 4.76) or ammonium formate buffer (pH 3.75) (mobile phase A), combined with organic solvents such as acetonitrile (ACN), methanol (MeOH) or tetrahydrofuran (THF) (mobile phase B). For monitoring OCLA in the stability tests, a Zorbax C18 (150 × 4.6 mm, 3.5 µm) column was utilized with ammonium formate buffer pH 3.2 and MeOH using a scouting gradient program (5%B at 0.0 min, 5%B from 0.0 to 5 min, 5-80%B from 5.0 to 55 min and 80-5%B from 55-57 min) delivered at 1 mL min<sup>-1</sup> flow rate. The analysis was conducted at 25 °C, with a 25 µL injection volume, and detection at 254 nm.

### ***Standard and sample preparation***

The stock solution of OCLA was prepared in MeOH to achieve a concentration of 1 mg mL<sup>-1</sup> and stored at -40 °C. For the stressing assays, the OCLA standard was prepared in MeOH with a stressing agent at a 50:50 (v/v) ratio, maintaining a final concentration of 1 mg mL<sup>-1</sup> and submitted to 60 °C. Prior to analysis, these solutions were neutralized if necessary, diluted with mobile phase to obtain a working solution with a concentration of 200 µg mL<sup>-1</sup>, and filtered through a 0.22 µm PTFE syringe filter before being subjected to chromatography.

### Forced degradation study

The degradation behavior of OCLA was acquired by subjecting the OCLA solution to various stress-inducing conditions, consisting of acid, alkaline, oxidative, photolytic, and thermal stress.<sup>13,19</sup> These assays were conducted under the following conditions: *i*) Hydrolytic stress (1 M HCl, 1 M NaOH, and neutral hydrolysis at 60 °C); *ii*) oxidative stress (3% H<sub>2</sub>O<sub>2</sub> at room temperature); *iii*) thermal stress (solid-state at 60 °C); and *iv*) photolytic stress (exposure to a light source option 2), in accordance with ICH recommendations.<sup>20</sup> The acid, alkaline, neutral hydrolysis, and oxidative stress tests were monitored for 7 days, thermal stress for 4 days, and photolytic stress for 1.75 days. The stability was assessed by monitoring the appearance of chromatographic peaks, the decrease in OCLA's peak area and comparison with control samples. Lastly, all DPs identified in the forced degradation assay were combined in equal proportions to produce the solution used for method development and optimization.

Preliminary tests were performed to previously establish some parameters such as detection wavelength and injection volume, in addition to a stable pH range to work with OCLA and its degradation products. The detection wavelength was established to allow the simultaneous observation of OCLA and the majority of its degradation products. An injection volume was determined to avoid interference of secondary and non-accumulative photolytic degradation products in the chromatogram, and a pH range was defined in which the ionization of OCLA degradation products remained stable.

### Development of the analytical method using the AQbD approach

The entire process, from ATP definition to validation, is summarized in Figure 2, which presents a flowchart of the AQbD strategy used for method development. All multivariate analyses were conducted using Design Expert v11.1 software.

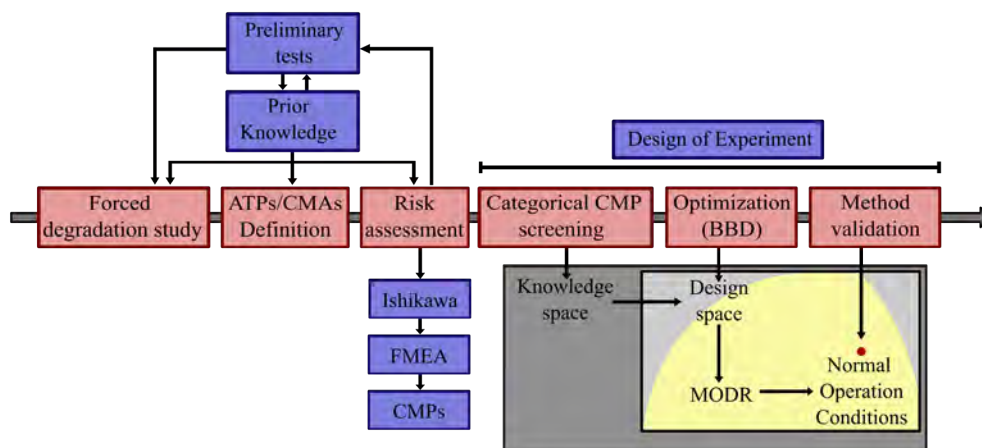


**Figure 2.** Flowchart of the AQbD method development process for OCLA.

### Establishment of analytical target profile and critical method attributes

An AQbD strategy was employed to develop a stability-indicating analytical method to estimate OCLA in the API among its DPs. The proposed Analytical Target Profile (ATP) was structured to outline the intended goals clearly. The ATP elements were categorized into characteristic and performance criteria, along with justifications and potential Critical Method Attributes (CMAs) associated with each element. These CMAs comprised OCLA's resolution, OCLA's adjacent peak resolution, OCLA's tailing factor, OCLA's capacity factor, and the last chromatographic peak capacity factor, intending to reduce the total run time. (Supplementary Figure S1).

### *Risk assessment*

An Ishikawa diagram was proposed to identify parameters that may impact the method's quality. The risk assessment of these parameters was carried out using the Failure Modes and Effects Analysis (FMEA) methodology. In this process, each parameter was evaluated on a scale from 1 to 10, for three key criteria: occurrence, severity, and detection. The likelihood of variation in each parameter will be assessed to assign an occurrence score, while the severity score will determine the potential impact of any variation on the analytical results. The difficulty in detecting such variations will also be evaluated, leading to a detection score. These scores will be multiplied to calculate the Risk Priority Number (RPN) for each parameter.<sup>21,22</sup> Parameters with an RPN above 124 that cannot be addressed through preventive measures or resolved during preliminary tests will be classified as Critical Method Parameters (CMPs). The CMPs will then, be grouped into categorical and continuous variables, based on their nature.

### *Categorical variables screening*

The categorical variables, including organic modifiers (ACN, MeOH and THF), mobile phase buffer (100 mM ammonium acetate buffer and 100 mM ammonium formate buffer), and stationary phases (Spherisorb® ODS2, XBridge BEH C8 and Zorbax Eclipse XBD C18), were combined and tested. The selection criteria for the combination were based on the OCLA capacity factor, with combinations exhibiting capacity factors outside the range of 3 to 15 being excluded. Additional factors considered included baseline stability, prioritizing combinations where the baseline remained stable without significant drift, and the absence of multiple coelutions, with combinations showing many overlapping peaks being discarded. Some OFaT experiments were conducted to establish the Initial Organic Ratio and Initial Organic Hold Time, which were optimized to minimize the loss of the acid degradation product in the dead volume.

### *Optimization*

All the experiments were modeled using Analysis of Variance (ANOVA). The goodness of fit was evaluated based on model significance ( $p$ -value  $< 0.05$ ), lack-of-fit ( $p$ -value  $> 0.05$ ), and higher determination coefficients ( $R^2$ ,  $R^2$ -adj, and  $R^2$ -pred). After establishing the regression for each CMA, the corresponding polynomial equations were used in an overlay plot with quality thresholds, including OCLA's resolution and OCLA's adjacent peak resolution greater than 3, OCLA's tailing factor between 0.8 and 1.5, and last chromatographic peak capacity factor below 22.1. The region encompassing the threshold compliances was designated as the method operable design range (MODR). The normal operating conditions (NOC) and the proven acceptable ranges (PAR's) were selected within this region and tested to evaluate the regression's ability to predict the experiments. The NOC and PARs were validated by comparing the CMA results with the tolerance interval (TI), using a 95% confidence level and a 99% tolerance proportion.

### *Control strategy*

A control strategy was established to ensure the reliability of the optimized method by the definition of the system suitability of the analytical procedure. The system suitability acceptance criteria will be established by analyzing the variation of parameters at the PARs points.<sup>22-24</sup>

### **Method validation**

The validation was conducted in accordance with the ICH Q2(R2) guideline (2005), and the RDC N° 166, from August 24, 2017, by ANVISA, encompassing selectivity, linearity, precision, accuracy, the limit of detection, and the limit of quantification.<sup>13,25</sup> Selectivity was evaluated by assessing spectral purity using the Chemstation peak purity function, the threshold was set at 99% of spectral peak purity. Linearity was assessed by analyzing three independent analytical curves at five levels of standard solution concentration, ranging from 80 to 240  $\mu\text{g mL}^{-1}$ . The regression model was evaluated using correlation ( $R$ ) and determination ( $R^2$ ) coefficients, residual normality by the Ryan-Joiner test and residual homoscedasticity by Levene's test. The significance of the coefficients (angular and linear) was tested using the Student's  $t$ -test, and the model

fit was evaluated through ANOVA. All statistical analyses were performed using Minitab® 17.1.0 (LEAD Technologies, North Carolina, USA) and Prism® 8 (GraphPad, Inc, California, USA). The limit of detection (LoD) and quantification (LoQ) were estimated from the calibration curve parameters, however, for operational purposes, the LoQ should be considered as the lowest concentration point on the calibration curve.

The method's accuracy and precision were assessed using the sample preparation protocol at three concentration levels (80, 160, and 240  $\mu\text{g mL}^{-1}$ ). Accuracy was determined by evaluating the percentage agreement between the values accepted as true values and the values obtained at the low, medium and high levels of the calibration curve. Repeatability of the analytical procedure was evaluated by calculating the relative standard deviation (RSD) at low, medium, and high concentration levels of the calibration curve under the same operating conditions over a short interval of time. Then, the intermediate precision was assessed by calculating the RSD of samples analyzed by different analysts on different days. The method was considered accurate if the recovery ranged between 98% and 102%, and precise if the data exhibited an RSD of less than 2% with similar variance for intermediate precision.<sup>13,25,26</sup>

## RESULTS AND DISCUSSION

### Forced degradation study

The degradation profile of OCLA was determined by subjecting the OCLA solution to acid, alkaline, hydrolytic, oxidative, photolytic and thermal degradation, resulting in the emergence of DPs under both acidic hydrolysis and photolytic conditions (Figure 3). The acidic condition generated a new DP (Figure 3A) with a retention time of 4.1 minutes, and the peak area of OCLA decreased by 19.13% during 7 days of exposure. Conversely, under photolytic stress (Figure 3B), seven DPs were observed across the chromatogram, indicating high sensitivity to light. The peak area of OCLA decreased by 41.08% during 42 h of photolytic exposure. Under alkaline, neutral, thermal, and oxidative stress conditions, no new chromatographic peaks emerged, and there was no notable decrease in the peak area of OCLA (less than 2%).

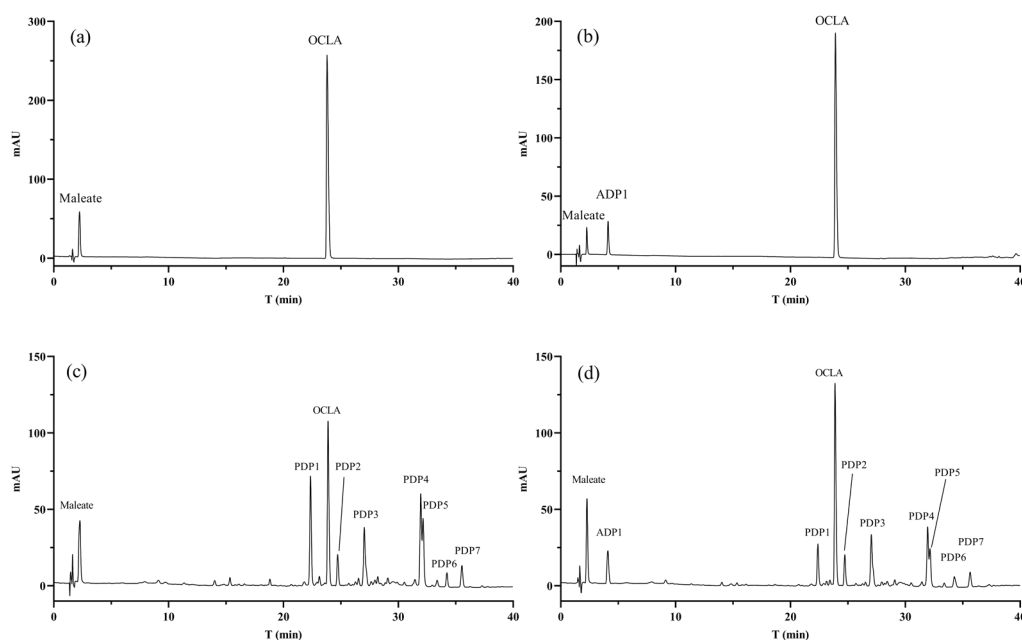


**Figure 3.** Chromatogram obtained from the stress conditions tested.

(Oclacitinib – OCLA; Acid Degradation Product – ADP; Photolytic Degradation Product – PDP) A - OCLA 200 mg B - HCl 1 M 60 °C, 7 days; C - Photolytic chamber (ICH's option 2), 44 hours; D - All degradation products combined. The chromatographic analysis was performed using a Zorbax XBD C18 column (150 × 4.6 mm, 3.5  $\mu\text{m}$ ). The mobile phase consisted of ammonium formate buffer pH 3.2 in combination with MeOH. A scouting gradient program was employed, with the following elution profile: 5%B at 0.0 min, 5%B from 0.0 to 5 min, 5-80%B from 5.0 to 55 min and 80-5%B from 55-57 min. The flow rate was maintained at 1.0 mL min<sup>-1</sup> throughout the analysis. The analysis was conducted at 25 °C, with a 25  $\mu\text{L}$  injection volume, and detection at 254 nm.



### **Development of the analytical method employing the AQbD strategies**

The development of the analytical target represents the initial steps in establishing the objectives and the required performance criteria for the method (Table I).<sup>27</sup> Based on these criteria, the CMAs were established, which directly correlate with the main goal of the method - To develop and validate an RP-HPLC-DAD method with stability-indicating properties for the detection and quantification OCLA avoiding interference from DPs (CMAs - OCLA's resolution and OCLA's adjacent peak resolution) ensuring the absence of chromatographic issues (CMA - OCLA's tailing factor), and minimizing analysis time (CMA - last chromatographic peak capacity factor).

**Table I.** Analytical target profile elements for the development of the stability-indicating method

<b>Purpose of the method</b>			
To develop and validate a stability-indicating RP-HPLC-DAD method capable of detecting and quantitating Oclacitinib without chromatographic issues, avoiding interference from degradation products, and minimizing analysis time.			
<b>ATP element</b>	<b>Target</b>	<b>Justification</b>	<b>Related CMA</b>
<b>Characteristic Criteria</b>			
Sample	OCLA API	Development of the indicative stability method for OCLA in the form of the active pharmaceutical ingredient.	–
Separation	Reversed-phase LC	Oclacitinib is a low polarity drug, and as a result, the reverse phase is often employed for its analysis.	–
Detection	UV-vis	The oclacitinib structure has a chromophore so that the diode array detector may be applied.	–
Method application	Stability study	The method applied to quantify oclacitinib among its degradation products in stability tests.	–
<b>Performance Criteria – Categorical Variables</b>			
Retention time optimization	OCLA's Optimal Retention	Ensuring OCLA's retention time falls within the optimal range is critical for consistent separation, minimizing overlapping peaks, and improving detection reliability.	OCLA's capacity factor > 3 and < 15
Chromatographic issue	Stable Baseline	A stable baseline is required to avoid interference with detection and quantification	Baseline Issues (+ or -)
Absence of interference	Little or no coelution	Multiple co-elutions in the early stages of method development can lead to difficulty in obtaining proper resolution	Multiple Co-elutions (+ or -)
<b>Performance Criteria – Continuous Variables</b>			
Resolution of Critical Pairs	Clear Separation between OCLA and adjacent peaks	Clear separation between oclacitinib and critical peaks prevents co-elution, ensuring accurate and reliable quantification by avoiding interference from adjacent compounds	OCLA's resolution and adjacent peak resolution (> 3)

(continues on next page)

**Table I.** Analytical target profile elements for the development of the stability-indicating method (continuation)

ATP element	Target	Justification	Related CMA
Performance Criteria – Continuous Variables			
Peak Symmetry	Reduce OCLA's tailing	Tailing in chromatographic peaks may affect the method's accuracy and precision, leading to quantification issues.	OCLA's tailing factor (0.8-1.5)
Time of analysis	Reduce total time of analysis	Reducing the total analysis time can result in mobile phase savings.	Capacity factor of the last chromatographic peak (<3Q)

ATP = Analytical target profile, OCLA = Oclacitinib, API = active pharmaceutical ingredient.

The Ishikawa diagram was used to identify parameters that may impact the quality of the method (Supplementary Figure S1). The potential critical method parameters found were grouped into method, sample preparation, mobile phase characteristics, detection and analysis, equipment and environment. These parameters had their degree of risk assessed through the application of the FMEA tool, where Risk Priority Number thresholds were considered as follows: >225 (high risk), 224–175 (unacceptable), 174–125 (need evaluation), 124–50 (acceptable), and <50 (negligible) (see supplementary table SI). This analysis identified the stationary phase, organic modifier, mobile phase buffer, oven temperature, flow rate, mobile phase pH, mobile phase gradient slope, injection volume, and wavelength as critical factors to the method. Other studies have also demonstrated that these variables are commonly considered critical parameters in method development.<sup>28–30</sup>

A screening step was conducted to select the categorical variables, which included the chromatographic column, organic modifier, and mobile phase buffer. The combination of Eclipse XDB C18, MeOH, and ammonium formate 100 mM (pH 3.0) (Supplementary figure S2A) yielded the most favorable profile regarding OCLA's capacity factor, peak resolutions and chromatogram baseline.

To reduce the dimensional space design, some of the continuous variables, such as the injection volume, wavelength, initial organic ratio and hold time were previously tested and fixed at 25  $\mu$ L, 254 nm, 5% and 4 min respectively. Initial tests showed that the analytes were divided into three sections along the chromatogram, an initial analyte for which the initial organic ratio and hold time were optimized, and two groups with four analytes each. To facilitate the modeling of resolution in critical pairs and reduce execution time, a stepwise gradient was developed, in which each of the previously mentioned groups of four analytes was assigned to a specific gradient segment with a defined slope. The slope corresponding to the segment containing only degradation products was fixed at 1.0 [% organic]  $\text{min}^{-1}$ , while the slope of the segment where OCLA elutes was taken to be modeled and optimized. A challenge identified during preliminary tests was the abrupt variation in the capacity factor of a degradation product adjacent to OCLA, depending on the pH applied. This change, likely resulting from an alteration in the molecule's ionization state, was observed around pH 3.3. Considering this effect and the fact that pH values above 3.3 led to the coelution of OCLA with this specific degradation product, the pH range selected for modeling was restricted to values below this threshold.

Finally, the ranges for the continuous variables were defined as follows: gradient slope (0.8–1.2 [% organic]  $\text{min}^{-1}$ ), flow rate (1.0–1.2  $\text{mL min}^{-1}$ ), buffer pH (3.0–3.2), and oven temperature (15–20  $^{\circ}\text{C}$ ). These ranges were applied on the Box-Behnken Design (BBD) to model the method and further optimize it. The stepwise approach ensured that the final method achieved the desired resolution and minimized analysis time. The BBD consisted of 28 experiments described in Supplementary Table SII.

The regression models along with their corresponding statistical parameters for each evaluated CMA are detailed in Table II. The data modeling indicated that a linear model best explained for the last peak capacity factor, the 2FI model more accurately described OCLA's tailing factor, and quadratic models were more suitable for OCLA's resolution and the resolution of its adjacent peak. Factors included in the model were selected based on the adjusted R-squared criterion, applying an output alpha of 0.05. During model

development, transformations such as square root, natural log, base 10 log, inverse, and inverse square root were tested, but none provided a significantly better fit than the raw data. For all modeled CMAs, the statistical analysis confirmed that the models were significant ( $p$ -value  $< 0.05$ ) and showed no lack of fit ( $p$ -value  $> 0.05$ ), suggesting that the model fits the data well and the variability is likely due to random errors. The  $R^2$  values of 0.9912, 0.9810, 0.8762, and 0.9639 for OCLA's resolution, OCLA's adjacent peak resolution (APR), OCLA's tailing factor, and last peak capacity factor, respectively, indicate that the model effectively captures the variability in the data. Furthermore, the  $R^2$ -adj values of 0.9881, 0.9767, 0.8473, and 0.9691 support the inclusion of the coefficients in the model, as their similarity to the  $R^2$  values of 0.9912, 0.9810, 0.8812 and 0.9736 indicates a low likelihood of overfitting. This assessment is further reinforced by the  $R^2$ -pred values of 0.9681, 0.9691, 0.8408, and 0.9600, which indicate strong predictive performance and consistency in the model's generalization capability.

**Table II.** Regression model of Box-Behnken Design experiments. A: mobile phase gradient slope; B: flow rate; C: buffer pH; D: oven temperature; Coef: term coefficients APR – adjacent peak resolution

OCLA's Resolution			OCLA's APR			OCLA's Tailing			Last Peak Capacity factor		
Quadratic model			Quadratic model			2FI Model			Linear Model		
Param	Coef	p-value	Param	Coef	p-value	Param	Coef	p-value	Param	Coef	p-value
A	-0.363	$< 0.001$	A	-0.073	$< 0.001$	A	-0.020	$< 0.001$	A	-2.090	$< 0.001$
B	0.151	$< 0.001$	B	-0.116	$< 0.001$	C	-0.044	$< 0.001$	B	2.170	$< 0.001$
C	-0.971	$< 0.001$	C	0.211	$< 0.001$	D	0.009	0.048	C	0.087	0.010
D	-0.339	$< 0.001$	D	0.080	$< 0.001$	AC	-0.022	0.008	-	-	-
BC	-0.107	0.018	C <sup>2</sup>	-0.055	$< 0.001$	AD	-0.018	0.021	-	-	-
A <sup>2</sup>	0.100	0.005	-	-	-	CD	0.017	0.028	-	-	-
C <sup>2</sup>	0.307	$< 0.001$	-	-	-	-	-	-	-	-	-
Model		$< 0.001$	Model		$< 0.001$	Model		$< 0.001$	Model		$< 0.001$
Lack of fit		0.0726	Lack of fit		0.6893	Lack of fit		0.9696	Lack of fit		0.2779
R <sup>2</sup>		0.9912	R <sup>2</sup>		0.9810	R <sup>2</sup>		0.8812	R <sup>2</sup>		0.9639
R <sup>2</sup> -adjusted		0.9881	R <sup>2</sup> -adjusted		0.9767	R <sup>2</sup> -adjusted		0.8473	R <sup>2</sup> -adjusted		0.9594
R <sup>2</sup> -predicted		0.9681	R <sup>2</sup> -predicted		0.9691	R <sup>2</sup> -predicted		0.8408	R <sup>2</sup> -predicted		0.9491

By analyzing the regression coefficients, related to the parameters and the parameter-interactions of the models of each CMA, it is possible to evaluate the effects of the CMPs and their interaction on the CMAs.<sup>31–33</sup> The buffer pH had a significant impact on the resolution of OCLA and its critical pairs, displaying an inverse relationship with OCLA Resolution but a direct proportional relationship with OCLA APR. This highlights the importance of carefully adjusting this CMP to achieve a balanced resolution. Additionally, the gradient slope influenced the Last Peak Retention Factor, while the flow rate affected both this response and the OCLA APR.

The MODR represents the range within which the combination of variables ensures the suitability of the analytical procedure for its intended application, as defined by the established CMAs. The MODR graph delineates a boundary that separates the regression model from the CMAs, signaling that the results fall within the acceptable range.<sup>34</sup> This robust region ensures the quality of the method by allowing adjustments within these defined limits. The quality verification of the method can be performed through a univariate test on experimental points to assess their concordance with the regression model.<sup>34,35</sup>

Once the model was fitted, the regressions were combined into an overlay plot (Figure 4). This plot was used to establish the quality thresholds for the CMAs, which included OCLA's Resolution and OCLA's APR below 3, OCLA's tailing factor between 0.8 and 1.5 and last peak capacity factor below 22.1. The MODR is depicted as the yellow area, where all CMAs meet the specified criteria.

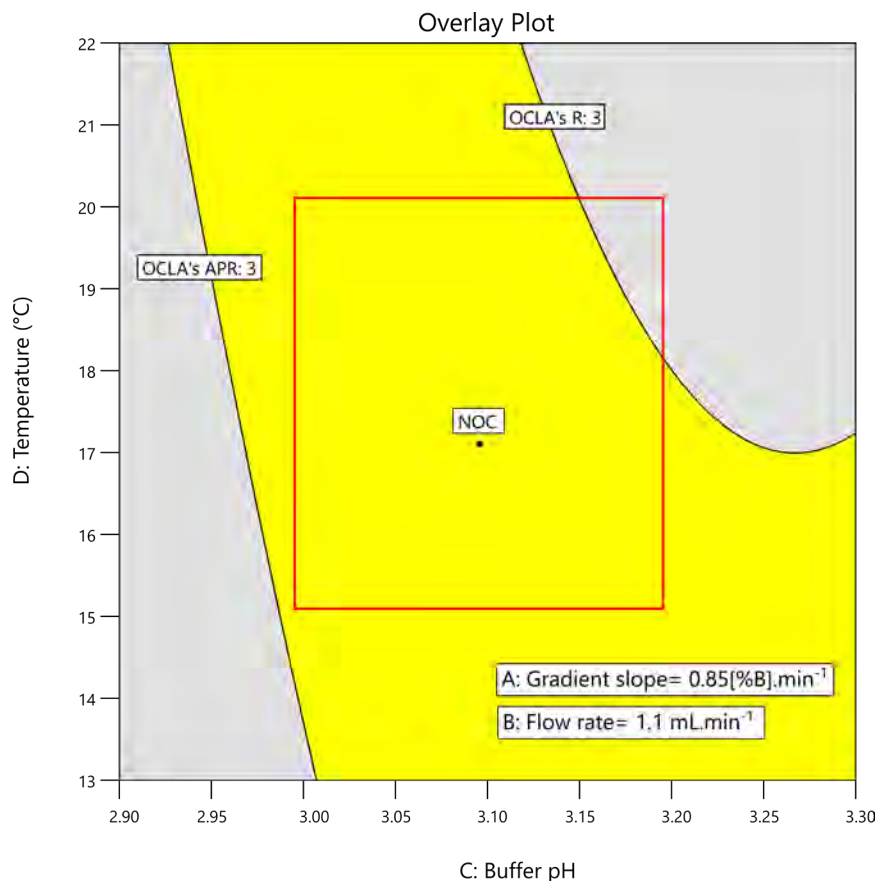


**Figure 4.** Overlay plot depicting the method operable design range and normal operating conditions. The area in the red square represents the Box-Behnken experimental range, while the black dot indicates the normal operating conditions.

Within the MODR, the PARs were established alongside the Normal Operating Conditions (NOC) to validate the model. The NOC was defined as comprising a mobile phase gradient slope of 0.85 [% organic] min<sup>-1</sup>, a flow rate of 1.1 mL min<sup>-1</sup>, a buffer pH of 3.1, and an oven temperature of 17 °C. The PARs (Supplementary figure S3) were defined as a fixed gradient slope of 0.85 [% organic] min<sup>-1</sup>, a flow rate range of 1.0 to 1.2 mL min<sup>-1</sup>, a buffer pH range of 3.05 to 3.15, and an oven temperature range of 16 to 18 °C. The tested points within the PARs, including the NOC, along with their corresponding results, are detailed in Supplementary Table SIII. The results obtained for the NOC and PARs demonstrate the robustness and validity of the model in predicting experimental results. The NOC and all PARs yielded results within the TI (95% confidence interval and 99% tolerance proportion) for all CMAs, except for the tailing factor, where PARs 2, 3, and 13 exceeded the predicted TI. Although most PARs produced results consistent with the model predictions for tailing factor, the occurrence of values outside the TI, together with the proximity of the results to the upper limit of the TI, suggests a slight tendency of the model to underestimate this CMA, indicating the presence of interactions not fully captured by the model. However, this does not compromise the applicability of the model, as most of the experimental results remain within the TI limits and all results remain within the acceptability criteria for tail factor (0.8 - 1.5).



The high reproducibility of the NOC metrics highlights the stability and reliability of the method at its optimal operating point. Overall, the model's predictive performance within the PARs and NOC supports its utility for method control and validation, while minor regions of variability suggest opportunities for further refinement to increase accuracy across the operating space.

A control strategy was established to ensure the method's reliability by defining system suitability criteria based on variations observed within the PARs. System suitability thresholds were determined from development and validation data, ensuring robustness in routine analysis.<sup>22–24</sup> The OCLA tailing factor varied between 1.262 and 1.405, the capacity factor ranged from 9.38 to 11.14, and the theoretical plates exceeded 34163, leading to the following acceptance criteria: tailing factor <1.405, capacity factor 9.38–11.14, and theoretical plates >34163. These system suitability criteria can be associated with control charts for continuous monitoring of the method. In this way, recurring deviations from the system suitability criteria can indicate problems such as equipment wear or column degradation, allowing timely maintenance or adjustments to ensure consistent method performance.

Figure 5 shows the NOC chromatogram that demonstrated the compliance of all CMAs in MODR. The final optimized method was achieved using an Zorbax C18 (150 x 4.6 mm, 3.5  $\mu$ m), mobile phase consisting of ammonium formate buffer 100 mM pH 3.1 with MeOH in a gradient program (5%B at 0.00 min, 5%B from 0.00 to 4.00 min, 5–25%B from 4.00 to 6.00 min, 25–37%B from 6.00 to 20.12 min, 37–45%B from 20.12 to 21.12 min, 45–55%B from 21.12 to 33.12 min, and 55–5%B from 33.12 to 37.12 min), with a flow rate of 1.1 mL min<sup>-1</sup>, injection volume of 25  $\mu$ L, the temperature set at 17 °C, and detection carried out at a wavelength of 254 nm. The DP1 shown in Figure 5 represents the OCLA's acidic stress degradation product, while the other seven originate from photolytic stress degradation products.

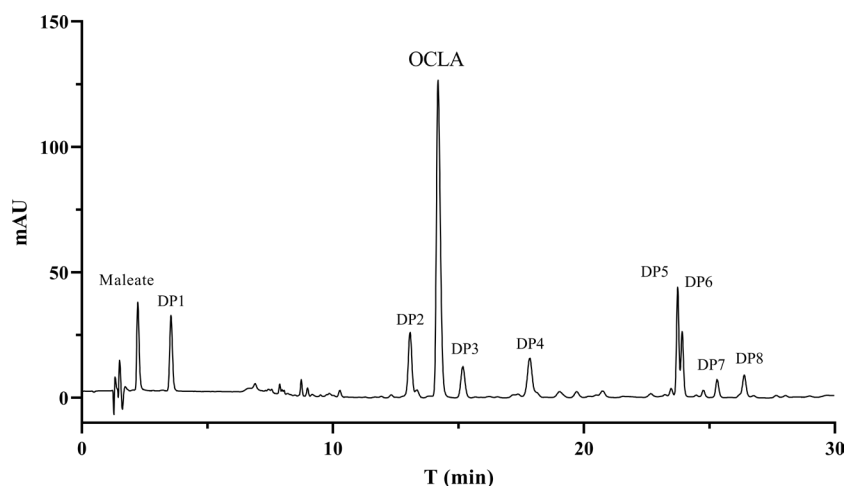


**Figure 5.** Stability-indicating method of Oclacitinib.

Chromatographic conditions: Zorbax C18 (150 x 4.6 mm, 3.5  $\mu$ m), mobile phase consisting of ammonium formate buffer 100mM pH 3.1 with MeOH in a gradient program (5%B at 0.00 min, 5%B from 0.00 to 4.00 min, 5–25%B from 4.00 to 6.00 min, 25–37%B from 6.00 to 20.12 min, 37–45%B from 20.12 to 21.12 min, 45–55%B from 21.12 to 33.12 min, and 55–5%B from 33.12 to 37.12 min) with a flow rate of 1.1 mL.min<sup>-1</sup>. The analysis was conducted at 17 °C, with a 25  $\mu$ L injection volume, and detection at 254 nm. DP1 from acidic stress; DP2–8 from photolytic stress.

### Method validation

The method demonstrated selectivity by ensuring there was no chromatographic peak overlap in the analysis of the OCLA sample. Each substance exhibited a distinct retention time. Additionally, the use of the peak purity tool revealed that the spectral congruence of the OCLA exceeded 99% in the NOC.

The regression analysis demonstrated linearity within the 80 to 240  $\mu$ g mL<sup>-1</sup> concentration range, displaying a strong correlation ( $R = 0.999$ ;  $R^2 = 0.999$ ). Linearity calibration curves can be viewed in Supplementary Figure S4. The Ryan-Joiner and Levene's tests yielded p-values >0.05, confirming the normal distribution and homogeneity of residuals. A regression fit with p-value below 0.05 indicates the statistical significance of the linear model concerning OCLA's content. The lack-of-fit parameter's p-value was above 0.05, suggesting

randomness in errors. The angular coefficient demonstrated deviation from zero ( $p$ -value  $< 0.05$ ), while the intercept showed no significant deviation from zero ( $p$ -value  $> 0.05$ ). Table III presents the parameters of the regression analysis.

**Table III.** Regression analysis of Oclacitinib. CI = Confidence interval, Sy.x = Standard error of estimate, LoD = Limit of detection, LoQ = Limit of Quantification.

Parameter	Value	p-value
Equation	$Y = 13.564 \cdot X - 47$	
Range	80 - 240 $\mu\text{g mL}^{-1}$	
R	0.999	
R <sup>2</sup>	0.999	
Angular coefficient	13.564 (CI 95% = 13.02-14.11)	$< 0.001$
Linear coefficient	-47 (CI 95% = -139,0 to 45,00)	0.041
Sy.x	21,55	
LoD	5.24 $\mu\text{g mL}^{-1}$	
LoQ	15.89 $\mu\text{g mL}^{-1}$	
Model fit		$< 0.001$
Lack-of-fit		0.1

The limits of detection (LoD) and quantification (LoQ) were established based on the calibration curve parameters, using the standard error of estimate. The LoD was determined to be 5.24  $\mu\text{g mL}^{-1}$ , while the LoQ was calculated as 15.89  $\mu\text{g mL}^{-1}$ .

Precision was evaluated through both repeatability and intermediate precision analyses. Repeatability findings are presented in Supplementary Table SIV, with a calculated RSD of less than 2%, indicating low variability. Additionally, intermediate precision (Supplementary Table SV) was evaluated using Student's  $t$ -test and  $F$ -test to compare means and variances between different days. The comparison showed no statistical significance, with  $p$ -values greater than 0.05. The accuracy of the method was evaluated based on data agreement, employing three concentration levels outlined in Table SVI. The results demonstrated recoveries of  $98.05\% \pm 0.14\%$ ,  $99.85\% \pm 0.32\%$ , and  $99.07\% \pm 0.50\%$  for the low, medium, and high concentration levels, respectively ( $n = 3$ , 95% CI), with RSD values below 2%, confirming the method's accuracy.<sup>13,26</sup>

## Discussion

As previously mentioned, current pharmacokinetic studies in dogs, cats and horses have frequently employed LC-MS methods for the quantification of Oclacitinib in plasma.<sup>15–17</sup> Although LC-MS methods have high sensitivity, their application in laboratory routines may be limited due to their high cost and the need for highly specialized equipment and operators. Alternative methods, such as UV spectrophotometry, have also been reported, but they present lower selectivity.<sup>18</sup>

In comparison, the method developed in this study provides a reliable, selective and low-cost alternative for the determination of OCLA and detection of its degradation products. In addition, the model with which this method was developed has a well-defined MODR, providing greater flexibility and analytical predictability, ensuring stability of the CMAs in the face of small changes in chromatographic parameters.

The robustness of the method was ensured by identifying and evaluating CMPs and their impact on CMAs. The use of a BBD to generate a response surface allowed the definition of a reliable operating space, where small variations in the mobile phase gradient, oven temperature, and flow do not compromise the resolution or the shape of the analytical peaks of OCLA. This stability allows operational adjustments to be made without the need for new regulatory validations, which is an important differential for the application of the method in the pharmaceutical industry.<sup>9–12</sup> Previous studies using AQbD have also demonstrated this advantage, allowing greater reproducibility and predictability of analytical methods.<sup>22,28–30,36</sup>

Despite the effectiveness of the method, some limitations can be explored in future studies. The present work focused on the determination of OCLA in API, but further investigations can evaluate the performance of the method in pharmaceutical formulations, such as tablets and oral suspensions. Another possible application is the quantification of OCLA in biological matrices (plasma, urine, tissues) for bioavailability and pharmacokinetic studies.

## CONCLUSION

Oclacitinib was found to be sensitive to photolytic and acidic stress, while oxidative, thermal, alkaline, and neutral stress did not lead to the generation of degradation products or decrease in API content. Eight DPs were detected, with seven arising from photolytic stress and one from acidic stress. The AQbD approach offers enhanced knowledge about method development and a deeper understanding of the interactions among analytical variables, thereby contributing to the overall method quality.

In addition, applying AQbD concepts not only leads to cost savings and faster method development but also allows for continuous improvement of the method through adjustments in MODR. The final optimized method utilized an Zorbax XBD C18 (150 x 4.6 mm, 3.5  $\mu$ m), mobile phase consisting of ammonium formate buffer 100 mM pH 3.1 with MeOH in a gradient program (5%B at 0.00 min, 5%B from 0.00 to 4.00 min, 5–25%B from 4.00 to 6.00 min, 25–37%B from 6.00 to 20.12 min, 37–45%B from 20.12 to 21.12 min, 45–55%B from 21.12 to 33.12 min, and 55–5%B from 33.12 to 37.12 min) a flow rate of 1.1 mL min<sup>-1</sup>, injection volume of 25  $\mu$ L, the temperature set at 17 °C, and detection wavelength of 254 nm.

This optimized method was undergoing successful validation and confirming its selectivity, linearity, precision, accuracy, and robustness. As a result, it can be effectively employed for the quantification of OCLA with its degradation products.

## Conflicts of interest

No conflicts of interest to disclose.

## Acknowledgements

The authors express their gratitude to the Brazilian National Council of Technological and Scientific Development (CNPq) and “Coordenação de Aperfeiçoamento de Pessoal de Nível Superior – Brasil” (CAPES) -Finance Code 001.

## REFERENCES

- (1) Roskoski, R. Janus Kinase (JAK) Inhibitors in the Treatment of Inflammatory and Neoplastic Diseases. *Pharmacol. Res.* **2016**, *111*, 784–803. <https://doi.org/10.1016/j.phrs.2016.07.038>
- (2) Santoro, D. Therapies in Canine Atopic Dermatitis. *Veterinary Clinics of North America: Small Animal Practice* **2019**, *49* (1), 9–26. <https://doi.org/10.1016/j.cvsm.2018.08.002>
- (3) Bäumer, W. Pharmacotherapy of Canine Atopic Dermatitis - Current State and New Trends. *Ankara Üniversitesi Veteriner Fakültesi Dergisi* **2019**, *67* (1), 107–111. <https://doi.org/10.33988/auvfd.644485>
- (4) Fukuyama, T.; Ganchingco, J. R.; Bäumer, W. Demonstration of Rebound Phenomenon Following Abrupt Withdrawal of the JAK1 Inhibitor Oclacitinib. *Eur. J. Pharmacol.* **2017**, *794*, 20–26. <https://doi.org/10.1016/j.ejphar.2016.11.020>

- (5) Haugh, I. M.; Watson, I. T.; Alan Menter, M. Successful Treatment of Atopic Dermatitis with the JAK1 Inhibitor Oclacitinib. *Baylor University Medical Center Proceedings* **2018**, 31 (4), 524–525. <https://doi.org/10.1080/08998280.2018.1480246>
- (6) Maggio, R. M.; Vignaduzzo, S. E.; Kaufman, T. S. Practical and Regulatory Considerations for Stability-Indicating Methods for the Assay of Bulk Drugs and Drug Formulations. *TrAC, Trends Anal. Chem.* **2013**, 49, 57–70. <https://doi.org/10.1016/j.trac.2013.05.008>
- (7) Zimmer, M. Forced Degradation and Long-Term Stability Testing for Oral Drug Products: A Practical Approach. In: Bajaj, S.; Singh, S. (Eds). *Methods for Stability Testing of Pharmaceuticals*. Part of the book series: Methods in Pharmacology and Toxicology (MIPT). Humana Press, New York, NY, 2018, pp 75–98. [https://doi.org/10.1007/978-1-4939-7686-7\\_4](https://doi.org/10.1007/978-1-4939-7686-7_4)
- (8) International Council for Harmonisation of Technical Requirements for Pharmaceuticals for Human Use. *Stability Testing of New Drug Substances and Products Q1A(R2)*, 2003. Available at: <https://database.ich.org/sites/default/files/Q1A%28R2%29%20Guideline.pdf> (accessed 2025-02-03).
- (9) Tome, T.; Žigart, N.; Časar, Z.; Obreza, A. Development and Optimization of Liquid Chromatography Analytical Methods by Using AQbD Principles: Overview and Recent Advances. *Org. Process Res. Dev.* **2019**, 23 (9), 1784–1802. <https://doi.org/10.1021/acs.oprd.9b00238>
- (10) Fukuda, I. M.; Pinto, C. F. F.; Moreira, C. dos S.; Saviano, A. M.; Lourenço, F. R. Design of Experiments (DoE) Applied to Pharmaceutical and Analytical Quality by Design (QbD). *Braz. J. Pharm. Sci.* **2018**, 54 (spe). <https://doi.org/10.1590/s2175-97902018000001006>
- (11) Veerubhotla, K.; Walker, R. B. Development and Validation of a Stability-Indicating RP-HPLC Method Using Quality by Design for Estimating Captopril. *Indian J. Pharm. Sci.* **2019**, 81 (1). <https://doi.org/10.4172/pharmaceutical-sciences.1000478>
- (12) Bhaskaran, N. A.; Kumar, L.; Reddy, M. S.; Pai, G. K. An Analytical “Quality by Design” Approach in RP-HPLC Method Development and Validation for Reliable and Rapid Estimation of Irinotecan in an Injectable Formulation. *Acta Pharm.* **2021**, 71 (1), 57–79. <https://doi.org/10.2478/acph-2021-0008>
- (13) International Council for Harmonisation of Technical Requirements for Pharmaceuticals for Human Use. *ICH Guideline Q2(R2) on Validation of Analytical Procedures*, 2022. Available at: [https://database.ich.org/sites/default/files/ICH\\_Q2-R2\\_Document\\_Step2\\_Guideline\\_2022\\_0324.pdf](https://database.ich.org/sites/default/files/ICH_Q2-R2_Document_Step2_Guideline_2022_0324.pdf) (accessed 2025-02-03).
- (14) United States Pharmacopeial Convention. *General Chapter <1220>: Analytical Procedure Life Cycle*. Rockville, 2022. [https://doi.org/10.31003/USPNF\\_M10975\\_02\\_01](https://doi.org/10.31003/USPNF_M10975_02_01)
- (15) Ferrer, L.; Carrasco, I.; Cristófol, C.; Puigdemont, A. A Pharmacokinetic Study of Oclacitinib Maleate in Six Cats. *Veterinary Dermatology* **2020**, 31 (2), 134–e24. <https://doi.org/10.1111/vde.12819>
- (16) Hunyadi, L.; Datta, P.; Rewers-Felkins, K.; Sundman, E.; Hale, T.; Fajt, V.; Wagner, S. Pharmacokinetics of a Single Dose of Oclacitinib Maleate as a Top Dress in Adult Horses. *J. Vet. Pharmacol. Ther.* **2022**, 45 (3), 320–324. <https://doi.org/10.1111/jvp.13043>
- (17) Collard, W. T.; Hummel, B. D.; Fielder, A. F.; King, V. L.; Boucher, J. F.; Mullins, M. A.; Malpas, P. B.; Stegemann, M. R. The Pharmacokinetics of Oclacitinib Maleate, a Janus Kinase Inhibitor, in the Dog. *J. Vet. Pharmacol. Ther.* **2014**, 37 (3), 279–285. <https://doi.org/10.1111/jvp.12087>
- (18) Momade, D. R. O.; Vilhena, R. de O.; Castro, C.; Regis, F.; Domingues, K. Z. A.; Schlichta, L. S.; Cobre, A. de F.; Pontarolo, R. Development and Validation of an UV-Vis Spectrophotometric Method for the Quantification of Oclacitinib in Capsule Formulation. *Revista de Ciências Farmacêutica Básica e Aplicadas - RCFBA* **2021**, 42. <https://doi.org/10.4322/2179-443X.0712>
- (19) Agência Nacional de Vigilância Sanitária (ANVISA). *RDC Nº 318 - Dispõe Sobre as Boas Práticas de Fabricação de Medicamentos*, 2019. Available at: [https://bvsms.saude.gov.br/bvs/saudelegis/anvisa/2019/rdc0318\\_06\\_11\\_2019.pdf](https://bvsms.saude.gov.br/bvs/saudelegis/anvisa/2019/rdc0318_06_11_2019.pdf) (accessed 2025-02-03).
- (20) Intl. Council for Harmonisation of Technical Requirements for Pharmaceuticals for Human Use. *ICH Topic Q1B Photostability Testing of New Active Substances and Medicinal Products Step 5*, 1996.
- (21) Mikulak, R. J.; McDermott, R.; Beauregard, M. *The Basics of FMEA* (2nd Ed.). Productivity Press, New York, 2017. <https://doi.org/10.1201/b16656>



- (22) Junkert, A. M.; Mieres, N. G.; Domingues, K. Z. A.; Ferreira, L. M.; Pontarolo, R. Development and Validation of a Stability-Indicating High-Performance Liquid Chromatography Method Coupled with a Diode Array Detector for Quantifying Haloperidol in Oral Solution Using the Analytical Quality-by-Design Approach. *J. Sep. Sci.* **2025**, *48* (1). <https://doi.org/10.1002/jssc.70067>
- (23) Lopes, I. J. N.; Fujimori, S. K.; Mendes, T. C.; de Almeida, R. A. D.; de Sousa, F. F. M.; de Oliveira, C. A.; do Nascimento, D. D.; Lourenço, F. R.; Rodrigues, M. I.; Prado, L. D. Application of Analytical Quality by Design (AQbD) for Stability-Indicating Method Development for Quantification of Nevirapine and Its Degradation Products. *Microchem. J.* **2024**, *199*. <https://doi.org/10.1016/j.microc.2024.109939>
- (24) Abdel-Moety, E. M.; Rezk, M. R.; Wadie, M.; Tantawy, M. A. A Combined Approach of Green Chemistry and Quality-by-Design for Sustainable and Robust Analysis of Two Newly Introduced Pharmaceutical Formulations Treating Benign Prostate Hyperplasia. *Microchem. J.* **2021**, *160*. <https://doi.org/10.1016/j.microc.2020.105711>
- (25) Agência Nacional de Vigilância Sanitária (ANVISA). *Resolução RDC Nº 166 – Dispõe Sobre a Validação de Métodos Analíticos e dá Outras Providências*, 2017. Available at: [https://bvsms.saude.gov.br/bvs/saudelegis/anvisa/2017/rdc0166\\_24\\_07\\_2017.pdf](https://bvsms.saude.gov.br/bvs/saudelegis/anvisa/2017/rdc0166_24_07_2017.pdf) (accessed 2025-02-03).
- (26) Marson, B.; Concentino, V.; Junkert, A.; Fachi, M.; Vilhena, R.; Pontarolo, R. Validation of analytical methods in a pharmaceutical quality system: An overview focused on HPLC methods. *Quim. Nova* **2020**, *43* (8), 1190-1203. <https://doi.org/10.21577/0100-4042.20170589>
- (27) Dewi, M.; Pratama, R.; Arifka, M.; Chaerunisaa, A. Quality by Design: Approach to Analytical Method Validation. *Sciences of Pharmacy* **2022**, *1* (1), 38–46. <https://doi.org/10.58920/sciphar01010033>
- (28) Zacharis, C. K.; Vastardi, E. Application of analytical quality by design principles for the determination of alkyl *p*-toluenesulfonates impurities in Aprepitant by HPLC. Validation using total-error concept. *J. Pharm. Biomed. Anal.* **2018**, *150*, 152–161. <https://doi.org/10.1016/j.jpba.2017.12.009>
- (29) Separovic, L.; Lourenço, F. R. Measurement Uncertainty Evaluation of an Analytical Procedure for Determination of Terbinafine Hydrochloride in Creams by HPLC and Optimization Strategies Using Analytical Quality by Design. *Microchem. J.* **2022**, *178*. <https://doi.org/10.1016/j.microc.2022.107386>
- (30) Kannaiah, K. P.; Sugumaran, A. Environmental Benign AQbD Based Estimation of Ketoconazole and Beclomethasone by RP-HPLC and Multi-Analytical UV Spectrophotometric Method. *Microchem. J.* **2022**, *172*. <https://doi.org/10.1016/j.microc.2021.106968>
- (31) Tai, Y.; Ren, D.; Zhao, W.; Qu, H.; Xiong, H.; Gong, X. Analytical Quality by Design Oriented Development of the UPLC Method for Analysing Multiple Pharmaceutical Process Intermediates: A Case Study of Compound Danshen Dripping Pills. *Microchem. J.* **2023**, *187*. <https://doi.org/10.1016/j.microc.2023.108438>
- (32) Sahu, P. K.; Ramiseti, N. R.; Cecchi, T.; Swain, S.; Patro, C. S.; Panda, J. An Overview of Experimental Designs in HPLC Method Development and Validation. *J. Pharm. Biomed. Anal.* **2018**, *147*, 590–611. <https://doi.org/10.1016/j.jpba.2017.05.006>
- (33) Tome, T.; Žigart, N.; Časar, Z.; Obreza, A. Development and Optimization of Liquid Chromatography Analytical Methods by Using AQbD Principles: Overview and Recent Advances. *Org. Process Res. Dev.* **2019**, *23* (9), 1784–1802. <https://doi.org/10.1021/acs.oprd.9b00238>
- (34) Breitzkreitz, M. Analytical Quality by Design. *Braz. J. Anal. Chem.* **2021**, *8* (32), 1–5. <https://doi.org/10.30744/brjac.2179-3425.editorial.mcbreitzkreitz.N32>
- (35) Saini, S.; Sharma, T.; Patel, A.; Kaur, R.; Tripathi, S. K.; Katore, O. P.; Singh, B. QbD-Steered Development and Validation of an RP-HPLC Method for Quantification of Ferulic Acid: Rational Application of Chemometric Tools. *J. Chrom. B* **2020**, *1155*. <https://doi.org/10.1016/j.jchromb.2020.122300>
- (36) Salwa, K. L. Quality-by-Design Driven Analytical Method (AQbD) Development and Validation of HPLC–UV Technique to Quantify Rivastigmine Hydrogen Tartrate in Lipidic Nanocarriers: Forced Degradation, and Assessment of Drug Content and in Vitro Release Studies. *Microchem. J.* **2023**, *193*. <https://doi.org/10.1016/j.microc.2023.108944>

## SUPPLEMENTARY MATERIAL

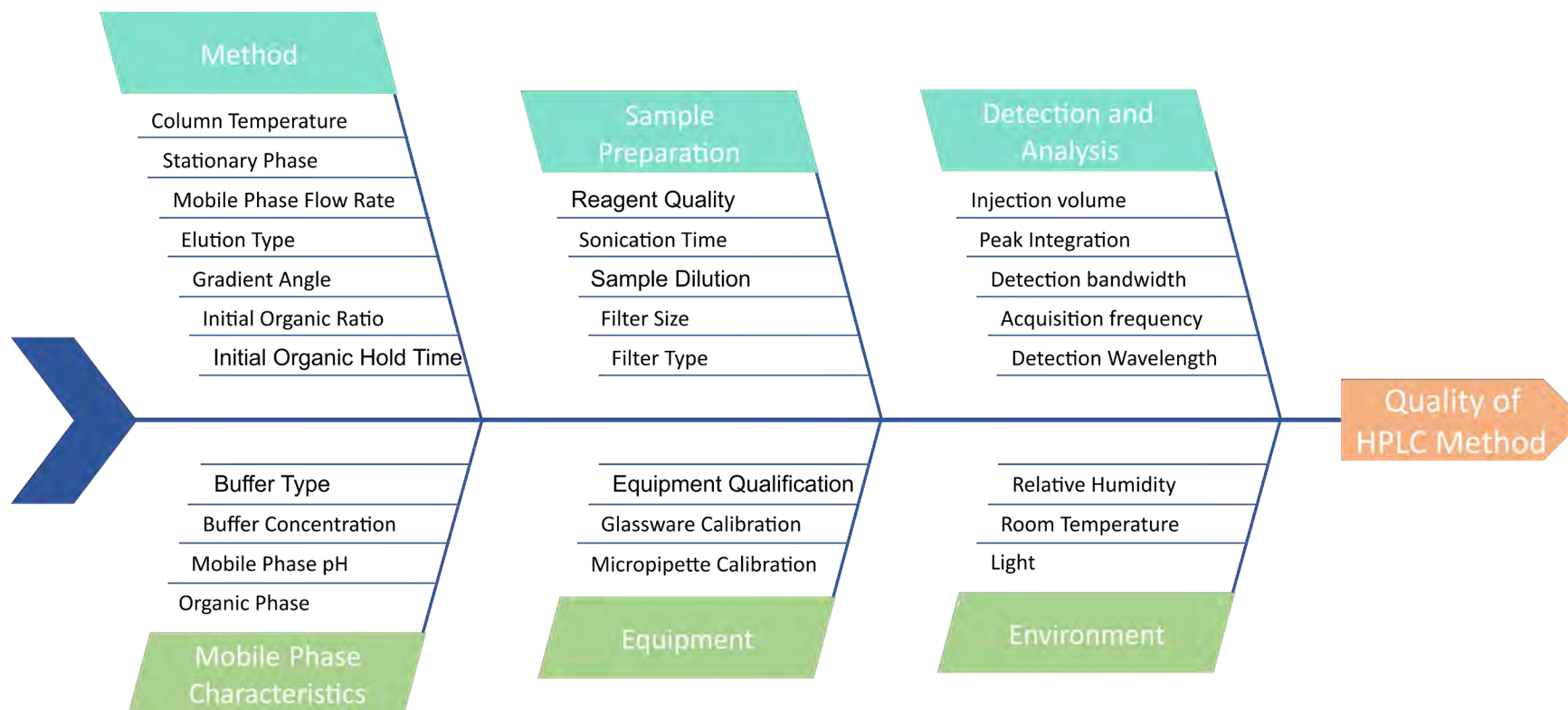


**Figure S1.** Ishikawa Diagram of Potential Critical Method Parameters.

**Table SI.** Risk Assessment Evaluation. Risk priority number thresholds: >225 (high risk), 224–175 (unacceptable), 174–125 (need evaluation), 124–50 (acceptable), and <50 (negligible).

Category	CMP	Occurrence	Severity	Detection	Risk priority number	Corrective action or exclusion justification
Method	Elution Type	1	10	1	10	Evaluated and defined in preliminary tests
	Initial Organic Ratio	1	7	5	35	Evaluated and defined after the screening tests
	Initial Organic Hold Time	2	7	4	56	Evaluated and defined after the screening tests
	Gradient Slope	3	10	6	180	Continuous parameter to be evaluated and modeled
	Stationary Phase	2	10	7	140	Categorical parameter to be tested and fixed
	Column Temperature	5	7	7	245	Continuous parameter to be evaluated and modeled
	Mobile Phase Flow Rate	6	8	8	384	Continuous parameter to be evaluated and modeled
Sample Preparation	Filter Size	1	3	1	3	Defined according to sample volume
	Filter Type	1	3	1	3	Defined according to sample type
	Sonication time	1	5	5	25	Previously assessed and fixed in the sample preparation protocol
	Reagent Quality	2	5	8	80	Supplier qualification
	Sample Dilution	3	7	5	105	Previously assessed and fixed in the sample preparation protocol
Detection and Analysis	Peak Integration	2	3	3	18	Defined and fixed at the beginning of the acquisitions
	Acquisition Frequency	3	4	4	48	Low impact on peak separation and quantification with good resolution
	Detection bandwidth	3	5	4	60	Defined and fixed at the beginning of the acquisitions
	Detection Wavelength	3	7	6	126	Evaluated and defined in preliminary tests
	Injection Volume	6	7	7	294	Evaluated and defined in preliminary tests
Mobile Phase Characteristics	Buffer Concentration	5	3	5	75	Low impact on separation and quantification
	Organic Phase	3	9	6	162	Categorical parameter to be tested and fixed
	Buffer Type	3	9	6	162	Categorical parameter to be tested and fixed
	Mobile Phase pH	7	9	8	504	Continuous parameter to be evaluated and modeled
Equipment	Glassware Calibration	5	8	5	200	Check and calibrate glassware
	Equipment Qualification	4	8	7	224	Check and calibrate equipment qualification
	Micropipette Calibration	4	8	7	224	Check and calibrate micropipette calibration
Environment	Room Temperature	3	3	4	36	Controlled room temperature
	Relative Humidity	3	4	4	48	Parameter controlled in sample storage
	Light	5	4	4	80	Parameter controlled in sample storage

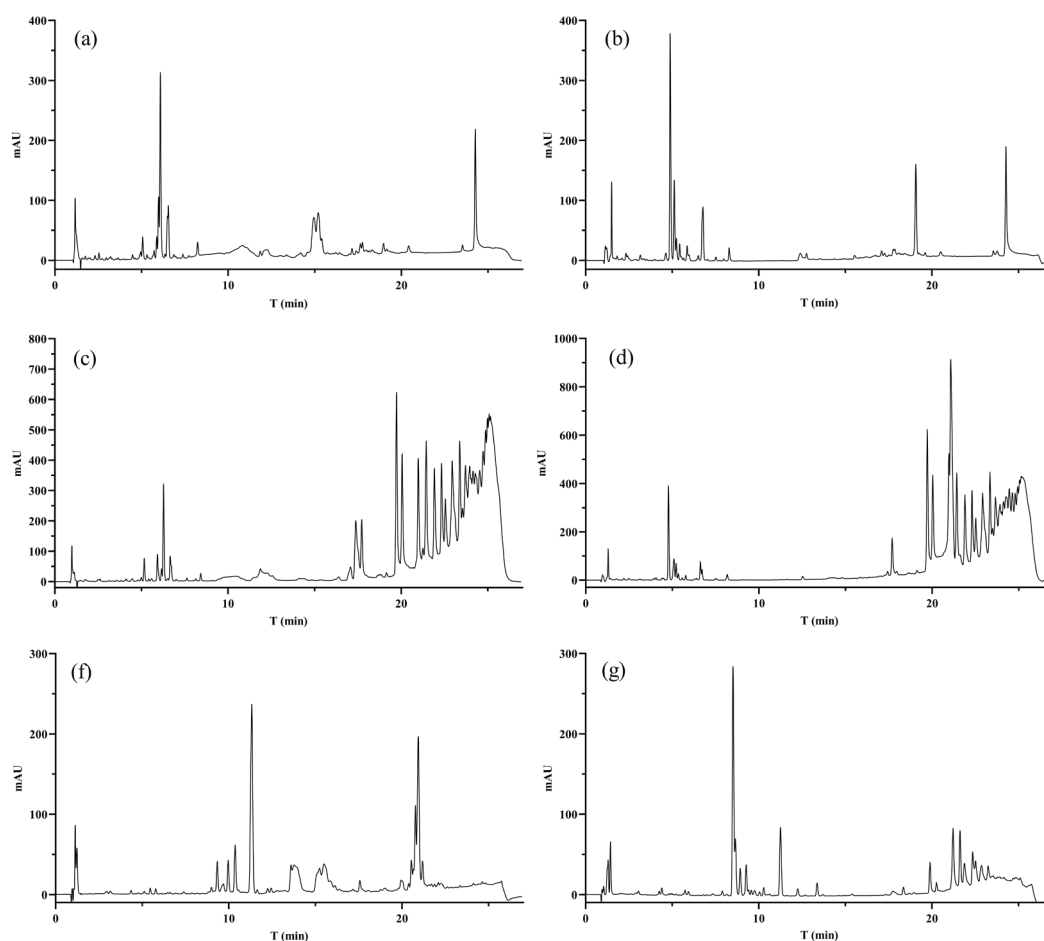


**Figure S2.** Screening test of categorical variables.

A - C8, ACN and acetate buffer; B - C8, ACN and formate buffer; C - C18, ACN and acetate buffer; D - C18, ACN and formate buffer; E - C18, MeOH and acetate buffer; F - C18, MeOH and formate buffer. The chromatographic analysis was performed using a Zorbax XBD C18 or XBridge BEH C8 column (150 × 4.6 mm, 3.5 μm). The mobile phase consisted of an ammonium acetate or ammonium formate buffer in combination with ACN or MeOH. A scouting gradient program was employed, with the following elution profile: 10%B at 0.0 min; 10-90%B from 0.0 to 24 min, and 90-10%B from 24 to 27 min. The flow rate was maintained at 1.5 mL/min throughout the analysis. The analysis was conducted at 25 °C, with a 40 μL injection volume, and detection at 254 nm.



**Table SII.** Results obtained from the Box-Behnken design. OCLA= Oclacitinib R= resolution factor, APR= Adjacent peak resolution factor, T= Tailing factor, and K'= Retention coefficient

n	A: Gradient slope	B: Flow rate	C: Buffer pH	D: Temperature	OCLA's R	OCLA's APR	OCLA's T	Last Peak K'
	[%B] min <sup>-1</sup>	mL min <sup>-1</sup>		°C				
1	0.8	1	3.1	17.5	3.895	3.503	1.323	19.87
2	1.2	1	3.1	17.5	3.069	3.307	1.3	16.44
3	0.8	1.4	3.1	17.5	4.215	3.241	1.325	25.37
4	1.2	1.4	3.1	17.5	3.451	3.106	1.271	20.87
5	1	1.2	3	15	5.273	2.929	1.347	20.43
6	1	1.2	3.2	15	3.275	3.332	1.226	20.76
7	1	1.2	3	20	4.499	3.053	1.33	19.70
8	1	1.2	3.2	20	2.487	3.510	1.278	19.96
9	0.8	1.2	3.1	15	4.448	3.263	1.29	22.62
10	1.2	1.2	3.1	15	3.595	3.124	1.291	18.97
11	0.8	1.2	3.1	20	3.647	3.385	1.351	22.18
12	1.2	1.2	3.1	20	2.986	3.264	1.279	18.34
13	1	1	3	17.5	4.758	3.130	1.35	17.51
14	1	1.4	3	17.5	4.778	2.884	1.331	22.11
15	1	1	3.2	17.5	2.672	3.530	1.264	17.80
16	1	1.4	3.2	17.5	3.119	3.289	1.243	22.84
17	0.8	1.2	3	17.5	5.180	3.075	1.343	20.90
18	1.2	1.2	3	17.5	4.482	2.981	1.338	18.21
19	0.8	1.2	3.2	17.5	3.210	3.553	1.298	22.73
20	1.2	1.2	3.2	17.5	2.651	3.368	1.207	18.80
21	1	1	3.1	15	3.676	3.302	1.266	18.04
22	1	1.4	3.1	15	4.017	3.060	1.282	22.62
23	1	1	3.1	20	3.098	3.480	1.285	17.36
24	1	1.4	3.1	20	3.299	3.278	1.285	22.21
25	1	1.2	3.1	17.5	3.572	3.264	1.288	20.04
26	1	1.2	3.1	17.5	3.592	3.248	1.32	20.10
27	1	1.2	3.1	17.5	3.548	3.252	1.271	20.49
28	1	1.2	3.1	17.5	3.534	3.314	1.318	19.79

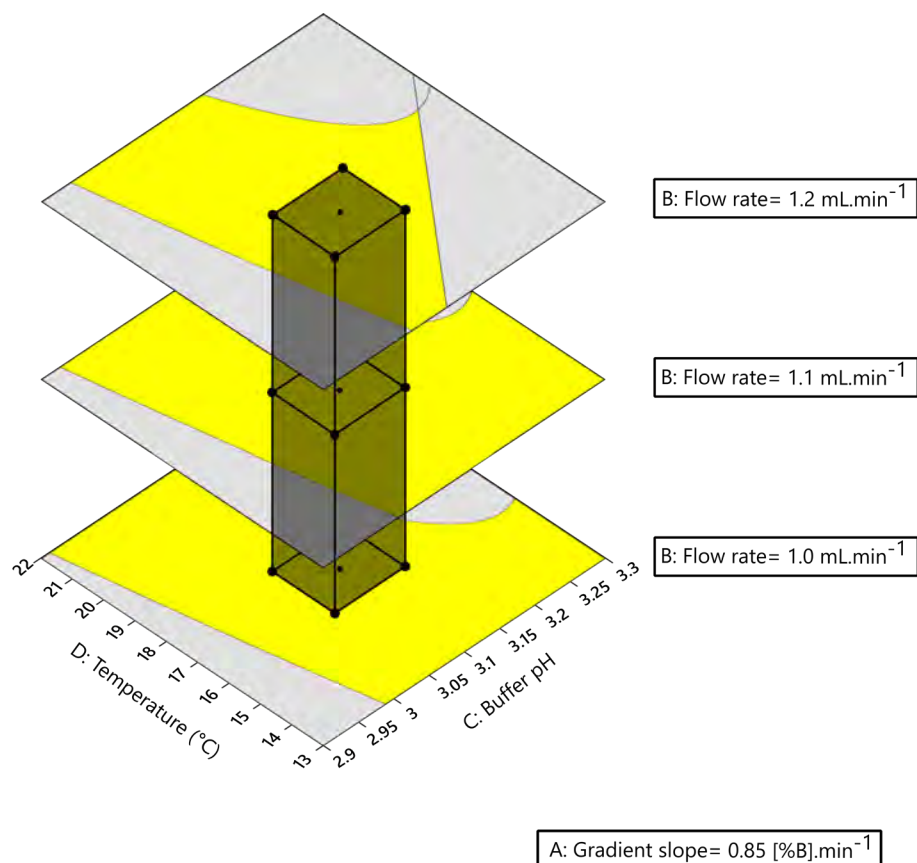


**Figure S3.** Combination of overlay plots at three flow rate levels. The Method Operable Design Range (MODR) are represented by the yellow area, the translucent parallelepiped delineates the Proven Acceptable Ranges (PARs) and the dots indicates each point that were tested.

**Table SIII.** Results from Proven Acceptable Ranges for model validation. OCLA= Oclacitinib R= resolution factor, APR= Adjacent peak resolution factor, T= Tailing factor, and K'= Retention coefficient

	A: Gradient slope	B: Flow rate	C: Buffer pH	D: Temperature	OCLAs R			OCLA's APR			OCLA's T			Last Peak K'		
PAR Points	[%B] min <sup>-1</sup>	mL min <sup>-1</sup>		°C	95% TI Low	Measured	95% TI High	95% TI Low	Measured	95% TI High	95% TI Low	Measured	95% TI High	95% TI Low	Measured	95% TI High
PAR 1	0.85	1	3.05	16.0	4.166	4.331	4.895	3.161	3.270	3.394	1.254	1.371	1.380	17.32	18.20	20.77
PAR 2	0.85	1	3.05	18.0	3.899	4.231	4.620	3.227	3.353	3.457	1.268	1.405	1.388	17.32	17.98	20.77
PAR 3	0.85	1	3.15	16.0	3.088	3.556	3.817	3.372	3.522	3.605	1.216	1.351	1.342	17.65	19.15	21.11
PAR 4	0.85	1	3.15	18.0	2.821	3.325	3.542	3.438	3.562	3.668	1.244	1.348	1.364	17.65	19.18	21.11
PAR 5	0.85	1	3.10	17.0	3.428	4.032	4.131	3.314	3.422	3.544	1.249	1.317	1.365	17.50	18.73	20.92
PAR 6	0.85	1.1	3.05	16.0	4.231	4.436	4.927	3.107	3.191	3.333	1.254	1.317	1.380	18.58	20.02	21.92
PAR 7	0.85	1.1	3.05	18.0	3.965	4.159	4.651	3.172	3.262	3.395	1.268	1.359	1.388	18.58	19.39	21.92
PAR 8	0.85	1.1	3.15	16.0	3.207	3.671	3.903	3.317	3.470	3.544	1.216	1.315	1.342	18.92	20.70	22.26
PAR 9	0.85	1.1	3.15	18.0	2.940	3.375	3.627	3.383	3.503	3.606	1.244	1.333	1.364	18.92	20.37	22.26
PAR 10	0.85	1.2	3.05	16.0	4.287	4.628	4.970	3.050	3.194	3.274	1.254	1.383	1.380	19.81	20.81	23.11
PAR 11	0.85	1.2	3.05	18.0	4.021	4.227	4.693	3.116	3.203	3.336	1.268	1.380	1.388	19.81	20.24	23.11
PAR 12	0.85	1.2	3.15	16.0	3.315	3.700	3.998	3.261	3.330	3.484	1.216	1.335	1.342	20.15	21.94	23.45
PAR 13	0.85	1.2	3.15	18.0	3.049	3.450	3.722	3.326	3.424	3.547	1.244	1.338	1.364	20.15	20.40	23.45
PAR 14	0.85	1.2	3.10	17.0	3.594	4.053	4.266	3.203	3.205	3.423	1.249	1.262	1.365	20.01	21.08	23.25
NOC	0.85	1.1	3.10	17.0	3.514	4.069	4.195	3.259	3.333	3.482	1.249	1.294	1.365	18.77	20.23	22.07
NOC	0.85	1.1	3.10	17.0	3.514	4.072	4.195	3.259	3.333	3.482	1.249	1.315	1.365	18.77	20.23	22.07
NOC	0.85	1.1	3.10	17.0	3.514	4.081	4.195	3.259	3.333	3.482	1.249	1.320	1.365	18.77	20.23	22.07

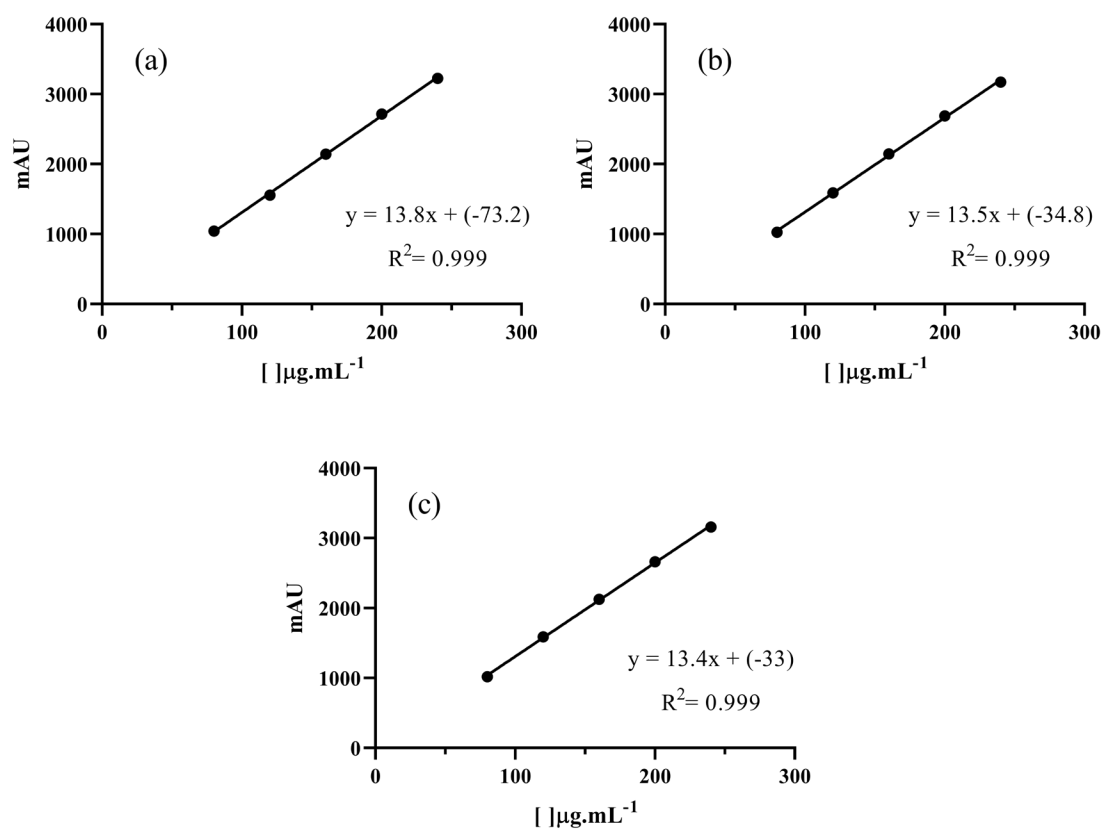


Figure S4. Linearity calibration curves A, B and C.

Table SIV. Repeatability results. SD = standard deviation, RSD = relative standard deviation

Concentration (µg mL <sup>-1</sup> )	Area	Mean	SD	RSD
80	1038.8	1035.9	11.67	1.13%
	1023.1			
	1045.9			
160	2116.4	2132.1	37.21	1.75%
	2105.4			
	2174.6			
240	3168.4	3174.6	32.35	1.02%
	3145.8			
	3209.6			



**Table SV.** Intermediate precision results. Note: SD = standard deviation, RSD = relative standard deviation.

Concentration ( $\mu\text{g mL}^{-1}$ )	Analyst 1	Analyst 2	Mean	SD	RSD	Test <i>t</i> (p-value)	Test <i>F</i> (p-value)
80	1072.1	1025.0	1041.7	18.20	1.75%	0.090	0.656
	1046.5	1021.1					
	1043.4	1041.8					
160	2176.9	2133.7	2126.1	33.91	1.60%	0.308	0.578
	2099.7	2084.2					
	2148.4	2113.5					
240	3217.6	3211.8	3178.7	39.38	1.24%	0.505	0.985
	3143.0	3132.1					
	3212.4	3155.0					


**Table SVI.** Accuracy results. SD = standard deviation, RSD = relative standard deviation, CI = confidence interval.


Level	( $\mu\text{g mL}^{-1}$ )	Theoretical area			Observed area			Recovery $\pm$ CI (95%)
		Area	Mean $\pm$ SD	RSD	Area	Mean $\pm$ SD	RSD	
Low	80	1058.7	1060.2 $\pm$ 16.3	1.54%	1035.3	1039.5 $\pm$ 14.4	1.67%	98.05% $\pm$ 0.14%
		1077.2			1058.6			
		1044.6			1024.6			
Medium	160	2164.5	2167.4 $\pm$ 32.6	1.51%	2172.9	2164.0 $\pm$ 27.3	1.26%	99.85% $\pm$ 0.32%
		2201.4			2185.9			
		2136.3			2133.4			
High	240	3270.2	3274.6 $\pm$ 49.0	1.50%	3216.5	3244.2 $\pm$ 37.4	1.15%	99.07% $\pm$ 0.50%
		3325.6			3286.8			
		3227.9			3229.2			

ARTICLE

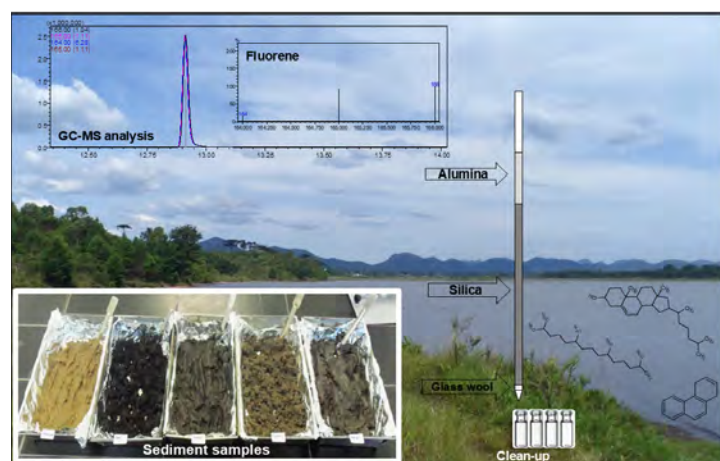
# Geochemical Hydrocarbon Markers in River Sediments from a Densely Populated Area of Curitiba, Brazil

Lucélia Taverna<sup>1</sup>, Fabricio Augusto Hansel<sup>2</sup> , Cesar Alexandro da Silva<sup>1,3</sup> , Vânia Ribeiro Ferreira<sup>1</sup>, Emerson Luís Yoshio Hara<sup>\*1,3</sup>  , Rafael Garrett Dolatto<sup>1</sup> , Marco Tadeu Grassi<sup>1</sup> 

<sup>1</sup>Grupo de Química Ambiental, Departamento de Química, Universidade Federal do Paraná.  PO Box 19032, 81531-980, Curitiba, PR, Brazil

<sup>2</sup>Centro Nacional de Pesquisa de Florestas, Empresa Brasileira de Pesquisa Agropecuária.  Estrada da Ribeira, Km 111, 83411-000, Colombo, PR, Brazil

<sup>3</sup>Laboratório de Geoquímica Ambiental e Poluição Marinha, Departamento de Oceanografia e Ecologia, Universidade Federal do Espírito Santo.  Campus Goiabeiras, 29055-460, Vitória, ES, Brazil



Employing geochemical hydrocarbon markers, this work aimed to identify the sources of organic matter in water bodies in the Metropolitan Region of Curitiba, State of Paraná, Brazil. Also, a reduced scale protocol assisted by ultrasonic bath was developed and applied to extraction, fractionation, and clean-up of the aliphatic hydrocarbons (AH), polycyclic aromatic hydrocarbons (PAH), and sterols in sediment samples from the rivers Barigui, Iguaçu, and Timbu and from the water supply reservoirs Iraí and Passaúna. The total concentrations determined in all samples ranged from 1.15 to 509.65  $\mu\text{g g}^{-1}$  for AH, between 97.3 and 440.65

$\text{ng g}^{-1}$  for PAH, and from 1.73 to 747.92  $\mu\text{g g}^{-1}$  for sterols. The highest concentration of the three markers was observed at the Timbu River, which is in an environmental protection area. About the samples from the Barigui River and both reservoirs, more than 95% of the molecules were classified as natural input. On the other hand, in the samples from the Iguaçu and Timbu rivers, densely urbanized area rivers, 53% and 88% of the markers, respectively, were classified as of anthropogenic origin. However, the ratios for PAH revealed the combustion of biomass as the main source of these compounds. The fecal marker coprostanol, which was detected in both the Iguaçu and Barigui rivers, shows contamination by domestic and industrial sewage, respectively. The ratios for sterols showed the presence of domestic sewage in rivers and reservoirs close to expanding urban areas. Thus, it was possible to conclude that the uncontrolled expansion of cities and their activities can compromise the integrity of the water bodies, their biota, and the supply of the population.

**Cite:** Taverna, T.; Hansel, F. A.; da Silva, C. A.; Ferreira, V. R.; Hara, E. L. Y.; Dolatto, R. G.; Grassi, M. T. Geochemical Hydrocarbon Markers in River Sediments from a Densely Populated Area of Curitiba, Brazil. *Braz. J. Anal. Chem.* 2025, 12 (49), pp 90-116. <http://dx.doi.org/10.30744/brjac.2179-3425.AR-188-2024>

Submitted December 27, 2024; Resubmitted February 10, 2025; 2<sup>nd</sup> time Resubmitted April 14, 2025; Accepted April 14, 2025; Available online June 4, 2025.

**Keywords:** emerging contaminants, sample preparation, gas chromatography, polycyclic aromatic hydrocarbons, environmental chemistry

## INTRODUCTION

The presence of elevated concentration levels of biogeochemical hydrocarbon markers, such as aliphatic hydrocarbons (AH), polycyclic aromatic hydrocarbons (PAH), and sterols in aquatic sediments, are frequently used as indicators of water pollution by persistent organic pollutants (POPs). Since sediments accumulate these POPs, the relative distribution or ratios are often used as an indicator of the origins and chemical/physical processes contributing to the pollution. Often, these POPs are continuously discharged into the water bodies through anthropogenic activities, worsened by deficiencies in the sewage collection and treatment services in municipalities from an emerging economy such as Brazil's.<sup>1-6</sup>

The analytical protocols to determine AH, PAH, and sterols, as well as other organic compounds in the sediment samples, comprise extraction, clean-up, and chromatographic determination. One of the most widely used extraction of organic compounds involves the use of the Soxhlet apparatus<sup>7,8</sup> and ultrasonic devices.<sup>9,10</sup>

Despite being efficient, the Soxhlet apparatus, which is recommended by the US EPA 3540C<sup>11</sup> method has disadvantages such as high consumption of organic solvents, significant waste generation, long extraction time, and considerable consumption of electrical power. To improve selectivity and minimize interferences, EPA 3540C recommends further purification procedures using alumina and silica gel chromatographic columns, as specified in US EPA 3610B<sup>12</sup> and US EPA 3630C<sup>13</sup> methods. However, these traditional clean-up methods have significant disadvantages, including high labor requirements, extensive solvent use, and substantial waste generation.

While these methods improve analytical precision, they inherently contradict the principles of green chemistry by increasing process inefficiencies and environmental burdens. Therefore, the development of alternative, eco-friendly purification strategies is crucial to minimizing solvent use, reducing waste production, and enhancing the sustainability of analytical methodologies. Ultrasonic devices have proven to be more attractive for routine analysis because they are an environmentally friendly alternative for extracting organic compounds from solid samples. These devices have a lower acquisition cost, require less time of use, allow reactions with smaller sample volumes, and, consequently, generate less waste generation<sup>9,14-17</sup>. Due to these advantages, the EPA 3550C ultrasonic extraction method<sup>18</sup> has been widely adopted over the EPA 3540 method.

For instance, Martinez et al.<sup>19</sup> used an ultrasonic device to extract 16 PAHs in water, sediment, and mussel samples 30 mL of HX/DCM (1:1) in three sonication cycles of 10 min, clean-up was optimized using a solid-phase extraction cartridge filled with alumina. From the recovery experiments, the values ranged from 22% to 112%. According to the authors, due to its easier use and faster operation, ultrasonic extraction was chosen as the preferred option ahead of the standard Soxhlet method.<sup>19</sup>

Considering these aspects, the aim of determining the presence of PAH, AH, and sterols in sediments is to assess the environmental impacts of unregulated urban expansion, especially in developing countries like Brazil. Despite the economic growth observed in recent decades, sewage treatment has not followed at the same pace.<sup>20,21</sup>

The objective of this work was to modify and optimize an environmentally friendly sample clean-up and fractionation protocol for the determination of AH, PAH, and sterols. The modification was aimed at having the following advantages: minimizing the amounts of solvents and sorbents used in the extraction and clean-up steps, and reducing the total time of analysis, power consumption, and the quantities of waste generated. After the optimization of the method, it was validated and applied in the analysis of sediments from rivers and reservoirs of the Metropolitan Region of Curitiba, Brazil.

## MATERIALS AND METHODS

### *Reagents and standards*

The organic solvents hexane (HX), dichloromethane (DCM), ethyl acetate (Et.Ac.), and methanol (MeOH) had a purity > 99% (Mallinckrodt, USA). The analytical standards androstanol (AND), cholestane (CLE), coprostanol (COP), epicoprostanol (ECOP), coprostanone (CTN), cholesterol (COL), cholestanol (CNL), stigmastanol (STN), stigmasterol (STR), and campesterol (CPL) as well derivatization reagent N,O-bis(trimethylsilyl)-trifluoro-acetamide trimethyl-chloro-silane (BSTFA/TMCS, 99:1) were purchased from same supplier (Sigma-Aldrich, USA).

To determine AH, a mixed solution of AH standards (n-C8 to n-C40, pristane, and phytane) was used for calibration, and deuterated standards n-C20D, n-C24D, and n-C30D from Accustandard, USA were used as surrogates.

A mixed solution of PAH: naphthalene (Nap), acenaphthylene (Acy), acenaphthene (Ace), fluorene (Flu), phenanthrene (Phe), anthracene (Ant), fluoranthene (Fla), pyrene (Pyr), benzo[a]anthracene (BaA), chrysene (Cry), benzo[b]fluoranthene (BbF), benzo[k]fluoranthene (BkF), benzo[a]pyrene (BaP), indene[1,2,3-cd]pyrene (InP), dibenzo[a,h]anthracene (DahA) and benzo[g,h,i]perylene (BghiP) was used as analytical standard (Accustandard, USA).

A mixed solution of deuterated PAH containing naphthalene-D8 (NapD8), acenaphthene-D10 (AceD10), phenanthrene-D10 (PheD10), chrysene-D12 (CryD12), perylene-D12 (PerD12) which was used as internal standard (IS), and p-terphenyl-D14 (Accustandard, USA) as surrogate standard. Alumina (Al<sub>2</sub>O<sub>3</sub>), anhydrous sodium sulfate (Na<sub>2</sub>SO<sub>4</sub>), and copper powder were obtained from J. T. Baker, USA.

The purity of the gases (hydrogen, nitrogen, synthetic air, and helium) was 99.999% and supplied by White Martins, Brazil. Before using anhydrous sodium sulfate, it was heated at 400 °C for 4 h to purge humidity and organic contaminants. Copper was activated using HCl (6.0 mol L<sup>-1</sup>) followed by MeOH rinsing, MeOH: DCM (1:1 v/v), and DCM. Silica and alumina gel, 70-230 mesh (Merck, Germany), were activated at 165 °C for 16 h and deactivated with ultra-pure water.

### *Assessing the efficiency of the extraction and clean-up steps*

Extraction and clean-up steps were adapted from Mater et al.<sup>22</sup> Experiments of fortification and recovery related to extraction and clean-up steps were performed with standard solutions of AH, PAH, and sterols at the following concentrations of 10 µg, 96 ng, and 75 µg, respectively. To optimize the extraction step, 1.0 g of activated copper and 3.0 g of Na<sub>2</sub>SO<sub>4</sub> were transferred into a glass conical tube, followed by the standard solutions of AH, PAH, and sterols.

The extractions were carried out in an ultrasonic bath (120 W, 25 kHz) using 7 mL of DCM: MeOH (2:1 v/v). Three cycles of extraction (20 min cycle<sup>-1</sup>) were carried out and, after each one, the tubes were centrifuged (2000 rpm for 6 min) and the supernatants were transferred to a glass beaker. The extract was preconcentrated in a rotary evaporator (50 °C) and then submitted to clean-up.

Recovery was evaluated after the extract pre-concentration to approximately 100 µL followed by reconstitution in 1.0 mL of HX. Clean-up optimization was performed in glass columns (7 mm i.d. × 30 cm length) packed with silica gel, neutral activated alumina, calcinated Na<sub>2</sub>SO<sub>4</sub>, and activated copper standard solutions of AH, PAH, and sterols. Different amounts of alumina were evaluated, as well as the silica activation influence on the compound's fractionation (Table I).

The initial 5.5 mL eluted from the AH fraction (F1) and the final 1.0 mL (Experiments 1 and 2 of Table I) were collected into distinct beakers. In all experiments, F1 and PAH fraction (F2) have been pre-concentrated in a rotary evaporator up to 2 mL and then up to 1 mL under N<sub>2</sub> (g) flow. The sterols fraction (F3) was pre-concentrated to dryness and derivatized (40 µL BSTFA/TMCS, 70 °C for 1 h). Then, the derivatizing reagent was volatilized under N<sub>2</sub> flow and redissolved with 1 mL of HX.



**Table I.** Terms used in experiments to elute the AH, PAH, and sterols

Experiment	m of SiO <sub>2</sub>	m of Al <sub>2</sub> O <sub>3</sub> <sup>a</sup>	V of HX (F1)	V of DCM:HX (F2)	V of Et.Ac.:MeOH (F3)
	g		mL		
1	2 <sup>b</sup>	2	6.5	10 (3:2 v/v)	12 (3:1 v/v)
2	2 <sup>b</sup>	1	6.5	10 (3:2 v/v)	12 (3:1 v/v)
3	2 <sup>b</sup>	1	5.5	10 (4:1 v/v)	12 (3:1 v/v)
4	2 <sup>c</sup>	1	5.5	10 (4:1 v/v)	12 (3:1 v/v)

<sup>a</sup> alumina was calcinated at 400 °C during 4 h and activated at 160 °C for 16 h; <sup>b</sup> silica gel activated at 160 °C, 16 h; <sup>c</sup> silica activated at 160 °C, 4 h, and then deactivated with 2% ultrapure water; F1: AH fraction; F2: PAH fraction, F3: sterols fraction; HX: hexane, DCM: dichloromethane, Et.Ac., ethyl acetate, MeOH: methanol.

### Instrumental analysis

AH determination was performed using a gas chromatograph (Focus GC, Thermo Corporation, USA) with a flame ionization detector (GC-FID), equipped with a DB-5 capillary column (30 m length × 0.32 mm i.d. × 0.25 µm film thickness). The injector was set at 280 °C and operated in splitless mode. The detector temperature was set at 300 °C. The injection was performed (1.0 µL) by an autosampler (AS 3000, Thermo Corporation, USA). GC oven's initial temperature was 60 °C held for 1.5 min, 6 °C min<sup>-1</sup> to 310 °C and held at 310 °C for 30 min. Nitrogen was used as carrier gas at a flow rate of 3 mL min<sup>-1</sup>.

PAH determination was performed using a GC-MS (Focus-GC Polaris Q, Thermo Corporation, USA). The capillary column specifications were: 30 m length, 0.25 mm i.d., 0.25 µm film thickness (DB-5ms, Agilent, USA) and helium as carrier gas at 1.0 mL min<sup>-1</sup>. F2 (1.0 µL) was injected in splitless mode. GC oven temperature was programmed from 50 °C (held for 5 min) to 230 °C at 5 °C min<sup>-1</sup>, up to 250 °C at 2 °C min<sup>-1</sup>, and finally to 300 °C at 5 °C min<sup>-1</sup> held for 8 min.

The mass spectrometer was operated in the electron ionization (EI) mode at 70 eV selected ion monitoring (SIM) mode, observing the ions in 3 segments: scan 1 (5-29 min): *m/z* 128, 136, 152, 154, 162, 164, 166, 178; scan 2 (30-47 min): *m/z* 178, 202, 228, 244; and scan 3 (47 min, until the end of run): *m/z* 228, 236, 240, 252, 260, 264, 276, 277, 278, 279. The ion source and the transfer line temperatures were kept at 250 °C. A dwell time of 0.2 seconds was used for each *m/z*, resulting in 15 cycles/s for each SIM segment.

The injector temperature was kept at 270 °C. PAH quantification was performed by injecting a standard mixed solution containing 16 PAH and comparing their mass spectra to the NIST MS library.

Derivatized sterols were determined by injecting 1.0 µL of the sample in split mode (split ratio 1/20). The injector temperature was set up to 300 °C, and GC oven temperature was programmed: 60 °C to 250 °C at 15 °C min<sup>-1</sup>, then up to 280 °C at 1 °C min<sup>-1</sup>, and finally up to 300 °C at 5 °C min<sup>-1</sup>, holding for 5 min. The mass spectrometer was operated in the EI mode at 70 eV. The ion source and transfer line temperatures were set up at 200 °C and 280 °C, respectively. Mass spectra were obtained in full scan mode (50 and 550 *m/z*).

### Quality assurance of the analytical method

Validation parameters and acceptance criteria used in our study were based on US EPA Method 8270E.<sup>23</sup> Blank sample extractions using sodium sulfate previously heated at 450 °C were performed. Calibration and linearity were measured by the correlation coefficient (R) obtained from analytical curves. The limit of detection (LOD) for PAH and sterols was calculated based on the parameters of the analytical curve: 3 times the ratio of the estimated standard deviation of the regression equation and the curve slope (Table S1 and S2).

To quantify AH, analytical curves (n=3) were plotted to range from 0.3 to 25 µg mL<sup>-1</sup> using n-C16D (10 µg mL<sup>-1</sup>) as internal standard and the concentration of surrogate standards (n-C20D, n-C24D, and n-C30D)

ranged from 1 to 25  $\mu\text{g mL}^{-1}$  (Table S3); analytical curves were used to obtain the response factor (RF<sub>x</sub>), which was used to determine the AH concentrations ( $C_{\text{HA}}$ ) according to Equation 1.

$$C_{\text{HA}} = \left( \frac{A_x}{A_{\text{IS}}} \right) \left( \frac{C_{\text{IS}}}{\text{RF}_x} \right) \quad (\text{Equation 1})$$

where  $A_x$  and  $A_{\text{IS}}$  correspond to area values obtained for target AH and C16D, respectively;  $C_{\text{IS}}$  corresponds to n-C16D concentration in the extract, and RF<sub>x</sub> is the response factor of target AH.

For PAH, linear analytical curves ( $n=3$ ) were plotted to range from 4.9 to 490  $\text{ng mL}^{-1}$  using a mixed solution of deuterated PAH containing NapD8, AceD10, PheD10, CryD12, PerD12 was used as internal standard (IS) at 102.4  $\text{ng mL}^{-1}$  (Table S1). Besides, linear analytical curves ( $n=3$ ) for the surrogate standard p-terphenyl-D14, whose concentrations ranged from 9.6 to 200  $\text{ng mL}^{-1}$ , were plotted. To quantify sterols, linear analytical curves were plotted ranging from 0.24 to 15  $\mu\text{g mL}^{-1}$  (COP, ECOP, CTN, COL, CNL, STR, and STN) and 0.4 to 20  $\mu\text{g mL}^{-1}$  for CPL using CLE as IS (15  $\mu\text{g mL}^{-1}$ ) (Table S2). Efficiency extraction was determined using AND as a surrogate standard, and analytical curves ( $n=3$ ) ranged from 2 to 20  $\mu\text{g mL}^{-1}$ . Concentrations of sterols were obtained from RF according to Equation 1.

The LOD values for AH were calculated based on the signal-to-noise ratio: 3 times the ratio of the lowest concentration of the calibration curve and the signal-to-noise ratio regarding the point of least concentration of the calibration curve (Table S3). The limit of quantification (LOQ) for the three classes of compounds was considered as the ratio of the lowest concentration of the calibration curve and the sediment mass.

Due to the absence of sediment certified containing sterols, the accuracy of the method was verified from recovery experiments using a sediment reference prepared in the laboratory. Reference material was prepared by decontaminating 20 g of natural sediment through Soxhlet extraction for 8 h, using 180 mL of DCM: MeOH (2:1 v/v). Then, 3.0 g of decontaminated sediment was transferred to an extraction tube with dichloromethane and spiked with 3.33  $\mu\text{g g}^{-1}$  of AH, 32  $\text{ng g}^{-1}$  of PAH, and 15  $\mu\text{g g}^{-1}$  of sterols standards. Surrogate standards at 5  $\mu\text{g mL}^{-1}$  n-C20D and n-C24D, 102.4  $\text{ng mL}^{-1}$  p-terphenyl-D14, and 15  $\mu\text{g mL}^{-1}$  androstanol were also added, followed by manual shaking. Analysis of spiked reference material was carried out in five replicates, and the precision was evaluated from relative standard deviation values obtained through recovery experiments.

### **Sediment sampling**

The study area is presented in Figure 1. Samples included three rivers and two reservoirs belonging to the Iguaçu River basin. The sampling sites were selected to include densely urbanized regions under intense industrial activity and environmental protection areas. This strategy was adopted to permit the evaluation of the effects of human occupation and its activities along the Iguaçu Basin.

Surface sediment samples were collected with a polyvinyl chloride sampler (50 mm diameter  $\times$  25 cm length). Samples were transferred and stored in previously combusted (450 °C) glass jars sealed with aluminum foil-lined lids and kept frozen (-30 °C) until drying in the laboratory. Thereafter, they were dried (40 °C) until constant weight was attained. Dried samples free of leaves and other impurities were ground in a porcelain mortar and, without sieving, stored in previously cleaned glass vials until analysis. The determination of AH, PAH, and sterols was performed in triplicate according to the modified method.

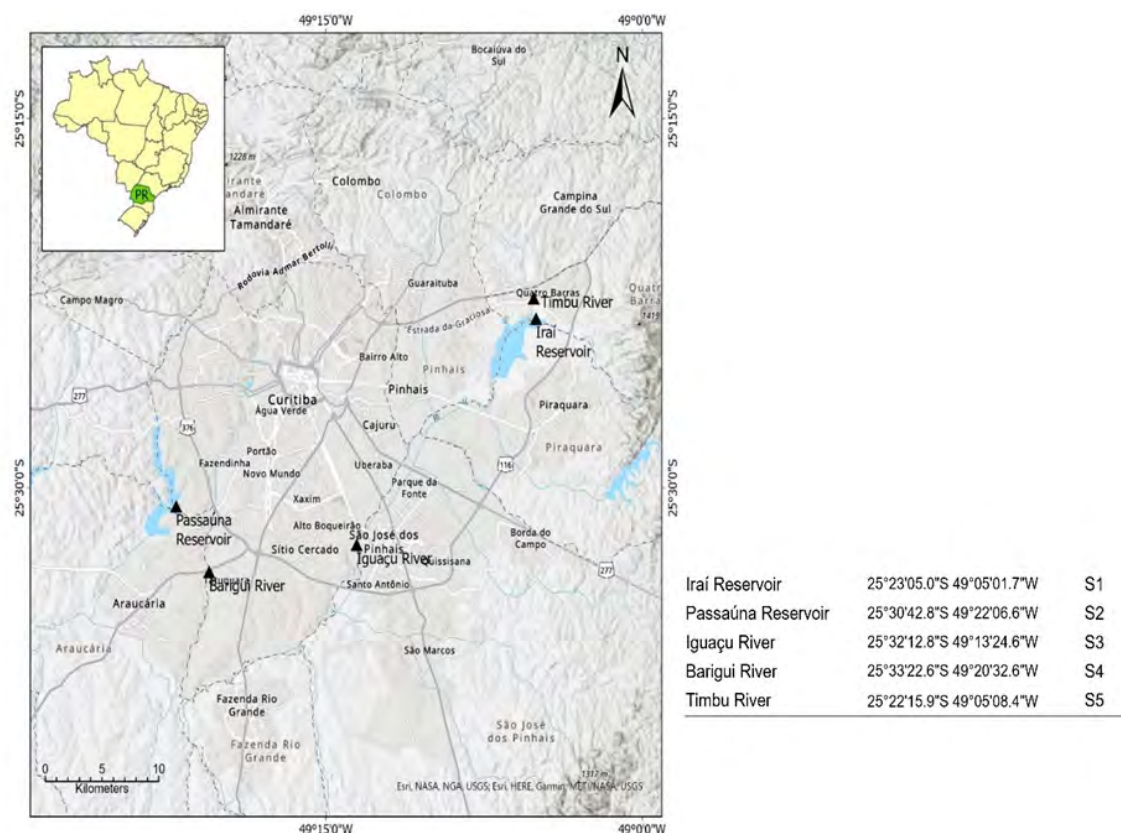


**Figure 1.** Main rivers and reservoirs of the Iguazu River Basin in the MRC. The marks (▲) indicate the approximate locations of sediment sampling in the Barigui River, Iguazu River, Timbu River, Irai Reservoir, and Passaúna Reservoir.

## RESULTS AND DISCUSSION

### Clean-up and fractionation

According to the literature, the clean-up step is essential for complex matrices such as aquatic sediments because it reduces the interferences, then increases the signal/noise ratio, provides greater analytical reliability, and minimizes maintenance of chromatographic system.<sup>24–26</sup> Based on this, the clean-up step was evaluated using different amounts of alumina (1.0 and 2.0 g), activated silica (2.0 g), and activated/deactivated silica (2.0 g), according to Table I.

The optimized conditions for AH, PAH, and sterols fractionation were obtained through Experiment 4 of Table I, that is, 2.0 g of deactivated  $\text{SiO}_2$  and 1.0 g of  $\text{Al}_2\text{O}_3$ . In this experiment, when the first aliquot of solvent was eluted through the column, corresponding to approximately 5.5 mL of hexane, the AH was separated. In the second fraction, PAH obtained after elution was 10 mL of DCM:HX (4:1 v/v), and the third fraction contained 12 mL of Et.Ac.:MeOH (3:1 v/v), the most polar compounds (sterols).<sup>27</sup>

Under these conditions, the obtained recoveries of AH ranged from 85% to 104%. The relative standard deviation (RSD) was up to 9.6%. PAH recoveries ranged from 65% to 112%, RSD was up to 21.2%, sterols recoveries were between 74% and 89%, and maximum RSD was up to 9.2%. These values of precision and accuracy were considered suitable for these three classes of compounds, and the conditions of Experiment 4 were selected to continue the next steps of the work.<sup>28</sup>

### Method performance

The performance of the proposed method was evaluated according to some parameters, such as correlation coefficient, limits of detection (LOD) and quantification (LOQ), recovery, and relative standard deviation (RSD). The analytical curves showed satisfactory linearity since the regression coefficients

varied from 0.9924 to 0.9998 for AH, 0.9861 to 0.9973 for PAH, and 0.9765 to 0.9957 for sterols and were considered satisfactory.<sup>29,30</sup>

LOD values ranged from 0.021 to 0.069  $\mu\text{g g}^{-1}$  for AH, 0.027 to 0.168  $\text{ng g}^{-1}$  for PAH, and 0.039 to 0.159  $\mu\text{g g}^{-1}$  for sterols. LOQ values were considered as the lowest concentration levels of the analytical curve (0.100  $\mu\text{g g}^{-1}$  for aliphatic, 1.633  $\text{ng g}^{-1}$  for 16 PAH, and 0.080  $\mu\text{g g}^{-1}$  for all sterols, except for campesterol, which was 0.133  $\mu\text{g g}^{-1}$ ).<sup>31</sup> Therefore, the values of LOD and LOQ demonstrated the high sensitivity of the optimized method. The average recovery ranges for experiments of accuracy and precision were 67% to 88% for AH, 44% to 105% for PAH, and 40% to 76% for sterols.<sup>29,32,33</sup>

Surrogate internal standards recoveries ranged satisfactorily from 82% and 83% to n-C20D and n-C24D, respectively, 85% for p-terphenyl-D14, and 83% for androstanol (Table S7). Some PAHs, like naphthalene, acenaphthylene, and acenaphthene, presented recoveries below 70%. It can be attributed to the loss by volatilization and co-elution in the fraction of aliphatic hydrocarbons, as previously mentioned. RSD of AH, PAH, and sterols ranged from 1% to 19%, these values are regarded as satisfactory since in trace analysis and complex matrices such as sediments, values of up to 20% were acceptable.

Table II summarizes the steps optimized in this work and compares them to a method described in the literature. Comparing our modified method to the US EPA 8270 method, there is a significant decrease in the amounts of reagent. Another key issue is also present, and this method is a substantial reduction in sample preparation and instrumental analysis elapsed time.

Thus, it is possible to conclude that the method proposed in this work presents satisfactory results when compared to the consolidated method. In addition, the results were obtained through less expensive and polluting processes and caused less harm to the health of the analysts.

In this sense, Da Silva et al.<sup>34</sup> presented very approximate recovery values; however, the number of reagents and their toxicity were greater when compared to this work. For example, the extraction was carried out with 200 mL of organochlorine solvent with the assistance of an ultrasound bath, and the mass of sorbent was 10 g. Likewise, Kawakami et al.<sup>7</sup> developed a method for the determination of sterols that was proposed using Soxhlet extraction followed by a clean-up step.

**Table II.** Summary of extraction and clean-up steps for the methods optimized, standard according to US EPA 8270, and performance from the recovery (%)

Variables	Proposed method	US EPA 8270 <sup>a</sup>
Clean-up column	7 mm i.d. x 30 cm	13 mm i.d. x 30 cm
Silica	2 g	8 g
Alumina	1 g	1 g
F1 Solvent	5.5 mL of Hexane	40 mL of Hexane
F2 Solvent	10 mL of HX/DCM (4:1)	75 mL of HX/DCM (1:1)
F3 Solvent	12 mL of Et.Ac./MeOH (3:1)	---
Equipment	Ultrasound	Soxhlet
Solvent <sup>b</sup>	21 mL DCM/MeOH (2:1)	200 mL of DCM
HA Recovery (%)	67 to 88%	45 to 110%
PAH Recovery (%)	44 to 105%	60 to 105%
Esterols Recovery (%)	40 to 76%	---
Elapsed time (h) <sup>c</sup>	1:30	5:00

<sup>a</sup> Optimization based on US EPA standard method; <sup>b</sup> Total volume of solvent in the extraction step,

<sup>c</sup> Total time of analysis, except chromatographic determination.



**Distribution of AH, PAH, and sterols in sediments of rivers in the MRC**

The modified method was then applied to sediment samples obtained from aquatic bodies in the MRC: Iraí and Passaúna reservoirs and the Iguaçu, Barigui, and Timbu rivers. Table III shows the concentrations of AH, PAH, and sterols obtained from these analyses.

The total AH concentrations ranged from 1.15  $\mu\text{g g}^{-1}$  to 509.69  $\mu\text{g g}^{-1}$ , and the highest concentration obtained was from the Timbu River sample. Regarding the total levels of PAH, the sediment collected in predominantly urban and industrial areas, represented by the Iguaçu and Barigui rivers, showed lower concentrations compared to the sample from the Timbu River, located in an environmental protection area.

According to the literature, it is possible to distinguish the degree of contamination in impacted hydrographic environments based on the correlation between the total concentrations of PAH present in its sediments. In this classification, values of concentrations greater than 500  $\text{ng g}^{-1}$  are called “highly contaminated”, between 250 to 500  $\text{ng g}^{-1}$  are “moderately contaminated,” and below 250  $\text{ng g}^{-1}$  are “slightly contaminated”, and these criteria are used in several studies involving environmental assessment.<sup>35–39</sup>

**Table III.** Determination of AH, PAH, and sterols in sediment samples obtained from the Iraí and Passaúna reservoirs and the Iguaçu, Barigui, and Timbu rivers (n=3)

Parameter	Iraí Reservoir	Passaúna Reservoir	Iguaçu River	Barigui River	Timbu River
<b>AH (<math>\mu\text{g g}^{-1}</math>)</b>					
$\Sigma$ alkanes ( $\text{C}_{16} - \text{C}_{36}/\text{UCM}$ )	3.05	1.18	1.15	4.18	509.69
UCM	-	-	-	-	488.26
REC (%) $\text{C}_{20}\text{d}$	69	84	82	86	118
REC (%) $\text{C}_{24}\text{d}$	65	85	65	78	84
<b>PAH (<math>\text{ng g}^{-1}</math>)</b>					
Nap	17.20	16.30	24.56	9.11	17.93
Ace	9.14	8.63	8.99	9.06	< 1.63
Acy	6.20	4.99	5.53	5.32	13.50
Fl	9.97	7.93	9.28	8.44	25.50
Phen	12.20	8.26	13.06	8.21	37.40
Ant	9.92	9.19	12.80	9.56	30.70
Flu	10.10	8.96	16.90	10.70	65.10
Pyr	7.67	6.46	16.20	8.91	56.40
BaA	< 1.63	< 1.63	2.38	2.51	5.62
Chry	5.89	5.13	11.80	7.93	20.50
BbF	3.59	3.30	10.20	12.40	39.70
BbK	7.79	7.62	12.40	9.94	26.60
BaP	5.79	6.64	16.10	6.84	34.90
IP	4.15	3.90	10.90	5.63	23.60
DahA	6.29	< 1.63	8.68	5.70	18.30

(continues on next page)

**Table III.** Determination of AH, PAH, and sterols in sediment samples obtained from the Iraí and Passaúna reservoirs and the Iguaçu, Barigui, and Timbu rivers (n=3) (continuation)

Parameter	Iraí Reservoir	Passaúna Reservoir	Iguaçu River	Barigui River	Timbu River
Bghi	< 1.63	< 1.63	10.70	8.84	24.90
ΣPAH	116	99	190	129	440
REC (%) p-terphenyl-D <sub>14</sub>	103	87	88	119	63
<b>Sterols (μg g<sup>-1</sup>)</b>					
Cop	< 0.08	< 0.08	0.75	0.15	410
E-cop	< 0.08	< 0.08	0.35	< 0.08	24.6
Coprostanone	< 0.08	< 0.08	0.27	< 0.08	173
Cholesterol	0.44	0.08	0.22	0.08	11.2
Cholestanol	0.48	0.10	0.47	< 0.08	36.1
Stigmasterol	3.06	0.37	0.28	0.14	7.67
Stigmastanol	2.11	0.37	0.60	0.68	13.8
β-sitosterol	3.33	0.36	0.28	0.22	7.15
Campesterol	10.3	1.34	0.52	0.46	64.4
Σsterols	19.8	2.62	3.73	1.73	749
REC (%) Androstanol	112	87	102	87	125

AH: Aliphatic Hydrocarbons; PAH: Polycyclic Aromatic Hydrocarbons; UCM: Unresolved complex mixture; REC: Surrogate standard recovery; \*Ratio is calculated from the area values of each compound.

Thus, the Timbu River sample is classified as moderately contaminated and the samples from the Iguaçu and Barigui Rivers and reservoirs samples as low level of contamination. Meniconi et al.<sup>40</sup> detected 532 ng g<sup>-1</sup> and 70 ng g<sup>-1</sup> (Σ16 PAH) in sediment samples collected in 2000 from the Barigui and Iguaçu rivers, respectively, after the rupture of the pipeline of a Petrobras oil refinery that caused the spill of 4000 m<sup>3</sup> of crude oil into the bed of the Barigui River. Leite et al.<sup>41</sup> showed that sediments from the rivers Iguaçu and Barigui collected in 2005 in the same local in this study were classified as highly contaminated, with total PAH concentrations of 1713 ng g<sup>-1</sup> and 1206 ng g<sup>-1</sup>, respectively.

The Timbu River and Iraí Reservoir samples were classified as slightly contaminated, with a total concentration of PAH 222 ng g<sup>-1</sup> and 131 ng g<sup>-1</sup>, respectively. Regarding the presence of sterols, the largest concentrations were found in the Timbu River and Iraí Reservoir.

Positive detection of coprostanol is widely used as evidence of sewage contamination in aquatic environments.<sup>42–44</sup> Other sterols were found in a broad range of concentrations, with the highest levels in the Timbu River.

### **Composition of organic matter sources and source quantified**

The composition of the total concentrations of each group of quantified compounds in Timbu, Barigui, and Iguaçu Rivers and Passaúna and Iraí Reservoirs is shown in Figure 2. For all samples, except the Barigui River, the quantified compounds were mainly composed of sterols. The Barigui River sample was characterized by the predominance of AH, while the PAH, molecular markers of anthropogenic source, had

the lowest contributions. Organic matter can have various sources, and when derived from the anthropogenic origin is directly related to the types of activities in that area.<sup>42,45,46</sup> Of the samples from the Barigui River and reservoirs, more than 95% of the compounds quantified were of natural input. For the samples from the Iguaçu and Timbu rivers, 53% and 88% of the markers quantified, respectively, are of anthropogenic origin, as presented in Figure 3.

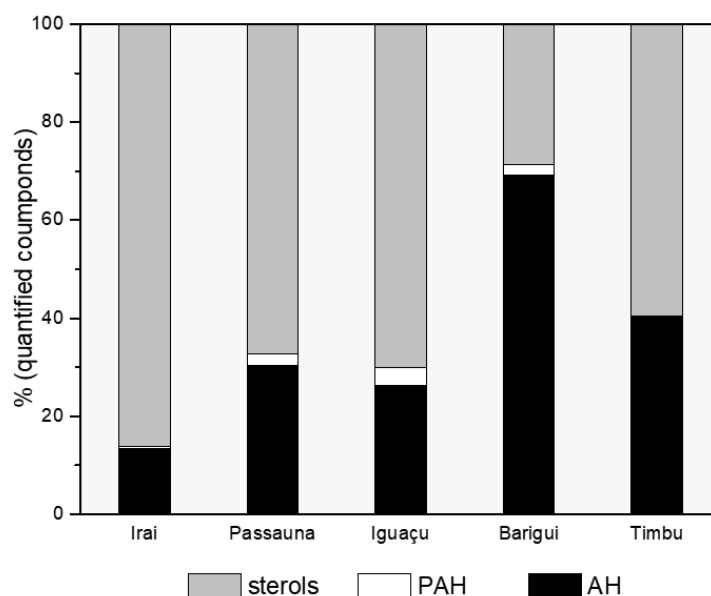


**Figure 2.** Composition of organic matter quantified. Sterols: Cop, e-cop, coprostanone, cholesterol, cholestanol, stigmasterol, stigmasterol and campesterol; PAH:  $\Sigma 16$  PAH; AH: C16 to C36, pristane, phytane and UCM.

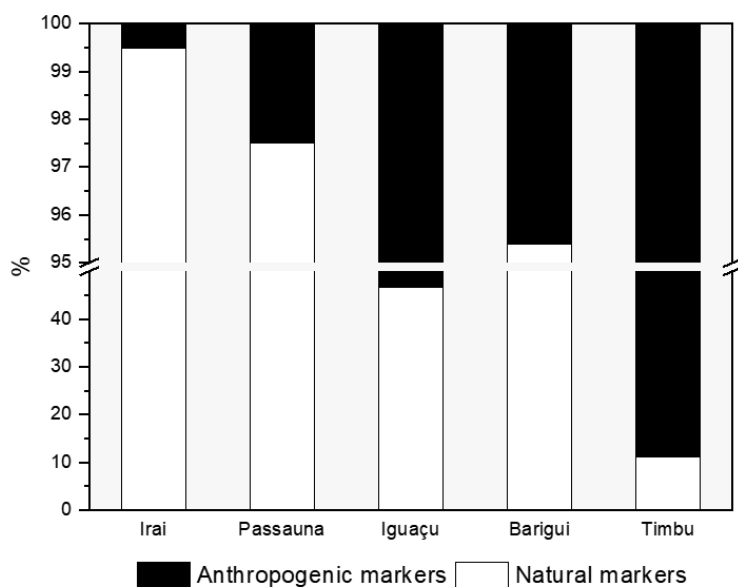


**Figure 3.** Comparison of quantitative molecular markers of natural and anthropogenic origin.

The sampling encompasses areas with different types of anthropogenic activities. The reservoirs are characterized by the presence of rural areas and proximity to industrialized regions. Barigui River is present in a densely urbanized area, and Timbu River in a region with high demographic expansion exhibits low levels of sanitation, finally the sample from the Iguaçu River is in an industrial site.<sup>45,47,48</sup>

The compounds quantified were classified according to their possible sources. The calculated (Table IV) by carbon preference index, CPI according to Equation 2.

$$CPI = \frac{1}{2} \times \left[ \left( \frac{C_{23}+C_{25}+C_{27}+C_{29}+C_{31}}{C_{22}+C_{24}+C_{26}+C_{28}+C_{30}} \right) + \left( \frac{C_{23}+C_{25}+C_{27}+C_{29}+C_{31}}{C_{24}+C_{26}+C_{28}+C_{30}+C_{32}} \right) \right] \quad (\text{Equation 2})$$

The distinction between PAH from petrogenic and pyrogenic sources can be made by the presence of a higher concentration of PAH of low molecular weight (2 – 3 rings) and alkylated PAH, which suggest petrogenic sources since PAH of high molecular weight (4 – 6 rings) are indicated pyrogenic sources.<sup>49</sup> Another very effective way to identify the possible sources of these compounds, in sediment, is the calculation of the ratio of isomers of molecular weight 202 (Flu, Pyr), 228 (BaA, Chry), and 276 (IP, BghiP), that, due to thermodynamic stability and to a greater abundance of these compounds.<sup>4</sup>

**Table IV.** Reasons and specific limits for distinguishing the origin of the AH, PAH, and sterols

AH and PAH			
	Petrogenic	Pyrogenic	Natural
CPI <sup>a</sup>	< or ≈ 1	–	> 1
Ant/(Ant+Fen) <sup>b</sup>	< 1	> 1: coal and diesel oil combustion	
Flu/(Flu+Pyr) <sup>b</sup>	< 0.4	> 0.5: biomass combustion < 0.5 e > 0.4: fossil fuels	
BaA/(BaA+Cris) <sup>b</sup>	< 0.2 0.2 to 0.35	0.2 to 0.35: fossil fuels > 0.35: biomass combustion	
IP/(IP+BghiP) <sup>b</sup>	< 0.2	0.2 to 0.5: fossil fuels > 0.50: biomass combustion	
Sterols			
		Domestic sewage	
% (cop + e-cop)/ ∑sterols <sup>c</sup>		> 50 %: highly contaminated	
e-cop/cop <sup>d</sup>		< 0.2: effluent not treated; > 0.8: treated effluent	
cop/cholesterol <sup>c</sup>		> 1.0: contaminated; < 1.0 natural	
cop / (cop + cholestanol) <sup>e</sup>		> 0.7 contaminated; < 0.3: not contaminated	

AH: Aliphatic Hydrocarbons; PAH: Polycyclic Aromatic Hydrocarbons; CPI: Carbon Preference Index; <sup>a</sup> Aboul-Kassim;<sup>50</sup>

<sup>b</sup> Yunker;<sup>4</sup> <sup>c</sup> Venkatesan;<sup>3</sup> <sup>d</sup> Mudge;<sup>51</sup> <sup>e</sup> Grimalt<sup>52</sup>.

According to the data shown in Table III and the data presented in Figure 4, it is noted that combustion was the predominant source of the isomeric pairs of PAH in the sediment analyzed. However, the combustion source cannot be made clear since there are discrepancies among the ratios used to determine them (Figure 3). Nevertheless, it is possible to assume that vegetation burning in the surrounding areas of the water reservoirs was the major source of these compounds related to the combustion of biomass.<sup>53,54</sup>



AH of biogenic origin is characterized by a predominance of compounds with odd carbon numbers. Small molecular chains, from 15 to 23 carbon atoms, indicate the presence of aquatic organisms, while the predominance of long molecular chains, between 23 and 33 carbons, suggests the presence of higher plants.<sup>55</sup>

For the samples of Iraí Reservoir and Barigui River, there is a predominance of AH containing an odd number of the linear carbon chain, especially those of higher molecular weight (n-C25, n-C27, and n-C29). The presence of n-C27 and n-C29 is typical of lacustrine sediments where higher plants are predominant, whereas the presence of n-C25 alkane is related to the proliferation of floating macrophytes.<sup>55-57</sup>

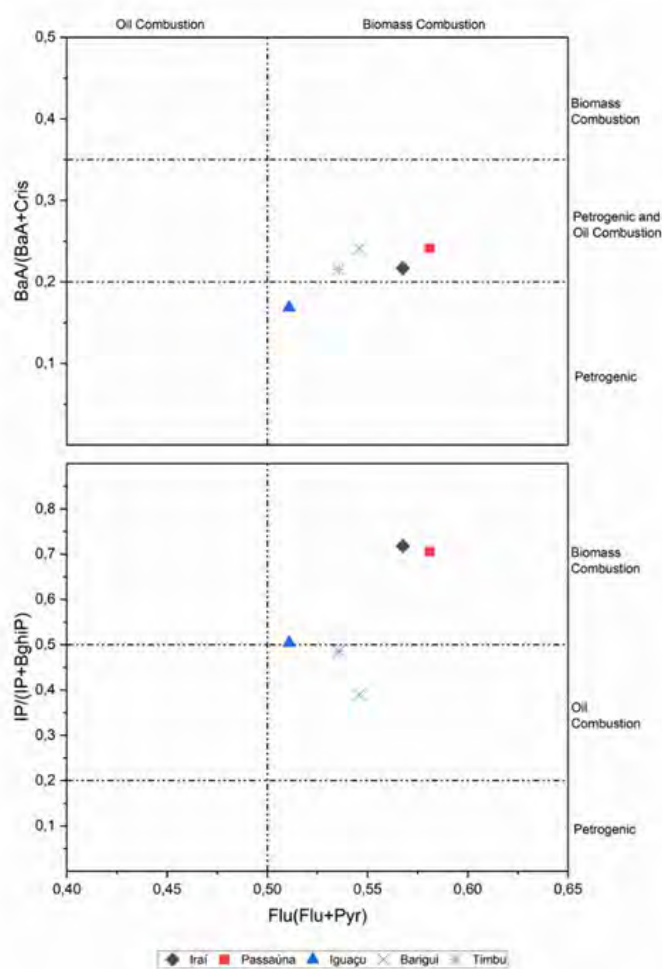


**Figure 4.** Representation of two-dimensional calculated ratios to identify specific sources of the isomeric pairs of PAHs (202, 228, and 276).

Due to the morphometric characteristics of the Iraí Reservoir, the proliferation of macrophytes plants is abundant, which justifies the presence of n-alkane n-C25 in the sample. The presence of AH of biogenic sources in the Barigui River and the reservoir samples can be confirmed by the CPI>1. CPI values for samples from the Iguaçu and Timbu Rivers (Table V) suggest the petrogenic input of AH (CPI<1).

The chromatographic profile of the Timbu River sample is characteristic of a UCM (Unresolved Complex Mixture) with a concentration of 488  $\mu\text{g g}^{-1}$ . UCM is characterized by a broad hump in the baseline of the chromatogram resulting from the analysis of sediment contaminated with biodegraded petroleum, unburned petroleum, lubricants, and asphalts from urban runoff.<sup>57,58</sup> The Timbu River, despite being present in the environmental protection area of Iraí, cuts across one of the busiest highways for motor vehicles in the MRC.

**Table V.** Values of AH calculated for specific reasons and sterols

Parameter	Irai Reservoir	Passaúna Reservoir	Iguaçu River	Barigui River	Timbu River
AH					
CPI	2.67	3.46	0.91	3.59	1,19
Sterols					
% (cop + e-cop) / $\Sigma$ sterols	0.31 <sup>a</sup>	1.32 <sup>a</sup>	30.44	9.06 <sup>a</sup>	75.62
e-cop / cop	0.42 <sup>a</sup>	0.37 <sup>a</sup>	0.46	0.10 <sup>a</sup>	0.06
cop/cholesterol	0.10 <sup>a</sup>	0.28 <sup>a</sup>	3.39	2.00	36.64
cop / (cholesterol + cholestanol)	0.05 <sup>a</sup>	0.12 <sup>a</sup>	1.00	1.14	8.68
cop / (cop + cholestanol)	0.08 <sup>a</sup>	0.16 <sup>a</sup>	0.59	0.73	0.92

AH: Aliphatic hydrocarbons; CPI: Carbon Preference Index; <sup>a</sup> Ratio calculated from the area values of each compound.

The chromatographic profile of the Timbu River sample is characteristic of a UCM (Unresolved Complex Mixture) with a concentration of 488  $\mu\text{g g}^{-1}$ . UCM is characterized by a broad hump in the baseline of the chromatogram resulting from the analysis of sediment contaminated with biodegraded petroleum, unburned petroleum, lubricants, and asphalts from urban runoff.<sup>57,58</sup> The Timbu River, despite being present in the environmental protection area of Irai, cuts across one of the busiest highways for motor vehicles in the MRC.

Thus, the presence of AH petrogenic sources in this river's sediments can be caused by the leaching of oil vehicles that travel on this road or asphalts from runoff. In general, we can say that the contribution of AH by petrogenic origin occurred in areas near roads with intense traffic of vehicles (Timbu River) and highly urbanized areas (Iguaçu River), thus giving a large anthropogenic input into these environments.

In contrast, the sediment from the Barigui River, despite being collected near a significant highway vehicle traffic in a highly industrialized and urbanized area, showed no indications of AH derived from petroleum and derivatives. Due to the specificity and high half-life of fecal sterols (coprostanol, epicoprostanol, and coprostanone), these compounds have been widely mentioned in studies involving fecal contamination and effluents.<sup>3,59,60</sup>

Coprostanol concentration  $> 0.1 \mu\text{g g}^{-1}$ , may be indicative of sewage contamination,<sup>52</sup> however, this parameter cannot be conclusive since this compound can be produced in situ anoxic conditions.<sup>61</sup> Thus, to confirm the sediment examined received input from domestic sewage is necessary to consider the concentrations of other sterols and the main relationships between them. The ratios used in this study and the results obtained are listed in Table III and Table IV, respectively.

The ratios obtained for the Timbu River indicate strong contamination by sewage. The discharge of sewage in nature in the vicinity of the Timbu River is a reality and accounts for more than 700 illegal connections to sewers along the bed of the river.<sup>60</sup> The value obtained from the E-COP/COP ratio (0.06) allows estimates of the degree of effluent treatment plant disposed of in an area. This value demonstrated that there is a predominance of coprostanol relative to epicoprostanol, noting the contribution of untreated sewage. Note also that for this sample, there is a relative abundance of coprostanone (173  $\mu\text{g g}^{-1}$ ). According to Grimalt et al.,<sup>52</sup> coprostanone is an estanone produced in smaller quantities than coprostanol in the biotransformation of cholesterol, and its presence is associated with fecal contamination, thus proving contamination by sewage at this site.

Regarding the Iguaçu River, it was found by the percentage ratio cop + e-cop/ $\Sigma$ sterols that the value obtained for the sampled sediment (30%) is slightly below the threshold to be considered highly polluted. The value of E-COP/COP for this sediment was 0.46 within the maximum and minimum levels used in

predicting the presence or absence of treated effluent. However, it can be said that this river receives the discharge of treated effluent since the collection point is located downstream of the WWTP-Belem. It was found for the sample Barigui River, which is an industrialized and urbanized region, which although not heavily polluted ( $COP + E-COP/\sum \text{sterols} = 9\%$ ), there is no influence of wastewater treated on-site sampled ( $e-cop/cop = 0.10$ ).

This result corroborates the study by Froehner and Martins,<sup>62</sup> which evaluated the presence of fecal sterols in 6 different regions of the river Barigui and found that all sampling sites were contaminated by sewage, especially in regions of greater human interference. The values of individual concentrations of fecal sterols obtained for the sources were below LOD, showing that there is little or no evidence that these samples are contaminated by sewage. The sterol that occurred at higher concentrations for these samples was campesterol, which is associated with sources of natural organic material of terrestrial or aquatic origin and, specifically, in this case, can result from the contribution of these algae present in the water reservoir.

From the evaluation of individual markers, it was possible to make an approximation of the relative contributions of anthropogenic markers quantified in this study (Figure 5). For reservoir samples, where no suppression demographic, combustion was the predominant source of molecular markers quantified, with no contribution of markers of the fecal source. However, for the samples of the Iguaçu, Barigui, and Timbu rivers, located in urbanized and industrialized areas, contributions of molecular markers from combustion and sewage were approximately the same proportion.

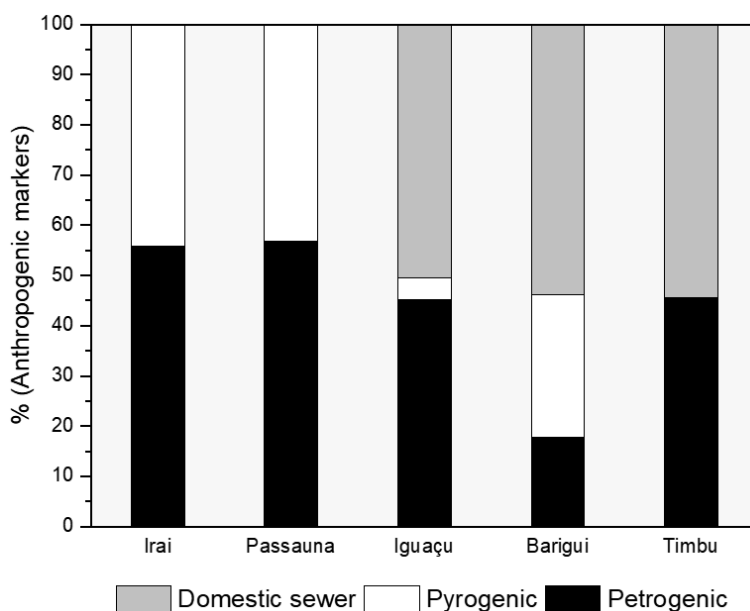


**Figure 5.** Distribution of quantitative molecular markers of anthropogenic origin for the samples analyzed.

### Comparative analysis with previous studies

PAH concentrations in sediment samples from rivers and reservoirs in Curitiba, Brazil, were evaluated against previously published data (Table S4). The total PAH concentrations ( $\sum \text{PAHs}$ ) ranged from 97.3 to 440.65  $\mu\text{g kg}^{-1}$ , which are relatively low compared to many other global regions. For example, the Yinma River Basin in China<sup>63</sup> reported concentrations between 1000 and 5750  $\mu\text{g kg}^{-1}$ , while the Niger Delta in Nigeria<sup>64</sup> had even higher levels, ranging from 1620 to 19800  $\mu\text{g kg}^{-1}$ . In southeastern Poland,<sup>65</sup>  $\sum \text{PAHs}$  reached as high as 33900  $\mu\text{g kg}^{-1}$ . In contrast, the Poxim River in Brazil showed much lower concentrations, between 2.2 and 28.4  $\mu\text{g kg}^{-1}$ .<sup>66</sup>

The PAH profile in Curitiba indicates a dominant contribution from pyrogenic sources, particularly biomass burning. This contrasts with numerous other areas where sources are typically mixed. For instance, petroleum-related pollution is significant in the Yinma River (China), Salt River (Taiwan), and Niger Delta (Nigeria), often accompanied by pyrogenic contributions from vehicle emissions and coal burning. This variation in source distribution may be indicative of different levels of industrialization and land-use practices. Regarding ecological and human health risks, the concentrations observed in Curitiba are likely to pose a lesser concern compared to heavily impacted environments such as the Salt River and the Tigris River.<sup>67,68</sup> In these regions, high molecular weight polycyclic aromatic hydrocarbons (PAHs) are prevalent and associated with increased carcinogenic risks. Studies in these areas frequently report moderate to high ecological threats, including significant adverse effects on aquatic biota.

In the present study, coprostanol concentrations ranged from 0.75 to 410  $\mu\text{g g}^{-1}$ . These values suggest moderate to high levels of fecal contamination, particularly in densely populated areas and regions with direct untreated sewage discharge. In comparison to other studies (Table S5), the levels in Curitiba ranged across a wide international spectrum, indicating different levels of urbanization, sanitation facilities, and anthropogenic influence. The Ipojuca River in Brazil showed a significantly elevated coprostanol concentration of 557.3  $\mu\text{g g}^{-1}$ , attributed to intense human activity and the proximity of urban settlements to the riverbanks.<sup>69</sup> In South Korea, the Geumho River exhibited a wide range of coprostanol concentrations (9 to 1282  $\mu\text{g g}^{-1}$ ), and these elevated levels were associated with extensive urbanization and industrialization in the area.<sup>70</sup> These findings highlight the significant impact of land-use patterns on sewage contamination levels. In contrast, the Guamá River in Brazil had a coprostanol concentration of 292.52  $\mu\text{g g}^{-1}$  linked to insufficient sewage treatment infrastructures and intense port operations.<sup>71</sup> The Kibera River in Kenya<sup>72</sup> showed considerable levels of contamination, ranging from 55 to 298  $\mu\text{g g}^{-1}$ , a result of the continuous discharge of untreated domestic wastewater, echoing the circumstances in Curitiba where direct sewage inputs are a major concern. On the other hand, rivers in areas with more advanced wastewater management systems exhibited considerably substantially reduced concentration levels. For instance, the Thames River in England presented coprostanol levels ranging from 0.0091 to 0.42  $\mu\text{g g}^{-1}$ .<sup>73</sup> Historical sediment core analyses revealed a significant decrease in coprostanol levels over time, correlating with the increasing use and effectiveness of sewage treatment systems. The results of this study highlight the urgent need for investments in basic sanitation infrastructure in urban centers to reduce environmental and public health risks associated with untreated sewage discharge.

Aliphatic hydrocarbon (AH) concentrations ranging from 0.75 to 410  $\mu\text{g g}^{-1}$  and these values suggest moderate contamination, primarily driven by the discharge of untreated sewage and the influence of a densely populated urban area. In comparison to other aquatic systems throughout the world (Table S6), AH levels in Curitiba varied widely, indicating variances in land use, pollution sources, and environmental management techniques. Whereas the Tehran River in Iran<sup>74</sup> had values ranging from 2.94 to 114.7  $\mu\text{g g}^{-1}$  in a densely populated region. However, in this situation, the hydrocarbon input was primarily petrogenic, as opposed to the Curitiba region, which is likely influenced by both anthropogenic and biogenic sources. Al Wajh Lagoon in Saudi Arabia, located near the Red Sea and vulnerable to hydrocarbon contamination from neighboring oil-related operations, showed a similar petrogenic effect (64-302.6  $\mu\text{g g}^{-1}$ ).<sup>75</sup> The concentration range in Brazil's rural aquatic system, the Mangueira Lagoon, was larger and wider (5.0–652.7  $\mu\text{g g}^{-1}$ ), with hydrocarbons mostly coming from petrogenic and biogenic sources.<sup>76</sup> This implies that natural and diffuse anthropogenic influences might cause significant AH levels to be present even in regions with lower metropolitan densities. Lower concentrations were recorded in the Lafayette River (USA), with values ranging from 4.94 to 40.83  $\mu\text{g g}^{-1}$ , where the sources were attributed to atmospheric deposition and automotive activity.<sup>77</sup> This scenario reflects a more diffuse contamination profile typical of urban areas with relatively controlled direct discharge. The Norilsk–Pyasino water system in Russia<sup>78</sup> had the highest AH values among the examined studies, with concentrations ranging from 15 to 1914  $\mu\text{g g}^{-1}$ , resulting from a large-scale diesel fuel spill. In contrast to the ongoing urban and domestic inputs seen in Curitiba, this is an acute contamination episode. In summary, the AH concentrations in Curitiba are moderate when viewed in the global context, with values



exceeding those of more regulated urban areas (e.g., Lafayette River) but significantly lower than those impacted by major industrial or accidental events (e.g., Norilsk–Pyasino). The sources in Curitiba appear to be primarily related to untreated domestic sewage and urban runoff, reinforcing the need for improved wastewater infrastructure to mitigate hydrocarbon inputs into aquatic systems.

## CONCLUSIONS

This work has resulted in a significant decrease in the number of reagents and the total analysis time compared to the official methodology described in the literature. Some figures of merit of the method demonstrated that the accuracy and precision obtained are suitable for the determination of the compounds in sediments; results were obtained with high-reliability analysis.

The use of geochemical markers for preliminary assessment of sources of organic matter and contamination in the sediments showed that the sediment with a higher input of organic matter of anthropogenic origin corresponds to the sample the Timbu River, this river despite being in an area of environmental protection. The presence of coprostanol as an indicator of fecal contamination showed that the pollution of the Iguaçu and Barigui rivers is heavily influenced by urban and industrial activities, respectively, and was a significant contribution to domestic sewage. Overall, the results obtained regarding the origin of the PAH demonstrate that combustion was the predominant source of this class of compounds evaluated for sediment.

## Conflicts of interest

The authors confirm that there are no known conflicts of interest associated with this publication.

## Acknowledgements

The authors would like to thank the “Ministério da Ciência, Tecnologia Inovações e Comunicações” (MCTIC), the “Financiadora de Estudos e Projetos” (FINEP), CTHIDRO 01/2013, the “Instituto Nacional de Ciências e Tecnologias Analíticas Avançadas” (INCTAA, 465768/2014-8), and PETROBRAS for the financial support. This study was also financed in part by the “Coordenação de Aperfeiçoamento de Pessoal de Nível Superior – Brasil” (CAPES) – Finance Code 001. M.T. Grassi is also thankful to the “Conselho Nacional de Desenvolvimento Científico e Tecnológico” (CNPq), grant number 308055/2017-9.

## REFERENCES

- (1) Isobe, K. O.; Tarao, M.; Zakaria, M. P.; Chiem, N. H.; Minh, L. Y.; Takada, H. Quantitative Application of Fecal Sterols Using Gas Chromatography - Mass Spectrometry to Investigate Fecal Pollution in Tropical Waters: Western Malaysia and Mekong Delta, Vietnam. *Environ. Sci. Technol.* **2002**, 36 (21), 4497–4507. <https://doi.org/10.1021/es020556h>
- (2) Kwan, C. S.; Takada, H.; Boonyatumanond, R.; Kato, Y.; Mizukawa, K.; Ito, M.; Dung, L. Q.; Zakaria, M. P.; Santiago, E. C. Historical Occurrences of Polybrominated Diphenyl Ethers and Polychlorinated Biphenyls in Manila Bay, Philippines, and in the Upper Gulf of Thailand. *Sci. Total Environ.* **2014**, 470–471, 427–437. <https://doi.org/10.1016/j.scitotenv.2013.09.076>
- (3) Venkatesan, M. I.; Kaplan, I. R. Sedimentary Coprostanol as an Index of Sewage Addition in Santa Monica Basin, Southern California. *Environ. Sci. Technol.* **1990**, 24 (2), 208–214. <https://doi.org/10.1021/es00072a009>
- (4) Yunker, M. B.; Macdonald, R. W.; Vingarzan, R.; Mitchell, R. H.; Goyette, D.; Sylvestre, S. PAHs in the Fraser River Basin: A Critical Appraisal of PAH Ratios as Indicators of PAH Source and Composition. *Org. Geochem.* **2002**, 33 (4), 489–515. [https://doi.org/10.1016/S0146-6380\(02\)00002-5](https://doi.org/10.1016/S0146-6380(02)00002-5)
- (5) Saito, Y.; Ueta, I. Miniaturization for the Development of High Performance Separation Systems. *Chromatography* **2017**, 38 (3), 85–94. <https://doi.org/10.15583/jpchrom.2017.019>
- (6) Kim, N. Y.; Loganathan, B. G.; Kim, G. B. Determination and Comparison of Freely Dissolved PAHs Using Different Types of Passive Samplers in Freshwater. *Sci. Total Environ.* **2023**. <https://doi.org/10.1016/j.scitotenv.2023.164802>

- (7) Kawakami, S. K.; Montone, R. C. An Efficient Ethanol-Based Analytical Protocol to Quantify Faecal Steroids in Marine Sediments. *J. Braz. Chem. Soc.* **2002**, *13* (2), 226–232. <https://doi.org/10.1590/S0103-50532002000200014>
- (8) Pouch, A.; Zaborska, A.; Mazurkiewicz, M.; Winogradow, A.; Pazdro, K. PCBs, HCB and PAHs in the Seawater of Arctic Fjords – Distribution, Sources and Risk Assessment. *Mar. Pollut. Bull.* **2021**, *164*. <https://doi.org/10.1016/j.marpolbul.2021.111980>
- (9) Fontana, A. R.; Lana, N. B.; Martinez, L. D.; Altamirano, J. C. Ultrasound-Assisted Leaching-Dispersive Solid-Phase Extraction Followed by Liquid-Liquid Microextraction for the Determination of Polybrominated Diphenyl Ethers in Sediment Samples by Gas Chromatography-Tandem Mass Spectrometry. *Talanta* **2010**, *82* (1), 359–366. <https://doi.org/10.1016/j.talanta.2010.04.050>
- (10) Zhao, L.; Zhao, Z.; Zhang, J.; Zhang, P. Seasonal Variation, Spatial Distribution, and Sources of PAHs in Surface Seawater from Zhanjiang Bay Influenced by Land-Based Inputs. *Mar. Environ. Res.* **2023**, *188*. <https://doi.org/10.1016/j.marenvres.2023.106028>
- (11) United States Environmental Protection Agency (US EPA). *Method 3540C: Soxhlet Extraction, part of Test Methods for Evaluating Solid Waste, Physical/Chemical Methods*, 1996. Available at: <https://www.epa.gov/sites/default/files/2015-12/documents/3540c.pdf> (accessed 03/2024).
- (12) United States Environmental Protection Agency (US EPA). *Method 3610B: Alumina Cleanup, part of Test Methods for Evaluating Solid Waste, Physical/Chemical Methods*, 1996. Available at: <https://www.epa.gov/sites/default/files/2015-12/documents/3610b.pdf> (accessed 03/2024).
- (13) United States Environmental Protection Agency (US EPA). *Method 3630C: Silica Gel Cleanup, part of Test Methods for Evaluating Solid Waste, Physical/Chemical Methods*, 1996. Available at: <https://www.epa.gov/sites/default/files/2015-12/documents/3630c.pdf> (accessed 03/2024).
- (14) Hara, E. L. Y.; da Silva, C. A.; Souza, R. S.; Saint Clair Colimo, A. G.; Grassi, M. T. Determination of Polybrominated Diphenyl Ethers in Riverine Sediments by Ultrasound-Assisted Microextraction (USAME), Reduced Scale Cleanup, and GC-MS. *Curr. Anal. Chem.* **2018**, *14* (6), 615–625. <https://doi.org/10.2174/1573411014666171229161613>
- (15) Martín-Pozo, L.; de Alarcón-Gómez, B.; Rodríguez-Gómez, R.; García-Córcoles, M. T.; Çipa, M.; Zafra-Gómez, A. Analytical Methods for the Determination of Emerging Contaminants in Sewage Sludge Samples. A Review. *Talanta* **2019**, *192*, 508–533. <https://doi.org/10.1016/j.talanta.2018.09.056>
- (16) Wacheski, T.; Hara, E.; Soares, B.; da Silva, B.; Abate, G.; Grassi, M. O-DGT Devices for the Determination of Emerging Contaminants in Aqueous Matrices. *J. Braz. Chem. Soc.* **2021**, *32* (1), 72–82. <https://doi.org/10.21577/0103-5053.20200157>
- (17) Orecchio, S.; Amorello, D.; Indelicato, R.; Barreca, S.; Orecchio, S. A Short Review of Simple Analytical Methods for the Evaluation of PAHs and PAEs as Indoor Pollutants in House Dust Samples. *Atmosphere (Basel)* **2022**, *13* (11). <https://doi.org/10.3390/atmos13111799>
- (18) United States Environmental Protection Agency (US EPA). *Method 3550C: Ultrasonic Extraction, part of Test Methods for Evaluating Solid Waste, Physical/Chemical Methods*, 2007. Available at: <https://www.epa.gov/sites/default/files/2015-12/documents/3550c.pdf> (accessed 2025-04-05).
- (19) Martinez, E.; Gros, M.; Lacorte, S.; Barceló, D. Simplified Procedures for the Analysis of Polycyclic Aromatic Hydrocarbons in Water, Sediments and Mussels. *J. Chromatogr. A* **2004**, *1047*, 181–188. <https://doi.org/10.1016/j.chroma.2004.07.003>
- (20) Patire, V. F.; de Albergaria-Barbosa, A. C. R.; Barreto, I. S.; Taniguchi, S.; Fernandez, W. S.; Dias, J. F.; da Silva, D. A. M.; Bicego, M. C. Bioavailability of Polycyclic Aromatic Hydrocarbons in Santos Bay (Brazil) and its Adjacent Continental Shelf. *Ocean and Coastal Research* **2023**, *71* (2), e23024. <https://doi.org/10.1590/2675-2824071.22047VFP>
- (21) Kawakami, S. K.; Mello, L.; Dergan, A. L.; Evangelista, C.; Aquino, R. F.; Mendes, R. A.; Carmo, A. M. C.; Amado, L. L. Sedimentary PAH and Oxidative Stress Biomarkers Responses on *Namalycastis Abiuma* (Polychaeta: Nereididae) from an Urbanized Amazon Estuary. *Reg. Stud. Mar. Sci.* **2023**, *57*. <https://doi.org/10.1016/J.RSMA.2022.102757>

- (22) Mater, L.; Alexandre, M. R.; Hansel, F. A.; Madureira, L. A. S. Assessment of Lipid Compounds and Phosphorus in Mangrove Sediments of Santa Catarina Island, SC, Brazil. *J. Braz. Chem. Soc.* **2004**, 15 (5), 725–734. <https://doi.org/10.1590/S0103-50532004000500019>
- (23) United States Environmental Protection Agency (US EPA). *Method 8270E (SW-846): Semivolatile Organic Compounds by Gas Chromatography/Mass Spectrometry (GC-MS)*. Available at: <https://www.epa.gov/esam/epa-method-8270e-sw-846-semivolatile-organic-compounds-gas-chromatographymass-spectrometry-gc> (accessed 2025-03-12).
- (24) Cavalcante, R. M.; De Lima, D. M.; Correia, L. M.; Nascimento, R. F.; Silveira, E. R.; Freire, G. S. S.; Viana, R. B. Técnicas de Extrações e Procedimentos de Clean-up Para a Determinação de Hidrocarbonetos Policíclicos Aromáticos (HPA) em Sedimentos da Costa do Ceará. *Quim. Nova* **2008**, 31 (6), 1371–1377. <https://doi.org/10.1590/S0100-40422008000600019>
- (25) Leite, N. F.; Peralta-Zamora, P.; Grassi, M. T. Multifactorial Optimization Approach for the Determination of Polycyclic Aromatic Hydrocarbons in River Sediments by Gas Chromatography-Quadrupole Ion Trap Selected Ion Storage Mass Spectrometry. *J. Chromatogr. A* **2008**, 1192 (2), 273–281. <https://doi.org/10.1016/j.chroma.2008.03.067>
- (26) Sánchez-Avila, J.; Fernandez-Sanjuan, M.; Vicente, J.; Lacorte, S. Development of a Multi-Residue Method for the Determination of Organic Micropollutants in Water, Sediment and Mussels Using Gas Chromatography-Tandem Mass Spectrometry. *J. Chromatogr. A* **2011**, 1218 (38), 6799–6811. <https://doi.org/10.1016/j.chroma.2011.07.056>
- (27) Jimenez Martinez, A. E.; Galoski, C. E.; Cardoso Borillo, G.; Moreton Godoi, R. H.; Lopes Figueira, R. C.; Alves de Lima Ferreira, P.; Froehner, S. Forensic Assessment of Polycyclic Aromatic Hydrocarbons to Reconstruct Anthropogenic Activities in a Nearby Urban Reservoir. *J. South Am. Earth Sci.* **2022**, 120. <https://doi.org/10.1016/J.JSAMES.2022.104104>
- (28) Teixeira, M.; Cesar, R.; Abessa, D.; Siqueira, C.; Lourenço, R.; Vezzzone, M.; Fernandes, Y.; Koifman, G.; Perina, F. C.; Meigikos dos Anjos, R.; Polivanov, H.; Castilhos, Z. Ecological Risk Assessment of Metal and Hydrocarbon Pollution in Sediments from an Urban Tropical Estuary: Tijuca Lagoon (Rio de Janeiro, Brazil). *Environ. Sci. Pollut. Res.* **2023**, 30 (1), 184–200. <https://doi.org/10.1007/S11356-022-22214-6>
- (29) Association of Official Analytical Collaboration (AOAC) International. *Guidelines for Single Laboratory Validation of Chemical Methods for Dietary Supplements and Botanicals*. AOAC International **2002**, 1–38.
- (30) Cai, Y.; Wang, Z.; Cui, L.; Wang, J.; Zuo, X.; Lei, Y.; Zhao, X.; Zhai, X.; Li, J.; Li, W. Distribution, Source Diagnostics, and Factors Influencing Polycyclic Aromatic Hydrocarbons in the Yellow River Delta Wetland. *Reg. Stud. Mar. Sci.* **2023**, 67. <https://doi.org/10.1016/J.RSMA.2023.103181>
- (31) Allouche, M.; Nasri, A.; Harrath, A. H.; Mansour, L.; Beyrem, H.; Boufahja, F. Migratory Behavior of Free-Living Marine Nematodes Surrounded by Sediments Experimentally Contaminated by Mixtures of Polycyclic Aromatic Hydrocarbons. *J. King Saud Univ., Sci.* **2020**, 32 (2), 1339–1345. <https://doi.org/10.1016/j.jksus.2019.11.025>
- (32) Bottoli, C. B. G.; Collins, C. H.; Jardim, I. C. S. F.; Ribani, M. Validação em métodos cromatográficos e eletroforéticos. *Quim. Nova* **2004**, 27 (5), 771–780. <https://doi.org/10.1590/S0100-40422004000500017>
- (33) Parra, Y. J.; Oloyede, O. O.; Pereira, G. M.; de Almeida Lima, P. H. A.; da Silva Caumo, S. E.; Morenikeji, O. A.; Vasconcellos, P. C. Polycyclic Aromatic Hydrocarbons in Soils and Sediments in Southwest Nigeria. *Environmental Pollution* **2020**, 259. <https://doi.org/10.1016/j.envpol.2019.113732>
- (34) Da Silva, T. F.; Azevedo, D. de A.; Neto, F. R. D. A. Distribution of Polycyclic Aromatic Hydrocarbons in Surface Sediments and Waters from Guanabara Bay, Rio de Janeiro, Brazil. *J. Braz. Chem. Soc.* **2007**, 18 (3), 628–637. <https://doi.org/10.1590/s0103-50532007000300021>
- (35) Venturini, N.; Tommasi, L. R. Polycyclic Aromatic Hydrocarbons and Changes in the Trophic Structure of Polychaete Assemblages in Sediments of Todos os Santos Bay, Northeastern, Brazil. *Mar. Pollut. Bull.* **2004**, 48 (1–2), 97–107. [https://doi.org/10.1016/S0025-326X\(03\)00331-X](https://doi.org/10.1016/S0025-326X(03)00331-X)



- (36) Benlahcen, K. T.; Chaoui, A.; Budzinski, H.; Bellocq, J.; Garrigues, P. Distribution and Sources of Polycyclic Aromatic Hydrocarbons in Some Mediterranean Coastal Sediments. *Mar. Pollut. Bull.* **1997**, *34* (5), 298–305. [https://doi.org/10.1016/S0025-326X\(96\)00098-7](https://doi.org/10.1016/S0025-326X(96)00098-7)
- (37) Johnson, A. C.; Larsen, P. F.; Gadbois, D. F.; Humason, A. W. The Distribution of Polycyclic Aromatic Hydrocarbons in the Surficial Sediments of Penobscot Bay (Maine, USA) in Relation to Possible Sources and to Other Sites Worldwide. *Mar. Environ. Res.* **1985**, *15* (1), 1–16. [https://doi.org/10.1016/0141-1136\(85\)90034-0](https://doi.org/10.1016/0141-1136(85)90034-0)
- (38) Notar, M.; Leskovšek, H.; Faganeli, J. Composition, Distribution and Sources of Polycyclic Aromatic Hydrocarbons in Sediments of the Gulf of Trieste, Northern Adriatic Sea. *Mar. Pollut. Bull.* **2001**, *42* (1), 36–44. [https://doi.org/10.1016/S0025-326X\(00\)00092-8](https://doi.org/10.1016/S0025-326X(00)00092-8)
- (39) Lin, X.; Lin, L.; Liao, Z.; Wu, P.; Yang, C. Occurrence and Distribution of Polycyclic Aromatic Hydrocarbons (PAHs) in Marine Organisms from Shenzhen Coastal Waters and Human Health Risk Assessment. *Mar. Pollut. Bull.* **2023**, *195*. <https://doi.org/10.1016/j.marpolbul.2023.115498>
- (40) Meniconi, M. D. F. G.; Gabardo, I. T.; Carneiro, M. E. R.; Barbanti, S. M.; da Silva, G. C.; Massone, C. G. Brazilian Oil Spills Chemical Characterization - Case Studies. *Environ. Forensics* **2002**, *3* (3–4), 303–321. <https://doi.org/10.1006/enfo.2002.0101>
- (41) Leite, N. F.; Peralta-Zamora, P.; Grassi, M. T. Distribution and Origin of Polycyclic Aromatic Hydrocarbons in Surface Sediments from an Urban River Basin at the Metropolitan Region of Curitiba, Brazil. *Journal of Environmental Sciences* **2011**, *23* (6), 904–911. [https://doi.org/10.1016/S1001-0742\(10\)60496-2](https://doi.org/10.1016/S1001-0742(10)60496-2)
- (42) Jeanneau, L.; Faure, P.; Montarges-Pelletier, E. Quantitative Multimolecular Marker Approach to Investigate the Spatial Variability of the Transfer of Pollution from the Fensch River to the Moselle River (France). *Sci. Total Environ.* **2008**, *389* (2–3), 503–513. <https://doi.org/10.1016/j.scitotenv.2007.09.023>
- (43) Martins, C. C.; Braun, J. A. F.; Seyffert, B. H.; Machado, E. C.; Fillmann, G. Anthropogenic Organic Matter Inputs Indicated by Sedimentary Fecal Steroids in a Large South American Tropical Estuary (Paranaguá Estuarine System, Brazil). *Mar. Pollut. Bull.* **2010**, *60* (11), 2137–2143. <https://doi.org/10.1016/j.marpolbul.2010.07.027>
- (44) Gurgatz, B. M.; Garcia, M. R.; Cabral, A. C.; de Souza, A. C.; Nagai, R. H.; Figueira, R. C. L.; de Mahiques, M. M.; Martins, C. C. Polycyclic Aromatic Hydrocarbons in a Natural Heritage Estuary Influenced by Anthropogenic Activities in the South Atlantic: Integrating Multiple Source Apportionment Approaches. *Mar. Pollut. Bull.* **2023**, *188*, 114678. <https://doi.org/10.1016/j.marpolbul.2023.114678>
- (45) Rodrigues, C. C. S.; Messias, M. S.; Morales, J. H. A.; Damasceno, F. C.; Corrêa, J. A. M. Insights about Levels and Sources of Organic Pollution in an Urbanized Amazon Estuary (Belém, PA, Northern Brazil). *Environ. Monit. Assess.* **2023**, *195* (6), 1–15. <https://doi.org/10.1007/S10661-023-11271-0>
- (46) Li, J.; Chang, R.; Ban, X.; Yuan, G. L.; Du, X.; Yin, G.; Lin, T. Aged Polycyclic Aromatic Hydrocarbons as Stratigraphic Marker in the Anthropocene: Evidence from Tibetan Lake Sediments. *Water Res.* **2023**, *245*. <https://doi.org/10.1016/j.watres.2023.120652>
- (47) Billah, M.; Bhuiyan, K. A.; Al Amran, I. U.; Cabral, A. C.; Garcia, M. R. D. Polycyclic Aromatic Hydrocarbons (PAHs) Pollution in Mangrove Ecosystems: Global Synthesis and Future Research Directions. *Rev. Environ. Sci. Bio/Technol.* **2022**, *21* (3), 747–770. <https://doi.org/10.1007/S11157-022-09625-0>
- (48) Gripp, L.; Carreira, R. S.; Moreira, D.; Scofield, A. L.; Massone, C. G. Method Development and Application to Sediments for Multi-Residue Analysis of Organic Contaminants Using Gas Chromatography-Tandem Mass Spectrometry. *Anal. Bioanal. Chem.* **2022**, *414* (19), 5845–5855. <https://doi.org/10.1007/S00216-022-04148-7>
- (49) Yonis, S.; Kahkashan, S.; Adelman, D.; Lohmann, R. Transects of Polycyclic Aromatic Hydrocarbons and Organochlorine Pesticides in an Urban Estuary Using Passive Samplers. *Mar. Pollut. Bull.* **2023**, *197*. <https://doi.org/10.1016/j.marpolbul.2023.115768>



- (50) Aboul-Kassim, T. A. T.; Simoneit, B. R. T. Lipid Geochemistry of Surficial Sediments from the Coastal Environment of Egypt I. Aliphatic Hydrocarbons-Characterization and Sources. *Mar. Chem.* **1996**, *54* (1–2), 135–158. [https://doi.org/10.1016/0304-4203\(95\)00098-4](https://doi.org/10.1016/0304-4203(95)00098-4)
- (51) Mudge, S. M.; Norris, C. E. Lipid Biomarkers in the Conwy Estuary (North Wales, U.K.): A Comparison between Fatty Alcohols and Sterols. *Mar. Chem.* **1997**, *57* (1–2), 61–84. [https://doi.org/10.1016/S0304-4203\(97\)00010-8](https://doi.org/10.1016/S0304-4203(97)00010-8)
- (52) Grimalt, J. O.; Fernández, P.; Bayona, J. M.; Albaigés, J. Assessment of Fecal Sterols and Ketones as Indicators of Urban Sewage Inputs to Coastal Waters. *Environ. Sci. Technol.* **1990**, *24* (3), 357–363. <https://doi.org/10.1021/es00073a011>
- (53) Lu, J.; Li, M.; Tan, J.; He, M.; Wu, H.; Kang, Y.; Hu, Z.; Zhang, J.; Guo, Z. Distribution, Sources, Ecological Risk and Microbial Response of Polycyclic Aromatic Hydrocarbons in Qingdao Bays, China. *Environmental Pollution* **2023**, *338*, 122687. <https://doi.org/10.1016/J.ENVPOL.2023.122687>
- (54) Bartley, M. C.; Tremblay, T.; De Silva, A. O.; Kamula, C. M.; Ciastek, S.; Kuzyk, Z. Z. A. Sedimentary Records of Contaminant Inputs in Frobisher Bay, Nunavut. *Environ. Sci. Ecotechnology* **2024**, *18*. <https://doi.org/10.1016/J.ESE.2023.100313>
- (55) Meyers, P. A.; Ishiwatari, R. Lacustrine Organic Geochemistry-an Overview of Indicators of Organic Matter Sources and Diagenesis in Lake Sediments. *Org. Geochem.* **1993**, *20* (7), 867–900. [https://doi.org/10.1016/0146-6380\(93\)90100-P](https://doi.org/10.1016/0146-6380(93)90100-P)
- (56) Meyers, P. A. Applications of Organic Geochemistry to Paleolimnological Reconstructions: A Summary of Examples from the Laurentian Great Lakes. *Org. Geochem.* **2003**, *34* (2), 261–289. [https://doi.org/10.1016/S0146-6380\(02\)00168-7](https://doi.org/10.1016/S0146-6380(02)00168-7)
- (57) Volkman, J. K.; Barrett, S. M.; Blackburn, S. I.; Mansour, M. P.; Sikes, E. L.; Gelin, F. Microalgal Biomarkers: A Review of Recent Research Developments. *Org. Geochem.* **1998**, *29* (5), 1163–1179. [https://doi.org/10.1016/S0146-6380\(98\)00062-X](https://doi.org/10.1016/S0146-6380(98)00062-X)
- (58) Gogou, A.; Bouloubassi, I.; Stephanou, E. G. Marine Organic Geochemistry of the Eastern Mediterranean: 1. Aliphatic and Polyaromatic Hydrocarbons in Cretan Sea Surficial Sediments. *Mar. Chem.* **2000**, *68* (4), 265–282. [https://doi.org/10.1016/S0304-4203\(99\)00082-1](https://doi.org/10.1016/S0304-4203(99)00082-1)
- (59) Froehner, S.; Martins, R. F.; Errera, M. R. Assessment of Fecal Sterols in Barigui River Sediments in Curitiba, Brazil. *Environ. Monit. Assess.* **2009**, *157* (1–4), 591–600. <https://doi.org/10.1007/s10661-008-0559-0>
- (60) Carneiro, C.; Kelderman, P.; Irvine, K. Assessment of Phosphorus Sediment–Water Exchange through Water and Mass Budget in Passaúna Reservoir (Paraná State, Brazil). *Environ. Earth Sci.* **2016**, *75* (7), article number 564. <https://doi.org/10.1007/s12665-016-5349-3>
- (61) Venkatesan, M. I.; Santiago, C. A. Sterols in Ocean Sediments: Novel Tracers to Examine Habitats of Cetaceans, Pinnipeds, Penguins and Humans. *Mar. Biol.* **1989**, *102* (4), 431–437. <https://doi.org/10.1007/BF00438343>
- (62) Froehner, S.; Martins, R. F. Avaliação Da Composição Química de Sedimentos Do Rio Barigüi Na Região Metropolitana de Curitiba. *Quim. Nova* **2008**, *31* (8), 2020–2026. <https://doi.org/10.1590/S0100-40422008000800020>
- (63) Sun, C.; Zhang, J.; Ma, Q.; Chen, Y.; Ju, H. Polycyclic Aromatic Hydrocarbons (PAHs) in Water and Sediment from a River Basin: Sediment–Water Partitioning, Source Identification and Environmental Health Risk Assessment. *Environ. Geochem. Health* **2017**, *39* (1), 63–74. <https://doi.org/10.1007/s10653-016-9807-3>
- (64) Iwegbue, C. M. A.; Ilerhievwie, G. O.; Tesi, G. O.; Olisah, C.; Nwajei, G. E.; Martincigh, B. S. Polycyclic Aromatic Hydrocarbons (PAHs) in Surficial Sediments from Selected Rivers in the Western Niger Delta of Nigeria: Spatial Distribution, Sources, and Ecological and Human Health Risks. *Mar. Pollut. Bull.* **2021**, *167*. <https://doi.org/10.1016/j.marpolbul.2021.112351>
- (65) Baran, A.; Tarnawski, M.; Urbański, K.; Klimkowicz-Pawlas, A.; Spalek, I. Concentration, Sources and Risk Assessment of PAHs in Bottom Sediments. *Environ. Sci. Pollut. Res.* **2017**, *24* (29), 23180–23195. <https://doi.org/10.1007/s11356-017-9944-y>

- (66) Souza, M. R. R.; Santos, E.; Suzarte, J. S.; Carmo, L. O.; Frena, M.; Damasceno, F. C.; Alexandre, M. R. Concentration, Distribution and Source Apportionment of Polycyclic Aromatic Hydrocarbons (PAH) in Poxim River Sediments, Brazil. *Mar. Pollut. Bull.* **2018**, 127, 478–483. <https://doi.org/10.1016/j.marpolbul.2017.12.045>
- (67) Chen, C.-F.; Ju, Y.-R.; Su, Y.-C.; Lim, Y. C.; Kao, C.-M.; Chen, C.-W.; Dong, C.-D. Distribution, Sources, and Behavior of PAHs in Estuarine Water Systems Exemplified by Salt River, Taiwan. *Mar. Pollut. Bull.* **2020**, 154. <https://doi.org/10.1016/j.marpolbul.2020.111029>
- (68) Grmasha, R. A.; Stenger-Kovács, C.; Bedewy, B. A. H.; Al-sareji, O. J.; Al-Juboori, R. A.; Meiczinger, M.; Hashim, K. S. Ecological and Human Health Risk Assessment of Polycyclic Aromatic Hydrocarbons (PAH) in Tigris River near the Oil Refineries in Iraq. *Environ. Res.* **2023**, 227. <https://doi.org/10.1016/j.envres.2023.115791>
- (69) de Oliveira, A. F.; Gomes, B.; França, R.; Moraes, A.; Bataglion, G.; Santos, J. Assessment of Urban Contamination by Sewage in Sediments from Ipojuca River in Caruaru City, Pernambuco, Brazil. *J. Braz. Chem. Soc.* **2022**, 33 (2), 163–172. <https://doi.org/10.21577/0103-5053.20210133>
- (70) Lee, D. H.; Kim, S. H.; Won, E. J.; Kim, M. S.; Hur, J.; Shin, K. H. Integrated Approach for Quantitative Estimation of Particulate Organic Carbon Sources in a Complex River System. *Water Res.* **2021**, 199. <https://doi.org/10.1016/J.WATRES.2021.117194>
- (71) Rodrigues, C. C. S.; Messias, M. S.; Morales, J. H. A.; Damasceno, F. C.; Corrêa, J. A. M. Insights about Levels and Sources of Organic Pollution in an Urbanized Amazon Estuary (Belém, PA, Northern Brazil). *Environ. Monit. Assess.* **2023**, 195 (6), article number 731. <https://doi.org/10.1007/s10661-023-11271-0>
- (72) Vane, C. H.; Kim, A. W.; dos Santos, R. A. L.; Gill, J. C.; Moss-Hayes, V.; Mulu, J. K.; Mackie, J. R.; Ferreira, A. M.; Chenery, S. R.; Olaka, L. A. Impact of Organic Pollutants from Urban Slum Informal Settlements on Sustainable Development Goals and River Sediment Quality, Nairobi, Kenya, Africa. *Appl. Geochem.* **2022**, 146. <https://doi.org/10.1016/J.APGEOCHEM.2022.105468>
- (73) Vane, C. H.; Kim, A. W.; dos Santos, R. A. L.; Moss-Hayes, V. Contrasting Sewage, Emerging and Persistent Organic Pollutants in Sediment Cores from the River Thames Estuary, London, England, UK. *Mar. Pollut. Bull.* **2022**, 175. <https://doi.org/10.1016/J.MARPOLBUL.2022.113340>
- (74) Moghaddam, A. H.; Hashemi, S. H.; Ghadiri, A. Aliphatic Hydrocarbons in Urban Runoff Sediments: A Case Study from the Megacity of Tehran, Iran. *J. Environ. Health Sci. Eng.* **2021**, 19 (1), 205–216. <https://doi.org/10.1007/s40201-020-00596-4>
- (75) Al-Otaibi, M. T.; Rushdi, A. I.; Rasul, N.; Bazeyad, A.; Al-Mutlaq, K. F.; Aloud, S. S.; Alharbi, H. A. Occurrence, Distribution, and Sources of Aliphatic and Cyclic Hydrocarbons in Sediments from Two Different Lagoons along the Red Sea Coast of Saudi Arabia. *Water (Switzerland)* **2024**, 16 (1). <https://doi.org/10.3390/w16010187>
- (76) Sanches Filho, P. J.; Andrade, G. O.; Moreira, K.; Rockenbach, C. K. Determination of Aliphatic Hydrocarbons in Surface Sediments of Mangueira Lagoon (RS—Brazil). *Environ. Earth Sci.* **2021**, 80 (21), article number 728. <https://doi.org/10.1007/s12665-021-10010-3>
- (77) Maynard, N.; Harvey, H. R. Distribution and Source Assignments of Polycyclic Aromatic and Aliphatic Hydrocarbons in Sediments and Biota of the Lafayette River, VA. *Environ. Sci. Pollut. Res.* **2023**, 30 (16), 47527–47543. <https://doi.org/10.1007/s11356-023-25563-y>
- (78) Nemirovskaya, I. A.; Glyaznetsova, Yu. S. The Effect of Accidental Spill of Diesel Fuel in Noril'sk on Hydrocarbon Concentrations and Composition in Bottom Sediments. *Water Resour.* **2022**, 49 (6), 1027–1039. <https://doi.org/10.1134/S0097807822060100>

## SUPPLEMENTARY MATERIAL

**Table S1.** Analytical curves, linear range, correlation coefficient, and detection and quantification limits for PAHs determination

Compound	Concentration range (ng mL <sup>-1</sup> )	R	LOD (ng g <sup>-1</sup> )	LOQ (ng g <sup>-1</sup> )
Nap	4.9 a 490	0.9946	0.087	1.633
Ace	4.9 a 490	0.9883	0.078	1.633
Acy	4.9 a 490	0.9967	0.093	1.633
Flu	4.9 a 490	0.9920	0.111	1.633
Phen	4.9 a 490	0.9937	0.123	1.633
Ant	4.9 a 490	0.9888	0.150	1.633
Flua	4.9 a 490	0.9909	0.168	1.633
Pyr	4.9 a 490	0.9970	0.105	1.633
BaA	4.9 a 490	0.9973	0.066	1.633
Chry	4.9 a 490	0.9965	0.027	1.633
BbF	4.9 a 490	0.9967	0.027	1.633
BbK	4.9 a 490	0.9861	0.078	1.633
BaP	4.9 a 490	0.9933	0.123	1.633
IP	4.9 a 490	0.9967	0.144	1.633
DahA	4.9 a 490	0.9970	0.129	1.633
Bghi	4.9 a 490	0.9941	0.111	1.633

**Table S2.** Analytical curves, linear range, correlation coefficient, and detection and quantification limits for determination of sterols

Compound	Concentration range (ng mL <sup>-1</sup> )	R	LOD (µg g <sup>-1</sup> )	LOQ (µg g <sup>-1</sup> )
Cop	0.24 a 15	0.9957	0.051	0.080
E-cop	0.24 a 15	0.9924	0.051	0.080
Coprostanone	0.24 a 15	0.9950	0.042	0.080
Cholesterol	0.24 a 15	0.9916	0.039	0.080
Cholestanol	0.24 a 15	0.9892	0.060	0.080
Stigmasterol	0.24 a 15	0.9960	0.051	0.080
Stigmastanol	0.24 a 15	0.9916	0.051	0.080
β-sitosterol	0.24 a 15	0.9952	0.051	0.080
Campesterol	0.40 a 20	0.9765	0.051	0.080

**Table S3.** Analytical curves, linear range, correlation coefficient, and detection and quantification limits for aliphatic hydrocarbon determination

Compound	Concentration range ( $\mu\text{g mL}^{-1}$ )	R	LOD ( $\mu\text{g g}^{-1}$ )	LOQ ( $\mu\text{g g}^{-1}$ )
Hexadecane (C16)	0.3 a 25	0.9993	0.069	0.100
Heptadecane (C17)	0.3 a 25	0.9985	0.045	0.100
Pristane	0.3 a 25	0.9992	0.048	0.100
Octadecane (C18)	0.3 a 25	0.9985	0.048	0.100
Phytane	0.3 a 25	0.9997	0.036	0.100
Nonadecane (C19)	0.3 a 25	0.9992	0.036	0.100
Eicosane (C20)	0.3 a 25	0.9995	0.021	0.100
Heneicosane (C21)	0.3 a 25	0.9924	0.027	0.100
Docosane (C22)	0.3 a 25	0.9950	0.024	0.100
Tricosane (C23)	0.3 a 25	0.9995	0.024	0.100
Tetracosane (C24)	0.3 a 25	0.9998	0.024	0.100
Pentacosane (C25)	0.3 a 25	0.9998	0.021	0.100
Hexacosane (C26)	0.3 a 25	0.9997	0.024	0.100
Heptacosane (C27)	0.3 a 25	0.9996	0.024	0.100
Octacosane (C28)	0.3 a 25	0.9997	0.027	0.100
Nonacosane (C29)	0.3 a 25	0.9996	0.027	0.100
triacontane (C30)	0.3 a 25	0.9995	0.042	0.100
n-Hentriacontane (C31)	0.3 a 25	0.9993	0.024	0.100
Dotriacontane (C32)	0.3 a 25	0.9992	0.027	0.100
Titriacontane (C33)	0.3 a 25	0.9992	0.063	0.100
Tetratriacontane (C34)	0.3 a 25	0.9994	0.024	0.100
Pentatriacontane (C35)	0.3 a 25	0.9991	0.078	0.100
Hexatriacontane (C36)	0.3 a 25	0.9995	0.027	0.100

**Table S4.** Polycyclic aromatic hydrocarbon (PAH) levels in sediment from rivers and reservoirs found in this study and globally

Study Area	Range $\Sigma\text{PAHs}$ ( $\mu\text{g kg}^{-1}$ )	Characteristics	Reference*
Rivers and Reservoirs Curitiba, Brazil	97.3 – 440.65	PAH revealed the combustion of biomass as the primary source	This work

(continues on next page)



**Table S4.** Polycyclic aromatic hydrocarbon (PAH) levels in sediment from rivers and reservoirs found in this study and globally (continuation)

Study Area	Range $\Sigma$ PAHs ( $\mu\text{g kg}^{-1}$ )	Characteristics	Reference*
Yinma River Basin, China	1000 – 5750	Predominantly light PAHs (2-3 rings), naphthalene: $825.06 \mu\text{g kg}^{-1}$ . Mixed sources: petroleum and combustion	Sun et al., 2017 <sup>1</sup>
Poxim River, Brazil	2.2 – 28.4	Predominantly pyrogenic sources, anthropogenic influence	Souza et al., 2018 <sup>2</sup>
Brisbane River, Australia	148 – 3079	Pyrogenic sources (vehicular emissions), low ecological risk, some degree of cancer risks for children	Duodu et al., 2017 <sup>3</sup>
South-Eastern Poland Reservoirs	150 – 33900	Both pyrolytic and petrogenic sources, varying ecological risks: moderate and substantial effects on biological communities	Baran et al., 2017 <sup>4</sup>
Salt River, Taiwan	343 – 29400	Coal and petroleum combustion, moderate to high ecological risks	Chen et al., 2020 <sup>5</sup>
Ovia River, Nigeria	5.25 – 573.33	Predominantly 2-3 ring PAHs, exceeding safe drinking water guidelines	Tongo et al., 2017 <sup>6</sup>
Niger Delta, Nigeria	1620 – 19800	High molecular weight PAHs, high ecological and human health risks	Iwegbue et al., 2021 <sup>7</sup>
Nenjiang and Second Songhua Rivers, China	76.5 – 9447	Biomass combustion and vehicle emissions are significant sources with negligible ecological risks.	Yang et al., 2023 <sup>8</sup>
Tigris River, Iraq	5619.2 – 12795.0	High molecular weight PAHs prevalent; pyrogenic sources; high cancer risk.	Grmasha et al., 2023 <sup>9</sup>

\*Supplementary Material Reference

**Table S5.** Coprostanol in sediment from rivers and reservoirs found in this study and globally

Study Area	Coprostanol ( $\mu\text{g g}^{-1}$ )	Characteristics	Reference*
Rivers and Reservoirs Curitiba, Brazil	0.75 – 410	Densely populated areas and discharge of untreated sewage directly into the river.	This work
Ipojuca River, Brazil	557.3	Contamination is due to intense anthropogenic activities close to the river.	Oliveira et al., 2022 <sup>10,11</sup>
Kibera River, Kenya	55 – 298	Discharge of untreated sewage directly into the river.	Vane et al., 2022 <sup>11</sup>
Thames River, England	0.0091 – 0.42	Decrease in COP concentration in sediment core over time due to the evolution of sewage treatment.	Vane et al., 2022 <sup>12</sup>
Geumho River, S. Korea	9 – 1282	High levels of urbanization and industrialization near the Geumho River and land-use types involving human activities	Lee et al., 2021 <sup>13</sup>
Guamá River, Brazil	292.52	Region with low sewage treatment, densely populated, and intense port activity	Rodrigues et al., 2023 <sup>14</sup>

\*Supplementary Material Reference

**Table S6.** Aliphatic hydrocarbons in sediment from rivers and reservoirs found in this study and globally

Study Area	AH ( $\mu\text{g g}^{-1}$ )	Characteristics	Reference*
Rivers and Reservoirs Curitiba, Brazil	0,75 – 410	Densely populated areas and discharge of untreated sewage directly into the river.	This work
Tehran river, Iran	2.94 - 114.7	Densely populated area with predominance of petrogenic origin of AH	Hasani et al., 2021 <sup>15</sup>
Mangueira Lagoon, Brazil	5.0 - 652.7	Relevant lagoon located in a rural area slightly by petrogenic and biogenic AH	Sanches et al., 2021 <sup>16</sup>
Al Wajh Lagoon, Saudi Arabia	64 - 302.6	Lagoon, located close to Red Sea, influenced by petrogenic activities	Al Otaibi et al., 2024 <sup>17</sup>
Lafayette River, USA	4.94 - 40.83	Possible sources such as automotive and atmospheric transport of coal dust contribute to the AH into urban area	Maynard et al., 2023 <sup>18</sup>
Norilsk-Pyasino water system, Russia	15 -1914	Accidental spill of Diesel fuel	Nemirovskaya et al., 2022 <sup>19</sup>

\*Supplementary Material Reference

**Table S7.** Recovery rates of AH, PAH, and sterols (%)

AH		PAH		Sterols	
C16	82	Nap	63	Coprostanol	93
C17	92	Acy	72	E-cop	82
Pristane	88	Ace	70	Coprostanone	60
C18	98	Flu	88	Cholesterol	87
Phytane	97	Phe	103	Cholestanol	88
C19	102	Ant	92	Stigmasterol	88
C20	102	Flt	98	$\beta$ -sitosterol	89
C21	103	Pyr	109	Stigmastanol	89
C22	104	BaA	99		
C23	104	Chr	108		
C24	104	BbF	54		
C25	102	BkF	114		
C26	104	BaP	113		
C27	107	IcdP	110		
C28	107	DahA	112		
C29	104	BghiP	119		
C30	105				
C31	104				
C32	105				
C33	103				
C34	102				
C35	103				
C36	99				

## SUPPLEMENTARY MATERIAL REFERENCES






- (1) Sun, C.; Zhang, J.; Ma, Q.; Chen, Y.; Ju, H. Polycyclic Aromatic Hydrocarbons (PAHs) in Water and Sediment from a River Basin: Sediment–Water Partitioning, Source Identification and Environmental Health Risk Assessment. *Environ. Geochem. Health* **2017**, 39 (1), 63–74. <https://doi.org/10.1007/s10653-016-9807-3>
- (2) Souza, M. R. R.; Santos, E.; Suzarte, J. S.; Carmo, L. O.; Frena, M.; Damasceno, F. C.; Alexandre, M. R. Concentration, Distribution and Source Apportionment of Polycyclic Aromatic Hydrocarbons (PAH) in Poxim River Sediments, Brazil. *Mar. Pollut. Bull.* **2018**, 127, 478–483. <https://doi.org/10.1016/J.MARPOLBUL.2017.12.045>
- (3) Duodu, G. O.; Ogogo, K. N.; Mummullage, S.; Harden, F.; Goonetilleke, A.; Ayoko, G. A. Source Apportionment and Risk Assessment of PAHs in Brisbane River Sediment, Australia. *Ecol. Indic.* **2017**, 73, 784–799. <https://doi.org/10.1016/J.ECOLIND.2016.10.038>
- (4) Baran, A.; Tarnawski, M.; Urbański, K.; Klimkowicz-Pawlas, A.; Spalek, I. Concentration, Sources and Risk Assessment of PAHs in Bottom Sediments. *Environ. Sci. Pollut. Res.* **2017**, 24 (29), 23180–23195. <https://doi.org/10.1007/S11356-017-9944-Y>
- (5) Chen, C. F.; Ju, Y. R.; Su, Y. C.; Lim, Y. C.; Kao, C. M.; Chen, C. W.; Dong, C. Distribution, Sources, and Behavior of PAHs in Estuarine Water Systems Exemplified by Salt River, Taiwan. *Mar. Pollut. Bull.* **2020**, 154. <https://doi.org/10.1016/J.MARPOLBUL.2020.111029>
- (6) Tongo, I.; Ezemonye, L.; Akpeh, K. Levels, Distribution and Characterization of Polycyclic Aromatic Hydrocarbons (PAHs) in Ovia River, Southern Nigeria. *J. Environ. Chem. Eng.* **2017**, 5 (1), 504–512. <https://doi.org/10.1016/J.JECE.2016.12.035>
- (7) Iwegbue, C. M. A.; Ilerhievwie, G. O.; Tesi, G. O.; Olisah, C.; Nwajei, G. E.; Martincigh, B. S. Polycyclic Aromatic Hydrocarbons (PAHs) in Surficial Sediments from Selected Rivers in the Western Niger Delta of Nigeria: Spatial Distribution, Sources, and Ecological and Human Health Risks. *Mar. Pollut. Bull.* **2021**, 167. <https://doi.org/10.1016/J.MARPOLBUL.2021.112351>
- (8) Yang, Y.; Zhao, Z.; Chang, Y.; Wang, H.; Wang, H.; Dong, W.; Yan, G. PAHs and PAEs in the Surface Sediments from Nenjiang River and the Second Songhua River, China: Distribution, Composition and Risk Assessment. *Process Saf. Environ. Prot.* **2023**, 178, 765–775. <https://doi.org/10.1016/J.PSEP.2023.08.037>
- (9) Grmasha, R. A.; Stenger-Kovács, C.; Bedewy, B. A. H.; Al-sareji, O. J.; Al-Juboory, R. A.; Meiczinger, M.; Hashim, K. S. Ecological and Human Health Risk Assessment of Polycyclic Aromatic Hydrocarbons (PAH) in Tigris River near the Oil Refineries in Iraq. *Environ. Res.* **2023**, 227. <https://doi.org/10.1016/J.ENVRES.2023.115791>
- (10) de Oliveira, A. F.; Gomes, B.; França, R.; Moraes, A.; Bataglion, G.; Santos, J. Assessment of Urban Contamination by Sewage in Sediments from Ipojuca River in Caruaru City, Pernambuco, Brazil. *J. Braz. Chem. Soc.* **2022**, 33 (2), 163–172. <https://doi.org/10.21577/0103-5053.20210133>
- (11) Vane, C. H.; Kim, A. W.; dos Santos, R. A. L.; Gill, J. C.; Moss-Hayes, V.; Mulu, J. K.; Mackie, J. R.; Ferreira, A. M.; Chenery, S. R.; Olaka, L. A. Impact of Organic Pollutants from Urban Slum Informal Settlements on Sustainable Development Goals and River Sediment Quality, Nairobi, Kenya, Africa. *Appl. Geochem.* **2022**, 146. <https://doi.org/10.1016/J.APGEOCHEM.2022.105468>
- (12) Vane, C. H.; Kim, A. W.; dos Santos, R. A. L.; Moss-Hayes, V. Contrasting Sewage, Emerging and Persistent Organic Pollutants in Sediment Cores from the River Thames Estuary, London, England, UK. *Mar. Pollut. Bull.* **2022**, 175. <https://doi.org/10.1016/J.MARPOLBUL.2022.113340>
- (13) Lee, D. H.; Kim, S. H.; Won, E. J.; Kim, M. S.; Hur, J.; Shin, K. H. Integrated Approach for Quantitative Estimation of Particulate Organic Carbon Sources in a Complex River System. *Water Res.* **2021**, 199. <https://doi.org/10.1016/J.WATRES.2021.117194>
- (14) Rodrigues, C. C. S.; Messias, M. S.; Morales, J. H. A.; Damasceno, F. C.; Corrêa, J. A. M. Insights about Levels and Sources of Organic Pollution in an Urbanized Amazon Estuary (Belém, PA, Northern Brazil). *Environ. Monit. Assess.* **2023**, 195 (6), 1–15. <https://doi.org/10.1007/s10661-023-11271-0>

- (15) Moghaddam, A. H.; Hashemi, S. H.; Ghadiri, A. Aliphatic Hydrocarbons in Urban Runoff Sediments: A Case Study from the Megacity of Tehran, Iran. *J. Environ. Health Sci. Eng.* **2021**, *19* (1), 205–216. <https://doi.org/10.1007/s40201-020-00596-4>
- (16) Sanches Filho, P. J.; Andrade, G. O.; Moreira, K.; Rockenbach, C. K. Determination of Aliphatic Hydrocarbons in Surface Sediments of Mangueira Lagoon (RS, Brazil). *Environ. Earth Sci.* **2021**, *80* (21), article number 728. <https://doi.org/10.1007/s12665-021-10010-3>
- (17) Al-Otaibi, M. T.; Rushdi, A. I.; Rasul, N.; Bazeyad, A.; Al-Mutlaq, K. F.; Aloud, S. S.; Alharbi, H. A. Occurrence, Distribution, and Sources of Aliphatic and Cyclic Hydrocarbons in Sediments from Two Different Lagoons along the Red Sea Coast of Saudi Arabia. *Water (Switzerland)* **2024**, *16* (1), 187. <https://doi.org/10.3390/w16010187>
- (18) Maynard, N.; Harvey, H. R. Distribution and Source Assignments of Polycyclic Aromatic and Aliphatic Hydrocarbons in Sediments and Biota of the Lafayette River, VA. *Environ. Sci. Pollut. Res.* **2023**, *30* (16), 47527–47543. <http://dx.doi.org/10.1007/s11356-023-25563-y>
- (19) Nemirovskaya, I. A.; Glyaznetsova, Y. S. The Effect of Accidental Spill of Diesel Fuel in Noril'sk on Hydrocarbon Concentrations and Composition in Bottom Sediments. *Water Resour.* **2022**, *49* (6), 1027–1039. <http://dx.doi.org/10.1134/S0097807822060100>



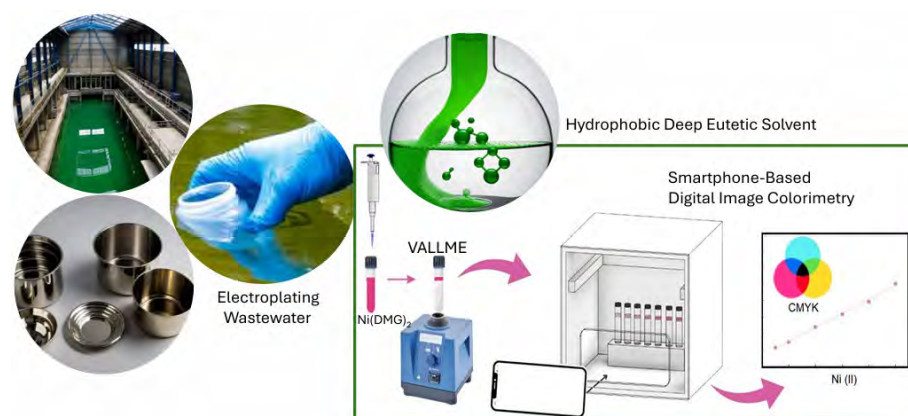
ARTICLE

# Vortex-Assisted Liquid-Liquid Microextraction Based on Hydrophobic Deep Eutectic Solvent for Nickel Determination in Water Samples by Smartphone Digital Image Colorimetry

Airton Vicente Pereira<sup>\*1</sup>  , Orlando Fatibello-Filho<sup>2</sup> , Geovanna Morgado da Penha<sup>2</sup> , Emily Amáble Tavares<sup>2</sup> 

<sup>1</sup>Departamento de Ciências Farmacêuticas, Universidade Estadual de Ponta Grossa , Av Carlos Cavalcanti, 4748, 84030-900, Ponta Grossa, PR, Brazil

<sup>2</sup>Departamento de Química, Universidade Federal de São Carlos , Rodovia Washington Luis, Km 235 13565-905, São Carlos, SP, Brazil



An environmentally friendly and sensitive vortex-assisted liquid-liquid microextraction (VALLME) method using a hydrophobic deep eutectic solvent (HDES) coupled with smartphone-based digital image colorimetry (SDIC) was developed for the preconcentration and determination of trace nickel in electroplating wastewater. Nickel cations were complexed with dimethylglyoxime (DMG) to form a pink-red complex

(Ni(DMG)<sub>2</sub>). Some important factors, including the HDES type, pH, volume of solvent, dimethylglyoxime concentration, and vortex time, were investigated and optimized. The extraction was performed in 1 minute using 250  $\mu$ L of HDES composed of tetrabutylammonium bromide (TBABr) with decanoic acid (1:2), with a sample volume of 10 mL at pH 8, and the image capture was made directly in the extraction tube without the need to separate the HDES phase. Under the optimum conditions, the method exhibited linearity within the concentration range of 0.45-5.9 mg L<sup>-1</sup>, detection and quantification limits of 0.15 and 0.45 mg L<sup>-1</sup>, and precision (RSD) of  $\pm$  2.6%. Application to water samples showed recoveries between 97% and 104%. The proposed HDES-based microextraction method offers an effective alternative for nickel determination in industrial wastewater.

**Keywords:** nickel, liquid-liquid microextraction, deep eutectic solvent, water samples, electroplating

**Cite:** Pereira, A. V.; Fatibello-Filho, O.; da Penha, G. M.; Tavares, E. A. Vortex-Assisted Liquid-Liquid Microextraction Based on Hydrophobic Deep Eutectic Solvent for Nickel Determination in Water Samples by Smartphone Digital Image Colorimetry. *Braz. J. Anal. Chem.* 2025, 12 (49), pp 117-131. <http://dx.doi.org/10.30744/brjac.2179-3425.AR-10-2025>

Submitted March 1, 2025; Resubmitted April 25, 2025; Accepted May 21, 2025; Available online June 6, 2025.

## INTRODUCTION

Ensuring universal access to drinking water is currently a sustainable global development goal.<sup>1</sup> However, water source contamination by numerous pollutants, both biological and chemical, due to various human activities, including urban development, inadequate waste disposal, industrial processes, and agricultural practices, impacts the environment and poses major health hazards to people.<sup>2</sup>

Heavy metal pollution has emerged as a critical global issue due to its high toxicity, bioaccumulation, and non-biodegradable nature.<sup>3</sup> Similarly to many other heavy metals, nickel is a naturally occurring element found in the soil and water. It is released into the atmosphere from natural sources, and low levels are present in fresh water, seawater, and groundwater.<sup>4,5</sup> However, anthropogenic activities such as burning fossil fuels, mining, metal processing and casting, and electroplating wastewater may elevate nickel levels in the environment.<sup>6</sup>

Apparently, the oral toxicity of nickel is low due to poor intestinal absorption when ingested with food; however, a higher percentage is absorbed when nickel cations are dissolved in water.<sup>7</sup> Fortunately, animal tissues rarely accumulate nickel compared to other heavy metals like lead, arsenic, and cadmium.<sup>8</sup> Nevertheless, depending on dose and exposure time, intake of nickel ions could potentially impact health. It is a potential carcinogen to the respiratory tract and can cause toxic effects, such as cardiovascular disease, asthma, and lung fibrosis.<sup>4,9</sup> Additionally, skin contact with stainless steel or nickel-plated objects (e.g., earrings, jewellery, orthodontic wires and appliances) and using cosmetics with nickel traces can cause allergic contact dermatitis.<sup>6</sup>

Environmental regulations play an important role in reducing water contamination by establishing standards for water quality. In Brazil, the National Environment Council (CONAMA), through resolution 357/2005, has set maximum allowed levels for several pollutants, including nickel, in various surface water bodies (freshwater, saltwater, brackish water, and effluent release).<sup>10</sup> According to the CONAMA resolution, the maximum allowable concentrations of nickel are 25  $\mu\text{g L}^{-1}$  and 2.0  $\text{mg L}^{-1}$  for freshwater and wastewater, respectively. One of the key challenges in monitoring and preventing metal contamination in water is the development of sensitive, reliable, and rapid methods for detecting heavy metals in water bodies.

Determination of trace nickel is usually based on traditional techniques such as flame atomic absorption spectrometry (FAAS),<sup>11,12</sup> HPLC UV-Vis with derivatization reagent,<sup>13,14</sup> differential pulse polarography,<sup>15</sup> voltammetry,<sup>16</sup> fluorimetry,<sup>17</sup> and spectrophotometry.<sup>18-20</sup> However, some of these methodologies have limitations, including time-consuming procedures, sophisticated equipment, and consumption of large amounts of solvents. Also, they are not portable for in situ analysis.

Among the numerous methods proposed for nickel determination, colorimetric procedures have some advantages, such as easy execution, low cost, and sensitivity. Oxime ligands such as dimethylglyoxime<sup>21</sup> and  $\alpha$ -furildioxime<sup>19</sup> and analogues (1-(2-pyridylazo)-2-naphthol, (PAN))<sup>20</sup> have been proposed for the colorimetric determination of nickel. Nickel forms a pink-red complex with dimethylglyoxime (DMG) in a moderate alkaline solution, which can be quantified by gravimetry<sup>22</sup> or extracted for subsequent colorimetric determination.<sup>21</sup>

To detect trace amounts of metal in water samples, a chemical separation and preconcentration step is required before analysis. In this regard, different procedures such as solid-phase extraction (SPE),<sup>23</sup> liquid-phase extraction,<sup>11,12</sup> cloud point extraction,<sup>18</sup> and flotation<sup>24</sup> have been developed for the extraction and preconcentration of nickel in water matrices. Nickel-DMG complex ( $\text{Ni}(\text{DMG})_2$ ) is insoluble in water and can be extracted with organic solvents such as *n*-hexane,<sup>24</sup> and chloroform<sup>25</sup> or ionic liquid.<sup>26</sup> However, these chemical solvents may cause pollution for the environment as well as harm to health.

Currently, there is a growing interest in environmentally friendly and sustainable extraction methods that utilize greener solvents. In this regard, the last two decades have seen remarkable advancements in green solvents. Deep eutectic solvents (DESs) have emerged as a promising solvent class capable of replacing toxic organic solvents.<sup>27</sup> Some advantages of DES include low-cost, biodegradability, low toxicity and are easily prepared with highly variable viscosities.<sup>28</sup> However, early DESs were highly hydrophilic and unstable in aqueous solutions, hence resulting in a breakdown of the hydrogen bonds between their components.

Hydrophobic deep eutectic solvents (HDESs) were introduced in 2015 as a mixture of hydrogen-bound donors (long-chain length organic acids) with different hydrogen-bound acceptors (quaternary ammonium salts).<sup>29</sup> In these systems, the anion of the salt (e.g., Br<sup>-</sup> of tetrabutylammonium bromide) serves as the hydrogen bond acceptor (HBA). Since then, HDESs have received much attention for broadening their applicability, including the removal of heavy metals from aqueous solutions.<sup>30</sup>

Smartphone-based digital image colorimetry (SDIC) is a novel, more accessible, and portable tool that enables quantitative analysis once limited to specialized laboratories with costly equipment.<sup>31</sup> Images captured with a smartphone camera are processed in different colour spaces (e.g., RGB, CMYK, CIELAB, and HSV) using software like Photometrix, Image J, Matlab, or Trigit, converting the colour data into analytical signals to establish a correlation between colour intensity and analyte concentration. Several studies have demonstrated the successful application of SDIC for monitoring metal concentrations in water.<sup>11,32-34</sup>

In this study, we introduce a method for preconcentration and determination of nickel in wastewater combining vortex-assisted liquid-liquid microextraction (VALLME) of the Ni(DMG)<sub>2</sub> complex with HDES composed of tetrabutylammonium bromide and decanoic acid (1:2) with smartphone-based DIC. An inexpensive image box equipped with a rechargeable, wireless illumination system was designed to capture images of the extraction tubes without the need to separate the HDES and aqueous phases. Colour space data were extracted from the digital images of the HDES phase using the free app Trigit,<sup>37</sup> with the magenta (M) channel of the CMYK model applied for nickel quantification.

## MATERIALS AND METHODS

### *Chemicals and solutions*

All chemicals were analytical grade and used as received without any further purification. Nickel chloride anhydrous (purity > 99%), DL-menthol (≥95%), thymol (98.5%) and ammonium chloride were purchased from Sigma Aldrich. Dimethylglyoxime, tetrabutylammonium bromide and ethanol absolute were purchased from Êxodo Científica (Sumaré, Brazil). Ammonium hydroxide, sodium phosphate monobasic monohydrate, sodium phosphate dibasic heptahydrate were purchased from Synth (São Paulo, Brazil). Octanoic acid and decanoic acid were purchased from Neon (São Paulo, Brazil). All solutions were prepared with ultra-purified water (electric resistivity of 18 Mohms cm) obtained from the Milli-Q system (Millipore).

A stock solution of nickel ions (1g L<sup>-1</sup>) was prepared by dissolving anhydrous nickel chloride, dried in an oven at 100 °C for 2 hours and left in a desiccator overnight, in ultrapure water. Working solutions of Ni(II) were prepared by diluting the stock solution. Dimethylglyoxime (DMG) stock solution (1.0 × 10<sup>-2</sup> mol L<sup>-1</sup>) was prepared by dissolving 0.1161 g of the reagent in absolute ethanol. Working solutions of DMG were prepared by diluting the stock solution in the same solvent.

### *HDES synthesis*

To prepare HDESs, two components (HBA and HBD) were mixed at appropriate molar ratios, as previously reported.<sup>35</sup> HDES1 was prepared by mixing menthol and thymol in a 1:1 molar ratio. For HDES2 and HDES3, TBABr was combined with octanoic acid or decanoic acid, respectively, at a 1:2 molar ratio. HDES4 was prepared by mixing thymol and decanoic acid in a 1:1 molar ratio. Briefly, each component was weighed and mixed in a closed round-bottom flask, then mechanically stirred at 100 rpm and 65 °C until a homogeneous liquid was formed. The HDESs were stored at room temperature in the amber glass flasks sealed with parafilm.

### *Samples*

Nickel electroplating bath, rinse water, and wastewater samples were collected from the electroplating, washing, and effluent tanks, respectively, at a local electroplating industry. The rinse bath and wastewater were kept in a polypropylene bottle and stored at 4 °C until analysis. All samples were analyzed without pre-treatment.

## Procedure

For wastewater, the preconcentration step was performed directly in the samples without any pretreatment. However, due to the high nickel concentrations, the electroplating bath and rinse water samples were diluted with ultrapure water. The general procedure for VALLME and determination of nickel by SDIC is illustrated in Figure 1. Nickel samples and working solutions were determined by the following procedure: 10-mL aliquots of the Ni (II) solutions were transferred to glass tubes with screw caps, and pH was adjusted to 8.0 using a phosphate buffer solution. Then, 200  $\mu\text{L}$  of  $4.0 \times 10^{-4} \text{ mol L}^{-1}$  dimethylglyoxime (DMG) were added, and the solution was mixed to ensure homogenization. After the formation of the pink  $\text{Ni}(\text{DMG})_2$  complex, 250  $\mu\text{L}$  of the HDES were added, and the tube was vortexed for 60 seconds. After phase separation, the HDES phase was analyzed directly in the tube using smartphone-based DIC, eliminating the need to transfer it to another sample holder (e.g., a cuvette). A blank sample was prepared following the same procedure, using ultrapure water instead of the nickel solution.

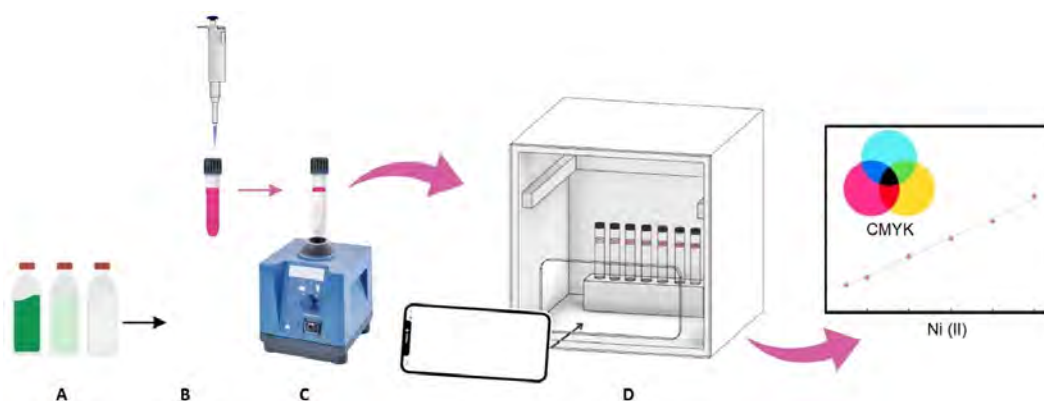


**Figure 1.** Schematic illustration of the procedure for nickel determination using SDIC: (A) Nickel samples (nickel bath, rinse water, and wastewater); (B) Ni-DMG complexation reaction; (C) VALLME with HDES; and (D) image capture.

To evaluate the greenness of the developed VALLME-DIC method for nickel determination, the Analytical Eco-Scale was employed.<sup>36</sup> This tool assigns penalty points (PPs) for factors such as toxicity, quantity of reagents, energy consumption, and waste, where a score  $\geq 75$  indicates excellent greenness.

## Apparatus

A custom image box ( $21 \times 21 \times 21 \text{ cm}$ ; height, width  $\times$  length) was constructed from a cardboard box lined with white paper for optimal light reflection. A microextraction tube holder was made by drilling holes into a white expanded polyethylene (EPE) foam sheet ( $12 \times 5 \times 2.5 \text{ cm}$ ; length  $\times$  width  $\times$  height), designed to hold the glass tubes in an upright position during image capture. An observation aperture ( $14.8 \times 7.2 \text{ cm}$ ) was created on the front of the box to accommodate the cell phone for capturing image samples. Wireless rechargeable LED lights with adjustable intensity controls and on/off switches were installed on the inner top and both sides of the box to ensure uniform illumination. The distance between the smartphone and the sample holder was kept constant at 15 cm throughout the experiments. Images were captured using an iPhone 15 (Apple), equipped with a 48 MP sensor camera, 26 mm focal length,  $f/1.6$  aperture, and sensor-shift optical image stabilization. The digital images were saved in JPEG format and analyzed using the Trigit web app.<sup>37</sup> A rectangular region of interest (ROI) was defined with a selection tool, and colour data were automatically generated across multiple colour spaces (RGB, CMYK, HSV, and CIELAB). The analytical signal was calculated using the M channel values from the CMYK colour space for each sample and standard solution, subtracting the blank value within the same image.



## RESULTS AND DISCUSSION

### *Nickel-DMG reaction and studied parameters*

The aim of this work was to develop a cost-effective and greener microextraction procedure using HDES for the rapid determination of nickel in wastewater samples. To achieve this, a colorimetric method was developed using the traditional reagent dimethylglyoxime (DMG) in combination with vortex-assisted liquid-liquid microextraction (VALLME) and smartphone-based digital image colorimetry. The proposed procedure involves the complexation of Ni(II) ions by DMG in an alkaline buffered medium to produce the characteristic pink-red Ni(DMG)<sub>2</sub> complex according to the reaction:  $\text{Ni}^{2+} + 2 \text{HDMG} \rightarrow \text{Ni(DMG)}_2 + 2\text{H}^+$ .

The Ni(DMG)<sub>2</sub> chelate is insoluble in water, forming the basis for gravimetric determination of Ni(II); however, it can be extracted into chloroform<sup>21</sup> or n-hexane<sup>24</sup> for subsequent colorimetric analysis. As an alternative to conventional volatile solvents, in this study four HDESs were evaluated for Ni(DMG)<sub>2</sub> extraction from aqueous solutions. These included two ionic, tetrabutylammonium-based HDES (TBABr:octanoic acid (1:2) and TBABr:decanoic acid (1:2)) and two nonionic, monoterpene-based HDES ((thymol-menthol (1:1) and thymol:decanoic acid (1:1)). Various extraction parameters were evaluated to optimize the VALLME of nickel-dimethylglyoximate, including the type and volume of HDES, pH of the nickel solution, DMG concentration, and vortex time. All experiments were conducted in triplicate using water samples spiked with nickel.

### *Image analysis*

The RGB colour space is the most common model used in digital image colorimetry. As expected, based on the colour of the Ni(DMG)<sub>2</sub> complex and complementary colours in the RGB model, a good correlation between analytical signal and nickel concentration was observed for the G (Green) channel, which corresponds to the complementary colour of the complex. However, pinkish-red colours in the RGB model lie midway between red and blue, which can lead to a less distinct signal. In contrast, the M (magenta) channel in the CMYK colour space closely corresponds with the colour of the Ni(DMG)<sub>2</sub> complex, resulting in improved sensitivity and linearity. Thus, the M channel was selected as the most effective for the analysis since it had the best correlation with nickel concentration.

### *HDES selection*

One of the most critical parameters affecting extraction efficiency is the extraction solvent. It is well-established that the extraction solvent should have some properties, such as lower density than water, low water miscibility, extraction capability of the target analyte, compatibility with the detection technique, and low toxicity.<sup>38</sup> HDESs can fulfil these requirements, making them quite useful as extraction solvents and a greener alternative to toxic volatile solvents. The obtained results confirmed the ability of HDESs for the extraction of Ni(DMG)<sub>2</sub> complex, with efficiency extraction values exceeding 90% (Figure 2).

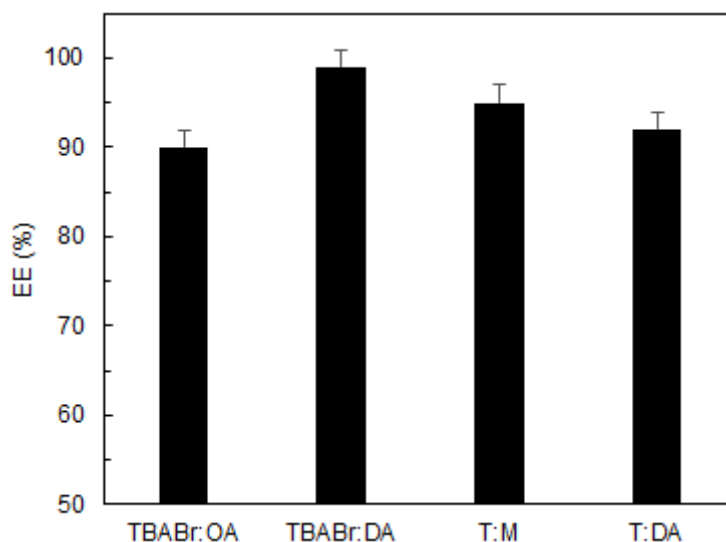


**Figure 2.** Effect of the type of HDES on the extraction efficiency. OA: octanoic acid, DA: decanoic acid, T: thymol, M: menthol. Experimental conditions:  $[\text{Ni}^{2+}] = 5 \text{ mg L}^{-1}$ , sample volume = 5 mL, pH = 9,  $[\text{DMG}] = 1\%$  (w/v) in ethanol, 200  $\mu\text{L}$ , HDES volume = 500  $\mu\text{L}$ , vortex time = 120 s.

Even HDESs present a capacity to absorb some amount of water that can influence the extraction of nonpolar analytes. The limited water solubility of  $\text{Ni}(\text{DMG})_2$  results from the formation of strong intramolecular  $\text{O}-\text{H}\cdots\text{O}$  bonds within the dimethylglyoxime chelate.<sup>39,40</sup> Consequently, hydrogen bonds tightly hold the hydrogen, limiting the interaction of the  $\text{O}-\text{H}$  groups with water and inhibiting dissolution.

Therefore, the higher extraction efficiency observed with TBABr:decanoic acid over TBABr:octanoic acid may be attributed to the slightly higher polarity of octanoic acid ( $\log K_{\text{ow}} = 3.03$ ) relative to decanoic acid ( $\log K_{\text{ow}} = 4.1$ ). Probably, the lower water intake of TBABr:decanoic acid HDES contributes to maintaining a low-polarity environment that stabilizes the chromophore structure of the  $\text{Ni}(\text{DMG})_2$ .

Furthermore, the HDESs composition affected the colour of the nickel-dimethylglyoximate. For both tetrabutylammonium-based HDESs the  $\text{Ni}(\text{DMG})_2$  complex formed exhibited its characteristic pink-red colour. In contrast, the non-ionic HDES thymol:menthol and thymol:decanoic acid presented distinct solvatochromic shifts, producing orange and pale-yellow complexes, respectively, which may be due to the nearly nonpolar environment.

Non-ionic HDES provided similarly high extraction efficiencies. However, the thymol:decanoic acid HDES exhibited emulsification and slow phase separation. Moreover, given that the weak colour of the complex in these nonionic HDESs could impact the sensitivity of colorimetric detection, TBABr:decanoic acid HDES was selected for further experiments.

### Effect of pH

Nickel-dimethylglyoximate formation and subsequent extraction are affected by the pH of the aqueous solution. Traditionally, the gravimetric determination and extraction of nickel-dimethylglyoximate from aqueous solution for colorimetric detection is achieved by adding a slight excess of ammonium hydroxide. The extraction of  $\text{Ni}(\text{DMG})_2$  by TBABr:decanoic acid HDES was investigated in the range of 5-10 (Figure 3). The results indicate that the extraction efficiency increased with pH, reaching a maximum at pH 7-9 before decreasing at pH 10, consistent with previously reported findings.<sup>21,23</sup>

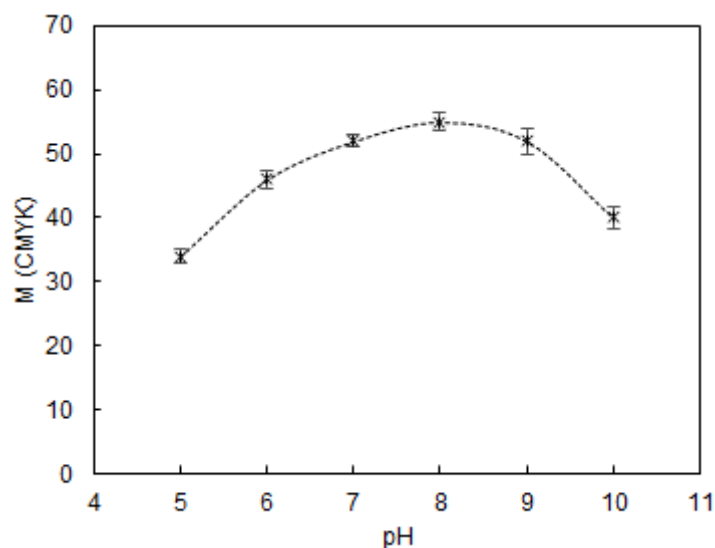


**Figure 3.** Effect of pH on analytical signal of Ni (II). Experimental conditions:  $[\text{Ni}^{2+}] = 5 \text{ mg L}^{-1}$ , sample volume = 10 mL,  $[\text{DMG}] = 1\%$  (w/v) in ethanol, 200  $\mu\text{L}$ , HDES volume = 500  $\mu\text{L}$ , vortex time = 120 s.

Remarkably, after vortexing, the HDES layer thickness at pH 8-10 remained consistent, in contrast to the noticeable thinning observed at pH levels 5 and 6. Studies have shown that the stability of HDESs when exposed to water depends heavily on the nature of both the HBA and HBD components.<sup>41</sup> If either the HBA or HBD component of an HDES is water-soluble, partial breakdown can occur, resulting in the hydrophilic component leaching into the aqueous phase.

Van Osch et al.<sup>29</sup> investigated the water stability of HDESs composed by ammonium salts and decanoic acid. The authors concluded that stability generally improves with longer alkyl chains in quaternary ammonium salts (HBAs), which lead to lower water content and reduced salt leaching. However, although the interfacial properties of HDESs with water have been explored,<sup>42</sup> the pH stability of HDESs in aqueous systems remains unexamined.

Our findings demonstrate the importance of pH to improve the stability of the HDES system. At basic solutions, the enhanced dissociation of decanoic acid ( $\text{pK}_a$  4.9) to its decanoate form at the oil-water interface could reduce hydrogen bonding interactions with the bromide anion, thereby promoting the leaching of the tetrabutylammonium cation ( $\text{TBA}^+$ ) into the aqueous phase. In contrast, the presence of decanoate enhances electrostatic interactions with  $\text{TBA}^+$ , thereby supporting greater structural integrity of the HDES. Based on these observations, pH 8 was selected for further analytical procedures.

### DMG concentration

DMG is a well-known vicinal dioxime widely used as a chelating ligand for nickel, forming a complex with a 1:2 stoichiometric ratio ( $\text{Ni(II):DMG}$ ). The effect of DMG concentration on the nickel extraction was examined in the range of  $2 \times 10^{-5}$  to  $8.0 \times 10^{-4} \text{ mol L}^{-1}$ . The analytical signal increased with the addition of DMG up to  $4.0 \times 10^{-4} \text{ mol L}^{-1}$ , reaching a plateau and remaining constant (Figure 4). This result is supported by previous studies<sup>24,26</sup> in which nickel determination is conducted with an excess of DMG. Therefore, a DMG concentration of  $4.0 \times 10^{-4} \text{ mol L}^{-1}$  was selected as the optimal concentration for  $\text{Ni(DMG)}_2$  extraction.

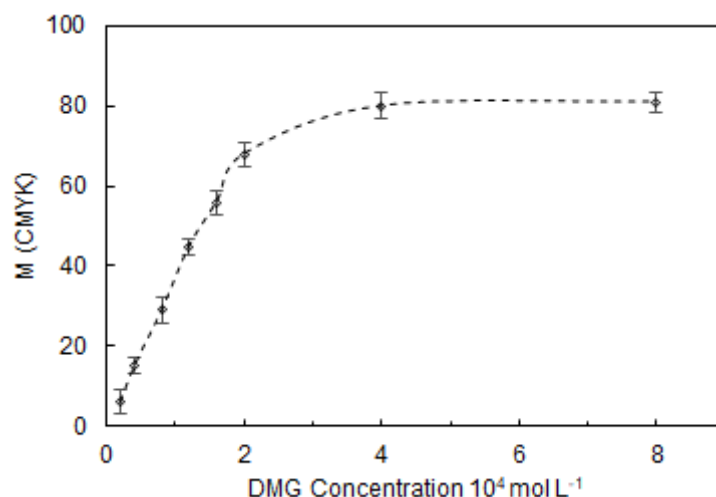


**Figure 4.** Effect of concentration of dimethylglyoxime (DMG). Experimental conditions:  $[\text{Ni}^{2+}] = 5 \text{ mg L}^{-1}$ , sample volume = 10 mL, pH = 8, DMG = 200  $\mu\text{L}$ , HDES volume = 500  $\mu\text{L}$ , vortex time = 120 s.

### Volume of HDES

To evaluate the effect of extraction solvent volume, different volumes of the TBABr: decanoic acid HDES, ranging from 125 to 1000  $\mu\text{L}$ , were tested. With increasing HDES volume, the extraction efficiency remained constant, but the analytical signal decreased, which can be attributed to the dilution effect of  $\text{Ni}(\text{DMG})_2$  in the larger solvent volume (Figure 5).

Although the 125  $\mu\text{L}$  volume provided greater sensitivity, the HDES phase volume was not sufficient to fill the internal diameter of the tube and form a uniform layer on the surface of the aqueous phase for precise analysis by smartphone-based DIC. Consequently, 250  $\mu\text{L}$  was selected as the optimal extraction HDES volume.

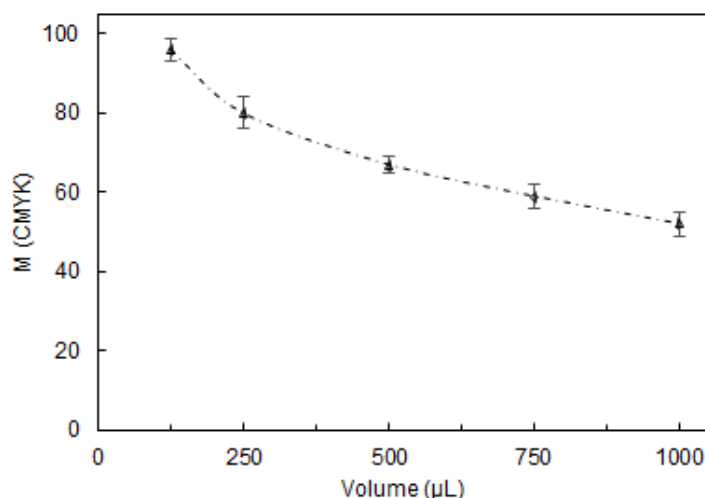


**Figure 5.** Effect of HDES volume on analytical signal. Experimental conditions:  $[\text{Ni}^{2+}] = 5 \text{ mg L}^{-1}$ , sample volume = 10 mL, pH = 8, DMG =  $4.0 \times 10^{-4} \text{ mol L}^{-1}$ , 200  $\mu\text{L}$ , vortex time = 120 s.



### Vortex time

Vortex-assisted liquid-liquid microextraction (VALLME) uses vortex mixing to disperse a microliter-sized droplet of extraction solvent in the aqueous samples.<sup>43</sup> This technique produces fine drops, which increase the interfacial area for mass transfer, decrease diffusion distance, and improve extraction efficiency. The effect of vortex time on extraction efficiency was evaluated over a range of 15 to 90 seconds at the maximum agitation speed (2,500 rpm). Figure 6 shows that the intensity of the analytical signal increased with vortex time up to 60 seconds over a range of 15 to 90 seconds at the maximum agitation speed (2,500 rpm). Therefore, 60 seconds was chosen as the optimal vortex time.

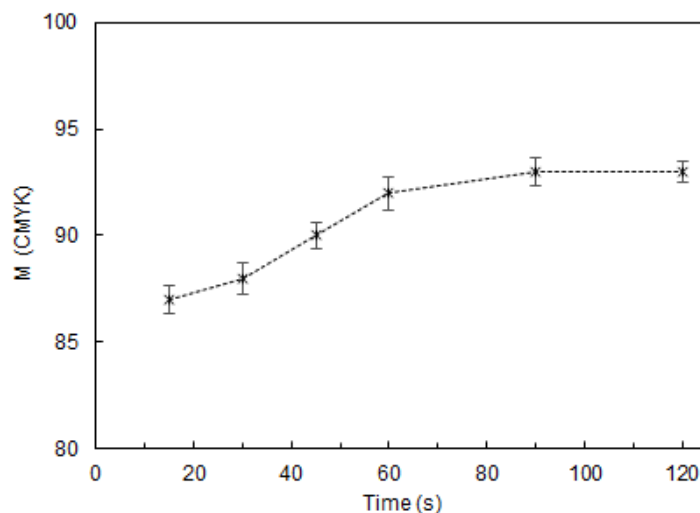


**Figure 6.** Effect of vortex time on analytical response. Experimental conditions:  $[\text{Ni}^{2+}] = 5 \text{ mg L}^{-1}$ , sample volume = 10 mL, pH = 8, DMG =  $4.0 \times 10^{-4} \text{ mol L}^{-1}$ , 200  $\mu\text{L}$ , HDES volume = 250  $\mu\text{L}$ .

### Interferences

Interference studies (Table I) were carried out using the proposed procedure to investigate the effects of  $\text{Cu}^{2+}$ ,  $\text{Cr}^{3+}$ ,  $\text{Fe}^{3+}$ ,  $\text{Co}^{2+}$ , and  $\text{Fe}^{2+}$ , which also may be present in wastewater from the electroplating process. The determination of  $\text{Ni}^{2+}$  ( $2 \text{ mg L}^{-1}$ ) in the presence of each metal cation at the  $5 \text{ mg mL}^{-1}$  level demonstrated no interference from  $\text{Cr}^{3+}$ ,  $\text{Fe}^{3+}$ ,  $\text{Co}^{2+}$ , or  $\text{Fe}^{2+}$ . It is important to highlight those metals like iron ( $\text{Fe}^{2+}$ ,  $\text{Fe}^{3+}$ ), chromium ( $\text{Cr}^{3+}$ ), and aluminum ( $\text{Al}^{3+}$ ) can be removed from rinsewater by chemical precipitation through pH adjustment. Raising the pH with the addition of an alkali (e.g.,  $\text{Ca}(\text{OH})_2$ ,  $\text{NaOH}$ ), these cations precipitate as hydroxides. Additionally, in the presence of oxygen,  $\text{Fe}^{2+}$  oxidizes to ferric ion ( $\text{Fe}^{3+}$ ), which precipitates as yellowish-orange ferric hydroxide at pH values above 3.5. Under experimental conditions,  $\text{Fe}^{2+}$  and  $\text{Cu}^{2+}$  affected the colour of the sample, although  $\text{Fe}^{2+}$  did not impact the detection of nickel.  $\text{Cu}^{2+}$  interfered with nickel determination, resulting in a decreased analytical signal, probably due to the formation of a thermodynamically stable chelating complex Cu-DMG. Copper interference became noticeable at concentrations approximately 1.5 times the level of nickel. However, there was no  $\text{Cu}^{2+}$  in the samples analyzed.

To address the potential interference from  $\text{Cu}^{2+}$  ions, which are commonly found in electroplating wastewater, additional experiments were conducted using a masking agent. As previously reported, a sodium thiosulfate masking solution was applied to eliminate the interference from  $\text{Cu}^{2+}$  on determination of  $\text{Ni}^{2+}$  by colorimetric analysis using 2-(2-thiazolylazo)-p-cresol.<sup>44</sup> The masking effect was observed after the addition of 1 mL of  $0.25 \text{ mol L}^{-1}$  sodium thiosulfate, as evidenced by the relatively lack of significant decrease in the analytical signal upon the addition of copper ion. The addition of masking solution did not

affect the signal of the  $\text{Ni}(\text{DMG})_2$  complex, confirming its suitability for improving method selectivity without compromising analytical performance.

**Table I.** Interference study of other metal ions on the nickel ( $2 \text{ mg L}^{-1}$ ) measurement by the proposed procedure

Interfering Cation	Concentration ( $\text{mg L}^{-1}$ )	$\text{Ni}^{2+}$ Recovery (%)	Interference (%)
Control	2	$100 \pm 2$	0
$\text{Cr}^{3+}$	5	$100 \pm 4$	0
$\text{Fe}^{3+}$	5	$98 \pm 3$	-2
$\text{Fe}^{2+}$	5	$102 \pm 2$	+2
$\text{Co}^{2+}$	5	$99 \pm 3$	-1
$\text{Cu}^{2+}$	3	$90 \pm 4$	-10
$\text{Cu}^{2+}$	5	$64 \pm 6$	-36
* $\text{Cu}^{2+}$	5	$97 \pm 4$	-3

\*after the addition of masking solution

### Analytical features

The analytical curve was linear in the concentration range of  $0.45$  to  $5.9 \text{ mg L}^{-1}$ . The regression equation was  $y = 1.35 + 16.06x$  (where  $y$  is the  $M$  value and  $x$  is the nickel concentration), with a correlation coefficient of  $R^2 = 0.9971$ . The limit of detection (LOD) calculated as three times the standard deviation of the blank signal divided by the slope of the analytical curve was equal to  $0.15 \text{ mg L}^{-1}$ . The limit of quantification (LOQ), determined as ten times the standard deviation of the blank signal divided by the slope of the analytical curve, was  $0.45 \text{ mg L}^{-1}$ . Precision studies were conducted using spiked samples, with percentage coefficient of variation (% CV) values observed within assays at (2.6%) and between assays at (3.4%), indicating consistent repeatability and reproducibility.

### Recovery

To assess recovery (%), water samples were fortified with three known nickel concentrations and analyzed by the proposed method following the procedure described in the experimental section. Recoveries (%) were calculated as the measured amount divided by the spiked amount, multiplied by 100. The recovery rates (Table II) for the water samples were excellent, ranging from 97% to 104%.

**Table II.** Results of recovery obtained for nickel ( $\text{mg L}^{-1}$ ) in water

Sample	Spiked	Found	Recovery (%)
A	0.50	$0.52 \pm 0.02$	104
	1.00	$0.97 \pm 0.04$	97
	2.00	$2.04 \pm 0.05$	102
B	0.50	$0.49 \pm 0.01$	98
	1.00	$1.03 \pm 0.02$	103
	2.00	$1.98 \pm 0.03$	99

### Applications to real samples

Nickel bath formulations typically combine nickel chloride, nickel sulphate, and boric acid. Rinsewaters is generated during the washing of plated items to remove residual plating solution and contaminants from metal electroplating operations and constitute a major portion of the waste. In general, in the electroplating industry, rinsewater is treated, and the final water can be then reused in the rinsing process or discharged. However, wastewater may still contain traces of heavy metals such as chromium, cadmium, copper, zinc, and nickel. The applicability of the proposed SDIC method following the VALLME procedure was evaluated through the analysis of nickel in nickel bath, rinsewater and wastewater samples of a galvanic industry (Table III).

**Table III.** Nickel amounts ( $\text{mg L}^{-1}$ ) found in the samples by proposed method and comparative method (mean  $\pm$  s)

Samples	Proposed Method	PAN colorimetric Method	Relative Error (%)
Nickel bath*	$81 \pm 1$	$79 \pm 2$	+2.5
Rinse water	$144 \pm 3$	$142 \pm 2$	+1.4
Rinse water	$158 \pm 3$	$159 \pm 3$	-0.6
Wastewater	$2.21 \pm 0.02$	$2.30 \pm 0.01$	-3.9
Wastewater	$2.44 \pm 0.01$	$2.37 \pm 0.04$	+2.9

\* $\text{g L}^{-1}$

To ensure readings remained within the linear range, the nickel bath sample was diluted 400,000-fold and the rinse water sample 100-fold. The results for the samples were compared with those from the 1-(2-pyridylazo)-2-naphthol (PAN) colorimetric method<sup>20</sup> for the measurement of Ni(II). Statistical analysis using a t-test indicated no significant difference between the methods at a 95% confidence level.

In this study, nickel levels in wastewater were slightly higher than the CONAMA-recommended limit ( $2 \text{ mg L}^{-1}$ ). However, this wastewater can be recycled back to the rinse baths.

### Comparison with other methods

For comparison purposes, the analytical features, including preconcentration technique, linear range, limit of detection (LOD), limit of quantification (LOQ), and sample volume of the proposed method and other extraction-based techniques coupled with FAAS, HPLC, and spectrophotometry, are compiled in Table IV.

**Table IV.** Comparison of analytical features of the proposed procedure and other published methods for the determination of nickel in water samples

Technique	Extraction procedure	Linear range ( $\text{mg L}^{-1}$ )	LOD ( $\text{mg L}^{-1}$ )	LOQ ( $\text{mg L}^{-1}$ )	Sample volume (mL)	Ref.
FAAS	Cloud point LLME	0.002-0.100	0.005	0.0016	50	11
FAAS	LPME	0.025-0.300	0.007	0.029	8	12
HPLC	LLME	0.001-0.010	0.008	0.001	5	13
HPLC	SPME	0.005-0.010	0.5	---	10	14
Spectrophotometry	Cloud point LLME	0.2-5.0	0.10	0.20	10	18

(continues on next page)

**Table IV.** Comparison of analytical features of the proposed procedure and other published methods for the determination of nickel in water samples (continuation)

Technique	Extraction procedure	Linear range (mg L <sup>-1</sup> )	LOD (mg L <sup>-1</sup> )	LOQ (mg L <sup>-1</sup> )	Sample volume (mL)	Ref.
Diffuse reflectance spectroscopy	SPME	0.5-5.0	0.47	0.50	1	23
Spectrophotometry	LLE	0.60-12	0.10	0.60	50	24
SDIC	VALLME	0.45-5.9	0.15	0.45	10	This work

Both the FAAS<sup>11,12</sup> and HPLC<sup>13,14</sup> methods are highly sensitive, with a lower linear range and limit of detection; however, they require expensive laboratory equipment and volatile, flammable solvents, such as methanol or acetonitrile. In Table S1, the calculated penalty points (PPs) for the technique were 21 points (5 points for reagents and 16 points for instrumentation occupational hazard, energy consumption, and waste) revealing the excellent greenness (Eco-scale score 79) of the proposed VALLME procedure. Compared to other analytical methods (e.g., cloud point extraction-FAAS, HPLC, spectrophotometry), our approach avoids the use of hazardous solvents like acetonitrile, methanol, and chloroform and reduces energy consumption and waste. Literature-reported methods for Ni determination have not been evaluated from this point of view, but the Eco-scale scores can be estimated between 50 and 70 due to higher solvent use, larger waste volumes, or non-portable instrumentation. Also, the cloud point LLME procedure is labour-intensive and time-consuming, allowing only 1-2 samples to be processed per hour. In addition to being inexpensive, the proposed smartphone-based method offers distinct advantages, with adequate sensitivity to monitor nickel levels in wastewater without requiring heating treatment, or dilution of the enriched phase, nor a skilled operator.

## CONCLUSIONS

In this study, VALLME of nickel-dimethylglyoxime complex with hydrophobic deep eutectic solvent for preconcentration and determination of Ni in water samples by smartphone-based DIC was presented and demonstrated for the first time. The significant advantage of the method is its simplicity because the image capture is performed directly in the extraction tube without the need to separate the extraction phase for subsequent analysis, unlike classical methods. The proposed procedure is fast, low-cost, eco-friendly, and demonstrates sufficient precision and accuracy for routine monitoring of nickel levels in electroplating industry wastewater.

## Conflicts of interest

The authors declare that there are no conflicts of interest.

## Acknowledgments

The authors thank grants #401681/2023-8 from CNPq, INCT Nanovida (CNPq/proc. 406079/2022-6) and 2024/04116-8 from FAPESP for the financial support granted during this research.

## REFERENCES

- (1) United Nations Sustainable Development Goals. Goal 6: *Ensure access to water and sanitation for all*. Available at: <https://www.un.org/sustainabledevelopment/water-and-sanitation/> (accessed February 2025).
- (2) Mishra, R. K.; Mentha, S. S.; Misra, Y.; Dwivedi, N. Emerging pollutants of severe environmental concern in water and wastewater: A comprehensive review on current developments and future research. *Water-Energy Nexus* **2023**, 6, 74-95. <https://doi.org/10.1016/j.wen.2023.08.002>



- (3) Kumar, P.; Gacem, A.; Ahmad, M. T.; Yadav, V. K.; Singh, S.; Yadav, K. K.; Alam, M. M.; Dawane, V.; Piplode, S.; Maurya, P.; Ahn, Y.; Jeon, B.-H.; Cabral-Pinto, M. M. S. Environmental and human health implications of metal(loid)s: Source identification, contamination, toxicity, and sustainable clean-up technologies. *Front. Environ. Sci.* **2022**, *10*. <https://doi.org/10.3389/fenvs.2022.949581>
- (4) Barceloux, D. G. Nickel. *J. Toxicol. Clin. Toxicol.* **1999**, *37* (2), 239-258. <https://doi.org/10.1081/clt-100102423>
- (5) Rinklebe, J.; Shaheen, S. M. Redox chemistry of nickel in soils and sediments: A review. *Chemosphere* **2017**, *179*, 265–278. <https://doi.org/10.1016/j.chemosphere.2017.02.153>
- (6) Begum, W.; Rai, S.; Banerjee, S.; Bhattacharjee, S.; Mondal, M. H.; Bhattarai, A.; Saha, B. A comprehensive review on the sources, essentiality and toxicological profile of nickel. *RSC Adv.* **2022**, *12* (15), 9139-9153. <https://doi.org/10.1039/d2ra00378c>
- (7) Schrenk, D.; Bignami, M.; Bodin, L.; Chipman, J. K.; Del Mazo, J.; Grasl-Kraupp, B.; Hogstrand, C.; Hoogenboom, L.; Leblanc, J.; Nebbia, C. S.; et al. Update of the risk assessment of nickel in food and drinking water. *EFSA J.* **2020**, *18* (11). <https://doi.org/10.2903/j.efsa.2020.6268>
- (8) Nielsen, F. Nickel. *Adv. Nutr.* **2020**, *12* (1), 281–282. <https://doi.org/10.1093/advances/nmaa154>
- (9) Genchi, G.; Carocci, A.; Lauria, G.; Sinicropi, M. S.; Catalano, A. Nickel: Human health and environmental toxicology. *Int. J. Environ. Res. Public Health* **2020**, *17* (3), 679. <https://doi.org/10.3390/ijerph17030679>
- (10) Conselho Nacional do Meio Ambiente (CONAMA). Resolution 357/05 – *Provisions for the classification of water bodies* – Brazilian resolution. Available at: <https://braziliannr.com/brazilian-environmental-legislation/conama-resolution-357-05-provisions-for-the-classification-of-water-bodies/> (accessed February 2025).
- (11) Abdolmohammad-Zadeh, H.; Ebrahimzadeh, E. Ligandless cloud point extraction for trace nickel determination in water samples by flame atomic absorption spectrometry. *J. Braz. Chem. Soc.* **2011**, *22* (3), 517-524. <https://doi.org/10.1590/s0103-50532011000300015>
- (12) Kartoğlu, B.; Tezgit, E.; Yiğit, A.; Zaman, B. T.; Bak irdere, E. G.; Bakirdere, S. Determination of trace nickel after complexation with a schiff base by switchable solvent – liquid phase microextraction (SS-LPME) and flame atomic absorption spectrometry (FAAS). *Anal. Lett.* **2021**, *55* (7), 1017-1026. <https://doi.org/10.1080/00032719.2021.1980797>
- (13) Ichinoki, S.; Onishi, C.; Fujii, Y. Selective determination of nickel ion in river water by solvent extraction with  $\alpha$ -furyldioxime, followed by reversed-phase HPLC with photometric detection. *J. Liq. Chromatogr. Relat. Technol.* **2006**, *29* (15), 2217-2228. <https://doi.org/10.1080/10826070600832905>
- (14) Comber, S. Determination of dissolved copper, nickel and cadmium in natural waters by high-performance liquid chromatography. *Analyst* **1993**, *118* (5), 505. <https://doi.org/10.1039/an9931800505>
- (15) Reyes-Salas, E. O.; Dosal-Gómez, M. A.; Barceló-Quintal, M. H.; Manzanilla-Cano, J. A. Simultaneous determination of nickel, cobalt, antimony, and arsenic in an aqueous sample by differential pulse polarography. *Anal. Lett.* **2002**, *35* (1), 123–133. <https://doi.org/10.1081/al-120002366>
- (16) Fendrych, K.; Porada, R.; Baś, B. Electrochemical sensing platform based on Zeolite/Graphite/Dimethylglyoxime nanocomposite for highly selective and ultrasensitive determination of nickel. *J. Hazard. Mater.* **2023**, *448*. <https://doi.org/10.1016/j.jhazmat.2023.130953>
- (17) Robert-Peillard, F.; Mouchtari, E. M. E.; Bonne, D.; Humbel, S.; Boudenne, J.-L.; Coulomb, B. Determination of dissolved nickel in natural waters using a rapid microplate fluorescence assay method. *Spectrochim. Acta, Part A* **2022**, 275. <https://doi.org/10.1016/j.saa.2022.121170>
- (18) Safavi, A.; Abdollahi, H.; Nezhad, H.; Kamali, R. Cloud point extraction, preconcentration and simultaneous spectrophotometric determination of nickel and cobalt in water samples. *Spectrochim. Acta Part A* **2004**, *60* (12), 2897–2901. <https://doi.org/10.1016/j.saa.2004.02.001>
- (19) Gahler, A.; Mitchell, A.; Mellon, M. Colorimetric determination of nickel with alpha-furildioxime. *Anal. Chem.* **1951**, *23* (3), 500–503. <https://doi.org/10.1021/ac60051a032>

- (20) Melgarejo, A. G.; Céspedes, A. G.; Pavón, J. M. C. Simultaneous determination of nickel, zinc and copper by second-derivative spectrophotometry using 1-(2-pyridylazo)-2-naphthol as reagent. *Analyst* **1989**, 114 (1), 109–111. <https://doi.org/10.1039/an9891400109>
- (21) Claassen, A.; Bastings, L. Notes on the extraction of nickeldimethylglyoxime by chloroform and on the photometric determination of nickel by the glyoxime method. *Recl. Trav. Chim. Pays-Bas* **1954**, 73 (9), 783–788. <https://doi.org/10.1002/recl.19540730909>
- (22) Junnila, P.; Latvala, M.; Matilainen, R.; Tummavuori, J. Optimization of the gravimetric determination method of nickel as dimethylglyoximate for nickel raw materials. *Fresenius J. Anal. Chem.* **1999**, 365 (4), 325–331. <https://doi.org/10.1007/s002160051495>
- (23) Gazda, D. B.; Fritz, J. S.; Porter, M. D. Determination of nickel(II) as the nickel dimethylglyoxime complex using colorimetric solid phase extraction. *Anal. Chim. Acta* **2004**, 508 (1), 53–59. <https://doi.org/10.1016/j.aca.2003.11.044>
- (24) Hashemi-Moghaddam, H. A selective flotation-spectrophotometric method for the determination of nickel using dimethylglyoxime. *J. Braz. Chem. Soc.* **2011**, 22 (6), 1056–1060. <https://doi.org/10.1590/s0103-50532011000600008>
- (25) Paping, L. R. M.; Rummens, C. P. J.; Vriens, P. H. A.; Van Wolput, J. H. M. C.; Beelen, T. P. M. Extraction of copper(II) and nickel(II) by long-chain aliphatic dioximes. *Polyhedron* **1985**, 4 (4), 723–729. [https://doi.org/10.1016/s0277-5387\(00\)86689-9](https://doi.org/10.1016/s0277-5387(00)86689-9)
- (26) Ebrahimi, B.; Bahar, S.; Moedi, S. E. Cold-induced aggregation microextraction technique based on ionic liquid for preconcentration and determination of nickel in food samples. *J. Braz. Chem. Soc.* **2013**, 24 (11). <https://doi.org/10.5935/0103-5053.20130228>
- (27) Raja, T.; Chandira, R.; Tamilvanan, S.; Rajesh, S.; Venkateswarlu, B. Deep eutectic solvents as an alternate to other harmful solvents. *Biointerface Res. Appl. Chem.* **2021**, 12 (1), 847–860. <https://doi.org/10.33263/briac121.847860>
- (28) Dzhevakhyan, M. A.; Prozhogina, Yu. E. Deep eutectic solvents: History, properties, and prospects. *Pharm. Chem. J.* **2023**, 57 (2), 296–299. <https://doi.org/10.1007/s11094-023-02879-0>
- (29) Van Osch, D. J. G. P.; Zubeir, L. F.; Van Den Bruinhorst, A.; Rocha, M. A. A.; Kroon, M. C. Hydrophobic deep eutectic solvents as water-immiscible extractants. *Green Chem.* **2015**, 17 (9), 4518–4521. <https://doi.org/10.1039/c5gc01451d>
- (30) Majidi, E.; Bakhshi, H. Hydrophobic deep eutectic solvents characterization and performance for efficient removal of heavy metals from aqueous media. *J. Water Process Eng.* **2024**, 57. <https://doi.org/10.1016/j.jwpe.2023.104680>
- (31) Soares, S.; Fernandes, G. M.; Rocha, F. R. P. Smartphone-based digital images in analytical chemistry: Why, when, and how to use. *TrAC, Trends Anal. Chem.* **2023**, 168. <https://doi.org/10.1016/j.trac.2023.117284>
- (32) Mahmoudian, N.; Zamani, A.; Fashi, A.; Richter, P.; Abdolmohammad-Zadeh, H. Ultra-trace determination of cadmium in water and food samples by a thin-film microextraction using a supported liquid membrane combined with smartphone-based colorimetric detection. *Food Chem.* **2023**, 421. <https://doi.org/10.1016/j.foodchem.2023.136193>
- (33) Balasubramanian, S.; Udayabhanu, A.; Kumar, P. S.; Muthamilselvi, P.; Eswari, C.; Vasantavada, A.; Kanetkar, S.; Kapoor, A. Digital colorimetric analysis for estimation of iron in water with smartphone-assisted microfluidic paper-based analytical devices. *Int. J. Environ. Anal. Chem.* **2021**, 103 (11), 2480–2497. <https://doi.org/10.1080/03067319.2021.1893711>
- (34) Sun, Y.; Yang, X.; Hu, J.; Ji, F.; Chi, H.; Liu, Y.; Hu, K.; Hao, F.; Wen, X. Portable one-step effervescence tablet-based microextraction combined with smartphone digital image colorimetry: Toward field and rapid detection of trace nickel ion. *Talanta* **2024**, 274. <https://doi.org/10.1016/j.talanta.2024.126036>
- (35) Piton, G.; Augusto, K.; Santos, D.; FatibelloFilho, O. Spectrophotometric determination of allura red AC and tartrazine in food products using hydrophobic deep eutectic solvents as an environmentally sustainable micro-extractor. *J. Braz. Chem. Soc.* **2021**, 32 (3), 564–571. <https://doi.org/10.21577/0103-5053.20200210>

- (36) Kowtharapu, L. P.; Katari, N. K.; Muchakayala, S. K.; Mariseti, V. M. Green metric tools for analytical methods assessment critical review, case studies and crucify. *TrAC, Trends Anal. Chem.* **2023**, 166. <https://doi.org/10.1016/j.trac.2023.117196>
- (37) Tjandra, A. D.; Heywood, T.; Chandrawati, R. Trigit: A free web application for rapid colorimetric analysis of images. *Biosens. Bioelectron.:X* **2023**, 14. <https://doi.org/10.1016/j.biosx.2023.100361>
- (38) Pérez, R. A.; Alberio, B. Ultrasound-assisted extraction methods for the determination of organic contaminants in solid and liquid samples. *TrAC, Trends Anal. Chem.* **2023**, 166. <https://doi.org/10.1016/j.trac.2023.117204>
- (39) Godycki, L. E.; Rundle, R. E. The structure of nickel dimethylglyoxime. *Acta Crystallogr.* **1953**, 6 (6), 487–495. <https://doi.org/10.1107/S0365110X5300137X>
- (40) Bruce-Smith, I. F.; Zakharov, B. A.; Stare, J.; Boldyreva, E. V.; Pulham, C. R. Structural properties of nickel dimethylglyoxime at high pressure: Single-crystal X-ray diffraction and DFT studies. *J. Phys. Chem. C* **2014**, 118 (42), 24705–24713. <https://doi.org/10.1021/jp508939g>
- (41) Makoś, P.; Słupek, E.; Gębicki, J. Hydrophobic deep eutectic solvents in microextraction techniques—A review. *Microchem. J.* **2019**, 152. <https://doi.org/10.1016/j.microc.2019.104384>
- (42) Salehi, H. S.; Moulτος, O. A.; Vlught, T. J. H. Interfacial properties of hydrophobic deep eutectic solvents with water. *J. Phys. Chem. B* **2021**, 125 (44), 12303–12314. <https://doi.org/10.1021/acs.jpcc.1c07796>
- (43) Psillakis, E. Vortex-assisted liquid-liquid microextraction revisited. *TrAC, Trends Ana. Chem.* **2018**, 113, 332–339. <https://doi.org/10.1016/j.trac.2018.11.007>
- (44) Ferreira, S. C. Spectrophotometric determination of nickel in copper-base alloy with 2-(2-thiazolylazo)-p-cresol. *Talanta* **1988**, 35 (6), 485–486. [https://doi.org/10.1016/0039-9140\(88\)80112-7](https://doi.org/10.1016/0039-9140(88)80112-7)

## SUPPLEMENTARY MATERIAL

**Table S1.** Eco-Scale evaluation for the VALLME-SDIC procedure

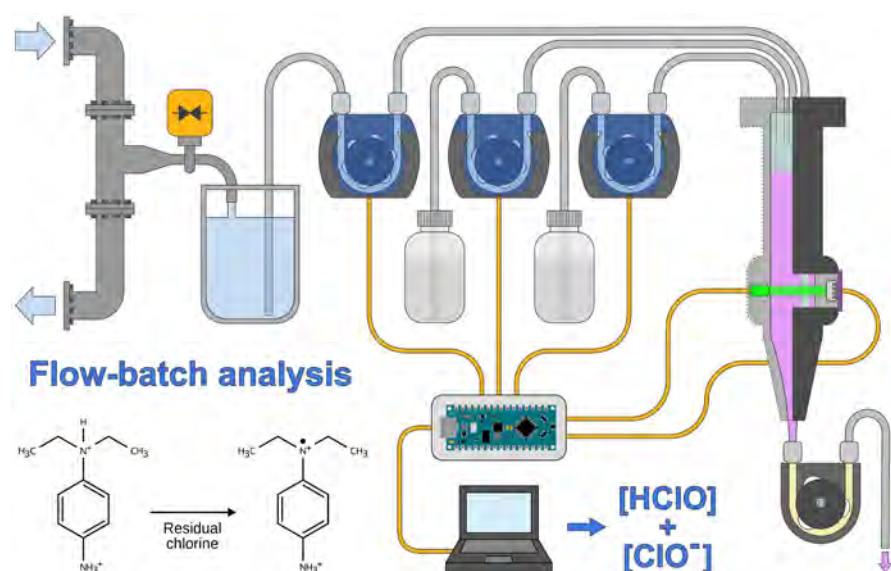
Reagents	Penalty Points (PPs)			Instruments/Others	PPs
	Amount PP	Hazard PP	Total PPs (Amount × Hazard)		
Ethanol (<1 mL)	1	4	4	Vortex	1
Tetrabutylammonium bromide (TBABr, <0.1 g)	1	6	6	Image capture (Smartphone)	0
Decanoic acid (<0.2 g)	1	2	2	Occupational hazard	0
Sodium thiosulfate (1 mL, 0.25 mol L <sup>-1</sup> )	1	1	1	Energy consumption (mild)	1
Phosphate buffer (1 mL, 0.1 mol L <sup>-1</sup> )	1	1	1	Waste (12.3 mL/sample)	3
Dimethylglyoxime (DMG, 200 µL of 4×10 <sup>-4</sup> mol L <sup>-1</sup> )	1	2	2		
<b>Subtotal PPs (reagents)</b>			<b>16</b>	<b>Subtotal instruments/others</b>	<b>5</b>
<b>Total PPs</b>					<b>21</b>
<b>Eco-Scale Score</b>					<b>79</b>

ARTICLE

# Development of a Flow-Batch Analyzer for the On-Site Automated Determination of Residual Chlorine in Drinking Water

Guillermo Roth<sup>ID</sup>, Justina Medina, Moisés Knochen\*<sup>ID</sup>✉

Universidad de la República <sup>FOR</sup>, Facultad de Química. DEC. Área Química Analítica. Grupo de Instrumentación y Automatización en Química Analítica (GIAQA). Av. Gral. Flores, 2124. 11800 Montevideo, Uruguay



A novel automated analyzer for the determination of residual chlorine in water was developed and evaluated. The analyzer is based on the technique of flow-batch analysis and employs the DPD photometric method for measurement of free chlorine. To decrease complexity, a stirrer was not used for mixing, resorting instead to the turbulence of the fluids to attain a satisfactory mixing of the reactants. The prototype was built using peristaltic pumps, a reaction-detection cell, and an LED-photodiode detection system. The open-source Arduino microcontroller

platform was used for data acquisition and control. The operational evaluation of the system included the study of the mixing process, the determination of the optimum concentration of DPD reagent and the calculation of analytical figures of merit: linear range, precision and accuracy of the results, as well as detection and quantification limits. The performance of the analyzer was deemed fit for the purpose of on-site analysis. This prototype is being taken as the basis for the design of an industrial-grade on-site on-line analyzer for the determination of residual chlorine in water treatment plants and drinking water distribution systems.

**Keywords:** residual chlorine, drinking water, flow-batch, automation, analyzer

## INTRODUCTION

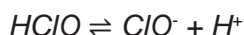
The addition of chlorine in water treatment plants and drinking-water distribution systems is a usual practice for the elimination of pathogenic microorganisms. Once dissolved in water, chlorine undergoes

**Cite:** Roth, G.; Medina, J.; Knochen, M. Development of a Flow-Batch Analyzer for the On-Site Automated Determination of Residual Chlorine in Drinking Water. *Braz. J. Anal. Chem.* 2025, 12 (49), pp 132-143. <http://dx.doi.org/10.30744/brjac.2179-3425.AR-19-2025>

Submitted March 29, 2025; Resubmitted June 16, 2025; Accepted August 3, 2025; Available online August 29, 2025.



several chemical reactions. A fraction may react with organic matter and microorganisms as well as with ammonia, generating substances with lower antimicrobial activity, such as monochloramine and dichloramine. The remaining chlorine species are known collectively as “residual chlorine” which is available for further antimicrobial activity. Molecular chlorine remains in a pH-dependent equilibrium with hypochlorite ion and hypochlorous acid:



The sum of molecular chlorine, hypochlorous acid and hypochlorite ion is called free chlorine.<sup>1-3</sup>

In drinking-water distribution lines, the decrease in residual chlorine levels along the pipes is detrimental to the desired antimicrobial activity. To maintain the required residual chlorine concentration, water utilities may install rechlorination stations at specific points in the system, ensuring it remains above the minimum threshold.

The concentration of residual chlorine is one of the key quality indicators in drinking water. The World Health Organization (WHO) recommends a minimum concentration of 0.2 mg L<sup>-1</sup> of free chlorine at the delivery point to ensure an effective disinfection.<sup>4</sup> On the other hand, high levels of free chlorine may produce unacceptable taste and odor, mainly due to byproducts formed through reaction with organic matter. The levels at which undesirable taste and odor become perceptible depend on composition of the raw water, temperature and individual sensitivity, but usually are above 2 mg L<sup>-1</sup>. Higher levels may even cause health issues. For that reason, maximum levels must also be established. The WHO has set a guideline value of 5 mg L<sup>-1</sup>, but due to sensorial aspects, local regulatory bodies often establish lower limits. In Uruguay, for instance, Decree 375/2011,<sup>5</sup> based on UNIT Technical Standard 833:2008,<sup>6</sup> establishes a maximum value of 2.5 mg L<sup>-1</sup> for free chlorine in drinking water.

From an analytical perspective, residual chlorine is determined by measuring free-chlorine levels. Several methods are available, including the amperometric method<sup>7</sup> and the spectrophotometric methods based on N,N'-diethyl-p-phenylenediamine (DPD)<sup>8,9</sup> and syringaldazine.<sup>10,11</sup> The DPD method is dependable and widely established, being listed in the APHA Standard Methods.<sup>12</sup> It relies on the oxidation of DPD solutions by free chlorine, forming a colored substance (Würster dye) with absorption maxima at around 515 and 550 nm. This reaction occurs at pH values around 6. However, in the presence of excess free chlorine, a secondary product, a colorless imine, may be produced. This is undesirable as it affects the quality of the analytical results.

Given the inherent instability of chlorine solutions, residual chlorine should not be determined on stored samples but rather determined on-site. Water treatment plants and drinking-water distribution systems require the use of on-line automated methods to ensure the necessary analytical frequency without the need for manual sampling and analysis.

Different techniques based on flow analysis have been proposed to automate free chlorine determinations. Flow injection analysis (FIA)<sup>13</sup> is the most frequently reported for this purpose.<sup>14-19</sup> This automation technique requires only small sample volumes and can provide high sampling frequencies with good precision, making it suitable for laboratory use and for the development of sophisticated analyzers. However, it is delicate and can be affected by issues such as the presence of gas bubbles as well as from refractive-index (“schlieren”) effects, which are problematic when photometric detection is used. Therefore, it is not the best option for on-site analyzers, where simplicity, robustness and dependability are absolute requirements.

Flow-batch analysis (FBA), first proposed by Honorato<sup>20</sup> and by Gonçalves,<sup>21</sup> is an automation technique that combines characteristics of both flow analysis and traditional batch analysis. It leverages the advantages of both modalities, resorting to in-flow fluid handling while retaining the batchwise styles of mixing and static detection. Although FBA does not achieve the high sampling frequencies of FIA, it has advantages in terms of simplicity and robustness. Reagents and sample are thoroughly mixed in a mixing chamber (usually with the aid of a stirrer), unlike the mixing coil used in FIA. As a result, no concentration gradient is



generated, avoiding the appearance of refractive-index effects. Detection can be carried out in static mode once mixing is complete. In fact, the mixing chamber can also be used as a detection cell, simplifying the design and avoiding the possible interference caused by gas bubbles, which rise to the surface and are easily eliminated.

FBA has been successfully used for several analytical applications in recent years.<sup>22-25</sup> However, a literature search for previous publications on the determination of free chlorine by means of FBA with photometric detection yielded no results. To date, only one paper has been found describing the use of a flow-batch analyzer for chlorine in water but using electrochemical detection.<sup>26</sup>

In this work, we describe the development and evaluation of a novel flow-batch analyzer for the determination of free chlorine in water samples. It was part of a larger project, in partnership with a local technological company, aimed at developing a cost-effective, internet-based network of automated on-line analyzers for the monitoring of residual chlorine, to be deployed in water treatment plants and drinking-water distribution lines. The analyzer was based on the DPD photometric method, utilizing the FBA technique for its inherent advantages, as discussed above. It used low-cost industrial peristaltic pumps, an LED-based detection system, and open-source Arduino-compatible hardware for control electronics. The final product at this first stage was a working prototype capable of performing the on-line determination of free chlorine at specified time intervals and transmitting the results to a PC via a USB port. This prototype can easily serve as a foundation for a more complex system capable of handling internet communications, which is currently being designed.

## MATERIALS AND METHODS

### *Reagents and samples*

Anhydrous DPD sulfate ( $\geq 98.0\%$ ) was from Sigma Aldrich (Burlington, MA, USA). All other reagents were also of analytical-reagent grade and obtained from Sigma-Aldrich.

DPD reagent solution was prepared according to APHA method,<sup>12</sup> except for DPD concentration, which was modified as described below.

Chlorine standard solutions were prepared daily from commercial sodium hypochlorite solution (nominal concentration  $40 \text{ g L}^{-1}$ ) which was periodically titrated according to the APHA standard method.<sup>12</sup>

Routine determinations by the manual method were carried out using Macherey-Nagel (Dueren, Germany) Visocolor DPD reagent powder pillows.

Samples of tap water with different levels of residual chlorine were collected from the local distribution system. Some samples were spiked to obtain concentrations in the upper range up to  $4 \text{ mg L}^{-1}$  free chlorine.

### *Apparatus*

Absorbance measurements in the laboratory were performed using a Shimadzu UV-1900i spectrophotometer fitted with 1-cm quartz cells.

The automated flow system was implemented using three 8-roller Kamoer (Shanghai, China) KCM peristaltic pumps, equipped with 24-V stepping motors and silicone pump tubing (1.61 mm internal diameter).

The reaction-detection cell, 110 mm in length, was constructed from stock 15-mm internal diameter clear glass tubing, fitted with a conical end where the drain pump was installed. The cell was fixed in a vertical position. An opaque shield, 3D-printed with black PLA filament, was used to isolate the cell from ambient light.

The detection system was composed of a high-intensity green LED with a nominal maximum emission at 515 nm (Kingbright, City of Industry, CA, USA) and an OPT101 (Texas Instruments, Dallas, TX, USA) detector/amplifier integrated circuit (IC), both mounted in a lab-made holder, also 3D-printed with black PLA filament. The LED and detector were arranged on opposite sides of the cell.

The final aspect of the cell is shown in Figure 1.

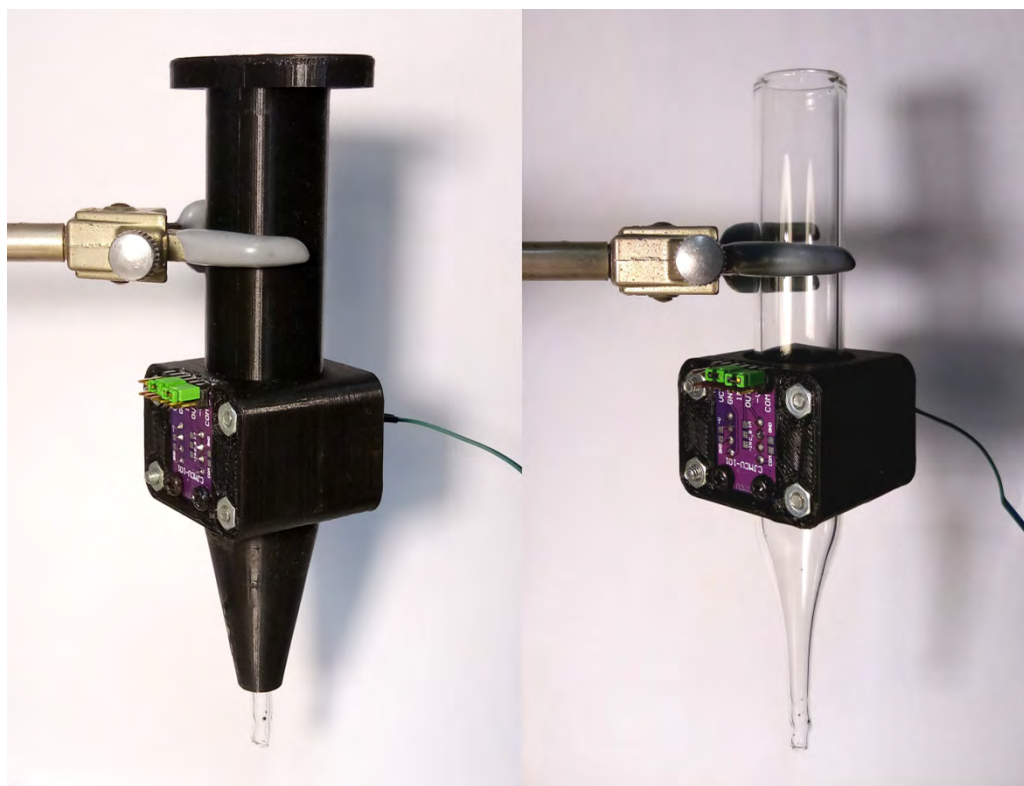


**Figure 1.** Reaction-detection cell, with and without the light shield installed, shown on the left and right, respectively.

Liquids (DPD reagent solution, buffer and sample) were delivered by the peristaltic pumps (P1 to P3) to the upper end of the reaction-detection cell via three pieces of stainless-steel tubing (0.75 mm internal diameter) fixed in a stopper. The flow rates and times were set at 3 mL min<sup>-1</sup> for 10 seconds (DPD reagent and buffer) and 30 mL min<sup>-1</sup> for 20 seconds (sample), corresponding to final volumes of 0.5, 0.5 and 10 mL respectively.

A generic peristaltic pump (P4) was used to empty the reaction cell to waste and also functioned as an effective blocking valve when turned off. Waste was collected in a reservoir for later disposal according to local regulations.

The water samples pumped by P3 were taken from an auxiliary intermediate reservoir which was emptied and refilled when changing samples.

The data acquisition and control system consisted of an Arduino Nano board with an ATmega 328P microcontroller and an ADS1115 (Texas Instruments) 16-bit data acquisition board, which received the analog signal from the OPT101. The ADS1115 was in turn connected to the Nano board by means of the I<sup>2</sup>C serial bus.

Control of the stepping motors for the three main peristaltic pumps was achieved with three A4988 digital drivers (Allegro, Manchester, NH, USA), interfaced with the Arduino Nano board. Pulse-width modulation (PWM) was employed to control the drain peristaltic pump via an NPN bipolar junction transistor. A separate transistor switched the LED, powered by an LM334 (Texas Instruments) constant-current source. The operating current of the LED was adjusted to ensure approximately 3.5 V at the output of the OPT101 when the cell was filled with water.

All necessary analytical calculations were carried out by the microcontroller, and the results were then transferred to a notebook computer via the USB connection. Firmware for the microcontroller was written and compiled in the Arduino Integrated Development Environment (IDE). The diagram of the fluidic system is depicted in Figure 2, while Figure 3 represents the schematics of the electronic circuit.

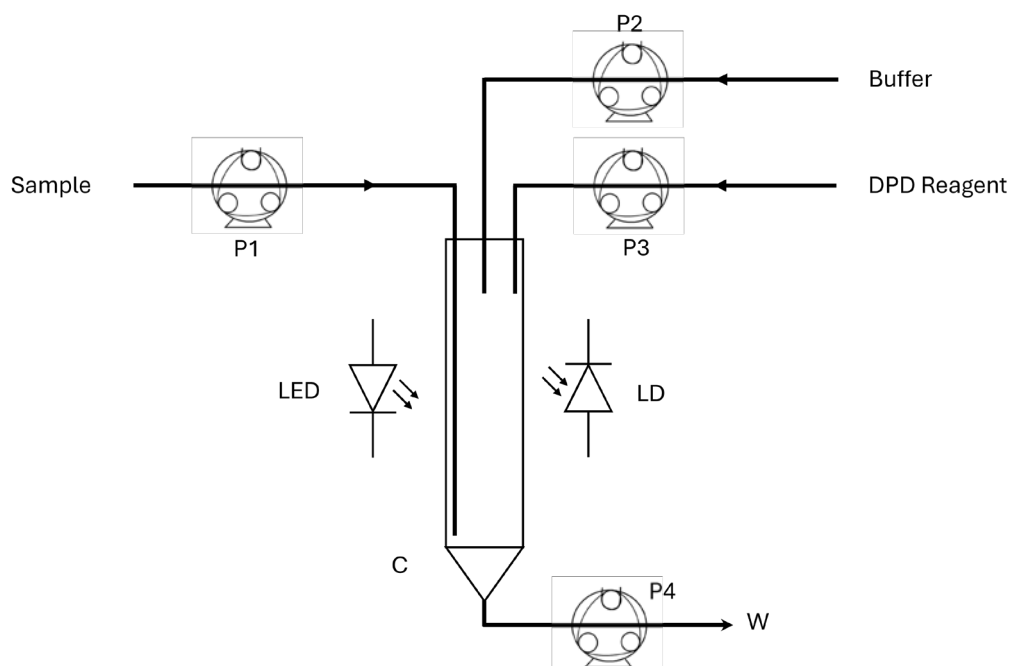


**Figure 2.** Schematics of the fluidic system. C: reaction-detection cell. P1, P2, P3: main peristaltic pumps. P4: auxiliary peristaltic pump. LED: light-emitting diode. LD: light detector. W: waste.

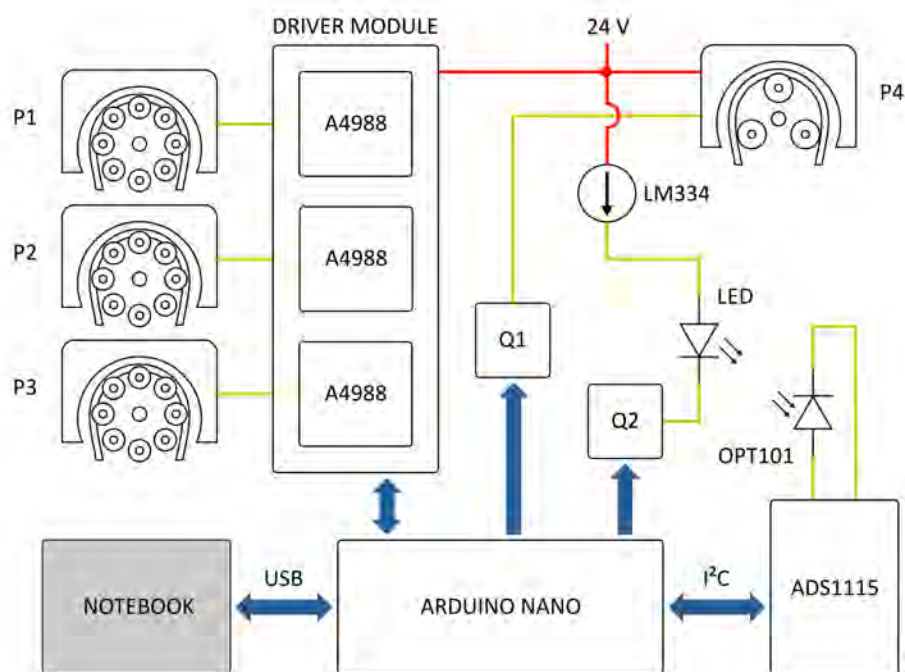


**Figure 3.** Schematic diagram of the electronic circuit. P1, P2, P3: main peristaltic pumps. P4: auxiliary peristaltic pump. Q1, Q2: NPN transistors.

### System operation

The system operates under the control of firmware loaded onto the Arduino microcontroller board. It typically remains in standby mode, with the analytical process initiated at predefined intervals (for example, every three hours), starting with several rinses of the flow system and reaction-detection cell using fresh sample.

The adjustment of the photometric measurement system begins with the LED turned off, measuring and storing the “dark current” signal. Next, with the cell filled up with water, the LED is turned on and the “full scale” (i.e. 100% T) signal is also measured and stored. Once these measurements are complete, the system is ready to begin absorbance measurements.

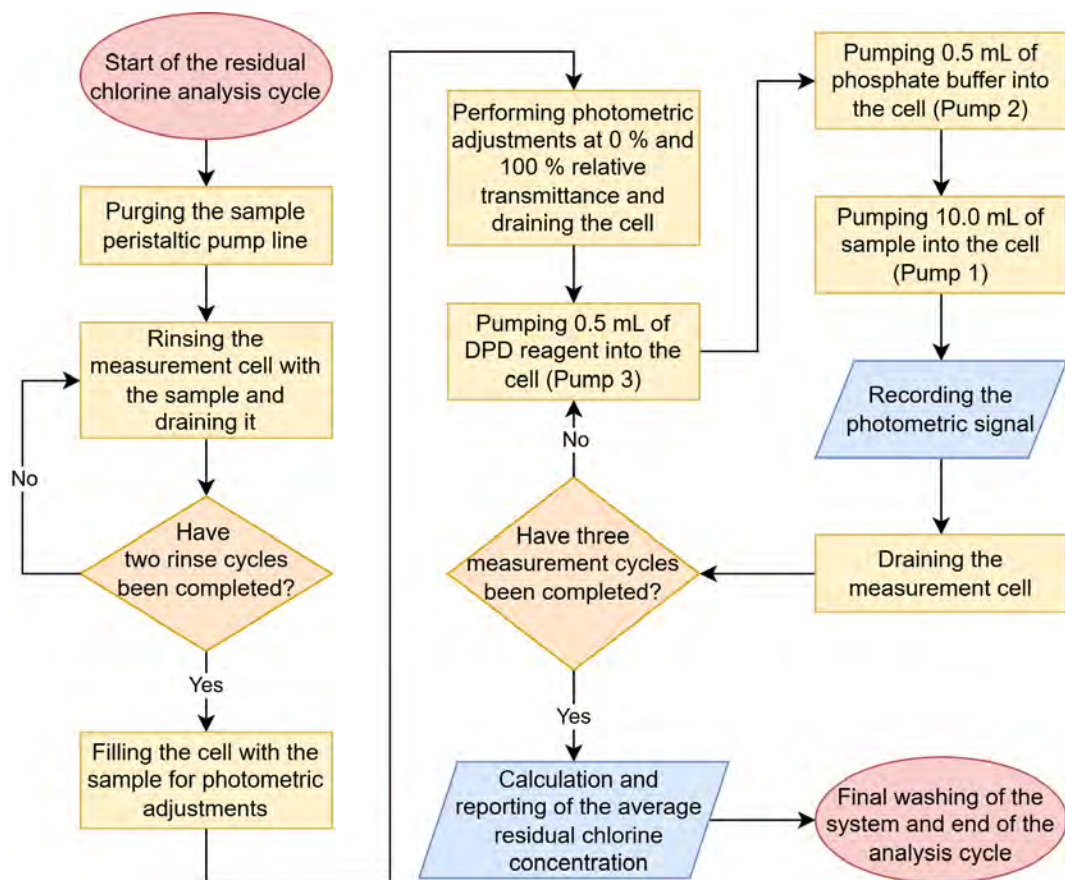


**Figure 4.** System operation flowchart, according to the selected operating conditions and carrying out the analysis in triplicate.

## RESULTS AND DISCUSSION

Given that the final use of the automated system will be under variable temperature conditions, a batch-wise study was conducted to assess the influence of temperature on the reaction. Reagent and buffer solutions and deionized water, as well as the spectrophotometer cell were thermostatted in a circulating water bath. The temperatures studied were 5.1, 20.9, 29.8 and 39.8 °C. For each temperature a 6-point calibration curve was plotted in the 0 – 4 mg L<sup>-1</sup> range of free chlorine. Chlorine standards, prepared at 10-fold concentrations (held at room temperature), were added to the thermostatted water and reagents in appropriate volumes to achieve final concentrations within the desired range. Measurements were carried out at 515 nm. The slopes of the linear calibration curves at these temperatures ranged from 0.2263 to



0.2384 L mg<sup>-1</sup>, showing a variability of about 5%. This value was deemed acceptable for on-site use and fit for the intended purpose.

One of the first considerations in the design was ensuring thorough mixing of the reagents and sample. Mechanical stirring is commonly employed in flow-batch systems. However, in this work, for increased simplicity it was decided to avoid the use of a stirrer. Instead, we explored the effectiveness of self-mixing based on turbulence, taking advantage of the high flow rate and volume of the last liquid added, which in this case was the sample itself.

The mixing process was studied by means of videos recorded at short distances, as well as by recording the absorbance signal as a function of time at 100-ms intervals, starting before the sample addition and ending once a stable absorbance was reached (Figure 5). It was found that, for the proposed flow rates and times, after an initial period of chaotic fluctuations due to turbulent mixing, a stable absorbance signal was achieved approximately 30 seconds after the sample was added. Consequently, a 30-second waiting time was incorporated into the software before beginning the measurement of the signals.

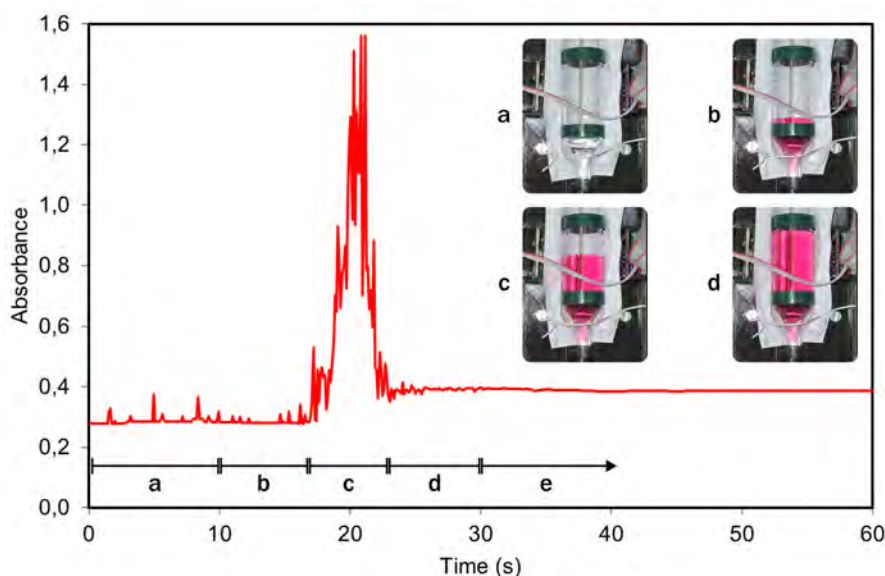


**Figure 5.** Plot of the absorbance signal (not adjusted to zero) as a function of time during and after the mixing stage, and pictures of the reaction/detection cell (without the detection system and the light shield) taken at different times showing the mixing of reagents and sample. a) Addition of reagent and buffer. b) Beginning of sample addition. Meniscus below the light path. c) Sample addition in progress. Meniscus overlapping the light path. d) End of sample addition. Meniscus above the light path. Mixture remains non-homogeneous. e) Stabilization period prior to absorbance measurement.

During these tests, it was noticed that the vertical position of the nozzle delivering the sample was critical. Due to the high flow rate, a nozzle with its tip positioned too high above the level of the liquid was prone to disperse sample drops, which would adhere to the dry upper portion of the cell wall and affect the analytical performance. To address this issue, the sample nozzle was extended so that its tip remained submerged in the liquid (near the bottom of the cell) from the early stages of the process. This adjustment was found to enhance the mixing effect and prevent sample drops from adhering to the cell wall.

Linearity was checked with standard solutions in the range up to 4 mg L<sup>-1</sup> of free chlorine. It was found that with the DPD concentration at 1.1 g L<sup>-1</sup>, the linear range was unsatisfactory, barely reaching 2 mg L<sup>-1</sup>. Thus, the effect of the concentration of DPD was also studied using concentrations of 4.4, 6.6 and 8.8 g L<sup>-1</sup> of anhydrous DPD sulfate, corresponding to 4, 6 and 8 times that established in the batch



APHA standard method (Figure 6). The four calibration curves were compared by visual inspection and considering the regression coefficients. A DPD sulfate concentration of  $6.6 \text{ g L}^{-1}$  was finally chosen as a tradeoff between economy and performance, the calibration equation being  $A = 0.314 C$ ,  $R^2 = 0.999$ . The very slight nonlinearity still observed was ascribed to the use of a cylindrical detection cell and to the polychromaticity of the light emitted by the LED, two obvious potential causes of deviation from Beer's Law.

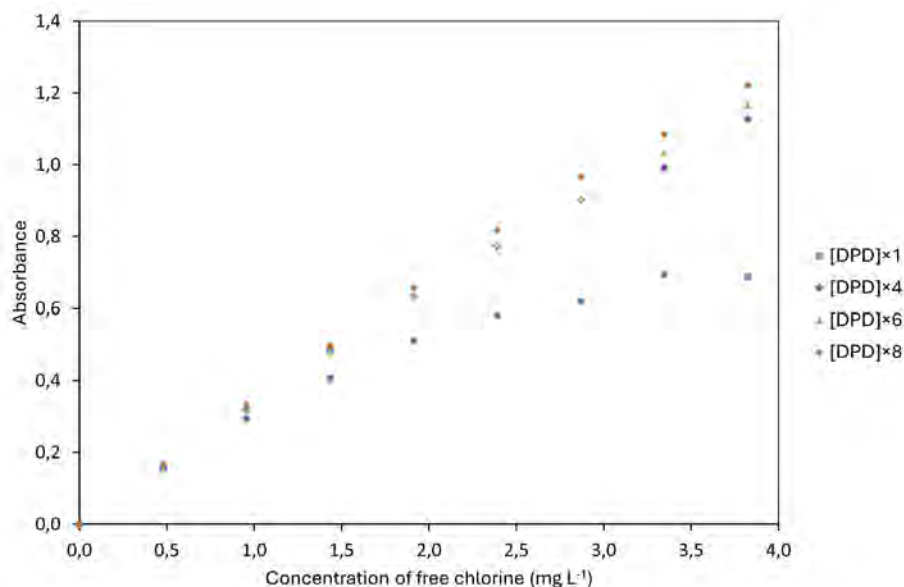


**Figure 6.** Absorbance as a function of free chlorine concentration at four different DPD concentrations.  $[\text{DPD}] \times 1 = 1.1 \text{ g L}^{-1}$  DPD sulfate.

Once the optimum DPD concentration was determined and linearity evaluated, the remaining analytical figures of merit were studied.

Precision (repeatability) was examined by repeating 10 times the determination of a sample containing around  $2 \text{ mg L}^{-1}$  free chlorine. The relative standard deviation found was 0.33%.

Carryover between successive determinations was studied in a worst-case scenario by first repeating 5 times the determination of a  $4 \text{ mg L}^{-1}$  free chlorine solution, followed by repeating 10 times the determination of a blank (deionized water). This experiment was also conducted in the opposite direction, first repeating 5 times the determination of the deionized water blank, followed by repeating 10 times the determination of the  $4 \text{ mg L}^{-1}$  free chlorine solution. Results are shown in Figure 7.

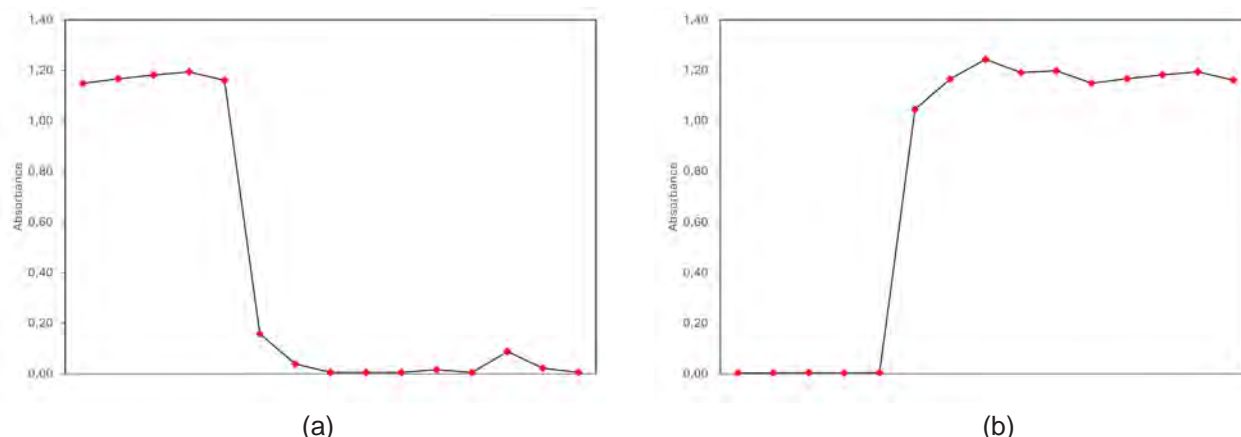


**Figure 7.** Carryover studies showing the changes in absorbance after a sudden change in free chlorine concentration. The figures show the results of 5 repetitions at the original concentration followed by 10 repetitions at the final concentration. (a) Concentrated sample before blank (b) Blank before the sample.

According to these results, to avoid the memory effect when changing samples, two rinsing steps with the new sample are necessary (loading and discarding each time) before carrying out the determination. Therefore, this routine was incorporated into the software controlling the process.

For accuracy verification, 90 samples with different free-chlorine concentrations within the linear range were analyzed by the proposed automated method and by the manual method using Macherey-Nagel reagent. The correlation curve for the results (automated method versus manual method), presented in Figure 8, fits a straight line ( $y = 1.001x + 0.0636$ ,  $R^2 = 0.9936$ ). It was concluded that the automated analyzer produced results equivalent to those obtained by the manual DPD method.

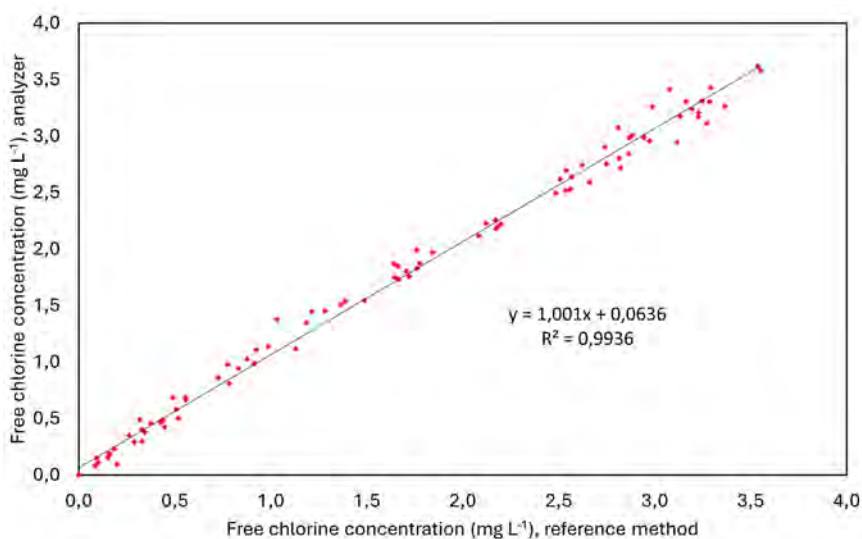


**Figure 8.** Correlation curve for the results for the analysis of 90 samples by the automated analyzer versus those obtained by the reference batch method with Macherey-Nagel DPD reagent.

Detection and quantification limits were calculated by repeating 10 times the determination of a blank (deionized water) and applying the 3s and 10s criteria respectively. The limit of detection found was 0.046 mg L<sup>-1</sup>, while the quantification limit was 0.15 mg L<sup>-1</sup>.

In each analytical cycle the system consumed 85 mL of water sample, 1.5 mL of DPD reagent and 1.5 mL of buffer. This included the two initial rinsings, photometric adjustment and the analysis carried out in triplicate. The total waste generated per analytical cycle was then 88 mL. Waste was collected in a large reservoir which should be emptied or changed during the periodic maintenance and its content disposed of according to local regulations.

It should be noted that for on-site use calibrations are difficult to automate. This would require not only an additional pump and reservoir (increasing complexity and cost), but also the storage of dilute standard solutions, which are unstable. Thus, it was planned that for field use recalibrations should be carried out simultaneously with periodic maintenance (i.e., replenishment of reagent reservoirs and emptying of the waste reservoir). This approach is usual in commercial automated analyzers for residual chlorine and is an accepted practice in the water industry. Other tradeoffs taken include the use of the water sample itself as the reference for 100% transmittance photometric adjustment, avoiding the need for a deionized water reservoir and an additional pump. This is also common practice in the water industry, but it assumes that the sample is not colored nor contains significant amounts of suspended solids.

The figures of merit obtained during the operation of the automated analyzer were deemed fit for the intended purpose. Unlike laboratory methods, which are carried out under highly controlled conditions, the design and operation of on-site analyzers require several tradeoffs explained above. This, together with the wide ambient temperature range necessarily leads to the adoption of less stringent acceptance criteria for the figures of merit, as compared to usual laboratory methods.

## CONCLUSIONS

It was demonstrated that flow-batch analysis is an appropriate analytical technique for automating the determination of residual chlorine in drinking water by means of the DPD photometric method. The system performed correctly without the need for a mechanical stirrer, resulting in increased simplicity.

Therefore, the project is now progressing to the next stage, which involves the design and construction of a robust industrial-grade prototype.

## Conflicts of interest

The authors have no conflicts of interest to declare, neither from the funding agency, from project partners nor from other origins.

## Acknowledgements

The authors thank “Agencia Nacional de Investigación e Innovación” (ANII, National Agency for Research and Innovation) for funding [Project ART\_X\_2021\_1\_170322]. This project is carried out by Universidad de la República in partnership with Spymovil SRL. Moisés Knochen also thanks ANII for a personal grant.

## REFERENCES

- (1) *Water Chlorination/chloramination practices and principles* (2<sup>nd</sup> ed.). American Water Works Association (AWWA). Denver, CO, 2006.
- (2) Edzwald, J. K. *Water Quality & Treatment. A Handbook on Drinking Water* (6<sup>th</sup> Ed.). American Water Works Association, Denver, CO, 2011.
- (3) Engelhardt, T. L.; Malkov, V. B. *Chlorination, Chloramination and Chlorine Measurement*. Hach, Loveland, CO, 2015.
- (4) World Health Organization (WHO). *Guidelines for Drinking Water Quality* (4<sup>th</sup> Ed.) Geneva, 2022.
- (5) Presidencia Uruguay. Executive Power. Decree 375/011. Montevideo, 2011. Available at: <https://www.gub.uy/presidencia/institucional/normativa/decreto-375011> (accessed March 2025).
- (6) Instituto Uruguayo de Normas Técnicas (UNIT). *Agua potable. Requisitos*. Standard N° 833:2008 (Reprint 2010); Montevideo, 2010. Available at: <https://www.unit.org.uy/normalizacion/norma/100000158/> (accessed March 2025).

- (7) Hazey, G. J. Amperometric Residual Chlorine Recording. *J. Am. Water Works Assoc.* **1951**, *43*, 292–298. Available at: <http://www.jstor.org/stable/41235740> (accessed March 2025).
- (8) Palin, A. T. The Determination of Free and Combined Chlorine in Water by the Use of Diethyl-p-Phenylene Diamine. *J. Am. Water Works Assoc.* **1957**, *49*, 873–880. Available at: <https://www.jstor.org/stable/41254900> (accessed March 2025).
- (9) Palin, A. T. Current DPD Methods for Residual Halogen Compounds and Ozone in Water. *J. Am. Water Works Assoc.* **1975**, *67*, 32–33. <https://doi.org/10.1002/j.1551-8833.1975.tb02149.x>
- (10) Bauer, R.; Rupe, C. O. Use of Syringaldazine in a Photometric Method for Estimating “Free” Chlorine in Water. *Anal. Chem.* **1971**, *43*, 421–425. <https://doi.org/10.1021/ac60298a003>
- (11) Cooper, W. J.; Sorber, C. A.; Meier, E. P. A Rapid Specific Free Available Chlorine Test with Syringaldazine (FACTS). *J. Am. Water Works Assoc.* **1975**, *67*, 34–39. <https://doi.org/10.1002/j.1551-8833.1975.tb02150.x>
- (12) Baird, R. B.; Eaton, A. D.; Rice, E. W.; Bridgewater, L. DPD Colorimetric Method – 4500-Cl G. *Standard Methods for the Examination of Water and Wastewater* (23<sup>rd</sup> Ed.). American Public Health Association, Washington, DC, 2017.
- (13) Ruzicka, J.; Hansen, E. H. *Flow Injection Analysis* (2<sup>nd</sup> Ed.). Wiley, New York, 1988.
- (14) Trojanowicz, M.; Matuszewski, W.; Hulanicki, A. Flow-Injection Potentiometric Determination of Residual Chlorine in Water. *Anal. Chim. Acta* **1982**, *136*, 85–92. [https://doi.org/10.1016/S0003-2670\(01\)95366-8](https://doi.org/10.1016/S0003-2670(01)95366-8)
- (15) Leggett, D. J.; Chen, N. H.; Mahadevappa, D. S. Rapid Determination of Residual Chlorine by Flow Injection Analysis. *Analyst* **1982**, *107*, 433–441. <https://doi.org/10.1039/AN9820700433>
- (16) Catalá Icardo, M.; García Mateo, J. V.; Martínez Calatayud, J. o-Dianisidine: A New Reagent for Selective Spectrophotometric, Flow Injection Determination of Chlorine. *Analyst* **2001**, *126*, 2087–2092. <https://doi.org/10.1039/B107000M>
- (17) Jin, J.; Suzuki, Y.; Ishikawa, N.; Takeuchi, T. A Miniaturized FIA System for the Determination of Residual Chlorine in Environmental Water Samples. *Anal. Sci.* **2004**, *20*, 205–207. <https://doi.org/10.2116/analsci.20.205>
- (18) Saad, B.; Wai, W. T.; Jab, M. S.; Ngah, W. S. W.; Saleh, M. I.; Slate, J. M. Development of Flow Injection Spectrophotometric Methods for the Determination of Free Available Chlorine and Total Available Chlorine: Comparative Study. *Anal. Chim. Acta* **2005**, *537*, 197–206. <https://doi.org/10.1016/j.aca.2005.01.002>
- (19) Zhou, M.; Li, T.; Zu, M.; Zhang, S.; Liu, Y.; Zhao, H. Membrane-Based Colorimetric Flow-Injection System for Online Free Chlorine Monitoring in Drinking Water. *Sens. Actuators, B* **2021**, *327*, 128905. <https://doi.org/10.1016/j.snb.2020.128905>
- (20) Honorato, R. S.; Ugulino de Araújo, M. C.; Lima, R. A. C.; Zagatto, E. A. G.; Lapa, R. A. S.; Costa Lima, J. L. F. A Flow-Batch Titrator Exploiting a One-Dimensional Optimization Algorithm for End Point Search. *Anal. Chim. Acta* **1999**, *396*, 91–97. [https://doi.org/10.1016/S0003-2670\(99\)00366-9](https://doi.org/10.1016/S0003-2670(99)00366-9)
- (21) Gonçalves Dias Diniz, P. H.; Farias de Almeida, L.; Harding, D. P.; Ugulino de Araújo, M. C. Flow-Batch Analysis. *TrAC, Trends Anal. Chem.* **2012**, *35*, 39–49. <https://doi.org/10.1016/j.trac.2012.02.009>
- (22) Liang, J.; Wei, Z.; Huang, Q.; Liang, J.; Zhao, X. C.; Zhou, Z.; Li, G. A novel approach for tea polyphenol detection based on flow batch analysis system in conjunction with diazotization coupling reaction. *Measurement* **2025** *246*, 116751. <https://doi.org/10.1016/j.measurement.2025.116751>
- (23) Costa, J. B. S.; de Paula, N. T. G.; da Silva, P. A. B.; de Souza, G. C. S.; Paim, A. P. S.; Lavorante, A. F. A spectrophotometric procedure for sialic acid determination in milk employing a flow-batch analysis system with direct heating. *Microchem. J.* **2019** *147*, 782–788. <https://doi.org/10.1016/j.microc.2019.03.086>
- (24) Chládková, G.; Kunovská, K.; Chocholouš, P.; Polášek, M.; Sklenářová, H. Automatic screening of antioxidants based on the evaluation of kinetics of suppression of chemiluminescence in luminol – hydrogen peroxide system using sequential injection analysis setup with the flow-batch detection cell. *Anal. Methods* **2019** *11*, 2531–2536. <https://doi.org/10.1039/C9AY00160C>

- (25) Zhu, X.; Deng, Y.; Li, P.; Yuan, D. X.; Ma, J. Automated syringe-pump-based flow-batch analysis for spectrophotometric determination of trace hexavalent chromium in water samples. *Microchem. J.* **2019** *145*, 1135–1142. <https://doi.org/10.1016/j.microc.2018.12.040>
- (26) Nascimento, V. B.; Selva, T. M. G.; Coelho, E. C. S.; Santos, F. P.; Antônio, J. L. S.; Silva, J. R.; Gaião, E. N.; Araújo, M. C. U. Automatic Determination of Chlorine without Standard Solutions Using a Biamperometric Flow-Batch Analysis System. *Talanta* **2010**, *81*, 609–613. <https://doi.org/10.1016/j.talanta.2009.12.049>

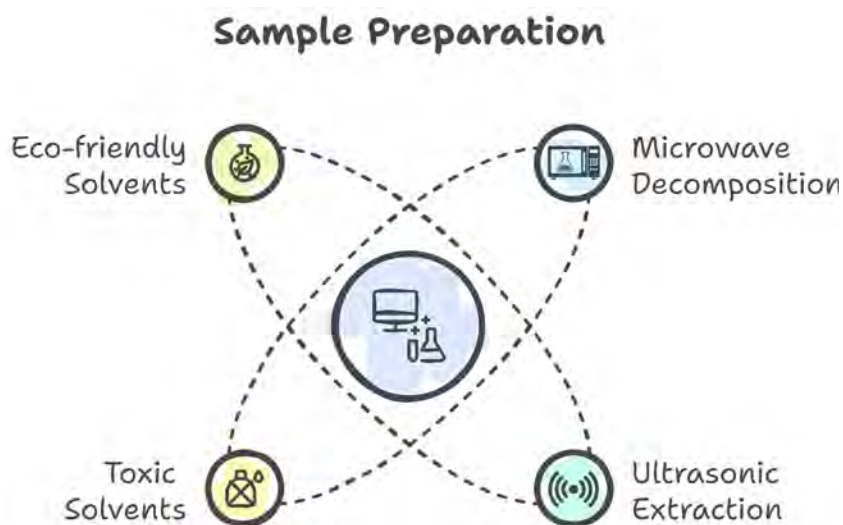


## TECHNICAL NOTE

# Sample Preparation Methods Focusing on Soy Biotechnological Samples: Towards Greener Application

João G. Veneziani Kamezawa<sup>ID</sup>, Lilian Seiko Kato<sup>ID</sup>, Elisânia Kelly Barbosa Fonseca<sup>ID</sup>,  
Marco Aurélio Zezzi Arruda\*<sup>ID</sup>✉

Instituto de Química, Universidade Estadual de Campinas (Unicamp) <sup>ROR</sup>, Rua Monteiro Lobato, 270, 13083-862, Campinas, SP, Brazil



Tissue and cell culture techniques have become pivotal in plant biotechnology, particularly for the improvement and mass propagation of economically important species such as soybean (*Glycine max*). Within this context, somatic embryogenesis has emerged as a powerful tool. Micronutrients like Fe, Mn, Mo, and Zn play essential roles in cellular metabolism and can serve as indicators of tissue growth and development. Inductively Coupled Plasma Mass Spectrometry (ICP-MS) is widely recognized for its sensitivity in multielement analysis at trace levels; however, sample preparation remains

a critical and often resource-intensive step. This study aims to develop and compare three distinct sample preparation methods for the determination of micronutrients in soybean calli using ICP-MS: (1) conventional acid decomposition, (2) acid extraction, and (3) acidless decomposition. The results indicated that all three methods provided statistically equivalent concentrations for all evaluated elements ( $p \geq 0.05$ ), with values ranging from  $0.54 \pm 0.08 \mu\text{g g}^{-1}$  for Mo to  $14 \pm 1 \mu\text{g g}^{-1}$  for Mn. Additionally, the residual chemical content (RCC) in the proposed methods was below the detection limit of  $8 \text{ mg L}^{-1}$ . Sustainability assessment using the AGREEprep tool highlighted acidless decomposition as the most environmentally friendly method, primarily due to its use of greener reagents and higher sample throughput. These findings suggest that acidless decomposition presents a viable and sustainable alternative for micronutrient analysis in plant tissue culture applications.

**Keywords:** soybean calli, sample preparation, ICP-MS, decomposition, extraction

**Cite:** Kamezawa, J. G. V.; Kato, L. S.; Fonseca, E. K. B.; Arruda, M. A. Z. Sample Preparation Methods Focusing on Soy Biotechnological Samples: Towards Greener Application. *Braz. J. Anal. Chem.* 2025, 12 (49), pp 144-151. <http://dx.doi.org/10.30744/brjac.2179-3425.TN-16-2025>

Submitted March 18, 2025, Resubmitted May 23, 2025, Accepted June 7, 2025, Available online June 18, 2025.

## INTRODUCTION

The production and exportation of soy is an important pillar of the Brazilian economy.<sup>1</sup> Many products are derived from soybeans, such as animal feed, oil, biodiesel and others. However, it is a cheap commodity and therefore needs large production to be profitable. Because there is a limit for the cultivated area for soy and an urge to improve the production and quality of the grains, the search for biotechnological tools is an important alternative for the producer countries. A technique that has been increasingly investigated in recent times is somatic embryogenesis (SE).

SE is an important tool in plant biotechnology; it is a process in which entire plants can be regenerated from a tissue named calli.<sup>2-7</sup> The calli is a tissue constituted by totipotent cells,<sup>2,5</sup> they are formed by the dedifferentiation of cells from an explant of a plant donor. The *in vitro* cultivation of totipotent cells, able to form every part of the organism, allows many applications as genetic improvements and rapid mass multiplication of varieties.<sup>4</sup> Therefore, the SE can be employed for the propagation and improvement of species with economic interests.<sup>4</sup> However, new technical methodologies need to be developed and adapted to measure these tissues and have confinable results about their applications.

The determination of the micronutrients of the calli can be very useful as an indicator of their development. Some of the most common micronutrients are iron (Fe), manganese (Mn), molybdenum (Mo) and zinc (Zn).<sup>8-10</sup> These nutrients are essential for the cells well-functioning, even though it is necessary at low concentrations, they perform important roles for the metabolism.<sup>9-11</sup> Besides its importance, no work has reported the micronutrients concentration in soybean calli. For this task, the inductively coupled plasma mass spectrometry (ICP-MS) is a well established technique for multielement determination at low concentrations.<sup>12-15</sup> However, the sample preparation step is crucial for ICP-MS analysis, as the technique requires a liquid sample with low residual acidity.<sup>12,16</sup>

More recently, the search for greener methods has gained importance in analytical chemistry. Besides being reliable, the new methods need to be environmentally friendly. The main goals are to reduce the amount of reagents consumed, avoid the use of toxic reagents and reduce the waste and energy consumption.<sup>17</sup> One excellent tool to evaluate the greenness of a sample preparation method is the AGREEprep,<sup>18</sup> a metric tool that uses ten principles, with different weights, to analyze the method. The criteria principles are based on minimizing waste, use of safer reagents, maximizing sample throughput besides the promotion of automation, secure of the operator and others.<sup>18</sup>

One of the most commonly used sample preparation techniques is microwave-assisted acid decomposition. In this method, acids act under high pressure and temperature in a closed-vessel system to effectively break down the organic matter in the sample matrix. To minimize the consumption of sample material and reagents, miniaturized systems can be employed. Despite its efficiency and widespread application, this technique is associated with significant reagent use, high waste generation, and extended preparation times.

In recent years, ultrasonic extraction has gained popularity for elemental analysis. Various ultrasonic devices can be utilized, including ultrasonic probes, baths, and focused ultrasonic baths. These methods operate under milder conditions of temperature and pressure and are capable of reducing sample preparation time. However, a key limitation of ultrasonic systems is their limited sample throughput, as typically only a few samples can be processed per run.

A novel approach was introduced by Silva et al. (2024),<sup>19</sup> who proposed a microwave-assisted acidless decomposition method for biological samples using only hydrogen peroxide as the oxidizing agent. This technique offers several advantages, including lower blank signals and reduced residual acidity, which are particularly beneficial for subsequent analysis by ICP-MS.

Therefore, this work aims to develop and compare three different methods, a microwave-assisted acid decomposition using minivials, an ultrasonic assisted acid extraction and a microwave-assisted acidless decomposition, to prepare soy calli for the determination of micronutrients (Fe, Mn, Mo and Zn) in soybean calli by ICP-MS, taken into account the greenness of such methods, through AGREEprep<sup>18</sup> software evaluation.

## MATERIALS AND METHODS

All the solutions were prepared with ultrapure water obtained from Direct-Q® 5 UV (Merck, Darmstadt, Germany). The ionic standards for the elements were from Fe, Mn, Mo and Zn. For the preparation methods were used sub-boiled nitric acid (14 mol L<sup>-1</sup>) (Synth, São Paulo, Brazil) and hydrogen peroxide (30% m/m) (Synth, São Paulo, Brazil).

The calli samples were produced in our laboratories, according previous protocol.<sup>20</sup> In brief, they were induced from the cotyledon of a 3-week-old soy plant of the line Roundup Ready (RR). After the induction, the calli were transferred to a propagation culture media for 4 weeks, then, the samples were collected and storage frozen at -18 °C. The samples were prepared in different ways for the determination by ICP-MS.

### *Microwave-assisted acid decomposition*

The calli were ground and homogenized still frozen in a porcelain mortar. About 25 mg of the sample were added to the microwave Teflon® mini vials.<sup>21</sup> Then, 250 µL of sub boiled nitric acid and 100 µL of hydrogen peroxide were added. Four mini vials were put inside each conventional microwave vial with 10 mL of water.<sup>22,23</sup> The decomposition program was 5 min at 240 W; 5 min at 420 W; 5 min at 600 W and 15 min at 800 W, and performed at a DTG-100 Plus (Provecto Analítica, Jundiaí, Brazil). After the digestion, the samples were collected and stored. To evaluate the decomposition efficiency, the same method was employed for the preparation of a certified reference material of rice flour (NIST 1568a).

### *Ultrasonic-assisted acid extraction*

For the extraction the same amount of calli was used and they were ground and homogenized in the same way. Then, 25 mg were added to an eppendorf tube with 250 µL of nitric acid, 100 µL of hydrogen peroxide and 150 µL of deionized water. Six flasks were attached to a plastic support that prevented them from opening during the sonication. A focalized ultrasonic bath (Cuphorn) attached to QQ700 sonicator (QSonica, USA) was used for 10 min with 60% of the amplitude in mode 1 min on/off. The maximum power achieved was around 90 W and the input energy was 50 kJ. After the extraction, the samples were filtered on 0.22 µm and storage for analysis.

### *Microwave-assisted using acidless method*

An acidless microwave-assisted decomposition, based on Silva et al.<sup>19</sup> previous work, was also evaluated. The same amount of calli (25 mg) was added to the microwave minivials, in the same system as the acid digestion. The reagent used for the decomposition was only 500 µL of hydrogen peroxide. The same microwave device was employed, and the program used was 5 min at 400 W, 20 min at 790 W and 3 min at 320 W, and after the digestion the samples were collected and stored. The residual carbon content (RCC) of the decomposition was evaluated by inductively coupled plasma optical emission spectroscopy (ICP OES), using a PlasmaQuant 9100 Series (Analytik Jena, Germany). The plasma power was 1000 W, the plasma gas flow 15 L min<sup>-1</sup>, the auxiliary gas flow 1.5 L min<sup>-1</sup>, and the nebulizer gas flow was set at 0.90 L min<sup>-1</sup>. A concentric nebulizer Micromist and cyclonic nebulization chamber were used, and the monitored wavelengths were 193.025 and 247.857 nm, both in axial mode. The calibration curve was prepared using sodium citrate (Synth, São Paulo, Brazil) from 60 mg L<sup>-1</sup> to 400 mg L<sup>-1</sup> of carbon.

### *Analytes determination*

The determination of the analytes was carried out in an iCAP-TQ (Thermo Fischer Scientific, Germany), and the conditions adjusted for the performance test of the device. All the samples were diluted to have 1% acidity (v/v), and the calibration curve performed with the same acidity as well. The plasma power used was 1550 W, the plasma gas flow rate as 14 L min<sup>-1</sup>, the auxiliary gas flow rate as 0.8 L min<sup>-1</sup> and the nebulizer gas flow rate of 0.950 – 1.013 L min<sup>-1</sup>. The introduction system was composed by a concentric nebulizer Micromist and cyclonic nebulization chamber. The monitoring mass charge ratio and the collision or reaction cell used are presented in the Table I. To avoid signal variations from the equipment, an Y connection was

added to the introduction system to inject the sample and a 10  $\mu\text{g L}^{-1}$  solution of Sc, Rh or Y as internal standard. The Rh was used to normalize the measurements made in KED mode and Sc and Y to normalize measurements in TQ- $\text{O}_2$  mode. The monitored mass/charge ratio from the internal standard are  $^{45}\text{Sc}^{16}\text{O}$ ,  $^{89}\text{Y}^{16}\text{O}$  and  $^{103}\text{Rh}$ .

**Table I.** Monitored mass charge ratio ( $m/z$ ) and acquisition mode in the ICP-MS

1 <sup>st</sup> Quadrupole		Collision/Reaction Cell	2 <sup>nd</sup> Quadrupole
<b>Fe</b>	NDA*	KED (He)	$^{57}\text{Fe}$
<b>Mn</b>	NDA*	KED (He)	$^{55}\text{Mn}$
<b>Mo</b>	$^{98}\text{Mo}$	$\text{O}_2$	$^{98}\text{Mo}^{16}\text{O}$
<b>Zn</b>	$^{66}\text{Zn}$	$\text{O}_2$	$^{66}\text{Zn}^{16}\text{O}$

\*NDA – No  $m/z$  filtered

## RESULTS AND DISCUSSION

The extraction process yielded a colorless solution containing fine particulate matter from the calli, necessitating filtration through a 0.22  $\mu\text{m}$  membrane to remove residual solids. Similarly, both decomposition methods also produced clear, particle-free solutions upon visual inspection; however, for precautionary purposes, these samples were also filtered using a 0.22  $\mu\text{m}$  membrane. This step is crucial for preventing particulate buildup in the ICP-MS injection system and minimizing the need for intensive cleaning between sample runs, thereby ensuring analytical consistency and instrument longevity.

As can be seen from Table II, the micronutrients were determined for the three different methods. Although there was few information about the presence of macro and micronutrients in soy calli, however, in plants, the Mo is the element that stands out because its lower concentration. This behavior can be attributed to the few numbers of proteins depending on this element.<sup>24,25</sup> Even at low concentrations it is important to determine Mo, since this micronutrient can alter significantly metabolism of amino acids and sugars.<sup>25</sup> Other micronutrients such as Fe, Mn, and Zn are present at higher concentration, around 10  $\mu\text{g g}^{-1}$ . The control of Fe in the cells is also very important, because the ions  $\text{Fe}^{2+}$  and  $\text{Fe}^{3+}$  can also form reactive oxygen species (ROS).<sup>26</sup> Manganese plays a role in diverse process in the cells, respiration, scavenging of ROS, pathogen defense and others. Interesting, the  $\text{Mn}^{2+}$  cation can act as antioxidant specie.<sup>27</sup> Also, the Zn control is very important, once it is an essential metal for more than 300 enzymes, including RNA polymerases, but at high concentrations it can be toxic for plants.<sup>28</sup>

**Table II.** Micronutrients concentration ( $\mu\text{g g}^{-1}$ ) for soy calli determined with different sample preparation methods (n=5)

Concentration ( $\mu\text{g g}^{-1}$ )	Fe	Mn	Mo	Zn
<b>Acid Decomposition</b>	$13 \pm 1$	$13 \pm 1$	$0.50 \pm 0.08$	$9 \pm 1$
<b>Acid Extraction</b>	$13 \pm 1$	$13 \pm 1$	$0.46 \pm 0.09$	$11 \pm 2$
<b>Acidless Decomposition</b>	$12 \pm 3$	$14 \pm 1$	$0.54 \pm 0.08$	$10 \pm 1$

The analytes concentration determined in the samples prepared by the different methods were compared with each other, and no statistical differences were found at 95% confidence level through  $t$ -student test. The concentration for Fe, Mn, Mo and Zn were statistically the same for all methods ( $p \geq 0.05$ ).

One of most common preparation technique is the microwave assisted acid decomposition.<sup>12,29,30</sup> The action of acid at high pressure and temperature in close vessel system decompose most of the organic matter in the matrix. Although this method is very effective and well known, it produces a large amount of waste and high use of reagents, even more it is highly time-consuming. Some alternatives have been proposed, such as the use of diluted acid,<sup>31,32</sup> and, in order to reduce sample and reagents the use of minivials,<sup>21</sup> and currently used for different proposals.<sup>12,22,33</sup> Ultrasonic extraction for elemental analysis has been increasing in recent years.<sup>34-37</sup> Many ultrasonic devices can be used, such as probe, bath or focalized bath.<sup>36</sup> Ultrasonic based techniques use mild conditions as temperature and pressure, moreover, can reduce the time in sample preparation.<sup>34</sup>

Taken into account more sustainable and green methods, recently an acidless decomposition was proposed<sup>19</sup> using only hydrogen peroxide as reagent. As seen in Table II, this method is equivalent to conventional methods, besides, the RCC was lower than the detection limit (8 mg L<sup>-1</sup>) for the calli and 0.02% for the reference material of rice flour, indicating the efficacy of the method. Furthermore, the determination of analytes in the certified reference material was in agreement with the certified values for Fe, Mn, and Mo, with the exception of Zn (Table III). Although Zn was not accurately quantified in the certified sample, its concentration was consistent across the different methods evaluated in this study (see Table II). Additionally, the low residual chemical content (RCC) values further support the reliability and applicability of the proposed method.

An acidless decomposition pay great attention once works with a more environmentally friendly reagent, it is a clean reagent (thus providing low blanks), the production of its decomposition is only O<sub>2</sub> and water, the costs are absurdly low (only few cents of Dolar/decomposition). Additionally, the mechanism for its action is already explained.<sup>19</sup>

**Table III.** Micronutrients concentration (µg g<sup>-1</sup>) for the reference material rice flour (NIST1568a) determined by acidless decomposition (n=4)

Concentration (µg g <sup>-1</sup> )	Fe	Mn	Mo	Zn
<b>Experimental</b>	7 ± 1	18 ± 4	1.3 ± 0.2	9 ± 1
<b>Certified</b>	7.4 ± 0.9	20.0 ± 1.6	1.46 ± 0.08	19.4 ± 0.5
<b>Agreement (%)</b>	108 ± 14	90 ± 18	89 ± 11	46 ± 8

The AGREEprep tool can be employed as a metric to evaluate and compare the sample preparation methods presented in this study. This tool is based on the ten principles of green sample preparation, which emphasize minimizing analytical steps, reducing the consumption of reagents, energy, and waste, and favoring the use of sustainable and renewable materials. Additionally, it promotes maximizing sample throughput through automation, ensuring operator safety, and adopting greener analytical techniques. Each criterion is scored from 0 to 1, with values closer to 1 indicating a greener and more sustainable approach.<sup>18</sup>

The decomposition methods demonstrated an advantage over extraction due to higher sample throughput and the use of reusable Teflon vessels, contributing to improved sustainability. Notably, the acidless decomposition method achieved a higher overall score, attributed to the use of safer and less hazardous reagents. However, all the methods evaluated in this study received lower scores for the number of analytical steps and for relying on ICP-MS as the analytical technique, which, while highly sensitive, is not considered green due to its energy demands and complexity.

The comparisons of the methods by the tool AGREEprep indicates the acidless method more adequately (Figure 1). The main advantages are the use of less hazard reagents, and less waste produced. Also, the miniaturized vessels of the microwave system allow a higher sample throughput, compared to the ultrasonic method, providing a better score at AGREEprep. Besides, using reusable Teflon vessels also contributes to the score.<sup>18</sup>



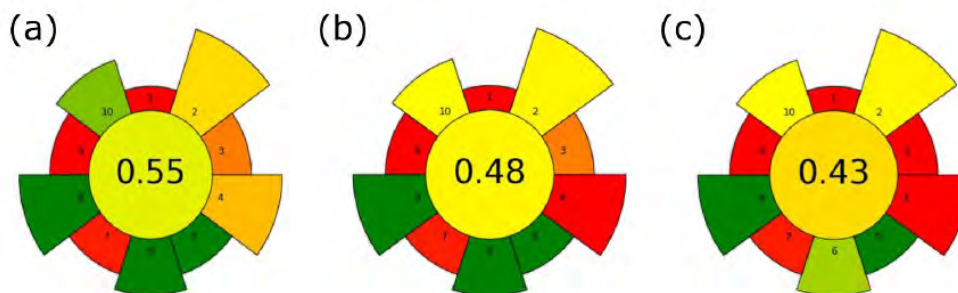


**Figure 1.** AGREEprep scores obtained for the acidless decomposition (a), acid decomposition (b) and acid extraction (c) methods.

## CONCLUSIONS

This study evaluated three distinct sample preparation methods for the determination of micronutrients (Fe, Mn, Mo, and Zn) in somatic soybean calli. All tested methods proved to be effective and reliable for elemental quantification. The microwave-assisted acid decomposition method, widely used in analytical laboratories, demonstrated consistent performance, while ultrasonic extraction emerged as a practical alternative for laboratories lacking access to microwave systems.

However, the microwave-assisted acidless decomposition method stands out as the most sustainable option, as highlighted by its superior performance in the AGREEprep assessment. This method showed no significant difference in analytical results compared to conventional techniques, while offering clear environmental and economic advantages. It requires only a few cents (USD) per decomposition, and the exclusive use of hydrogen peroxide enhances both safety and analytical compatibility. Additionally, the use of miniaturized vials markedly reduced sample and reagent volumes, further improving the method's greenness and cost-efficiency. Collectively, these features make the acidless method a promising and eco-friendly alternative for routine micronutrient analysis in plant tissue studies.

## Conflicts of interest

The authors declare that they have no conflict of interest.

## Acknowledgements

The authors thank the São Paulo Research Foundation (FAPESP) (grants 2014/50867-3, 2018/25207-0, 2019/24445-8, 2021/15218-8, 2022/13166-3), National Council of Research (CNPq) (grant number 303231/2020-3), Council for the Improvement of Higher Education Teachers (CAPES) (fellowship number 88887.653200/2021-00).

## REFERENCES

- (1) Flach, R.; Abrahão, G.; Bryant, B.; Scarabello, M.; Soterroni, A. C.; Ramos, F. M.; Valin, H.; Obersteiner, M.; Cohn, A. S. Conserving the Cerrado and Amazon Biomes of Brazil Protects the Soy Economy from Damaging Warming. *World Dev.* **2021**, *146*. <https://doi.org/10.1016/j.worlddev.2021.105582>
- (2) Fehér, A. Callus, Dedifferentiation, Totipotency, Somatic Embryogenesis: What These Terms Mean in the Era of Molecular Plant Biology? *Front. Plant Sci.* **2019**, *10*. <https://doi.org/10.3389/fpls.2019.00536>.
- (3) Midhu, C. K.; Hima, S.; Binoy, J.; Satheeshkumar, K. Influence of Incubation Period on Callus Tissues for Plant Regeneration in *Ophiorrhiza Pectinata* Arn. Through Somatic Embryogenesis. *Proc. Natl. Acad. Sci., India, Sect. B* **2019**, *89* (4), 1439–1446. <https://doi.org/10.1007/s40011-018-01061-x>
- (4) Behera, P. P.; Sivasankarreddy, K.; Prasanna, V. S. S. V. Somatic Embryogenesis and Plant Regeneration in Horticultural Crops. In: Gupta, S.; Chaturvedi, P. (Eds.) *Commercial Scale Tissue Culture for Horticulture and Plantation Crops* (1<sup>st</sup> ed.). Springer Singapore, 2022, pp 197 – 218. <https://doi.org/10.1007/978-981-19-0055-6>

- (5) Loyola-Vargas, V. M.; Ochoa-Alejo, N. Somatic Embryogenesis. An Overview. In: Loyola-Vargas, V. M.; Ochoa-Alejo, N. (Eds.). *Somatic Embryogenesis: Fundamentals Aspects and Applications* (1<sup>st</sup> ed.). Springer Cham, 2016, pp 1 – 10. <https://doi.org/10.1007/978-3-319-33705-0>
- (6) Méndez-Hernández, H. A.; Ledezma-Rodríguez, M.; Avilez-Montalvo, R. N.; Juárez-Gómez, Y. L.; Skeete, A.; Avilez-Montalvo, J.; De-la-Peña, C.; Loyola-Vargas, V. M. Signaling Overview of Plant Somatic Embryogenesis. *Front. Plant Sci.* **2019**, *10*. <https://doi.org/10.3389/fpls.2019.00077>
- (7) Arruda, M. A. Z.; da Silva, A. B. S.; Kato, L. S. There is Plenty of Room in Plant Science: Nanobiotechnology as an Emerging Area Applied to Somatic Embryogenesis. *J. Agric. Food Chem.* **2023**, *71*, 3651–3657. <https://doi.org/10.1021/acs.jafc.2c08065>
- (8) Thapa, S.; Bhandari, A.; Ghimire, R.; Xue, Q.; Kidwaro, F.; Ghatrehsamani, S.; Maharjan, B.; Goodwin, M. Managing Micronutrients for Improving Soil Fertility, Health, and Soybean Yield. *Sustainability* (Switzerland) **2021**, *13*. <https://doi.org/10.3390/su132111766>
- (9) Bagale, S. Nutrient Management for Soybean Crops. *Int. J. Agron.* **2021**, *2021* (1). <https://doi.org/10.1155/2021/3304634>
- (10) Bradley, M.; Brown, P.; Cakmak, I.; Rengel, Z.; Zhao, F. Function of Nutrients: Micronutrients. In: Marschner, P. (Ed.). *Marschner's Mineral Nutrition of Higher Plants* (3<sup>rd</sup> Ed.). Academic Press, 2012. Chapter 7, pp 191-248. <https://doi.org/10.1016/B978-0-12-384905-2.00007-8>
- (11) Jatav, H. S., Sharma, L. D., Sadhukhan, R., Singh, S. K., Singh, S., Rajput, V. D. An overview of micronutrients: prospects and implication in crop production. In: Aftab, T.; Hakeem, K. R. (Eds.). *Plant Micronutrients: Deficiency and Toxicity Management*. Springer Cham, 2020, pp 1-30. [https://doi.org/10.1007/978-3-030-49856-6\\_1](https://doi.org/10.1007/978-3-030-49856-6_1)
- (12) Bizzi, C. A.; Pedrotti, M. F.; Silva, J. S.; Barin, J. S.; Nóbrega, J. A.; Flores, E. M. M. Microwave-Assisted Digestion Methods: Towards Greener Approaches for Plasma-Based Analytical Techniques. *J. Anal. At. Spectrom.* **2017**, *32*, 1448–1466. <https://doi.org/10.1039/c7ja00108h>
- (13) Chen, W.; Yang, Y.; Fu, K.; Zhang, D.; Wang, Z. Progress in ICP-MS Analysis of Minerals and Heavy Metals in Traditional Medicine. *Front. Pharmacol.* **2022**, *13*. <https://doi.org/10.3389/fphar.2022.891273>.
- (14) Ahmad, R.; Shaaban, H.; Issa, S. Y.; Alsaad, A.; Alghamdi, M.; Hamid, N.; Osama, R.; Algarni, S.; Mostafa, A.; Alqarni, A. M.; Aldholmi, M.; Riaz, M. ICP-MS Determination of Elemental Abundance in Traditional Medicinal Plants Commonly Used in the Kingdom of Saudi Arabia. *Food Addit. Contam.: Part B* **2022**, *15* (2), 129–141. <https://doi.org/10.1080/19393210.2022.2053591>
- (15) Varhan Oral, E.; Tokul-Ölmez, Ö.; Yener, İ.; Firat, M.; Tunay, Z.; Terzioğlu, P.; Aydin, F.; Öztürk, M.; Ertaş, A. Trace Elemental Analysis of Allium Species by Inductively Coupled Plasma-Mass Spectrometry (ICP-MS) with Multivariate Chemometrics. *Anal. Lett.* **2019**, *52* (2), 320–336. <https://doi.org/10.1080/00032719.2018.1460376>
- (16) Damak, F.; Asano, M.; Baba, K.; Ksibi, M.; Tamura, K. Comparison of Sample Preparation Methods for Multielements Analysis of Olive Oil by Icp-Ms. *Methods and Protoc.* **2019**, *2* (3), 1–14. <https://doi.org/10.3390/mps2030072>
- (17) Shi, M.; Zheng, X.; Zhang, N.; Guo, Y.; Liu, M.; Yin, L. Overview of Sixteen Green Analytical Chemistry Metrics for Evaluation of the Greenness of Analytical Methods. *TrAC, Trends Anal. Chem.* **2023**, *166*. <https://doi.org/10.1016/j.trac.2023.117211>
- (18) Wojnowski, W.; Tobiszewski, M.; Pena-Pereira, F.; Psillakis, E. AGREEprep – Analytical Greenness Metric for Sample Preparation. *TrAC, Trends Anal. Chem.* **2022**, *149*. <https://doi.org/10.1016/j.trac.2022.116553>
- (19) Silva, A. B. S.; da Silva Leal, K. N.; Arruda, M. A. Z. An Acidless Microwave-Assisted Wet Digestion of Biological Samples as a Greener Alternative: Applications from COVID-19 Monitoring to Plant Nanobiotechnology. *Anal. Bioanal. Chem.* **2024**. <https://doi.org/10.1007/s00216-024-05472-w>
- (20) Silva, A. B. S.; Arruda, M. A. Z. Exploring Single-Particle ICP-MS as an Important Tool for the Characterization and Quantification of Silver Nanoparticles in a Soybean Cell Culture. *Spectrochim. Acta, Part B* **2023**, *203*. <https://doi.org/10.1016/j.sab.2023.106663>

- (21) Flores, E. M. M.; Saidelles, A. P. F.; Barin, J. S.; Mortari, S. R.; Martins, A. F. Hair Sample Decomposition Using Polypropylene Vials for Determination of Arsenic by Hydride Generation Atomic Absorption Spectrometry. *J. Anal. At. Spectrom.* **2001**, 16 (12), 1419–1423. <https://doi.org/10.1039/b107910g>
- (22) Santa Cruz, E. C.; Madrid, K. C.; Arruda, M. A. Z.; Sussulini, A. Association between Trace Elements in Serum from Bipolar Disorder and Schizophrenia Patients Considering Treatment Effects. *J. Trace Elem. Med. Biol.* **2020**, 59. <https://doi.org/10.1016/j.jtemb.2020.126467>
- (23) da Costa, L.; Arruda, M. A. Simultaneous Hydride Generation Inductively Coupled Plasma Mass Spectrometry for the Evaluation of Different Generations of Soybean Seeds. *Braz. J. Anal. Chem.* **2023**, 10 (39), 113-123. <https://doi.org/10.30744/brjac.2179-3425.ar-135-2022>
- (24) Hänsch, R.; Mendel, R. R. Physiological Functions of Mineral Micronutrients (Cu, Zn, Mn, Fe, Ni, Mo, B, Cl). *Curr. Opin. Plant Biol.* **2009**, 12, 259–266. <https://doi.org/10.1016/j.pbi.2009.05.006>
- (25) Tejada-Jiménez, M.; Chamizo-Ampudia, A.; Galván, A.; Fernández, E.; Llamas, Á. Molybdenum Metabolism in Plants. *Metallomics* **2013**, 5, 1191–1203. <https://doi.org/10.1039/c3mt00078h>
- (26) Lal, M. A.; Bhatla, S. C. Sulfur, Phosphorus, and Iron Metabolism. In: Bhatla, S. C.; Lal, M. A. *Plant Physiology, Development and Metabolism* (2<sup>nd</sup> ed.). Springer, Singapore, 2023, pp 351 – 357. [https://doi.org/10.1007/978-981-99-5736-1\\_12](https://doi.org/10.1007/978-981-99-5736-1_12)
- (27) Alejandro, S.; Höller, S.; Meier, B.; Peiter, E. Manganese in Plants: From Acquisition to Subcellular Allocation. *Front. Plant Sci.* **2020**, 11. <https://doi.org/10.3389/fpls.2020.00300>
- (28) Kaur, H.; Garg, N. Zinc Toxicity in Plants: A Review. *Planta* **2021**, 253, 129. <https://doi.org/10.1007/s00425-021-03642-z>
- (29) Costa, L. M.; Silva, F. V.; Gouveia, S. T.; Nogueira, A. R. A.; Nóbrega, J. A. Focused Microwave-Assisted Acid Digestion of Oils: An Evaluation of the Residual Carbon Content. *Spectrochim. Acta, Part B* **2001**, 56 (10), 1981–1985. [https://doi.org/10.1016/S0584-8547\(01\)00308-1](https://doi.org/10.1016/S0584-8547(01)00308-1)
- (30) Kwon, S. Y.; Kim, Y. I.; Kim, Y. K.; Lee, Y. B.; Mok, J. H. Microwave-Assisted Sample Preparation for Screening of Heavy Metal Elements in Food Additives by ICP-MS. *LWT* **2024**, 208. <https://doi.org/10.1016/j.lwt.2024.116708>
- (31) Gonzalez, M. H.; Souza, G. B.; Oliveira, R. V.; Forato, L. A.; Nóbrega, J. A.; Nogueira, A. R. A. Microwave-Assisted Digestion Procedures for Biological Samples with Diluted Nitric Acid: Identification of Reaction Products. *Talanta* **2009**, 79 (2), 396–401. <https://doi.org/10.1016/j.talanta.2009.04.001>
- (32) Bizzi, C. A.; Flores, E. M. M.; Barin, J. S.; Garcia, E. E.; Nóbrega, J. A. Understanding the Process of Microwave-Assisted Digestion Combining Diluted Nitric Acid and Oxygen as Auxiliary Reagent. *Microchem. J.* **2011**, 99 (2), 193–196. <https://doi.org/10.1016/j.microc.2011.05.002>
- (33) Brancalion, M. L.; Zezzi Arruda, M. A. Evaluation of Medicinal Plant Decomposition Efficiency Using Microwave Ovens and Mini-Vials for Cd Determination by TS-FF-AAS. *Microchim. Acta* **2005**, 150, 283–290. <https://doi.org/10.1007/s00604-005-0357-0>
- (34) Gamela, R. R.; Costa, V. C.; Pereira-Filho, E. R. Multivariate Optimization of Ultrasound-Assisted Extraction Procedure for the Determination of Ca, Fe, K, Mg, Mn, P, and Zn in Pepper Samples by ICP OES. *Food Analytical Methods* **2020**, 13 (1), 69–77. <https://doi.org/10.1007/s12161-019-01524-5>
- (35) Coelho, T. L. S.; Silva, D. S. N.; Filho, L. B. de S.; Rocha, J. M.; de Higuera, J. M.; de Sá, I. P.; Gamela, R. R.; Nogueira, A. R. de A.; Lopes Júnior, C. A.; Vieira, E. C. High Enhancement of Macro and Micronutrients Quantification in Cajuína by ICP OES Using Ultrasound and Multivariate Analysis. *Food Chemistry Advances* **2023**, 2. <https://doi.org/10.1016/j.focha.2023.100265>
- (36) De La Calle, I.; Costas, M.; Cabaleiro, N.; Lavilla, I.; Bendicho, C. Use of High-Intensity Sonication for Pre-Treatment of Biological Tissues Prior to Multielemental Analysis by Total Reflection X-Ray Fluorescence Spectrometry. *Spectrochim. Acta, Part B* **2012**, 67, 43–49. <https://doi.org/10.1016/j.sab.2011.12.007>
- (37) Manjusha, R.; Shekhar, R.; Kumar, S. J. Ultrasound-Assisted Extraction of Pb, Cd, Cr, Mn, Fe, Cu, Zn from Edible Oils with Tetramethylammonium Hydroxide and EDTA Followed by Determination Using Graphite Furnace Atomic Absorption Spectrometer. *Food Chem.* **2019**, 294, 384–389. <https://doi.org/10.1016/j.foodchem.2019.04.104>

## FEATURE

# 48<sup>th</sup> RASBQ 2025: Brazilian Chemistry's Stage for Innovation and Collaboration

From June 8 to 11, 2025, Campinas, São Paulo, hosted the 48<sup>th</sup> Annual Meeting of the Brazilian Chemical Society (RASBQ), the largest chemistry event in Latin America. Held at Expo Dom Pedro, the event welcomed approximately 2,500 participants, including researchers, students, and professionals in the field, under the central theme: "Climate Emergencies? Chemistry Acts and Reacts."



Opening session of the 48<sup>th</sup> RASBQ - Photo: SBQ 2025

The program featured over 90 activities and 100 speakers across symposia, workshops, mini-courses, breakout sessions, and panels. Highlights included 140 oral presentations, 1,650 posters, and interactive activities through the SBQ in School program, which engaged approximately 500 high school students.

For the first time, the registration process collected data on gender, race/ethnicity, and specific needs, helping to increase the diversity of the presentations. Expo Dom Pedro's infrastructure also stood out, offering full accessibility, a baby changing room, a quiet room for neurodivergent individuals, kids' areas, and sign language interpretation for parts of the program.





One of the Poster Sessions – Photo: SBQ 2025

The event also included technical visits to the National Center for Research in Energy and Materials (CNPEM), highlighting laboratories such as the Brazilian Nanotechnology Laboratory (LNNano) and the Brazilian Synchrotron Light Laboratory (LNLS). Key topics addressed included green chemistry, microplastics, chemical safety, innovation, and intellectual property.

The meeting received financial support from CAPES, UNICAMP, CNPQ, OPCW, and sponsors such as the Federal Council of Chemistry, American Chemical Society, Horiba, Shimadzu, Agilent, Analytik Jena, AUTEC, CNPEM, dPUnion, Laborglass, Malvern Panalytical, Royal Society of Chemistry, Waters, and Tescan. Attendees also visited exhibitor booths from companies like Nova Analítica, Metrohm, PerkinElmer, Jasco, and others.



Exhibitors' area – Photo: SBQ 2025



## Awards and Tribute Session

The SBQ awards aim to recognize and encourage outstanding contributions to chemistry in Brazil. This year's honorees included:

### *Simon Matias Medal*

Awarded to individuals who have made significant contributions to the development of chemistry in Brazil and to the Brazilian Chemical Society. The honorees at this event were: Prof. Dr. Boaventura Freire dos Reis (CENA-USP), Prof. Dr. Maria Eunice Ribeiro Marcondes (IQ-USP), and Prof. Dr. Marian Rosaly Davolos (IQAr -UNESP).

### *Vanderlan da Silva Bolzani Award*

Recognizes women who have excelled in advancing chemistry in Brazil and/or strengthening the SBQ. Awarded biannually. The honorees at this event were: Prof. Dr. Marília Oliveira Fonseca Goulart. (UFAL) and Prof. Dr. Ana Paula de Carvalho Teixeira (UFMG).

### *Hans Viertler Award*

Given biennially to SBQ members under 35 who have distinguished themselves in scientific and/or technological research in the previous year. The honoree at this event was: Prof. Dr. Leandro Wang Hantao (UNICAMP).



Awardees and Honorees during the 48<sup>th</sup> RASBQ – Photo: SBQ 2025

### **Journal of the Brazilian Chemical Society (JBCS) Medal**

Honors individuals or institutions for their contributions to the creation, dissemination, consolidation, and scientific growth of the JBCS. The honoree at this event was: Prof. Dr. José Walkimar de Mesquita Carneiro (UFF).

### **“Química Nova” Award for Young Authors**

Awarded biennially to scientists under 40 who are current SBQ members and have published in “Química Nova” within the two years preceding the award. The honoree at this event was: Prof. Dr. Vagner Bezerra dos Santos (UFPE).

### **“Revista Virtual de Química” Award**

Awarded annually by the editors of the “Revista Virtual de Química” to researchers who have made significant contributions to the journal. The honoree at this event was: Prof. Dr. Norberto Peporine Lopes (FCFRP-USP).

### **Angelo da Cunha Pinto – Publications of the Brazilian Chemical Society (PubliSBQ) Award**

Awarded biennially to Brazilian individuals and/or institutions for excellence in scientific publishing across all fields. The honoree at this event was: Editora EDUSP (University of São Paulo Press).

### **Young Researcher Award – RSC-RASBQ 2025** (in partnership with the Royal Society of Chemistry)

- **Category 1** – Doctoral Student or Young Doctor: Luís Cláudio Martins (CENA-USP)
- **Category 2** – Early-Career Scientist: Beatriz dos Santos Cugnasca (IQ-USP)

### **Honorable mentions**

- **Category 1:** Marcelo Henrique Reis Carvalho (UFJF) and Naralyne Martins Pesqueira (UNESP)
- **Category 2:** Gabriel Toneto Druzian (UFSM) and Sthéphany Zaida Silva do Amparo (UFMG)

Additionally, the winners of the 8<sup>th</sup> SBQ-ACS “Brazilian Women in Chemistry” Award were announced, recognizing their leadership and achievements. The honorees at this event were:

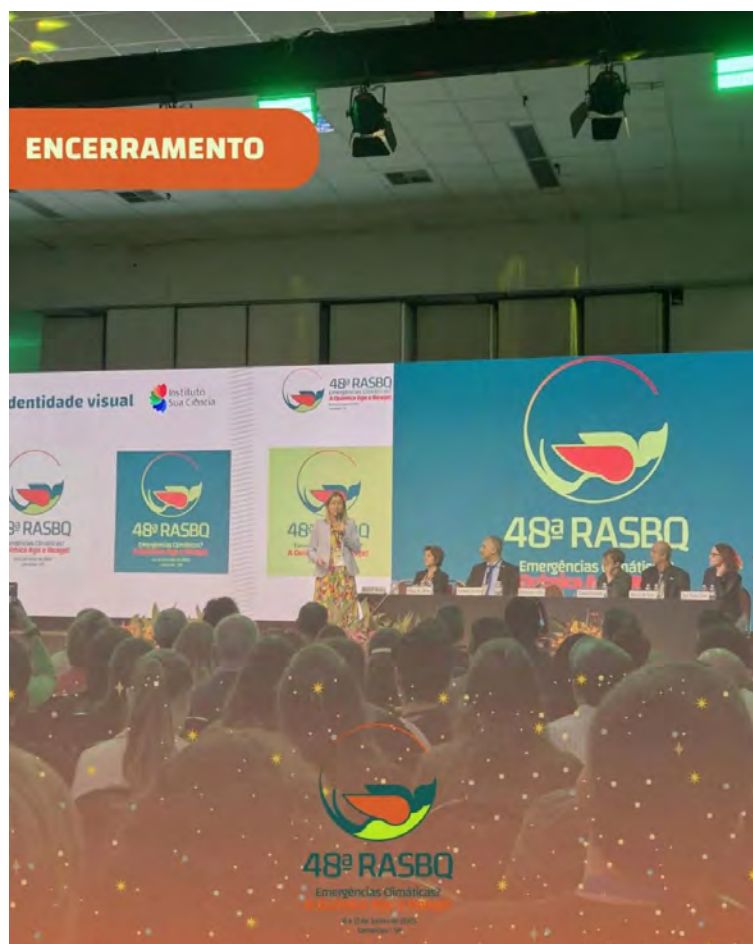
- **Emerging Leader:** Denise Brentan da Silva (Federal University of Mato Grosso do Sul)
- **Leadership in Academia:** Arlene Gonçalves Corrêa (Federal University of São Carlos)
- **Industry Leadership:** Fernanda de Oliveira Barreto Costa (Indorama Ventures)

The award ceremony took place on June 10, during the SBQ Women’s Center Symposium, where the winners shared their journeys and contributions to science in Brazil.

### **About the Brazilian Chemical Society (SBQ)**

The SBQ, organizer of this 48<sup>th</sup> Annual Meeting, is one of Brazil’s most important scientific societies, with strong international engagement. Its structure includes a dedicated volunteer Board of Directors and Advisory Board (14 members), a Fiscal Council (5 members), 13 Scientific Divisions (each with 3 members), 26 Regional Secretariats (each with 3 members), a Young Researchers Committee (3 members), a Women’s Center (3 members), and the newly established Inclusion and Diversity Center (3 members). Additionally, the SBQ has a dedicated secretarial team for event management, communications, and publishing (PubliSBQ).

Approaching its 50<sup>th</sup> anniversary, the SBQ was recently awarded the “Insígnia da Ordem do Rio Branco”, the highest honor from Brazil’s Ministry of Foreign Affairs, in a ceremony held on May 27, 2025, in Brasília.



**Closing Session – Photo: SBQ 2025**

The 48<sup>th</sup> RASBQ 2025 firmly established itself as a vital platform for knowledge exchange, strengthening the scientific community, and developing strategies to address global environmental challenges.

Text: Lilian Freitas

Source: SBQ - <https://www.s bq.org.br/48ra/>

## SPONSOR REPORT

PDF

This section is dedicated for sponsor responsibility articles.

# Impurity analysis of gabapentin by HPLC-UV-CAD

Ruben Pawellek, Adrian Leistner, Ulrike Holzgrabe

*Institute of Pharmacy, University of Wuerzburg, Germany*

This report was extracted from the Thermo Scientific Customer Application Note 74011

**Keywords:** Gabapentin, impurity analysis, Vanquish Horizon Charged Aerosol Detector, Variable Wavelength Detector

### Application benefits

- Simultaneous and sensitive detection of chromophore- deficient and volatile impurities with one single HPLC method instead of two separate methods, due to hyphenated detection techniques
- Shortened overall time of analysis and reduced consumption of consumables compared to two separate compendial methods
- Improved limits of quantitation (LOQs) for the chromophore-deficient impurities in accordance with the compendial requirements

### Goal

This application aims to replace the two separate compendial methods for the impurity analysis of gabapentin employed in the European Pharmacopoeia (Ph. Eur.) with one single HPLC method with hyphenated ultraviolet and charged aerosol detectors (UV-CAD). The complementary hyphenated detection techniques will enable the simultaneous detection of analytes with divergent physico-chemical properties. The UV-CAD method meets the required LOQs for a compendial application.

## INTRODUCTION

Gabapentin is commonly used for the treatment of focal seizures and, more recently, neuropathic pain. As its dosage may exceed an average daily intake of 2 g, regulatory authorities, such as the International Council on Harmonisation (ICH), impose strict requirements on the quality control of the drug by demanding a reporting threshold of 0.03% with respect to the concentration of main substance for possible impurities.<sup>1</sup> The requested limits of quantitation (LOQs) cannot be accomplished when applying the routinely used HPLC-UV procedure, as gabapentin and some of its impurities are chromophore- deficient substances (Figure 1). Chromophore-deficient substances lack UV-absorbing structural elements, such as an aromatic ring or conjugated double bonds.

The impurity profile of gabapentin entirely consists of compounds with saturated ring systems. Thus, the UV absorbance of the impurities, except for impurities A and D, is negligible. Quantitation of the impurities in the gabapentin monograph of the Ph. Eur. is accomplished by two separate HPLC-UV methods.<sup>2</sup> The compendial reporting threshold for possible impurities is therefore restricted to 0.05%, which contradicts the ICH directive.

The hyphenation of ultraviolet and charged aerosol detectors offers a solution to the challenging impurity profiling of gabapentin, since the complementary detection techniques enable the quantitation of all putative impurities with one single method at the required LOQs.

In this application, we report a HPLC-UV-CAD method for the impurity analysis of gabapentin that allows simultaneous determination of the volatile impurity A and the chromophore-deficient impurities B, D, E, and G in one single chromatographic run at a quantitation limit of at least 0.03%.<sup>3</sup> Consequently, overall analysis time and costs are effectively reduced compared to the two separate compendial methods.

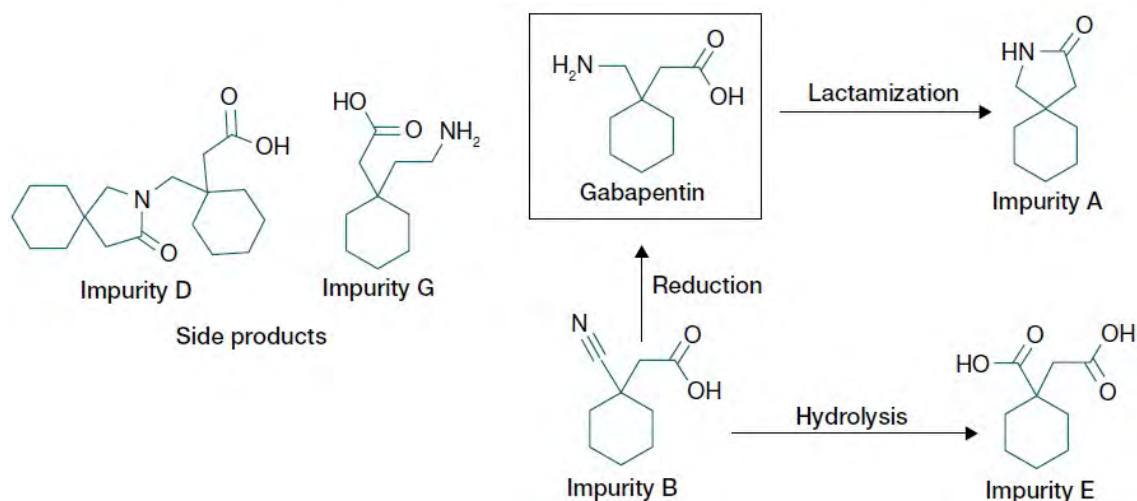


Figure 1. Impurity profile of gabapentin with respect to the Ph. Eur. 10.3.<sup>2</sup>

## EXPERIMENTAL DETAILS

### Chemicals

- Deionized water, 18.2 MΩ·cm resistivity or higher
- Fisher Scientific™ Acetonitrile, Optima™ LC/MS grade (ACN) (P/N A955-212)
- Fisher Scientific™ Ammonium formate, Optima™ LC/MS grade (P/N A11550)
- Fisher Scientific™ Formic acid, Optima™ LC/MS grade (P/N A117-50)
- Gabapentin and impurities A, B, D, E, G were purchased from a reputable vendor

### Sample handling

- Fisher Scientific™ Fisherbrand™ Mini Vortex Mixer (P/N 14-955-152)
- Vials (amber, 2 mL), Fisher Scientific (P/N 03-391-6)
- Cap with Septum (Silicone/PTFE), Fisher Scientific (P/N 13-622-292)

### Sample preparation

Stock solutions of the impurities A, E, and G were prepared by accurately weighing 10 mg of the respective impurity and dissolving it in 10.0 mL deionized water. Stock solutions of the impurities B and D were prepared accordingly, except for dissolution in methanol. The stock solutions were used for preparing the calibration standards and for spiking of the sample solutions by appropriate dilution with mobile phase A. The stock solutions were stored at 8 °C (-20 °C for impurity B) and were stable for at least one week.

Sample solutions were freshly prepared daily by weighing 80 mg of gabapentin and dissolving in 10.0 mL mobile phase A. The sample solutions were stable for at least one day at room temperature.

### Instrumentation

Thermo Scientific™ Vanquish™ Flex Binary UHPLC system consisting of:

- Vanquish System Base (P/N VF-S01-A-02)
- Vanquish Binary Pump F (P/N VF-P10-A)
- Vanquish Split Sampler HT (P/N VH-A10-A)
- Vanquish Column Compartment H (P/N VH-C10-A-02)
- Vanquish Variable Wavelength Detector F (P/N VF-D40-A)
- Standard flow cell, biocompatible, 11 µL (P/N 6077.0200)
- Vanquish Charged Aerosol Detector H (P/N VH-D20-A)



**Gabapentin method****Table 1. Chromatographic conditions**

Parameter	Value
Column	Agilent™ Zorbax™-SB C8 (250 × 4.6 mm, 5 µm)
Mobile phase	A: 20 mM Ammonium formate pH 2.8 in water B: 20 mM Ammonium formate pH 2.8 in water/ACN 10/90 (v/v)
Gradient	Time (min)      %B
	0–1                25
	1–5                25–60
	5–11              60
	11–12            60–25
	12–15            25
Run time	15 min
Flow rate	1.2 mL/min
Column temperature	25 °C (still air mode)
Autosampler temperature	8 °C
Autosampler wash solvent	Methanol
Injection volume	20 µL
Detector settings (CAD)	Evaporation temperature: 30 °C Power function value: 1.3 Filter constant: 5 s Data collection rate: 10 Hz
Detector settings (UV)	Detection wavelength: 210 nm Data collection rate: 20 Hz Response time: 0.20 s

**Chromatography Data System**

The Thermo Scientific™ Chromeleon™ Chromatography Data system (CDS), version 7.2.6 was used for data acquisition and analysis.

**RESULTS AND DISCUSSION****Method development**

The polarity of the zwitterionic  $\gamma$ -aminobutyric acid derivative gabapentin is higher compared to its increasingly alkyl-substituted impurities (Figure 1). Since all analytes share a cyclohexyl group as part of their molecular structure, they can be separated by reversed-phase (RP)-HPLC. Stationary phases of moderate hydrophobicity, such as C8, phenyl, or biphenyl, represent a good compromise for the separation of gabapentin and its medium hydrophobic impurities when applying reversed-phase RP-HPLC. Various C8 and phenyl columns were tested for their separation efficacy toward the analytes. A C8 column was selected for further method development that provided the best resolution for the critical peak pair of impurities B and A and, in addition, adequate peak shapes for all analytes. The pH of the ammonium formate buffer used in the method was adjusted with formic acid to 2.8 to suppress deprotonation of the acidic analytes, resulting in improved peak shapes and prolonged retention times of the latter. Using a 20 mM ammonium formate buffer pH 2.8 in a mixture of water/ACN resulted in sharp gaussian peak shapes for all analytes. To facilitate the elution of the most hydrophobic impurity D subsequent to the other analytes in one chromatographic run, a gradient program had to be applied. The flow rate of the pump was set at 1.2 mL/min resulting in

a relatively short run time of 15 min including re-equilibration time. The instrumental settings of the CAD were optimized toward sensitive detection of semi-volatile impurity B. Adjustment of the CAD's evaporation temperature (30 °C) and filter constant (5 s) settings enabled the accurate quantitation of semi-volatile impurity B at the required reporting threshold (0.03%).

### **UV-CAD detection**

As gabapentin itself and the impurities B, E, and G lack suitable chromophores in their structures, applying low wavelength UV detection <220 nm is not sufficient to compensate the structural deficits. A method solely based on UV detection suffers from poor sensitivity.

This issue can be overcome by employing a CAD for the determination of the chromophore-deficient impurities B, E, and G. However, a sensitive quantitation of impurity A is not possible with CAD due to the compound's relatively high volatility.

Hyphenation of UV and CAD is beneficial in this case, since impurity A can be detected by UV with sufficient sensitivity, while the remaining chromophore-deficient impurities are subsequently covered by CAD. The in-line coupling of the complementary detectors thereby enabled simultaneous quantitation of all putative impurities at the ICH claimed reporting threshold of 0.03% being equivalent to 50 ng on column injected mass. Excellent LOQs (<10 ng injected mass) were obtained for the non-volatile impurities, while the method was sufficiently sensitive toward the UV detected impurity A (50 ng) and the semi-volatile impurity B (50 ng) (Table 2).

### **Method validation**

The method was validated with respect to the requirements outlined in ICH guideline Q2(R1).<sup>4</sup> Specificity of the method was demonstrated by injection of a sample solution spiked with 0.1% of each impurity (Figure 2). The resolution was >1.5 for all peak pairs, proving adequate selectivity. Linearity was evaluated over a concentration range from 0.03 to 0.24%. Calibration curves for the impurities were established by linear regression of six equally distributed calibration levels. The coefficients of determination ( $R^2$ ) were >0.999 (Table 2) and the residual plots showed evenly scattered calibration points indicating a good quality of fit. Accuracy and precision were both evaluated on spiked sample solutions. The % recovery rates obtained from calculation by linear regression and the %RSD for intra- and inter-day repeatability are illustrated in Table 2. With recovery rates ranging from 97 to 105% and repeatability %RSD values ranging from 0.8 to 4.7% for the non-volatile impurities, the method can be considered as sufficiently accurate and precise for the intended purpose. The recovery rates (93–112%) as well as the repeatability %RSD (4.6–8.4%) were slightly increased for semi-volatile impurity B compared to the non-volatile analytes. However, the results were still within an acceptable range. The limits of detection (LOQs) of the method were calculated using the S/N approach of ICH guideline Q2(R1)<sup>4</sup> (Table 2). LOQs of ≤50 ng injected mass were achieved for the impurities, which enabled accurate quantitation at the required reporting threshold of 0.03%. For evaluation of the method's robustness, the resolution for each peak pair was monitored against small variations of flow rate (1.1–1.3 mL/min), temperature of the column chamber (20–30 °C), initial % of mobile phase B (23–27%), and final % of mobile phase B (60–62%). The method can be regarded as robust against these small changes.

### **UV-CAD method vs. compendial procedures**

The most evident benefit of the UV-CAD method over the two separate compendial methods employed in the Ph. Eur.<sup>2</sup> is the improved sensitivity for the chromophore-deficient analytes. Sample concentration was reduced from 14 mg/mL in the compendial method to 8 mg/mL in the UV-CAD methods, accompanied with a lowered reporting threshold. Consequently, the general reporting threshold for the impurities can be reduced from 0.05 to 0.03% to comply with the requirements of ICH guideline Q3A (R2)<sup>1</sup> for drugs with an average daily intake >2 g. Moreover, combining two separate methods with a respective run time of 15 min to one single method with just 15 min run time substantially shortens the overall analysis time and reduces the number of required consumables and instrumentation.

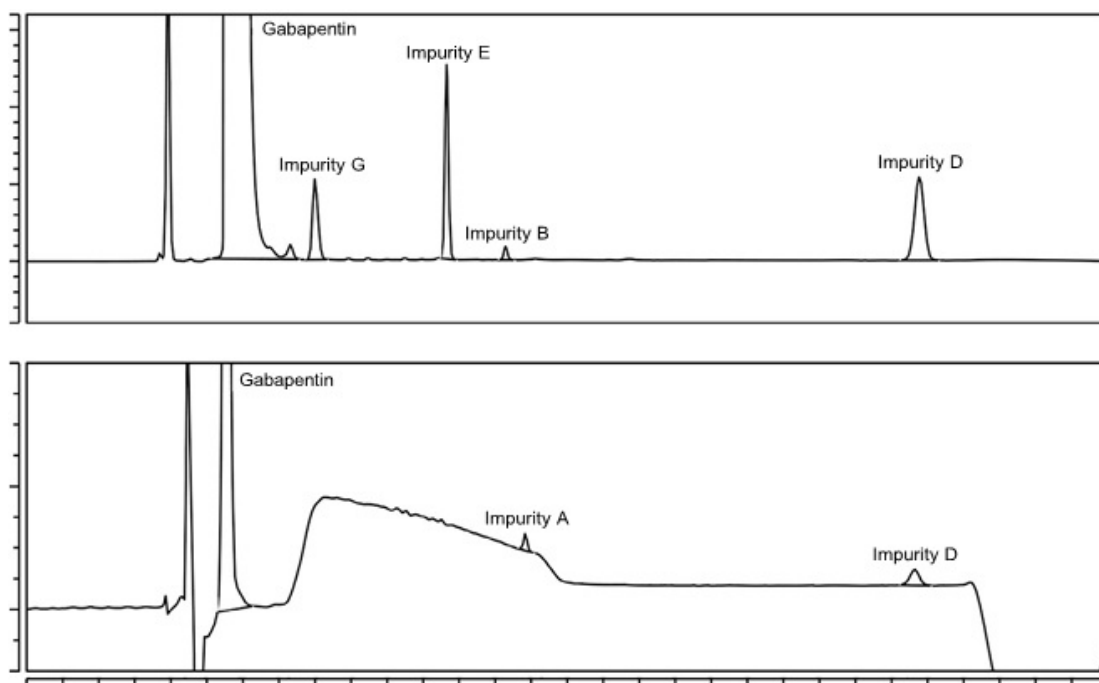


**Figure 2.** Chromatograms of the CAD (upper chromatogram) and UV signal for a gabapentin sample solution (8 mg/mL) spiked with 0.1% of each impurity.

**Table 2.** Validation results of the gabapentin method

Parameter	Condition/ concentration	Gabapentin	Impurity A <sup>a</sup>	Impurity B	Impurity D	Impurity E	Impurity G
Linearity	Equation <sup>b</sup> $y = mx + t$	$0.0017x - 0.0032$	$0.0064x - 0.0145$	$0.00017x - 0.0041$	$0.0024x - 0.0213$	$0.0021x - 0.0164$	$0.0013x - 0.0052$
	$R^2$	0.9995	0.9996	0.9993	0.9999	0.9995	0.9996
	SD slope [pA/ng]	$1.8 \times 10^{-5}$	$6.5 \times 10^{-5}$ <sup>a</sup>	$2.3 \times 10^{-6}$	$1.3 \times 10^{-5}$	$2.4 \times 10^{-5}$	$1.2 \times 10^{-5}$
	SD intercept [pA]	0.0048	0.018 <sup>a</sup>	0.00057	0.0034	0.0065	0.0033
Accuracy (% recovery rate)	0.03%, n=3	n.d. <sup>c</sup>	99	98	102	105	98
	0.10%, n=3	n.d.	n.d.	93	102	103	97
	0.20%, n=3	n.d.	n.d.	112	102	101	99
LOQ	Inject. mass (ng)	3	50	50	4	2	3
LOD	Inject. mass (ng)	1	n.d.	n.d.	2	1	1
Intraday precision	0.03%, n=6	n.d.	2.7 <sup>d</sup>	8.4	2.1	3.1	2.2
	0.10%, n=6	n.d.	1.3	7.7	1.2	1.6	1.6
	0.20%, n=6	n.d.	0.8	5.4	1.0	1.4	1.1
Interday precision	0.03%, n=2	n.d.	3.8	8.2	1.9	2.8	4.7
	0.10%, n=2	n.d.	1.1	6.0	1.2	2.0	2.4
	0.20%, n=2	n.d.	0.9	4.6	1.1	1.5	1.6

<sup>a</sup>Detected by UV, SD slope [mAu/ng], SD intercept [mAU]; <sup>b</sup>Obtained from linear regression of the 6 calibration points; <sup>c</sup>Not determined; <sup>d</sup>%RSD.

## CONCLUSION

A simple, rapid, and selective HPLC-UV-CAD method for the impurity profiling of gabapentin was developed. Hyphenation of UV and CAD enabled the simultaneous detection of volatile impurity A and the

chromophore-deficient impurities B, D, E, and G in one chromatographic run. Compared to the two separate compendial methods employed in the Ph. Eur., the reporting threshold was improved, besides time and costs savings by reducing the mobile phase and column consumption.

## REFERENCES

- (1) International Council for Harmonisation, Guideline Q3A (R2) Impurities in New Drug Products, 2006. <https://database.ich.org/sites/default/files/Q3A%28R2%29%20Guideline.pdf>
- (2) Council of Europe, European Pharmacopoeia Online 10.2, EDQM, Strasbourg, France, 2020, Monograph no. 2173. Available from: <https://pheur.edqm.eu/app/10-3/content/10-3/2173E.htm?highlight=on&terms=gabapentin>
- (3) Pawellek, R.; Muellner, T.; Gamache, P.; Holzgrabe, U. Power function setting in charged aerosol detection for the linearization of detector response – optimization strategies and their application, *J. Chromatogr. A* 2021, 1637, 461844.
- (4) International Council for Harmonisation, Guideline Q2 (R1) Validation of Analytical Procedures: Text and Methodology, 2005. <https://database.ich.org/sites/default/files/Q2%28R1%29%20Guideline.pdf>

Find out more at [thermofisher.com/CAD](https://thermofisher.com/CAD)

*This Sponsor Report is the responsibility of Thermo Fisher Scientific.*

**For research use only.** © 2021 Thermo Fisher Scientific Inc. Agilent and ZORBAX are trademarks of Agilent Technologies, Inc. All other trademarks are the property of Thermo Fisher Scientific and its subsidiaries. This information is presented as an example of the capabilities of Thermo Fisher Scientific Inc. products. It is not intended to encourage use of these products in any manners that might infringe the intellectual property rights of others. Specifications, terms and pricing are subject to change. Not all products are available in all countries. Please consult your local sales representative for details. **CAN74011-EN 0321S**



## SPONSOR REPORT

PDF

This section is dedicated for sponsor responsibility articles.

# A streamlined laboratory workflow for the analysis of common contaminants according to the U.S. EPA 8270E and 8081B methods using GC-MS/MS

Sarah Crumlett<sup>1</sup>, Mark Belmont<sup>1</sup>, Terry Jeffers<sup>1</sup>, Adam Ladak<sup>2</sup>, Giulia Riccardino<sup>3</sup>, and Daniel Kutscher<sup>4</sup>

<sup>1</sup>Thermo Fisher Scientific, Bannockburn, IL, USA

<sup>2</sup>Thermo Fisher Scientific, Hemel Hempstead, UK

<sup>3</sup>Thermo Fisher Scientific, Milan, IT

<sup>4</sup>Thermo Fisher Scientific, Bremen, DE

This report was extracted from the Thermo Scientific Application Note 003362

**Keywords:** U.S. EPA, semivolatile compounds, pesticides, polycyclic aromatic hydrocarbons (PAHs), U.S. EPA 8270E, U.S. EPA 8081B, gas chromatography, triple quadrupole mass spectrometry, TSQ 9610 mass spectrometer, TriPlus RSH Smart AS, method consolidation

**Goal:** The goal of this application note is to demonstrate a modernized workflow for the analysis of semivolatile compounds (SVOCs) and pesticide residues according to EPA 8270E<sup>1</sup> and EPA 8081B<sup>2</sup> methods using a single instrument platform based on gas chromatography coupled to triple quadrupole mass spectrometry (GC-MS/MS). This method could also be expanded to include similar environmental methods, providing users with a simplified analysis workflow that can be applied across a variety of application areas to simplify adoption in high-throughput environmental laboratories.

## INTRODUCTION

Analytical testing laboratories dealing with environmental analysis must monitor diverse compound classes (SVOCs, pesticides, PCBs, etc.) in multiple matrices (drinking water, surface water, wastewater, soils, sludges) often requiring different instrument configurations and settings. This poses some challenges in terms of reduced productivity and sample throughput as well as increased time and costs for multiple platform maintenance, dedicated consumable usage, as well as staff training. Moreover, staff turnover or reduced laboratory personnel requires analysts to run multiple instrumentation and methods, adding unneeded complexity to their daily work.

Many U.S. EPA methods for environmental analysis recommend the use of gas chromatography coupled to analog detectors such as electron capture detection (ECD),<sup>1</sup> nitrogen phosphorous detection (NPD),<sup>2</sup> and photometric detection (FPD)<sup>3</sup> because they provide a very specific detection for certain functional classes (e.g., organochlorine or organophosphorus pesticides). Despite their high specificity, extensive sample preparation and adequate chromatographic separation are required to differentiate between the target compounds and other co-eluting compounds or matrix interferences. This can result in sample reanalysis using alternative columns and conditions to confirm results. These reruns are often run by mass spectrometry to provide better identification and confirmations. A more effective approach is the use of triple quadrupole mass spectrometry (MS/MS). The selected reaction monitoring (SRM) acquisition mode provides greater selectivity compared to single ion monitoring, allowing for simplified sample preparation protocols. Hundreds

of analytes can be monitored within a single chromatographic run as typical ion transitions are monitored for each compound. This allows for confident identification of analytes at sub-ppb level sensitivities even without full chromatographic resolution between compounds. Furthermore, timed-SRM mode (t-SRM) allows the operator to process a specific method's list of target analytes, set an acquisition window around each elution time, and subsequently optimize the mass spectrometers dwell time, leading not only to simpler data with smaller file sizes, but also better sensitivity. The adoption of such a platform that can be used for multiple analytical methods would improve laboratories' sample throughput and productivity while reducing the cost of spare parts inventory and instrument management, streamlining operations.

In this study, the same Thermo Scientific™ TSQ™ 9610 GC-MS/MS system configuration was used for analysis of SVOCs and organochlorine pesticides according to the EPA 8270E and EPA 8081B methods. Overall method performance, including linearity, sensitivity, and precision, were evaluated thoroughly for use in a working water testing laboratory.

Key hardware and software for method modernization As part of workflow modernization and cost reduction, many laboratories investigate automation of the sample preparation procedures to promote a safer work environment (reducing the analyst's exposure to toxic chemicals) and save analyst's valuable time, improve data quality, and reduce possible errors, cross-contamination, and waste. The Thermo Scientific™ TriPlus™ RSH Smart autosampler<sup>4</sup> combines highly versatile sample injection capability (liquid, headspace, and solid-phase microextraction (SPME)) with automated sample preparation procedures, eliminating typical GC-MS workflow bottlenecks. Daily operations such as dilutions, standard curve generation, and derivatization up to more complex, multi-step sample preparation protocols can be fully automated leading to substantial cost savings, while gaining efficiency and productivity from system's unattended operations.

Containing costs does not mean that laboratories must give up flexibility and advances in technology. The Thermo Scientific™ TRACE™ 1610 series GC,<sup>5</sup> the only GC with a user-installable modular concept, is designed to enhance the workflow experience through the use of interchangeable injector and detector modules that allow the analyst to easily modify the instrument configuration in minutes without special tools or training and simplify troubleshooting operations without the need for service calls. The GC's advanced multi-functional touch screen with instrument health monitoring of common

maintenance items such as inlet liner or septum changes (among many others) can help avoid unplanned downtime through user-settable alerts on consumables usage and maintenance. The TSQ 9610 GC-MS/MS<sup>6</sup> system using NeverVent™ technology allows for column replacement and ion source cleaning without venting the mass spectrometer, increasing uptime. The ultra-sensitive, ultra-robust Thermo Scientific™ Advanced Electron Ionization™ (AEI) ion source combined with the Thermo Scientific™ XLXR™ electron multiplier detector provide class leading sensitivity and extended dynamic range enables method consolidation for analysis of low- and high-concentrated compounds in a single GC run.

Software is key for a streamlined workflow. The Thermo Scientific™ Chromeleon™ Chromatography Data System (CDS)<sup>7</sup> provides flexibility and scalability to control chromatography (GC, LC, and IC) instruments, as well as single and triple quadrupole mass spectrometers, and even HRAM mass spectrometry instruments like the Thermo Scientific™ Orbitrap Exploris™ GC mass spectrometer with one single software, all while meeting data integrity regulatory requirements of the U.S. Food and Drug Administration Title 21 Code of Federal Regulations Part 11 (21 CFR Part 11). Users can easily switch between instruments, platforms, and methods, managing all the analytical processes and data, from a variety of locations. From instrument control to raw data storage, processing, and generation of the results and approvals, Chromeleon CDS can seamlessly connect multiple sites and worldwide locations to a central data center with the same performance as a fully local operation

## EXPERIMENTAL

In all the experiments described here, a TSQ 9610 triple quadrupole mass spectrometer equipped with NeverVent AEI ion source was coupled to a TRACE 1610 gas chromatograph equipped with a Thermo Scientific™ iConnect™ split/splitless (iConnect-SSL) injector and a Thermo Scientific™ AI/AS 1610 liquid

autosampler. The same instrument configuration, chromatographic column, and consumables were used for assessing instrument compliance to EPA 8270E and EPA 8081B methods (Figure 1). A TriPlus RSH SMART autosampler was placed on the bench and used as an off-line sample preparation station for calibration curve dilution and internal standard addition. The use of an automated approach improved analyst's safety by reducing exposure to toxic chemicals such as dichloromethane (DCM).

Chromatographic separation was achieved on a Thermo Scientific™ TraceGOLD™ TG-5SilMS capillary column 30 m × 0.25 mm × 0.25 μm (with integrated 5 m SafeGuard column, P/N 26096-1425). The “-Sil” indicates silylarene groups are incorporated in the polymer backbone, ensuring improved thermal stability and reduced susceptibility to oxidation, resulting in low column bleed and outstanding inertness.

Additional GC-MS/MS and autosampler parameters as well as a complete list of the target compounds are detailed in Table 1 and [Appendix 1](#), respectively.

### **Data acquisition, processing and reporting**

Data was acquired, processed, and reported using the Chromeleon CDS, version 7.3.2. Integrated instrument control ensures full automation of the analytical workflow combined with an intuitive user interface for data analysis, processing, customizable reporting, and storage in compliance with 21 CFR Part 11. This integrated instrument control enables users to perform in-sequence tuning, and when combined with the scheduling capability of Chromeleon CDS, instruments can be checked automatically at a desired time, so that additional operator time can be saved and used for more productive purposes.

In addition, the Chromeleon Environmental Analysis Extension Pack for U.S. EPA-based environmental applications provides a comprehensive set of instrument methods, processing methods, and reports, designed for quick sequence set-up and reporting to allow rapid implementation of new instruments with ease.



**Figure 1. Unified environmental method schematic for analysis of multiple compound classes using a single analytical platform.**

**Table 1. GC-MS/MS and autosampler parameters applied for SVOCs and multi-residue analysis of pesticides according to EPA 8270E and EPA 8081B methods as well as parameters used for DFTPP, tailing and degradation performance verification as per EPA 8270E method**

AI/AS 1610 autosampler parameters		
Injection type	Standard	
Sample mode	Standard	
Fill strokes	6	
Air volume (µL)	1	
Sample depth	Bottom	
Injection mode	Fast	
Pre-injection wash cycles	0	
Pre-injection solvent wash volume (µL)	0	
Post-injection wash cycles	6	
Post-injection solvent wash volume (DCM, µL)	5	
Sample wash cycles	3	
Sample wash volume (µL)	1.5	
Injection volume (µL)	1	
Syringe	10 µL Fixed needle, gas tight syringe 26 Gauge, 50 mm, Cone tip, (P/N 365D2977)	
iConnect-SSL parameters		
	EPA 8081	EPA 8270 and DFTPP
Injection temperature (°C)	225	
Liner	For splitless injection: Thermo Scientific™ LinerGOLD™ Splitless liner, Single taper with quartz wool (P/N 453A1925-UI)	
Oven equilibration time (min)	0.2	
Inlet module and mode	SSL, split with surge	SSL, splitless with surge
Surge pressure (psi)	35	35
Surge duration (min)	0.8	0.8
Splitless time (min)	--	0.8
Split flow (mL/min)	--	60
Split ratio	5:1	--
Septum purge flow (mL/min)	Constant 5.0	

(continues on next page)

iConnect-SSL parameters		
	EPA 8081	EPA 8270 and DFTPP
Gas saver flow (mL/min)	5	5
Gas saver time (min)	5	5
Carrier gas, flow (mL/min)	Ramped, 1.2 mL/min hold 20 min 1.0 mL/min to 2.0 mL/min hold 9.20 min	Constant, 1.2

TRACE 1610 GC parameters		
	EPA 8081 / 8270	DFTPP
Oven temperature program		
Oven equilibration time (min)	0.2	0.2
Temperature (°C)	40	90
Hold time (min)	2	1
Rate (°C/min)	50	30
Temperature 2 (°C)	125	310
Rate (°C/min)	12	--
Temperature 3 (°C)	150	--
Rate (°C/min)	20	--
Temperature 4 (°C)	200	--
Rate (°C/min)	5	--
Temperature 5 (°C)	280	--
Rate (°C/min)	30	--
Temperature 6 (°C)	330	--
Hold time (min)	4.05	5
GC run time (min)	30	15
Column		
Trace GOLD TG-5SilMS with integrated 5 m SafeGuard	30 m, 0.25 mm, 0.25 µm (P/N 26096-1425)	

(continues on next page)



TSQ 9610 mass spectrometer parameters		
	EPA 8081 / 8270	DFTPP
Transfer line temperature (°C)	300	300
Ion source type and temperature (°C)	NeverVent AEI, 300	NeverVent AEI, 300
Ionization type	EI	EI
Acquisition mode	Timed SRM	Full Scan, 35–500
Filament delay (min)	--	3.5
Dwell or scan time (s)	--	0.0988
Tuning parameters	AEI Smart Tune	AEI Smart Tune
Collision gas and pressure (psi)	Argon at 70	Argon at 70
Minimum desired peak width (s)	3	--
Desired scans per peak	20	--
Set resolution for each unique transition	Enabled (see table in <a href="#">Appendix 1</a> for individual resolution)	--
Use last tune detector gain	X7	--
Use specified emission current (μA)	25	25

## RESULTS AND DISCUSSION

### ***EPA Method 8270E***

U.S. EPA Method 8270E is used to determine the concentration of semivolatile organic compounds, such as polycyclic aromatic hydrocarbons (PAHs), in many types of solid waste matrices, soils, air, and water samples by using gas chromatography coupled to mass spectrometry (GC-MS). One of the challenges of this method is that multiple analytes spanning wide concentration ranges must be analyzed in one single run, often leading to non-ideal calibration curves. The Thermo Scientific XLXR detector provides an extended dynamic range that allows laboratories to easily overcome this issue and provides wider calibration ranges, with better linearity, leading to more accurate and repeatable results. Moreover, since many diverse pesticides are listed in the EPA 8270E method, high selectivity is mandatory for a confident identification of compounds. The timed-selected reaction monitoring (t-SRM) acquisition mode allows for simultaneous acquisition of multiple characteristic ion transitions for each target analyte, maintaining high sensitivity combined with high selectivity to discriminate between the target compounds and matrix, thus ensuring a reliable and confident identification of analytes.

### ***Instrument performance verification: DFTPP tune, tailing, and degradation***

The EPA 8270E method provides a list of performance criteria that need to be assessed to check instrument suitability for sample analysis. A decafluorotriphenylphosphine (DFTPP) tune check standard is used to assess the instrument response in terms of spectral quality. Other test probes such as benzidine and pentachlorophenol are used to assess instrument inertness, specifically in the sample flow path, and yet more compounds like endrin and DDT breakdown products are used to assess sample degradation within the injector. Although not requested when analysis is performed using product ions for quantitation, a quality control sample containing all test analytes was injected at least once daily to ensure that the system

fulfilled all method requirements in terms of ion abundance, tailing, and degradation. The TSQ 9610 GC-MS/MS met all ion ratio performance criteria without requiring any adjustments of the default instrument tuning. Moreover, the high inertness of the GC flow path allowed the peak tailing and degradation evaluation criteria to be easily met. The Chromeleon CDS reporting capability allows for customized tune and breakdown reports, and the Chromeleon 7.3.2 Report Designer 2.0 features allow for quick and easy visual review of the performance tests by using conditional formatting with a Pass/Fail indicator as shown in Figure 2.

### **Chromatography**

Structural isomers are compounds having the same molecular formula but different physical arrangement of the atoms in space; therefore, they often elute very closely to each other in pairs. The EPA 8270E method requires calculations of chromatographic resolution for these “critical pairs” to ensure that the fundamental chromatographic separation is adequate for analysis so that, for example, analytical columns can be exchanged before degradation may affect data quality. Typically, if the peaks are separated by at least 50% resolution, they can be considered chromatographically separated. An example of typical chromatograms for a reference standard mix prepared in DCM at a concentration of 500 µg/L (ppb) is shown in Figure 3. The insets show some examples of critical pair resolution achieved for closely eluting isomers. Resolution was calculated as per the EPA method using the formula in Equation 1 and was  $\geq 50\%$ , thus meeting the method suitability requirements.

$$\text{Equation 1: } \text{Resolution} = 1 - [\text{valley height}] / [\text{average peak height}]$$

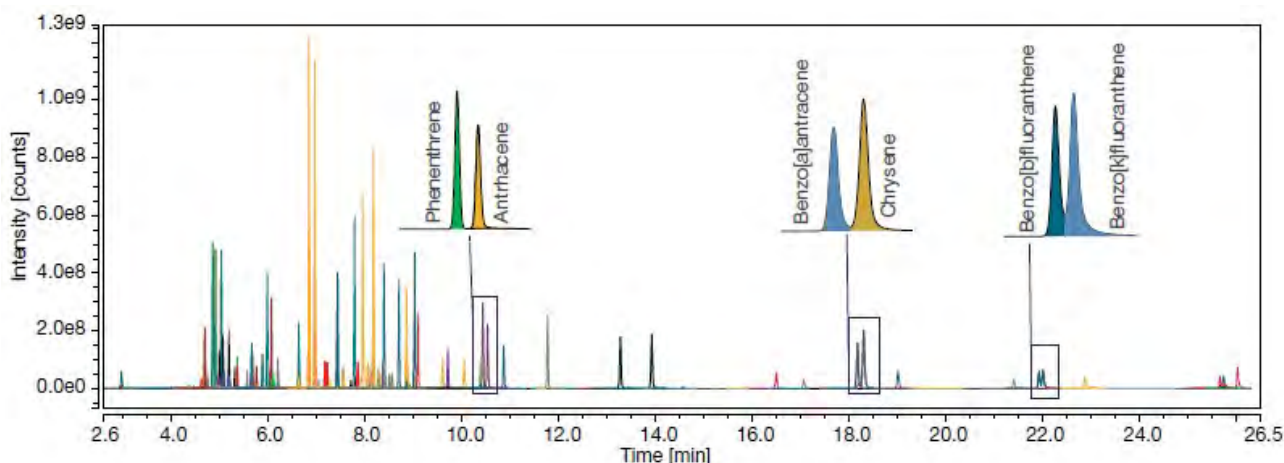
### **Linearity and detection limits**

Linearity and detection limits were assessed by preparing multiple calibration curves diluted in solvent (DCM) ranging from 0.5 µg/L to 250 µg/L. Linearity was determined using an internal standard method by calculating the relative standard deviation (RSD) of the response factor (RF) for each analyte and comparing the result to the limit specified in the EPA methods. All target analytes showed a linear trend with RF %RSD in agreement to the <20% limit specified in the method, thus confirming that a very wide linear range can be easily achieved with the XLXR detector. Full range calibration curves (0.5–250 µg/L) for some selected analytes and the quantifier and qualifier ions at 0.5 µg/L are reported as an example in Figure 4.

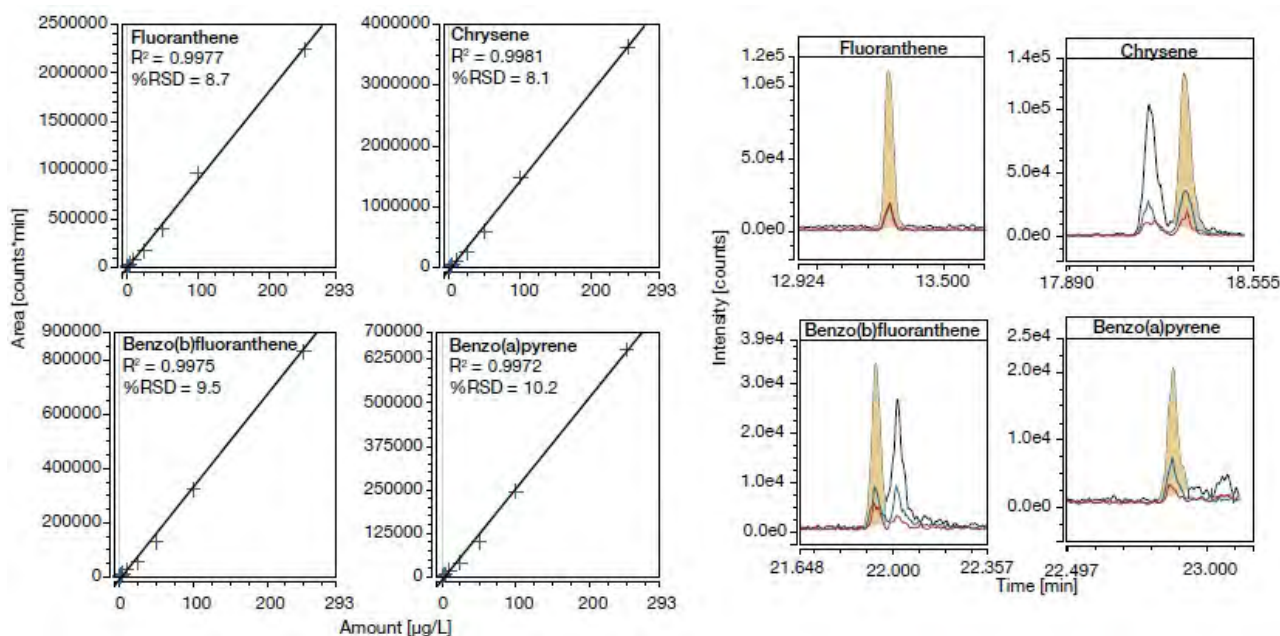
Method detection limits (MDLs) are firmly established with many regulatory bodies and can be defined in multiple ways. According to the most recent U.S. Code of Federal Regulations,<sup>8</sup> MDL is defined as: “the minimum concentration of a substance that can be measured and reported with 99% confidence that the analyte concentration is greater than zero and is determined from analysis of a sample in a given matrix containing the analyte.” This methodology can be seamlessly transferred when calculating instrument detection limits (IDLs). Unlike MDL, IDL uses solvent based standards containing the test chemical at concentrations that give a consistent response over several repeat injections.



Figure 2. Chromeleon CDS browser showing a customized report for an easy and quick review of the instrument performance criteria (DFTPP ion ratios, tailing, and degradation) results fulfilling the EPA 8270E method requirements.



**Figure 3.** Example of chromatography achieved for a solvent standard spiked at 500 µg/L. The insets show examples of resolution for some critical pairs in compliance with the EPA 8270E method.



**Figure 4.** Example of calibration curves prepared in DCM (range: 0.5–250 µg/L) for some selected target analytes as well as quantifier and qualifier ions at 0.5 µg/L. Coefficients of determination ( $R^2$ ) and RF %RSD are annotated.

Therefore, the IDL is a statistically rigorous method that uses the precision of a measurement at low analyte levels and accurately reflects the true detection limit of an instrument, ultimately defining how sensitive an analytical system is.<sup>9</sup> The IDL was determined for all the target compounds by preparing  $n=7$  solvent standard in DCM at 1 µg/L. IDLs were calculated using the Students t-test values for the corresponding  $n-1$  degrees of freedom at 99% confidence, the amount of analyte on column, and the absolute peak area %RSD for each analyte as per Equation 2.<sup>10</sup> MDL calculation reports are already available for Chromeleon CDS.



$$\text{Equation 2: } IDL = t * \text{Amount} * \%RSD$$

$t$  = Student  $t$ -value for one-tailed distribution

Amount = Amount of analyte (on-column)

%RSD = Relative standard deviation of the response

Calculated IDLs for selected compounds covering the entire volatility range are reported as an example in Figure 5. IDLs ranged from 5 to 45 µg/L with peak area RSD <10% for the majority of the target compounds. Details of the calculations are reported in [Appendix 2](#).

### EPA Method 8081B

U.S. EPA Method 8081B provides validated procedures for the determination of organochlorine pesticides (OCPs). OCPs are a group of synthetic chlorinated hydrocarbon derivatives, which were commonly used to protect crops, livestock, buildings, and households from the damaging effects of insects. OCPs have been banned in the United States and many other countries across the world because of their persistent presence in the environment and the threat they pose to food safety and animal health. EPA Method 8081B suggests the use of dual-column gas chromatography with electron capture detector (ECD) as this allows detection and measurement of electronegative chemical compounds (most notably halogens, organohalides, and nitrogen-containing compounds) with extremely high sensitivity. Despite the high sensitivity provided towards electronegative compounds, the ECD poses some concerns in terms of compound identification and laboratory safety and operations due to the use of a  $^{63}\text{Ni}$  radioactive source. Because of the complexity of an analog-style chromatographic separation, the second column is still needed to confirm IDs and discriminate between the target analytes and matrix interferences.

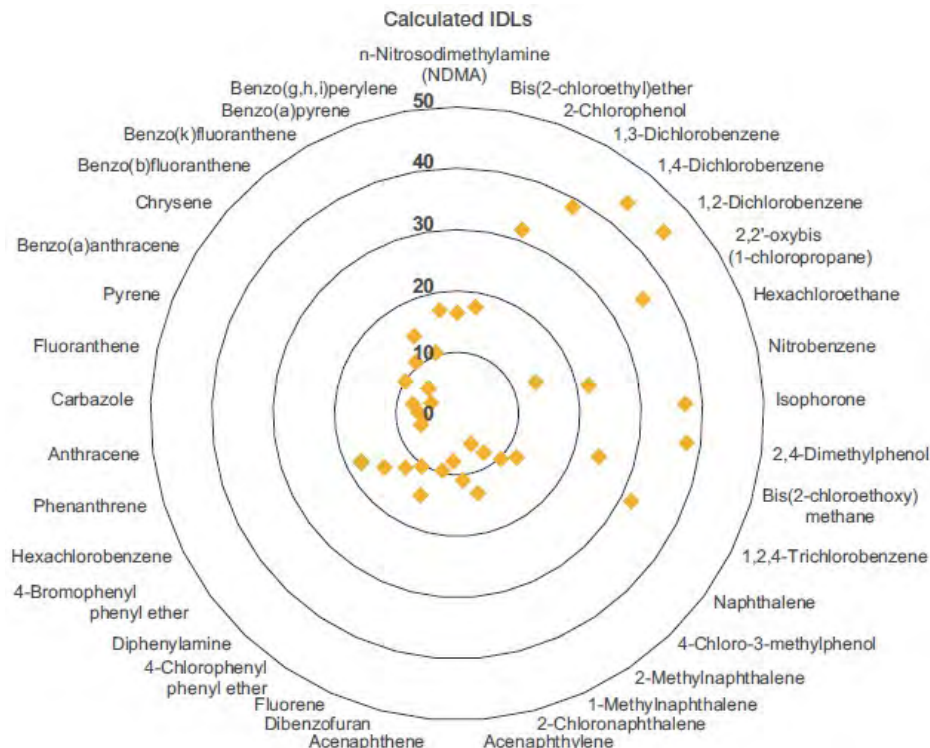


**Figure 5. Examples of calculated IDLs for some selected compounds covering the whole volatility range.** Calculated IDLs for solvent standard spiked at 1 µg/L resulted in the range from 5 to 45 µg/L with peak area %RSD <10 for the majority of the compounds.



The dual-column configuration also requires twice as much carrier gas, as well as an additional analytical column and unions, which makes continued operations costly from a consumable standpoint. Although ECD cells contain a small radioactive Ni63 and are generally considered safe to maintain and handle by trained operators, their use may require certain registrations and licensing fees on a yearly basis to maintain compliance with the radiation safety procedures stated in the regulations of the Nuclear Regulatory Commission (NRC) and state and local guidelines.

The use of GC-MS/MS can overcome challenges associated with using ECD as it is sensitive enough to provide equivalent detection limits but adds the advantage of selectivity, as compounds can be identified based on their unique mass and fragmentation pattern. These two features allow the end user to monitor unique ion transitions for each compound of interest, thus improving confidence in compound identification and quantitation, all while removing safety concerns related to the use of a radioactive source. An example of typical chromatogram for a solvent standard spiked at 1,000 µg/L obtained using GC-MS/MS with t-SRM is reported in Figure 6. Endosulfan I and γ-chlordane as well as endrin and dieldrin tend to coelute on the 5% phenyl 95% dimethylpolysiloxane stationary phase used for this application; therefore, the capability of selecting unique mass ions allowed the discrimination between two compounds that are not chromatographically resolved.

#### **Linearity, instrument detection limit (IDL), and limit of detection (LOQ)**

The TSQ 9610 NeverVent AEI is equipped with the XLXR detector, which is an electron multiplier that offers extended detector lifetime and dynamic range. Calibration curves in DCM were automatically prepared using an off-line TriPlus RSH autosampler by diluting a pesticide mix in the range from 0.5 to 1,000 µg/L. Linearity was evaluated using the internal standard method by calculating the calibration factor for each analyte at each concentration, the mean calibration factor, and the relative standard deviation (RSD) of the calibration factors. The calibration factor RSD were <20% for each analyte, therefore confirming the linear trend and demonstrated in Table 2. The advantage of using internal standard calibration is to account for routine change in response of the chromatographic system as well as variation in the volume of the introduced sample or sample extract.

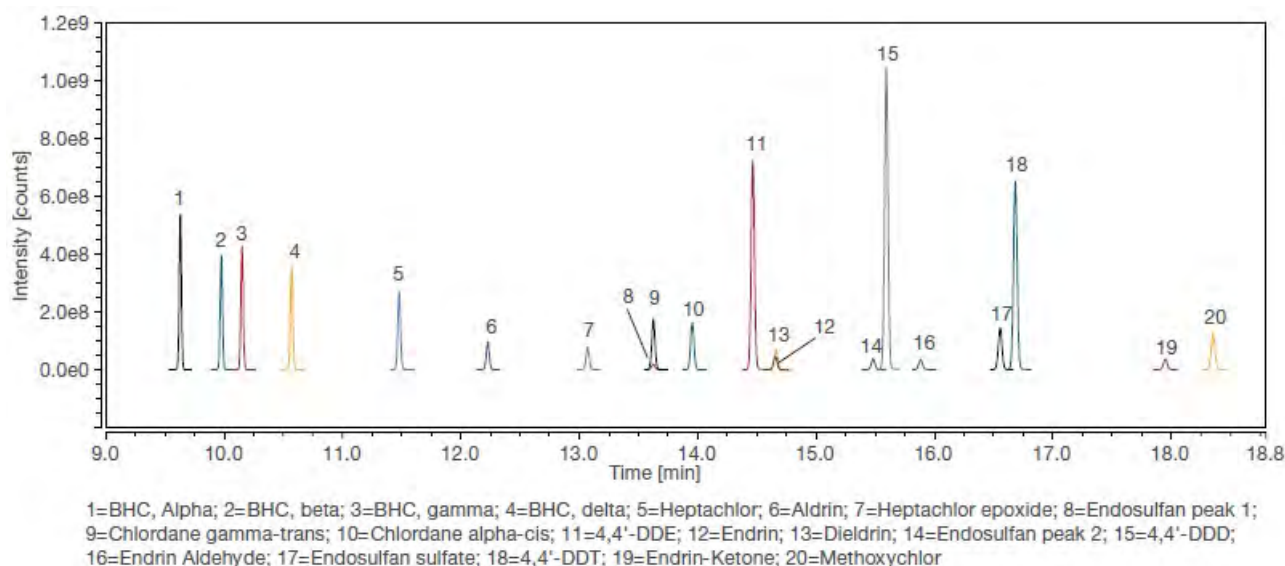


**Figure 6. Typical chromatogram for a solvent standard spiked at 1,000 µg/L. The capability of monitoring typical transitions allowed for the confident identification of the coeluting peaks as shown in the insets.**

Method detection limit and instrument repeatability were assessed for all the target compounds by preparing n=10 solvent standards at a concentration of 1 µg/L. IDLs were calculated by using Equation 2 and resulted within 0.10 to 0.68 µg/L with peak area %RSD for 10 replicated injections <20, with the only exception of endosulfan (peak 1) for which peak area %RSD was 24, as reported in Table 2. Overlaid chromatograms showing peak area repeatability obtained for n=10 replicated injections for aldrin are reported as an example in Figure 7.

The best-in-class t-SRM acquisition mode coupled to the ultra- sensitive AEI ion source delivered unprecedented sensitivity with improved S/N ratio. Figure 8 demonstrates the intensity signal obtained for alpha, beta, gamma, and delta BHC at the lowest calibration point (0.5 µg/L). The calculated S/N resulted in detectability far surpassing the minimum S/N > 3 threshold often reported, therefore suggesting that limits of detection could be potentially lowered even further for future proof analysis.

**Table 2. Calculated IDLs, peak area %RSD, and average calibration factor %RSD for the investigated pesticides. IDLs ranged from 0.16 to 0.68 µg/L with average RF and peak area %RSD <20%, with the only exception of endosulfan (peak 1) for which peak area %RSD was 24.**

Compound	RT (min)	Average RF %RSD	Calculated IDL (µg/L)	Peak area %RSD
BHC, alpha	9.63	5.2	0.18	6.5
BHC, beta	9.98	7.8	0.31	11.4
BHC, gamma	10.15	5.9	0.16	5.8
BHC, delta	10.58	9.1	0.12	4.2
Heptachlor	11.49	9.2	0.35	11.6
Aldrin	12.23	8.6	0.33	11.3
Heptachlor epoxide	13.08	8.7	0.32	11.3
Chlordane, gamma- <i>trans</i>	13.64	7.3	0.18	6.6
Endosulfan, peak1	13.64	17.7	0.68	23.7
Chlordane, alpha- <i>cis</i>	13.94	9.3	0.28	10.0
4,4'-DDE	14.48	9.4	0.1	3.7
Endrin	14.66	8.5	0.18	6.6
Dieldrin	14.68	14.4	0.35	16.4
Endosulfan, peak 2	15.5	15.9	0.43	12.5
4,4'-DDD	15.61	15.7	0.14	4.9
Endrin aldehyde	15.89	19.2	0.5	16.7
Endosulfan sulfate	16.57	9.8	0.16	6.5
4,4'-DDT	16.7	11.7	0.22	7.4
Endrin ketone	17.96	13	0.26	9.2
Metoxychlor	18.36	15.5	0.48	17.0

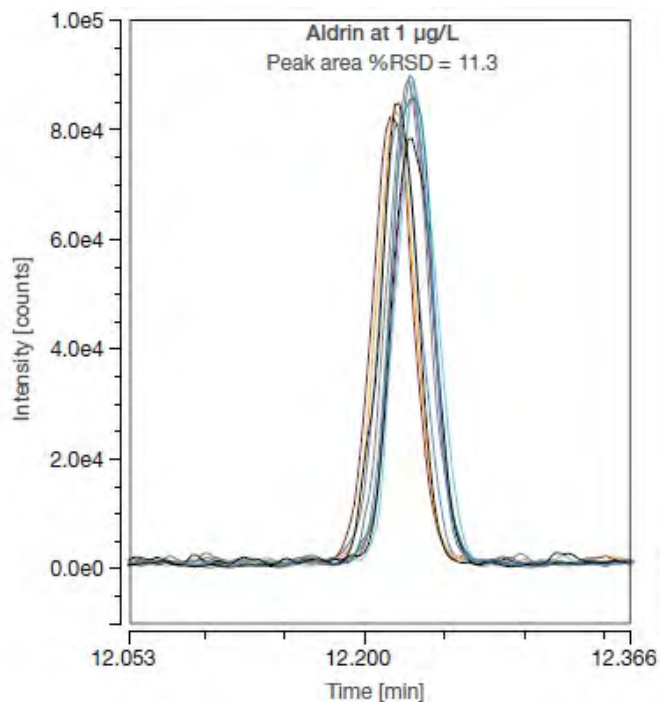


**Figure 7. Overlaid chromatograms showing aldrin peak area repeatability obtained for n=10 replicated injections of solvent standard at 1 µg/L.**

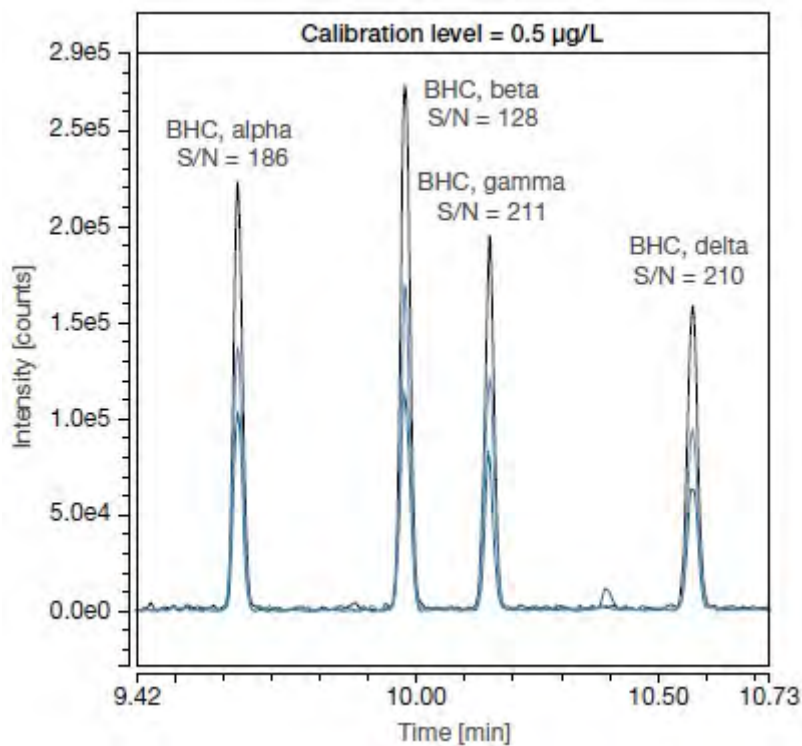


**Figure 8. Intensity signal obtained for alpha, beta, gamma, and delta BHC at the lowest calibration point (0.5 µg/L).** The best-in-class t-SRM acquisition mode coupled to the ultra-sensitive AEI ion source allowed for improved S/N ratio. Quantifier ion = black trace. Qualifier ions = blue and red traces.

## CONCLUSIONS

Modern environmental laboratories benefit greatly from the next generation of gas chromatography-mass spectrometry instrumentation that allows analysts to be more productive with simpler to use, more rugged, and more sensitive instrumentation.

Advances in the Thermo Scientific line of GC-MS/MS allow for modernization of common environmental workflows for the analysis of SVOCs and organochlorine pesticides, as well as many more target analytes, all from a single, easy-to-use platform.

Modernizing instrumentation leads to simplified streamlined laboratory operations:

- Using a single hardware platform translates into increased sample throughput and the potential for consolidating multiple methods in a single GC run for streamlined operations.
- Harmonization of consumables and supplies, as well as decreasing the amount of expensive carrier gas, leads to more efficient lab operations and better ROI.
- A single software interface for acquisition, tuning, and reporting that can be used in an enterprise environment provides traceability and simplicity.
- Improved analyst's safety while reducing the risk of errors and cross-contaminations through the use of automated sample preparation benefits all ranges of lab staff.
- Accelerated routine maintenance operation through the NeverVent technology, allows a user to maintain the system without breaking the vacuum, and the modular concept of the TRACE 1610 GC allows for flexible configurations and reduced instrument downtime.
- Future-proof analysis with the GC-MS/MS timed-SRM acquisition and the AEI ion source for lower limits of detection and confident compound identification and quantitation, far surpassing current regulations.

## REFERENCES

- (1) U.S. EPA, SW-846 Test Method 8081B: Organochlorine Pesticides by Gas Chromatography, Rev. 2, February 2007. <https://www.epa.gov/sites/default/files/2015-12/documents/8081b.pdf>
- (2) U.S. EPA, SW-846 Test Method 8270E: Semivolatile Organic Compounds by Gas Chromatography/Mass Spectrometry (GC-MS), Rev. 6, June 2018. [https://www.epa.gov/sites/default/files/2020-10/documents/method\\_8270e\\_update\\_vi\\_06-2018\\_0.pdf](https://www.epa.gov/sites/default/files/2020-10/documents/method_8270e_update_vi_06-2018_0.pdf)
- (3) U.S. EPA, SW-846 Test Method 8141B: Organophosphorus Compounds by Gas Chromatography, Rev. 2, February 2007. <https://www.epa.gov/sites/default/files/2015-12/documents/8141b.pdf>
- (4) Thermo Fisher Scientific, BR52235-EN 0921C, TriPlus RSH SMART robotic sampling system. <https://www.thermofisher.com/document-connect/document-connect.html?url=https://assets.thermofisher.com/TFS-Assets%2FCMD%2Fbrochures%2Fbr-52235-gc-autosampler-br52235-en-lr.pdf>
- (5) Thermo Fisher Scientific, BR74090-EN 0123S, Stay ahead with measurably more production. <https://www.thermofisher.com/document-connect/document-connect.html?url=https://assets.thermofisher.com/TFS-Assets%2FCMD%2Fbrochures%2Fbr-740900-gs-trace-1600-series-br740900-en.pdf>
- (6) Thermo Fisher Scientific, BR000161-EN 0422C, Stay ahead with unstoppable confidence. <https://www.thermofisher.com/document-connect/document-connect.html?url=https://assets.thermofisher.com/TFS-Assets%2FCMD%2Fbrochures%2Fbr-000161-gc-ms-tsq-9610-br000161-en.pdf>
- (7) Thermo Fisher Scientific, BR001975-EN 0723M, Built for stability. Built for performance. Why compromise? <https://www.thermofisher.com/documentconnect/document-connect.html?url=https://assets.thermofisher.com/TFS-Assets%2FCMD%2Fbrochures%2Fbr-001975-sw-chromeleon-cds-7-3-2-br001975-en.pdf>
- (8) U.S. Code of Federal Regulations, 49 FR 43430, (Oct. 26, 1984); 50 FR 694, 696(Jan. 4, 1985), as amended at 51 FR 23703 (June 30, 1986). [http://www.ecfr.gov/cgi-bin/text-idx?SID=efe93db42854f88dffc66ba8de737e6&mc=true&node=ap40.23.136\\_17.b&rgn=div9](http://www.ecfr.gov/cgi-bin/text-idx?SID=efe93db42854f88dffc66ba8de737e6&mc=true&node=ap40.23.136_17.b&rgn=div9)

- (9) Thermo Fisher Scientific, TN 10494, Practical Determination and Validation of Instrument Detection Limit of Thermo Scientific™ ISQ™ LT Single Quadrupole GC-MS. <https://tools.thermofisher.com/content/sfs/brochures/TN-10494-GC-MS-ISQ-LTSingle-Quadrupole-TN10494-EN.pdf>
- (10) International Union of Pure and Applied Chemists (IUPAC). [http://www.iupac.org/publications/analytical\\_compendium/Cha18sec437.pdf](http://www.iupac.org/publications/analytical_compendium/Cha18sec437.pdf)

Learn more at [thermofisher.com/triple-quadrupole-gc-ms](https://thermofisher.com/triple-quadrupole-gc-ms)

*This Sponsor Report is the responsibility of Thermo Fisher Scientific.*

**General Laboratory Equipment – Not For Diagnostic Procedures.** © 2024 Thermo Fisher Scientific Inc. All rights reserved. All trademarks are the property of Thermo Fisher Scientific and its subsidiaries unless otherwise specified. This information is presented as an example of the capabilities of Thermo Fisher Scientific products. It is not intended to encourage use of these products in any manner that might infringe the intellectual property rights of others. Specifications, terms and pricing are subject to change. Not all products are available in all countries. Please consult your local sales representative for details. AN003362-EN 1024S



## SPONSOR REPORT

PDF

This section is dedicated for sponsor responsibility articles.

# New Performance for High Volume Agriculture Laboratories

*Enabling high throughput in elemental analysis of several agriculture matrices using Milestone's ETHOS UP with MAXI 24 HP*

This report was extracted from the Milestone Industry Report Ethos UP – Maxi-24 HP | Agriculture

## INTRODUCTION

Fertilizer is a fundamental component for the growing of plants. However, too much of the wrong nutrient can have adverse effects such as burning the roots. Characterizing the fertilizer content will indicate the formula's macronutrient content, as well as other nutrients such as calcium, magnesium, potassium, etc. Analysis on a fertilizer product gives the ratio of each macronutrient, which must be correct to ensure optimal efficacy. ICP analysis can provide a lot of information on fertilizer composition but the choice of the correct sample preparation technique is fundamental. Traditional sample preparation techniques include hot block digestion, closed vessel microwave digestion and ashing; each of them posing different challenges. Hot block digestions suffer from long run times, airborne contamination, poor digestion quality, and poor recovery of volatile compounds. Closed vessel microwave digestion has proven to be an effective technique with fast, complete digestions, a clean environment, and full recovery of volatile compounds. Milestone's ETHOS UP equipped with the MAXI 24 High Performance (HP) rotor incorporates all of the benefits of closed vessel microwave digestion while making sample preparation fast, easy, effective, and of the highest quality. This innovative solution perfectly integrates with the powerful ETHOS UP, matching both performance and throughput requirements of agricultural elemental analysis.

## EXPERIMENTAL

In this industry report, a recovery study on certified reference materials has been performed to prove the efficacy of the ETHOS UP in sample preparation for metal analysis.

### Instrument

The ETHOS UP is the most advanced microwave sample preparation equipment. It meets the requirements of modern analytical labs.



Figure 1. Milestone's ETHOS UP.



Figure 2. MAXI-24 HP Rotor.

The ETHOS UP used in this study was equipped with MAXI-24 HP rotor controlled via Milestone's easyTEMP contactless temperature. The superior temperature measurement of easyTEMP allows the processing of different samples of similar reactivities, thus reducing labor time and increasing the overall throughput.

### **MAXI-24 HP Rotor**

The latest Milestone's development is the MAXI-24 HP, which combines performance and throughput within a single rotor-based platform. It completely innovates the rotor-base solutions providing high throughput without sacrificing the performance. Thanks to its 24 positions, it is the first high pressure and throughput rotor available in the market. The completely new design of its vessels allows to achieve conditions never seen for high throughput rotors. Thicker high purity PTFE-TFM vessels and caps, along with rugged PEEK shields are key ingredients to handle the conditions required to completely digest these samples.

### **Procedure**

Table 1 reports the conditions used to prepare the sample.

**Table 1.** Sample amount and acid mixture used for the microwave digestion run

SAMPLE	SAMPLE AMOUNT	ACID MIXTURE
Multi-nutrient	0.2 g	8 mL of HNO <sub>3</sub> (65%), 0.5 mL of H <sub>2</sub> SO <sub>4</sub> (96%), 2 mL of HF (48%)
Marine sediment (IAEA-457)*	0.5 g	9 mL of HNO <sub>3</sub> (65%), 3 mL of HCl (37%)
San Joaquin soil (NIST 2709a)*	0.5 g	9 mL of HNO <sub>3</sub> (65%), 3 mL of HCl (37%)
Tomato leaves (NIST 1573a)	0.5 g	5 mL of HNO <sub>3</sub> (65%) + 1 mL of H <sub>2</sub> O <sub>2</sub> (30%)
Cabbage (IAEA-359)	0.5 g	5 mL of HNO <sub>3</sub> (65%) + 1 mL of H <sub>2</sub> O <sub>2</sub> (30%)

\* EPA 3051A was applied

All samples were weighted into the MAXI-24 HP vessel, approximately 0.5 g (as reported in Table 1). The acid mixture (trace metal grade) was added according to the data reported in Table 1 and the proper microwave method has been used as reported in Table 2.

**Table 2.** Microwave program

STEP	TIME	T2	POWER
1	00:10:00	160 °C	1500 W
2	00:15:00	210 °C	1800 W
3	00:10:00	210 °C	1800 W

After microwave digestion, the samples were diluted to 50 mL with deionized water and analyzed by ICP-OES.

### **Quantification**

ICP-OES Instrumental Parameters: RF power (W): 1300; Plasma flow (L/min): 15.0; Auxiliary Flow (L/min): 1.5; Nebulizer Flow (L/min): 0.75; Replicate read time (s): 10; Instrument stabilization delay (s): 15; Sample Uptake Delay (s): 30; Pump Rate (rpm): 15; Rinse Time (s): 10; Replicates: 3.

## RESULTS AND DISCUSSION

The performance of the Milestone ETHOS UP equipped with MAXI-24 HP rotor and easyTEMP technology was evaluated through a recovery study on multi-nutrient fertilizer (NIST SRM695), marine sediment (IAEA 457), San Joaquin soil (NIST 2709a), tomato leaves (NIST 1573a) and cabbage (IAEA 359) samples. The samples were digested with Milestone's ETHOS UP and subsequently analyzed via ICP-OES.

**Table 3.** Data of the recovery study on multi-nutrient fertilizer (NIST SRM695) sample

	<b>Certified value</b>	<b>Recovery % (n=3)</b>	<b>RSD (%)</b>
<b>Al</b>	0.61 ± 0.03%	89.3	2.3
<b>As</b>	200 ± 5 mg/Kg	96.7	2.6
<b>Ca</b>	2.26 ± 0.04%	103.5	2.8
<b>Cd</b>	16.9 ± 0.2 mg/Kg	93.5	1.7
<b>Co</b>	65.3 ± 2.4 mg/Kg	94.1	2.3
<b>Cr</b>	244 ± 6 mg/Kg	88.9	2.6
<b>Cu</b>	1225 ± 9 mg/Kg	91.7	1.7
<b>Fe</b>	3.99 ± 0.08%	89.7	2.3
<b>Hg</b>	1955 ± 0.036 mg/Kg	95.6	2.6
<b>K</b>	11.65 ± 0.13%	92.6	1.9
<b>Mg</b>	1.79 ± 0.05%	105.9	2.7
<b>Mn</b>	0.305 ± 0.005%	101.5	2.4
<b>Mo</b>	20.0 ± 0.3 mg/Kg	93.3	1.4
<b>Na</b>	0.405 ± 0.007%	95.6	2.2
<b>Ni</b>	135 ± 2 mg/Kg	90.0	2.3
<b>Pb</b>	273 ± 17 mg/Kg	102.3	2.6
<b>V</b>	122 ± 3 mg/Kg	99.6	1.0
<b>Zn</b>	0.325 ± 0.005 mg/Kg	101.3	2.1

**Table 4.** Data of the recovery study on marine sediment (IAEA-457) sample

	<b>Certified value</b>	<b>Recovery % (n=3)</b>	<b>RSD (%)</b>
<b>Ag</b>	1.93 ± 0.38 mg/Kg	94.1	1.4
<b>Al</b>	82660 ± 3430 mg/Kg	96.3	1.3
<b>As</b>	10.2 ± 1.0 mg/Kg	109.4	2.5
<b>Cd</b>	1.09 ± 0.08 mg/Kg	102.9	1.9
<b>Co</b>	14.7 ± 1.0 mg/Kg	90.0	2.1

(continues on next page)

**Table 4.** Data of the recovery study on marine sediment (IAEA-457) sample (continuation)

	<b>Certified value</b>	<b>Recovery % (n=3)</b>	<b>RSD (%)</b>
<b>Cr</b>	144 ± 8 mg/Kg	89.9	2.0
<b>Cu</b>	365 ± 19 mg/Kg	91.3	1.4
<b>Fe</b>	41450 ± 2240 mg/Kg	91.6	0.9
<b>Hg</b>	0.143 ± 0.012 mg/Kg	93.2	1.3
<b>Li</b>	64.2 ± 5.5 mg/Kg	94.7	1.8
<b>Mn</b>	427 ± 30 mg/Kg	93.1	2.8
<b>Ni</b>	53.1 ± 2.7 mg/Kg	93.0	1.4
<b>Pb</b>	105 ± 7 mg/kg	91.4	1.2
<b>Sn</b>	27.40 ± 0.75 mg/Kg	93.7	2.1
<b>Sr</b>	137 ± 10 mg/Kg	94.1	1.1
<b>V</b>	87.4 ± 8.1 mg/Kg	101.3	2.0
<b>Zn</b>	425 ± 25.8 mg/Kg	96.8	2.5

**Table 5.** Data of the recovery study on San Joaquin soil (NIST 2709a) sample

	<b>Certified value</b>	<b>Recovery % (n=3)</b>	<b>RSD (%)</b>
<b>Al</b>	7.37 ± 0.16%	93.4	2.3
<b>Ba</b>	979 ± 28 mg/Kg	91.6	2.6
<b>Ca</b>	1.91 ± 0.09%	89.9	2.8
<b>Cd</b>	0.371 ± 0.002 mg/Kg	<LOQ	—
<b>Co</b>	12.8 ± 0.2 mg/Kg	94.2	2.7
<b>Cr</b>	130 ± 9 mg/Kg	90.7	2.4
<b>Fe</b>	3.36 ± 0.07%	83.3	1.4
<b>K</b>	2.11 ± 0.06%	92.8	2.2
<b>Mg</b>	1.46 ± 0.02%	102.8	2.3
<b>Mn</b>	529 ± 18 mg/Kg	98.1	2.6
<b>Na</b>	1.22 ± 0.03 %	93.6	2.8
<b>P</b>	0.0688 ± 0.0013%	113.1	1.7
<b>Pb</b>	17.3 ± 0.1 mg/kg	92.4	1.4
<b>Sb</b>	1.55 ± 0.06 mg/Kg	<LOQ	1.9
<b>Si</b>	30.3 ± 0.4%	96.3	1.2
<b>Sr</b>	239 ± 6 mg/Kg	95.7	2.3

(continues on next page)

**Table 5.** Data of the recovery study on San Joaquin soil (NIST 2709a) sample (continuation)

	<b>Certified value</b>	<b>Recovery % (n=3)</b>	<b>RSD (%)</b>
<b>Ti</b>	0.336 ± 0.007%	91.3	2.6
<b>V</b>	110 ± 11 mg/Kg	102.0	2.8
<b>Zr</b>	195 ± 46 mg/Kg	94.4	1.7

**Table 6.** Data of the recovery study on tomato leaves (NIST 1573A) sample

	<b>Certified value</b>	<b>Recovery % (n=3)</b>	<b>RSD (%)</b>
<b>Al</b>	598.4 ± 7.1 mg/Kg	94.1	2.3
<b>As</b>	0.1126 ± 0.0032 mg/Kg	<LOQ	—
<b>Ca</b>	50450 ± 550 mg/Kg	96.7	1.0
<b>Cd</b>	1.517 ± 0.027 mg/Kg	92.1	2.1
<b>Co</b>	0.5773 ± 0.0071 mg/Kg	<LOQ	—
<b>Cr</b>	1.988 ± 0.034 mg/Kg	90.9	2.6
<b>Cu</b>	4.70 ± 0.14 mg/Kg	96.0	2.8
<b>Fe</b>	367.5 ± 4.3 mg/Kg	96.8	1.7
<b>Hg</b>	0.0341 ± 0.0015 mg/Kg	92.3	2.3
<b>K</b>	26760 ± 480 mg/kg	99.7	2.6
<b>Mn</b>	246.3 ± 7.1 mg/Kg	101.0	1.7
<b>Na</b>	136.1 ± 3.7 mg/Kg	97.1	2.3
<b>Ni</b>	1.582 ± 0.041 mg/Kg	93.5	2.6
<b>P</b>	2161 ± 28 mg/Kg	90.6	2.2
<b>Rb</b>	14.83 ± 0.31 mg/K.g	90.2	1.4
<b>Sb</b>	0.0619 ± 0.0032 mg/kg	<LOQ	—
<b>Se</b>	0.0543 ± 0.0020 mg/Kg	<LOQ	—
<b>V</b>	0.835 ± 0.034 mg/Kg	<LOQ	—
<b>Zn</b>	30.94 ± 0.55 mg/Kg	94.5	2.4

**Table 7.** Data of the recovery study on cabbage (IAEA-359) sample

	<b>Certified value</b>	<b>Recovery % (n=3)</b>	<b>RSD (%)</b>
<b>As</b>	0.10 ± 0.004 mg/Kg	<LOQ	—
<b>Ba</b>	11.0 ± 0.5 mg/Kg	91.6	1.2
<b>Ca</b>	18500 ± 510 mg/Kg	92.5	2.6

(continues on next page)

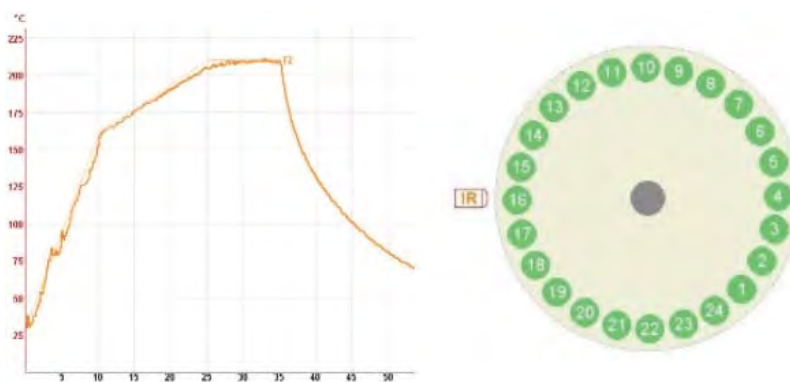


**Table 7.** Data of the recovery study on cabbage (IAEA-359) sample (continuation)

	Certified value	Recovery % (n=3)	RSD (%)
<b>Cd</b>	0.12 ± 0.005 mg/Kg	<LOQ	—
<b>Cr</b>	1.30 ± 0.06 mg/Kg	90.3	2.0
<b>Cu</b>	5.67 ± 0.18 mg/Kg	94.8	2.1
<b>Fe</b>	148 ± 3.9 mg/Kg	95.2	1.6
<b>Hg</b>	0.013 ± 0.002 mg/Kg	94.1	0.7
<b>K</b>	32500 ± 690 mg/Kg	96.3	1.6
<b>Mg</b>	2160 ± 50 mg/Kg	91.4	1.7
<b>Mn</b>	31.9 ± 0.6 mg/Kg	98.9	2.9
<b>Na</b>	580 ± 21 mg/Kg	103.4	1.1
<b>Ni</b>	1.05 ± 0.05 mg/kg	95.5	1.4
<b>Se</b>	0.12 ± 0.011 mg/Kg	<LOQ	—
<b>Sr</b>	49.2 ± 1.4 mg/Kg	93.1	1.9
<b>Zn</b>	38.6 ± 0.7 mg/Kg	91.9	2.1

The analytical results were shown in Tables 3-7 with good recoveries of all elements and RSDs below 3%. This demonstrates the robustness and reproducibility of the digestion process with the ETHOS UP – MAXI-24 HP.

Figure 3 shows the temperature profile of the digestion as well as the multiple temperature visualization and recording for all the samples digest in the run.

**Figure 3.** MAXI-24 HP Microwave Run Report and Multiple temperature traceability.

## CONCLUSION

The data shown in this industry report demonstrates full recovery of the elements reported in the certificates of the reference material. Highly reactive samples such as fertilizer has been completely digested even in large sample amounts. The digestion process has been accurately controlled by the easyTEMP sensor,

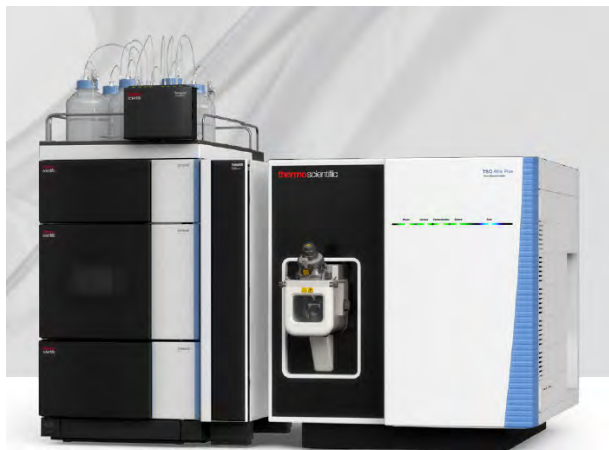
ensuring same digestion quality and reliable results. In addition, microwave digestion using the Milestone ETHOS UP with easyTEMP control, provides the highest level of reproducibility and great ease of use, ensuring high quality digestion run after run.

Further reading [here](#)

*This Sponsor Report is the responsibility of Milestone.*

## **ABOUT MILESTONE**

At Milestone we help chemists by providing the most innovative technology for metals analysis, direct mercury analysis and the application of microwave technology to extraction, ashing and synthesis. Since 1988 Milestone has helped chemists in their work to enhance food, pharmaceutical and consumer product safety, and to improve our world by controlling pollutants in the environment.

**RELEASE****TSQ Altis Plus Triple Quadrupole Mass Spectrometer****Ultimate quantitative performance made possible**

Overcome the most demanding quantitative workflow challenges. With superior acquisition speeds, enhanced sensitivity, prototypical selectivity, and exceptional robustness, the TSQ Altis Plus mass spectrometer delivers unprecedented accuracy and precision for low-level compound detection and quantitation in complex matrices that redefines ultimate instrument performance.

**Achieve the highest confidence in targeted compound detection and quantitation**

Greater than 6 orders of linear dynamic range with high selectivity. Enhanced acquisition speeds empower large-scale studies for translational workflow development

or method optimization with effective dwell time settings as low as 0.3 – 5 millisecond polarity switching maximizes productivity in fewer experiments.

**High-throughput screening and quantitation**

Innovations in the ion source, mass analyzer, active Q2 collision cell, and RF electronics offer high sensitivity, selectivity, and superior acquisition speeds/polarity switching times that are ideal with UHPLC separations.

**Expanded experimental capabilities**

Integrated workflow solutions centered on the TSQ Altis Plus mass spectrometer address regulated requirements targeting a growing list of diverse compounds. New UHPLC and ion chromatography (IC) systems maximize sample delivery and separation capabilities, maintaining the sensitivity to meet minimum residue limits without costly sample preparation or derivatization steps.

**Operational simplicity**

Simplified calibration approach consolidates steps needed by the operator, combining an intelligent instrument check and calibration routine. Experimental determination of dwell times assigned to each transition has been automated based on user-defined chromatographic peak width and the option of fixed cycle time or optimal number of data points per chromatographic peak.

**Database integration**

Utilization of experimental libraries created from discovery experiments can by-pass the need for purified standards and lengthy optimization routines. The output from processed data in Thermo Scientific TraceFinder software can be directly imported into the instrument method editor, streamlining large-scale study creation.

Discovery experiments, however, may not contain all compounds targeted in a study. Integration with Thermo Scientific mzCloud databases enables selection of additional compounds from the most advanced mass spectral database to be added into existing experimental methods.

[Read more](#)

# Confident Quantitation



Any compound, any matrix, any user.

To achieve your business and scientific goals, you need results you can count on. Regardless of your application, the new Thermo Scientific TSQ™ Series Triple Quadrupole Mass Spectrometers deliver unprecedented precision for your quantitative workflows. Selective high-resolution SRM, robustness, reliability and sensitivity come together—now every user in every lab can obtain high-confidence data, regardless of the matrix and molecule analyzed.

Find out more at [thermofisher.com/Altis-Quantis](http://thermofisher.com/Altis-Quantis)

VIDEO

WEBSITE

For Research Use Only. Not for use in diagnostic procedures. © 2017 Thermo Fisher Scientific Inc. All rights reserved. All trademarks are the property of Thermo Fisher Scientific and its subsidiaries unless otherwise specified. AD65064EN-1117S

**ThermoFisher**  
SCIENTIFIC

**RELEASE****Thermo Scientific TSQ 9610 Triple Quadrupole GC-MS/MS System*****Unstoppable confidence for analytical testing***

To confidently stay ahead, your GC-MS/MS system must deliver ultimate performance while consistently producing trusted quantitative results. That's the reason for the Thermo Scientific™ TSQ™ 9610 Triple Quadrupole GC-MS/MS System. User-centric Thermo Scientific™ NeverVent™ technology, extended-life detector, and intelligent software eliminate unnecessary downtime to maximize your sample throughput and return on investment (ROI). New extended linear dynamic range combined with proven high sensitivity ensures you keep ahead of the toughest regulatory methods and business demands.

Combine the TSQ 9610 Triple Quadrupole GC-MS/MS System with the Thermo Scientific™ TRACE™ 1600 Series Gas Chromatograph (GC) and Thermo Scientific™ AI/AS 1610 Liquid Autosampler to optimize the performance and productivity of your solution.

***Increase instrument uptime***

Eliminate unnecessary and unplanned instrument downtime to deliver high-confidence quantitative results, day after day. The TSQ 9610 Triple Quadrupole GC-MS/MS System combines unstoppable robustness with the ability to change the GC column and clean the ion source without interrupting analytical workflows.

***Maximize sample throughput***

When high sample throughput is essential, the system delivers results on time and with ease. Automated workflows and simplified operation ensure every user produces consistent results, sample after sample. Extended linear range and rapid selected reaction monitoring (SRM) scanning enable method consolidation so you can analyze more compounds in a single run. When these capabilities are combined with best-in-class uptime and sensitivity, you stay ahead of any productivity demand.

***Realize rapid return on investment***

Ensuring your system delivers results as soon as it's installed is necessary to achieving rapid ROI. With built-in intelligence that simplifies instrument set up, analytical methods, and everyday operation, the TSQ 9610 Triple Quadrupole GC-MS/MS System is designed for accelerated deployment. Reduced needs for operator training and faster time to full productivity together with maximum sample throughput provide fast return on your instrument investment.

**Find out more at [thermofisher.com/TSQ9610](http://thermofisher.com/TSQ9610)**





## Mass Spectrometry

# Stay ahead with unstoppable confidence

To confidently stay ahead, your GC-MS/MS system must deliver ultimate performance while consistently producing trusted quantitative results. That's the reason for the Thermo Scientific™ TSQ™ 9610 Triple Quadrupole GC-MS/MS System. User-centric Thermo Scientific™ NeverVent™ technology, extended-life detector, and intelligent software eliminate unnecessary downtime to maximize your sample throughput and return on investment (ROI). New extended linear dynamic range combined with proven high sensitivity ensures you keep ahead of the toughest regulatory methods and business demands.

GC-MS that's ready to run when you are.



**VIDEO**

**WEBSITE**

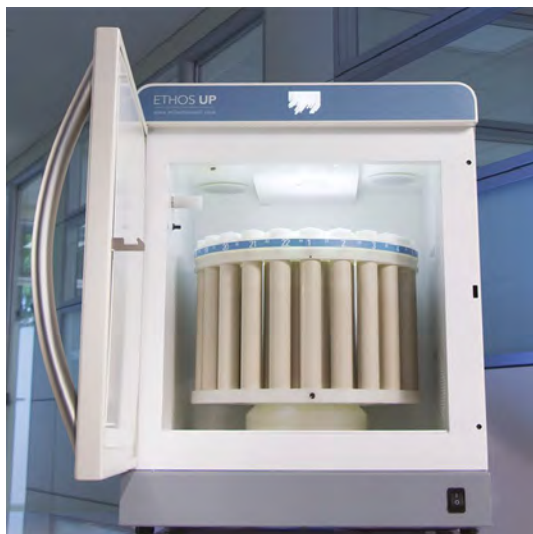
Find out more at **[thermofisher.com/TSQ9610](https://thermofisher.com/TSQ9610)**

For Research Use Only. Not for use in diagnostic procedures. © 2022 Thermo Fisher Scientific Inc. All rights reserved. All trademarks are the property of Thermo Fisher Scientific and its subsidiaries unless otherwise specified. ad000XXX-na-en 0122

**thermo**scientific

## RELEASE

# ETHOS UP High Performance Microwave Digestion System



### Quality Analysis Starts with Great Sample Prep

The ETHOS UP™ fully embodies Milestone's philosophy in microwave sample preparation. Specifically designed for closed vessel microwave acid digestion, it offers productivity, safety, ease of use, connectivity, expertise and application flexibility.

### Safety and reliability

Best microwave hardware, temperature and pressure sensors. The cavity has a volume in excess of 70 L, and is constructed entirely of stainless steel to ensure longevity and structural integrity. Its unique pressure responsive door, also made of stainless steel, ensures superior safety even with the most reactive samples. The safeVIEW high definition digital camera, allows to safely look into the microwave cavity.

### Performance and throughput

The MAXI-24 High Performance (HP) and high throughput rotor was designed with double pressure limits and greater capacity than other high throughput rotors. It processes increased volumes of sample and a wide variety of matrices within a single rotor-based platform. Quick-assembly vessels are closed with a simple hand-tightening, improving your daily productivity.

### EasyCONTROL operating software

Milestone pioneered the use of infrared sensors combined with an in-situ temperature sensor to more accurately control the digestion cycle.

Today, Milestone innovates again by combining all the benefits of in-situ and infrared sensors into a single solution: **the Milestone easyTEMP, a direct contactless temperature sensor**. The MAXI-24 HP, along with the built-in easyTEMP, contactless temperature control in all vessels, automatically controls the temperature even in case of exothermic reactions.

### Flexibility

Rotors and pressure vessels are crucial components to ensure high digestion quality and safety. Milestone's rotors are built with high-purity PTFE-TFM, PEEK safety shields and a unique safety release mechanism.

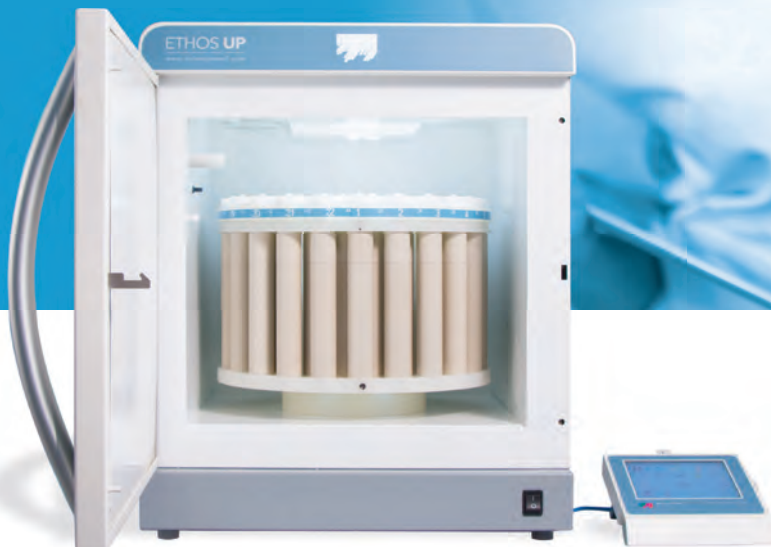
### Smart software to save your time

The ETHOS UP comes with a dedicated touch screen terminal with easyCONTROL software which incorporates our expertise and knowledge in microwave sample preparation. The ETHOS UP user-interface provides full control of all digestion parameters, complete documentation and improves the overall procedure.

[Read more](#)



Productivity UP.  
Simplicity UP.  
Safety UP.  
**Ethos UP.**



HIGHEST THROUGHPUT ROTORS

NO METHOD DEVELOPMENT

REMOTE SYSTEM CONTROL

ENHANCED SAFETY FEATURES

## JUST WHEN YOU THINK METALS PREP TECHNOLOGY CANT GET ANY BETTER, IT DOES.

The Milestone Ethos UP isnt just intelligent, its the most powerful microwave digestion system on the market today.

Featuring the highest throughput rotors, stainless steel construction and patented vent-and-reseal technology, the Ethos UP ensures market-leading safety and productivity.

Plus, new Milestone Connect offers remote system control, 24/7 technical support and direct access to a comprehensive library of content developed especially for lab professionals.

See how Ethos UP can help you work smarter.  
Go to [www.milestonesrl.com/ethosup](http://www.milestonesrl.com/ethosup)



VIDEO

WEBSITE



MICROWAVE DIGESTION

MERCURY CLEAN CHEMISTRY ASHING EXTRACTION SYNTHESIS

[milestonesrl.com](http://milestonesrl.com)

**RELEASE**

## Pittcon Conference & Expo

Pittcon is a catalyst for the exchange of information, a showcase for the latest advances in laboratory science, and a venue for international connectivity.



Pittcon is a dynamic, transnational conference and exposition on laboratory science, a venue for presenting the latest advances in analytical research and scientific instrumentation, and a platform for continuing education and science-enhancing opportunity. Pittcon is for anyone who develops, buys, or sells laboratory equipment, performs physical or chemical analyses, develops analysis methods, or manages these scientists.

### **Pittcon Awards**

*Honoring scientists who have made outstanding contributions to Analytical Chemistry*



Each year, Pittcon provides a venue where scientists who have made outstanding contributions to laboratory science, analytical chemistry, and applied spectroscopy are honored.

Among these awards is the **Pittcon Heritage Award** which honors those visionaries whose entrepreneurial careers shaped the instrumentation and laboratory supplies community and by doing so have transformed the scientific community at large.

The award has been presented jointly with Pittcon since 2002 and is given out each year at a special ceremony during the Pittcon Conference and Expo. The recipient's name and achievements are added to the Pittcon Hall of Fame, which conference attendees can visit at the show each year.

### **Pittcon 2026 – Conference on Analytical Chemistry and Applied Spectroscopy**

March 7-11, 2026

Henry B. González Convention Center  
San Antonio, Texas, USA


**Pittcon**<sup>®</sup>  
Conference and Exposition




Sí Science  
Sí San Antonio


## SPURRING SCIENTIFIC INNOVATION

Pittcon is the place. A place of purpose. Of progress. And discovery. A place of infinite promise.

 What is Pittcon?

 2026 Highlights

 Why Attend

 Why Exhibit

Find Your Next  
'A-Ha' Moment

March 7-11, 2026  
San Antonio, Texas, USA

Registration Opens in  
September

**Pittcon**  
Conference and Exposition

ATTEND PITTCON ▾

CONFERENCE ▾

EXPOSITION ▾

EXHIBIT AT PITTCON ▾



### Pittcon 2026 Conference + Expo

Connect. Cultivate. Collaborate.

Find that spark that drives your research, your career, and above all, your scientific perspective forward.

Dates

March 7 - 11  
2026

Venue

Henry B. González  
Convention Center

WHY ATTEND?

WHY EXHIBIT?



### What is Pittcon?

Pittcon is a dynamic, international conference and exposition on laboratory science, a venue for presenting the latest advances in analytical research and scientific instrumentation, and a platform for continuing education and science-enhancing opportunity.

LEARN MORE

## So What is Pittcon?

Pittcon is a dynamic, international conference and exposition on laboratory science, a venue for presenting the latest advances in analytical research and scientific instrumentation, and a platform for continuing education and science-enhancing opportunity.

WHO SHOULD ATTEND?

EXPLORE PITTCON

**Pittcon**  
Conference and Exposition



**RELEASE****SelectScience® Pioneers online Communication and Promotes Scientific Success**

SelectScience® promotes scientists and their work, accelerating the communication of successful science. Through trusted lab product reviews, virtual events, thought-leading webinars, features on hot scientific topics, eBooks and more, independent online publisher SelectScience® provides scientists across the world with vital information about the best products and techniques to use in their work.

**Some recent contributions from SelecScience® to the scientific community****Resource*****The green energy transition enabling sustainability through science***

In last decade, the growth of renewable energy has outperformed expectations. Renewables like wind and solar are more efficient, economical, and available than ever. Explore this interactive resource for the latest on renewable energy sources. Discover how you can transition to greener energy for your R&D, performance testing, and quality assurance laboratory. Access [here](#)

**Webinar*****Size exclusion chromatography with light scattering for biopharmaceuticals***

This two-part webinar series where Dr. Jelle De Vos from RIC group and Dr. Sonja Schneider from Agilent Technologies will discuss how SEC is evolving to meet the demands of modern biopharma. In Part 1, the experts will cover the fundamentals of SEC and demonstrate how combining it with light scattering detection can enhance the characterization and development of biopharmaceuticals. Access [here](#)

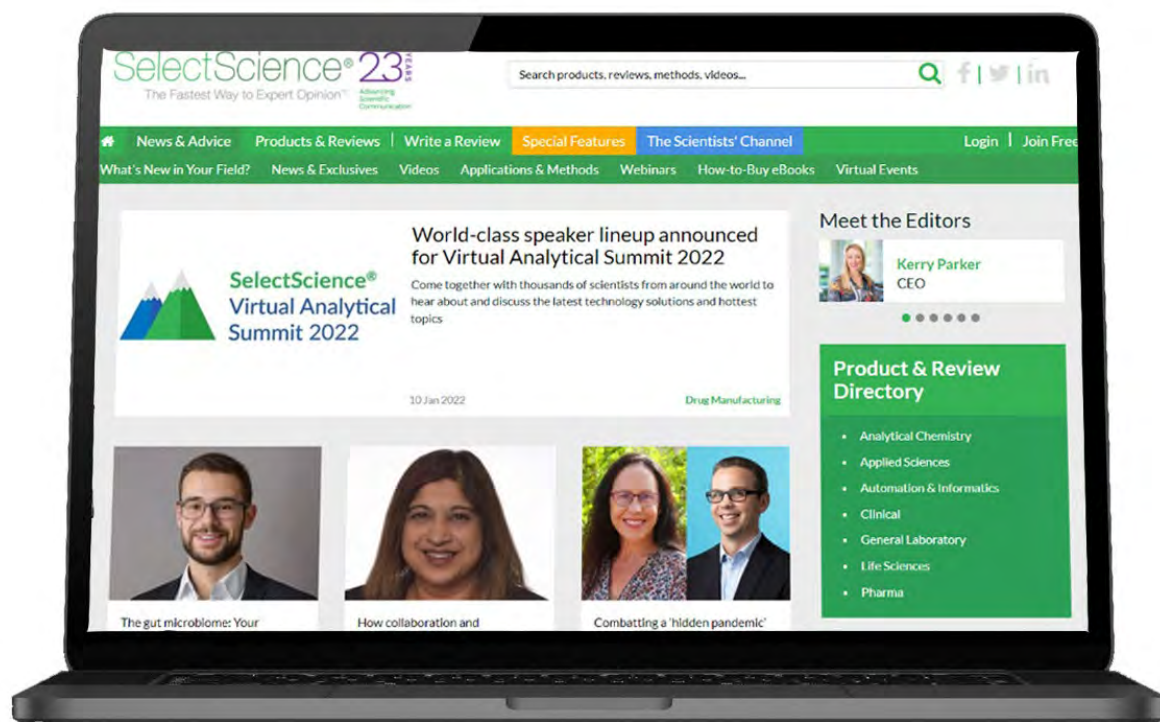
**News*****Unlock the future of PFAS detection with high-resolution mass spectrometry***

High-resolution mass spectrometry (HRMS) stands out as a powerful tool for PFAS analysis, offering more specificity and comprehensive characterization of PFAS contamination compared to traditional methods. Its effectiveness shines in analyzing complex samples, identifying multiple PFAS compounds, even minor components, and distinguishing similar substances. Access [here](#)

***Blue/Green LED technology — key to more sustainable chocolate***

Learn how Blue/Green LED technology is revolutionizing gel imaging in labs producing chocolate alternatives. In the rapidly evolving field of biotechnology, the demand for more efficient, safe, and accurate tools continues to grow. One of the key advancements driving this change is Blue/Green LED technology, a safer and more effective alternative to traditional UVlight for gel imaging. Access [here](#)

# SelectScience® is the leading independent online publisher connecting scientists to the best laboratory products and applications.



- Working with Scientists to Make the Future Healthier.
- Informing scientists about the best products and applications.
- Connecting manufacturers with their customers to develop, promote and sell technologies.

**RELEASE****CHROMacademy is the leading provider of eLearning for analytical science**

*CHROMacademy helps scientific organizations acquire and maintain excellence in their laboratories.*

For over 10 years, CHROMacademy has increased knowledge, efficiency and productivity across all applications of chromatography. With a comprehensive library of learning resources, members can improve their skills and knowledge at a pace that suits them.

CHROMacademy covers all chromatographic applications – HPLC, GC, mass spec, sample preparation, basic lab skills, and bio chromatography. Each paradigm contains dozens of modules across theory, application, method development, troubleshooting, and more. Invest in analytical eLearning and supercharge your lab.



For more information, please visit [www.chromacademy.com/](http://www.chromacademy.com/)



CHROMacademy Lite members have access  
to less than 5% of our content.  
Premier members get so much more !

## Video Training courses

Fundamental HPLC  
Fundamental GC  
Fundamental LCMS  
Fundamental GCMS  
HPLC Method Development  
GC Method Development



## Ask the Expert

We are always on hand to help fix your  
instrument and chromatographic  
problems, offer advice on method  
development, help select a column for  
your application and more.

**To find out more about Premier Membership contact:**

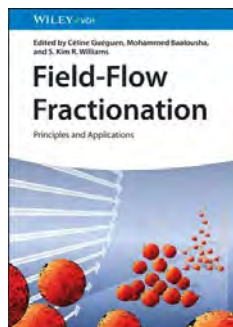
Glen Murry: +1 732.346.3056 | Glen.Murry@ubm.com

Peter Romillo: +1 732.346.3074 | Peter.Romillo@ubm.com

**[www.chromacademy.com](http://www.chromacademy.com)**

The worlds largest e-Learning website for analytical scientists

## NOTICES OF BOOKS



### **Field Flow Fractionation: Principles and Applications**

*Céline Guéguen, Mohammed Baalousha, Kim R. Williams*

February 2026, Wiley

This book offers a comprehensive and topical one-stop reference on field flow fractionation, an important separation technique which has been proven successful in the analysis of natural and engineered nanoparticles, pharmaceuticals, proteins, polymers, soils, and food. [Read more](#)

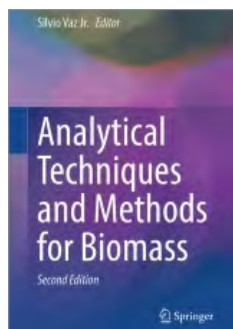


### **Analysis of Variance for High-Dimensional Data: Applications in Life, Food, and Chemical Sciences**

*Age K. Smilde, Federico Marini, Johan A. Westerhuis, Kristian Hovde Liland*

July 2025, Wiley

This book is an essential reference for practitioners involved in data analysis in the natural sciences, including professionals working in chemometrics, bioinformatics, data science, statistics, and machine learning. The book is valuable for developers of new methods in high dimensional data analysis. [Read more](#)

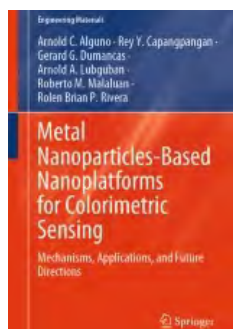


### **Analytical Techniques and Methods for Biomass**

*Silvio Vaz Jr. (Ed.)*

2025, Springer Cham

This book deals with the application of techniques and methods of chemical analysis for the study of biomass and its conversion processes. It aims to fill the existing gap in the literature on this subject. The application of various techniques and analytical methods is presented straightforwardly, enabling readers to choose the most appropriate methodologies for analyzing the major classes of plant biomass and their products. [doi](#)



### **Metal Nanoparticles-Based Nanoplatfoms for Colorimetric Sensing**

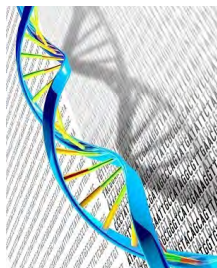
*Arnold C. Alguno, Rey Y. Capangpangan, Gerard G. Dumancas, Arnold A. Lubguban, Roberto M. Malaluan, Rolan Brian P. Rivera*

2025, Springer Singapore

This book highlights an in-depth examination of metal nanoparticles as transformative agents in colorimetric sensing technology. Targeted toward researchers, practitioners, and students in nanotechnology, analytical chemistry, and related fields, this book consolidates the latest advancements in nanoparticle-based colorimetric systems for highly sensitive and selective detection. [doi](#)



## PERIODICALS & WEBSITES



**American Laboratory®** is a platform that addresses basic research, clinical diagnostics, drug discovery, environmental, food and beverage, forensics and other markets, and combines in-depth articles, news, and video to deliver the latest advances in their fields.

**Study:** *NGS Should Be Go-to Technology on Day Zero of the Next Pandemic*. By Michelle Taylor, Editor-in-Chief. While the world was eventually able to get COVID-19 under control, it was obvious better planning was needed in the case of another—likely—pandemic. [Access here](#)




### LCGC

Chromatographyonline delivers practical, nuts-and-bolts information to help scientists and lab managers become more proficient in the use of chromatographic techniques and instrumentation. **Article:** *Challenges and Solutions in Oligonucleotide Analysis, Part I: An Overview of Liquid Chromatography Methods and Applications*. By Martin Gilar; Dwight R. Stoll. This article explores advanced oligonucleotide analysis techniques, including chromatography methods for therapeutic RNA, siRNA, and mRNA, enhancing nucleic acid research. [Read more](#)



### Scientia Chromatographica

*Scientia Chromatographica* is the first and to date the only Latin American scientific journal dedicated exclusively to Chromatographic and Related Techniques. With a highly qualified and internationally recognized Editorial Board, it covers all chromatography topics in all their formats, in addition to discussing related topics such as “The Pillars of Chromatography”, Quality Management, Troubleshooting, Hyphenation (GC-MS, LC-MS, SPE-LC-MS/MS) and others. It also provides columns containing general information, such as: calendar, meeting report, bookstore, etc. [Read more](#) 



### Select Science

SelectScience® has transformed global scientific communications and digital marketing. It informs scientists about the best products and applications, connects manufacturers with their customers to develop, promote, and sell technologies, and promotes scientists and their work. This accelerates the communication of successful science. Scientists can make better decisions using independent expert information and easily access manufacturers. SelectScience® informs the global scientific community through editorial, feature, video, and webinar programs. [Read more](#)



### Spectroscopy

With the *Spectroscopy* journal, scientists, technicians, and lab managers gain proficiency through unbiased, peer-reviewed technical articles, trusted troubleshooting advice, and best-practice application solutions. **Article:** *New Infrared Device Measures Blood Sugar Without a Prick*. By Jerome Workman, Jr. Researchers have developed a miniature non-invasive blood glucose monitoring system using NIR technology. The compact, low-cost device uses infrared light to measure sugar levels through the fingertip, offering a painless alternative to traditional finger-prick tests. [Read more](#)

## **EVENTS in 2025**

**October 20 to 23**

**XXV Brazilian Symposium of Electrochemistry and Electroanalytical (SIBEE)**

Águas de Lindóia, SP, Brazil

<https://www.sibee.com.br/>

**October 28 to 31**

**Congresso Latino-Americano de Cromatografia e Técnicas Relacionadas (COLACRO-2025)**

Campos do Jordão Arts & Convention Center, Campos do Jordão, SP, Brazil

<https://www.colacro.org/>

**November 9 to 14**

**8<sup>th</sup> EspeQBrasil and 17<sup>th</sup> Rio Symposium–RSAS 2025**

Hotel Fazenda Colina Verde, São Pedro, SP, Brazil

[Access info](#)

## **EVENTS in 2026**

**March 7 to 11**

**PITTCON Conference & Expo**

Henry B. González Convention Center

San Antonio, Texas, USA

<https://pittcon.org/>

**April 06 to 07**

**XX International Conference on Chemometrics in Analytical Chemistry**

Rome, Italy

<https://waset.org/chemometrics-in-analytical-chemistry-conference>

**May 17 to 22**

**44<sup>th</sup> International Symposium on Capillary Chromatography and 21<sup>st</sup> GCXGC Symposium**

Congress Centre, Riva del Garda, Italy

<https://iscc44.chromaleont.it/>

**June 8 to 9**

**MassSpecMeet 2026**

Lisbon, Portugal

**July 23 to 24**

**ANALYTICA ACTA 2026**

Paris, France

**August 22 to 28**

**26<sup>th</sup> International Mass Spectrometry Conference (IMSC)**

Lyon, France

<https://imsc26.com/>

## AUTHOR GUIDELINES

### Aims & Scope

*Brazilian Journal of Analytical Chemistry* is a double-blind peer-reviewed research journal dedicated to the diffusion of significant and original knowledge in all branches of Analytical and Bioanalytical Chemistry. It is addressed to professionals involved in science, technology, and innovation projects at universities, research centers and in industry. **BrJAC welcomes** the submission of research papers reporting studies devoted to new and significant analytical methodologies, putting in evidence the scientific novelty, the impact of the research and demonstrating the analytical or bioanalytical applicability. BrJAC **strongly discourages** those simple applications of routine analytical methodologies, or the extension of these methods to new sample matrices, unless the proposal contains substantial novelty and unpublished data, clearly demonstrating advantages over existing ones.

Additionally, there are other submission categories to BrJAC such as:

**Reviews:** They should be sufficiently broad in scope, but specific enough to permit an appropriate depth discussion, including critical analyses of the bibliographic references and conclusions. Manuscripts submitted for publication as Reviews must be original and unpublished. Reviews undergo double-blind full peer review and are handled by the Editor of Reviews.

**Technical Notes:** Concise descriptions of developments in analytical methods, new techniques, procedures, or equipment falling within the scope of the BrJAC. Technical notes also undergo double-blind full peer review.

**Letters:** Discussions, comments, and suggestions on issues related to Analytical Chemistry or Bioanalytical Chemistry. Letters are welcome and will be published at the discretion of the BrJAC Editor-in-Chief.

**Point of View:** This category is exclusively invited by the Editor-in-Chief.

See the next items for more information on the journal, the documents preparation, manuscript types, and how to prepare the submission.

### Professional Ethics

**Originality:** manuscripts submitted for publication in BrJAC cannot have been previously published or be currently submitted for publication in another journal.

**Preprint:** BrJAC does not accept manuscripts that have been posted on preprint servers prior to the submission.

**Integrity:** the submitted manuscripts are the full responsibility of the authors. Manipulation/invention/omission of data, duplication of publications, the publication of papers under contract and confidentiality agreements, company data, material obtained from non-ethical experiments, publications without consent, the omission of authors, plagiarism, the publication of confidential data and undeclared conflicts of interests are considered serious ethical faults.

BrJAC discourages and restricts the practice of excessive self-citation by the authors.

BrJAC does not practice coercive citation, that is, it does not require authors to include references from BrJAC as a condition for achieving acceptance, purely to increase the number of citations to articles from BrJAC without any scientific justification.

**Transparency:** The use of artificial intelligence (AI) by authors must comply with the transparency guidelines below:

- Authors are responsible for all content submitted to BrJAC, including the accuracy of AI-generated content.

- The authors must provide a declaration regarding the use of artificial intelligence in preparing the submitted manuscript. A template for this declaration is available for download [here](#). Authors must use this template when writing their declaration.
- AI tools should not be listed as authors, as they cannot be held responsible for the published work.
- Any use of AI tools for text or image generation must be declared in the Methods section of the manuscript, with a description of how and for what purpose the AI tools were used.
- If AI is used to create graphics and the cover artwork, the name of the tool(s) used and a brief description of how the image was created should be included in the figure caption. Authors are responsible for ensuring that the terms of use of the tools used state that the result is not the property of the generating site.
- The Editor may, at his/her discretion, determine that the use of AI in a particular submission is too extensive. This determination may result in rejection of the manuscript or a request to remove or reduce the AI-generated portions of the manuscript.
- In the peer review process, the BrJAC states that the opinion of the reviewers consulted is solely that of the reviewer. The use of AI tools in the review of manuscripts is not accepted. This BrJAC standard is intended to protect the confidentiality of the manuscript.

**Self-citation:** BrJAC discourages and restricts the practice of excessive self-citation by the authors. The maximum percentage of self-citations acceptable by BrJAC is 20%.

**Coercive citation:** BrJAC does not practice coercive citation. That is, BrJAC does not require authors to include BrJAC references as a condition for acceptance, purely to increase BrJAC articles citations without scientific justification.

**Similarities:** Manuscripts submitted to BrJAC are analyzed for similarities using specialized software. The maximum total similarity index accepted by the BrJAC is 25%, with a maximum of 3% for each source.

**Conflicts of interest:** when submitting their manuscript for publication, the authors must include all potential sources of bias such as affiliations, funding sources and financial, management or personal relationships which may affect the work.

**Copyright:** will become the property of the Brazilian Journal of Analytical Chemistry, if and when a manuscript is accepted for publication. The copyright comprises exclusive rights of reproduction and distribution of the articles, including reprints, photographic reproductions, microfilms or any other reproductions similar in nature, including translations.

**Request for permission to reuse figures and tables published in the BrJAC:** researchers who want to reuse any document or part of a document published in the BrJAC should request reuse permission from the BrJAC Editor-in-Chief, even if they are the authors of such document. A template for requesting reuse permission can be downloaded [here](#).

**Misconduct will be treated according to** the COPE's recommendations (<https://publicationethics.org/>) and the Council of Science Editors White Paper on Promoting Integrity in Scientific Journal Publications (<https://www.councilscienceeditors.org/>).

### ***Manuscript submission***

**The BrJAC does not charge authors an article processing fee.**

Manuscripts must be prepared according to the BrJAC manuscript template. Manuscripts in disagreement with the BrJAC guidelines are not accepted for revision.

The submission of manuscripts is done online by a submitting author through a digital manuscript manager system, which guides the author step by step through the entire submission process.

After the submitting author logs in to the system and enters his/her personal and affiliation details, the submission can be started.

All co-authors must be added to the Authors section.

Five documents are mandatorily uploaded by the submitting author: Cover letter, Title Page, Declaration of AI usage, Novelty Statement and the Manuscript. Templates for these documents are available for download [here](#).

The manuscript and the title page must be uploaded as Word files. The cover letter, declaration of AI usage, and novelty statement may be uploaded as PDF files. The manuscript Word file will be converted by the system to a PDF file which will be used in the double-blind peer review process.

All correspondence, including notification of the Editor's decision and requests for revision, is sent by e-mail to the submitting author through the manuscript manager system.

### ***Documents Preparation***

It is highly recommended that authors download and use the [templates](#) to create their five mandatory documents to avoid the suspension of a submission that does not meet the BrJAC guidelines.

#### **Cover Letter**

The cover letter template should be downloaded and filled out carefully.

Any financial conflict of interest or lack thereof and agreement with BrJAC's copyright policy must be declared. It is the duty of the submitting author to inform his/her collaborators about the submission of the manuscript and its eventual publication.

The Cover Letter must be signed by the corresponding author.

#### **Declaration on the Use of Artificial Intelligence**

The Declaration on the AI Use template must be downloaded and filled out carefully.

The corresponding author must sign the Declaration on the AI Use.

In the declaration on the use of artificial intelligence, the corresponding author must indicate whether or not AI tools were used in preparing the manuscript.

If AI tools were used, the author must state which tools were used and for what purpose.

#### **Title Page**

The Title Page must contain information for each author: full name, affiliation and full international postal address, and information on the contribution of each author to the work. Acknowledgments must be entered on the Title Page. The submitting author must sign the Title Page.

#### **Novelty Statement**

The Novelty Statement must contain clear and succinct information about what is new and innovative in the study in relation to previously related works, including the works of the authors themselves.

#### **Manuscript (all submission categories)**

It is highly recommended that authors download the Manuscript template and create their manuscript in this template, keeping the layout of this file.

- **Language: English** is the language adopted by BrJAC. The correct use of English is of utmost importance. We highly recommend [Proof-Reading-Service.com](#), a professional language editing service that specializes in [journal article proofreading](#) and [manuscript editing](#) for submissions to this journal. Upon completion of the proofreading, please provide a certificate confirming that the service has been carried out.
- **Required items:** the manuscript must include a title, abstract, keywords, and the following sections: Introduction, Materials and Methods, Results and Discussion, Conclusion, and References.
- **Identification of authors:** as the BrJAC adopts a double-blind review, the manuscript file must **NOT** contain the authors' names, affiliations nor acknowledgments. Full details of the authors and their acknowledgements should be on the Title Page.



- **Layout:** the lines in the manuscript must be numbered consecutively and double-spaced.
- **Graphics and Tables:** must appear close to the discussion about them in the manuscript. For **figures** use **Arabic** numbers, and for **tables** use **Roman** numbers.
- **Figure files:** when a manuscript is approved for publication, the BrJAC production team will contact the corresponding author to request separate files of each figure and a graphical abstract. These files must have **good resolution** and the extension **PNG or JPG**. The graphical abstract should preferably be created in landscape format. In the article diagrammed in the journal, the graphical abstract will occupy a space of 8 to 9 cm in length and 6 cm in height. Chemical structures must have always the same dimensions.
- **Studies involving biological material:** for studies involving human and animal material for research purposes, authors must state in the manuscript that the research has been approved by the research ethics committee of the institution where the study was conducted.
- **Permission to use content already published:** to use figures, graphs, diagrams, tables, etc. identical to others previously published in the literature, even if these materials have been published by the same submitting authors, a reuse permission from the publisher or scientific society holding the copyrights must be requested by the submitting authors and included among the documents uploaded in the manuscript management system at the time of manuscript submission.
- **Chemical nomenclature, units and symbols:** should conform to the rules of the International Union of Pure and Applied Chemistry (IUPAC) and Chemical Abstracts Service. It is recommended that, whenever possible, the authors follow the International System of Units, the International Vocabulary of Metrology (VIM) and the NIST General Table of Units of Measurement. Abbreviations are not recommended except for those recognized by the International Bureau of Weights and Measures or those recorded and established in scientific publications. Use L for liters. Always use superscripts rather than /. For instance: use mg mL<sup>-1</sup> and NOT mg/mL. Leave a space between numeric values and their units.
- **References throughout the manuscript:** the references must be cited as superscript numbers. It is recommended that references older than 5 (five) years be avoided, except in relevant cases. Include references that are accessible to readers.
- **References item:** This item must be thoroughly checked for errors by the authors before submission. From 2022, BrJAC is adopting the American Chemical Society's Style in the Reference item. Mendeley Reference Manager users will find the Journal of American Chemical Society citation style in the Mendeley View menu. Non-users of the Mendeley Reference Manager may refer to the ACS Reference Style Quick Guide DOI: <https://doi.org/10.1021/acsguide.40303>

### **Review process**

Manuscripts submitted to the BrJAC undergo an initial check for compliance with all of the journal's guidelines. Submissions that do not meet the journal's guidelines will be suspended and an alert sent to the corresponding author. The authors will be able to resend the submission within 30 days. If the submission according to the journal's guidelines is not made within 30 days, it will be deleted from the BrJAC system on the first subsequent day, and an alert will be sent to the corresponding author.

Manuscripts that are in accordance with the journal's guidelines undergo a similarity analysis using specialized software.

The manuscript is then forwarded to the Editor-in-Chief who will check whether the manuscript is in accordance with the journal's scope and will analyze the similarity report. The maximum total similarity index accepted by the BrJAC is 25%, with a maximum of 3% for each source.

If the manuscript passes the screening described above, it will be forwarded to an Associate Editor who will also analyze the similarity report and invite reviewers.

Manuscripts are reviewed in double-blind mode by at least 2 reviewers. A larger number of reviewers may be used at the discretion of the Editor. As evaluation criteria, the reviewers employ originality, scientific quality,

contribution to knowledge in the field of Analytical Chemistry, the theoretical foundation and bibliography, the presentation of relevant and consistent results, compliance with the BrJAC's guidelines, clarity of writing and presentation, and the use of grammatically correct English.

**Note:** In case the Editors and Reviewers consider the manuscript to require an English revision, the authors will be required to send an English proofreading certificate, by the ProofReading Service or equivalent service, before the final approval of the manuscript by the BrJAC.

The 1<sup>st</sup>-round review process usually takes around 5-6 weeks. If the manuscript is not rejected but requires corrections, the authors will have one month to submit a corrected version of the manuscript. In another 3-4 weeks, a new decision on the manuscript may be presented to the corresponding author.

The manuscripts accepted for publication are forwarded to the BrJAC production department. Minor changes to the manuscripts may be made, when necessary, to adapt them to BrJAC guidelines or to make them clearer in style, respecting the original content. The articles are sent to the authors for approval before publication. Once published online, a DOI number is assigned to the article.

### ***Final Considerations***

Whatever the nature of the submitted manuscript, it must be original in terms of methodology, information, interpretation or criticism.

With regard to the contents of published articles and advertisements, the sole responsibility belongs to the respective authors and advertisers; the BrJAC, its editors, editorial board, editorial office and collaborators are fully exempt from any responsibility for the data, opinions or unfounded statements.

**Manuscript submission at [www.brjac.com.br](http://www.brjac.com.br)**